Vanja Buvik

Stability of amines for CO$_2$ capture

Doctoral thesis

NTNU
Norwegian University of
Science and Technology

Vanja Buvik

Stability of amines for CO$_2$ capture

Thesis for the Degree of Philosophiae Doctor

Trondheim, August 2021

Norwegian University of Science and Technology
Faculty of Natural Sciences
Department of Chemical Engineering

NTNU
Norwegian University of
Science and Technology

Abstract

Despite of being a well-tested and highly attractive technology for capture of carbon dioxide (CO_2), amine scrubbing encounters economic and operational challenges originating from degradation of the amine solvent, in particular oxidative degradation. By finding means of tackling of solvent degradation, associated problems like corrosion, emissions, and environmental concerns can also be significantly reduced. Degradation mechanisms have been studied for more than two decades and have yet to be fully understood within the whole process. This, mainly experimental work aims to contribute to further understanding of amine degradation in the CO_2 capture process and how it can be avoided.

Measurement of oxygen solubility is a central part of the study, as oxygen plays a vital role in the degradation reactions. It was found that all studied amines seem to have comparable oxygen solubility to water in the absence of CO_2. The parameters that influence oxygen solubility the most are the presence of CO_2, temperature, and mass transfer limitations due to rapidly occurring degradation reactions in unstable amines like ethanolamine (MEA).

Experiments where aqueous amine solvents were subjected to sparging with 98% oxygen gas at 60 °C, with addition of ferrous (Fe^{2+}) and under constant stirring were used to assess oxidative amine degradation. The oxidative stability of 18 different amines was studied, and seen in context of thermal, and biological stability. Low thermal, and oxidative degradability are highly desirable properties, while a low biodegradability is undesirable. It was found that, despite of an overarching trend of correlation, there are amine solvents that have high biodegradability but also low degradability under oxidative conditions. No correlation between literature data for thermal degradation and oxidative stability in this work was found. The oxidative degradation experiments show the correlations between structural features of the amine and stability, where MEA is the least stable of alle those studied. Tertiary and sterically hindered amines are the most stable under oxidative conditions, and only naturally occurring amines were found to be readily biodegradable.

The most thoroughly studied amine in this work was MEA, because of its relatively fast degradation rate compared to most other amines. It was found that CO_2-free MEA hardly degrades under oxidative conditions, that Fe^{2+} and Cu^{2+} have similar catalytic abilities on oxidative MEA degradation, and potassium iodide (KI) was identified as an inhibitor for MEA degradation under laboratory-scale oxidative degradation experiments.

Acknowledgements

First of all, thank you Prof Hanna Knuutila for giving me this chance, for your guidance, wisdom, understanding, flexibility, and good jokes. I knew I shouldn't let the chance pass when a PhD position under your supervision came up four years ago, and I was right. Thank you also for the encouragement and support when I did not always want to follow the straightest path through my PhD, taking detours into other departments to learn new things outside the scope of chemical engineering, and learning and practicing public dissemination. You always have a million things going on, yet I always find you have time for me. I have learned so very much from you and of all that I am thankful. I really could not have had a better advisor.

I am quite convinced that this work would have taken me very much longer if it wasn't for the help and advice of my co-supervisor Dr Solrun Johanne Vevelstad. You are an amine degradation oracle who always knows where to start looking, you know every suggested degradation mechanism, and always have time to talk to me when I don't know where to begin, continue, or what to take from the results I have gotten. Your guidance through these years has been extremely valuable to me and I greatly appreciate getting the chance to follow in your footsteps. I am also so grateful to Dr Diego Pinto, who hired me at the department of chemical engineering in the first place, and opened my eyes to this very interesting, and important research topic.

Outside the department of chemical engineering I have also met great people that have taught me a lot. I want to thank Prof Richard Strimbeck for taking me in to the world of plants when I wanted to do biodegradation experiments, for teaching me about plant and soil metabolism, setting up experiments with living things, patiently helping me score the plants twice a week, and then for all the advice on the statistical analyses! Thank you, Dr Odd Gunnar Brakstad, for your time and efforts helping with biodegradation experiments in sea water, and for introducing me to biodegradation in general. I learned a lot from you both and would love to work with you again in the future.

Some people have given me priceless technical support throughout my time here. Gøril Flatberg, I don't know what I would have done without you. Thank you for being a great colleague that I love working alongside with, and for making sure the lab is always well-equipped. I could always count on your help when something needed fixing in the lab, and without you I think a certain instrument, who's name we do not mention, would have broken my spirits. Thank you also Mikael Hammer for fixing every computer issue, whether in the lab or in the office, and always providing me with all kinds of equipment I have needed the past four years, you've made it very easy for me. I also want to thank Dr Susana Villa Gonzales here, although the thesis

Contents

List of abbreviations

Abbreviations

α	$mol_{CO2} \, mol_{amine}^{-1}$
abs	absolute
aq.	aqueous
ATR	attenuated total reflectance
BECCS	bioenergy with carbon capture and storage
BOD	biological oxygen demand
BOD28	biological oxygen demand after 28 days
c	concentration
CAS	Chemical Abstracts Service reference number
CCS	carbon capture and storage
CCUS	carbon capture, utilisation, and storage
CPH	combined heat and power
CV	coefficient of variation; ratio of SD to the mean
DAC	direct air capture
$DeSO_X$	removal of sulphur oxides (SO_X)
$DeNO_X$	removal of nitrogen oxides (NO_X)
dil.	diluted
DO	dissolved oxygen
EC50	effective concentration of test substance inhibiting growth by 50%
ED	electrodialysis
EDX	energy dispersive X-ray microanalysis
ELPI	electrical low-pressure impactor
EOR	enhanced oil recovery
ESP	electrostatic precipitator
FGD	flue gas desulphurisation
FMPS	fast mobility particle sizer

FT-IR	Fourier transform infrared
GC	gas chromatography
GDT	gas distribution tube
GHG	greenhouse gas
h	hour
h	Planck's constant ($6.626 \cdot 10^{-34}$ J·s)
HSE	health, safety, and environment
HSS	heat stable salts
IC	ion chromatography
ICP	Inductively coupled plasma
IEA	International Energy Agency
IPCC	Intergovernmental Panel on Climate Change
LC	liquid chromatography
LOD	limit of detection
LOQ	limit of quantification
m	mass
M	mol L^{-1}
mL	millilitre
mM	mmol per kg
mmol	millimoles
MS	mass spectrometry
MS/MS	tandem mass spectrometry
NCCS	Norwegian CCS Research Centre
NDIR	nondispersive infrared
NOAA	National Oceanic and Atmospheric Administration
OECD	Organisation for Economic Co-operation and Development
OES	optical emission spectroscopy
OPC	optical particle counter
PCCC	post-combustion CO_2 capture
ppb	parts per billion

ppm	parts per million
PR	particle removal
PTR	proton-transfer reaction
QTOF	quad time-of-flight
RFCC	residual fluidised cracker
RSD	relative standard deviation
SAS	salted amine solvents
SCR	selective catalytic reduction
SD	standard deviation
SDR	solvent degradation rig
SEM	scanning electron microscope
T	temperature
TCM	Technology Centre Mongstad
ThOD	theoretical oxygen demand
TIC	total inorganic carbon
TN	total nitrogen
TOC	total organic carbon
TOF	time of flight
TONO	total nitrosamine
TRL	technology readiness level
UNFCCC	United Nations Framework Convention on Climate Change
USN	University of South-Eastern Norway
v	frequency
V	volume
VOC	volatile organic compounds
WESP	wet electrostatic precipitator
WFGD	wet flue gas desulphurisation
wt	weight

Chemical and compound abbreviations, and CAS-numbers

AB	4-amino-1-butanol	13325-10-5
AEP	1-(2-aminoethyl)-piperazine	140-31-8
AMP	2-amino-2-methyl-1-propanol	124-68-5
AP	3-aminopropan-1-ol	156-87-6
BHEOX	*N,N'*-bis(2-hydroxyethyl) oxamide	1871-89-2
BzA	benzylamine	100-46-9
1,2-DAP	propane-1,2-diamine	78-90-0
DEEA	2-(diethylamino)ethanol	100-37-8
DGA	Diglycolamine® / 2-(2-aminoethoxy)-ethanol	929-06-6
DIPA	diisopropanolamine	110-97-4
1DMA2P	1-dimethylamino-2-propanol	108-16-7
DMAPA	3-(dimethylamino)-1-propylamine	109-55-7
DMMEA	2-(dimethyl)-aminoethanol	108-01-0
DMPA	3-dimethylamino-1-propanol	3179-63-3
DNPH	2,4- dinitrophenylhydrazine	119-26-6
EA	ethylamine	75-04-7
EAE	2-(ethylamino)ethanol	110-73-6
Gly	Glycine	56-40-6
HEA	*N*-(2-hydroxyethyl)-acetamide	142-26-7
HEEDA	2-(2-hydroxyethylamino)-ethanol	111-41-1
HEF	*N*-(2-hydroxyethyl)-formamide	693-06-1
HEI	*N*-(2-hydroxyethyl)-imidazole	1615-14-1
HEIA	*N*-(2-hydroxyethyl)-2-imidazolidione	3699-54-5
HEPO	4-(2-hydroxyethyl)-2-piperazinone	23936-04-1
1-(2HE)PP	1-(2-hydroxyethyl)-piperidine	3040-44-6
MAPA	3-(methylamino)-propylamine	6291-84-5
MAPD	3-(methylamino)-propane-1,2-diol	40137-22-2
MDEA	*N*-methyl diethanolamine	105-59-9
MEA	2-aminoethano-1-ol	141-43-5

MEG	ethane-1,2-diol	107-21-1
MIPA	amino-2-propanol	78-96-6
MMEA	2-(methyl)-aminoethanol	109-83-1
MSA	methanesulfonic acid	75-75-2
OZD	2-oxazolidinone	497-25-6
PZ	piperazine	110-85-0
Sar	Sarcosine	107-97-1
TEA	triethanolamine	102-71-6

Chapter 1

Introduction

This first chapter contains a general description of the issues in focus in the work conducted for this PhD thesis. A short background on the need for CO_2 capture and the status of amine scrubbing as a means of CO_2 capture is given, followed by the scope of the work, a list of publications, and the author's contribution to them.

1.1 Background

Anthropogenic greenhouse gas emissions have caused the atmospheric concentrations of these gases to increase exponentially since pre-industrial times. The largest contribution to the heating imbalance the global climate is experiencing is caused by carbon dioxide (CO_2) (Butler and Montzka, 2020), which in April 2021 reached an average of 419 ppm (NOAA, 2021), greatly exceeding the pre-industrial concentrations of around 280 ppm (Etheridge et al., 1996). The goal of the legally binding Paris agreement from 2015 is to limit the increase of global average temperatures from pre-industrial time, to less than 2 °C, and preferably even less than 1.5 °C (UNFCCC, 2015). In their report from 2018, the Intergovernmental Panel on Climate Change (IPCC) highlighted three out of four imaginable scenarios for achieving this, in which carbon capture and storage (CCS) or carbon capture, utilization and storage (CCUS) was included as part of the solution (Rogelj et al., 2018). The International Energy Agency (IEA) also highlight the importance of CCUS for reaching net-zero emissions (IEA, 2020). As well as being an important measure to keep unavoidable industrial processes, such as steel and cement production emission-free in the future, CCUS is an immediate solution to supply zero- to low-emission energy in the transition to renewable energy sources in a global society with high electrical energy demand.

There are a wide range of technologies at different technology readiness levels (TRLs) applicable for CO_2 separation from industrial sources. These include chemical and physical absorption (TRL 9 = commercial scale), membrane separation (TRL 7 = demonstration scale), adsorption (TRL 7), cryogenic distillation, and calcium looping (TRL 6 = pilot scale) (Bui et al., 2018). Additionally, there are processes such as oxyfuel-combustion, chemical looping, or pre-combustion capture that allow for combustion processes with low CO_2 emissions. Direct air capture (DAC) technologies are emerging fast and have gained a high popularity, with the concept of capturing CO_2 directly from atmospheric concentrations. The energy intensity of DAC technologies is for now much higher than conventional capture processes (Bui et al., 2018), but it may play a significant role in the future, when high-concentration streams of CO_2 from industrial sources have been abated. DAC is, together with the production of bioenergy with CCS (BECCS), reforestation/afforestation, enhanced weathering, soil management and ocean fertilisation, a negative-emission technology (Minx et al., 2018).

Despite of a broad consensus on the scientific side, CCUS is a controversial topic that meets much scepticism in media and the general public. Main concerns include the fact that the oil and gas industries stand behind much of the research funding in the field, causing worries that CCUS is merely an excuse to prolong the fossil fuel age. In the past, one of the incentives for CCS was to use the captures CO_2 for enhanced oil recovery (EOR), meaning that it simply is used to extract larger amounts of oil

from the reservoirs. Additionally, geological storage of CO_2 can sound unsafe, and for some as a means of moving the problem from one location to another. In a time where false information and fear spreads faster than viruses, the CCUS experts face the challenge of conveying the enormous scientific knowledge base that exists, as well as the success stories from all sides of the chain: capture, utilisation, and storage. The only alternative scenario for reaching zero-emissions without implementation of CCUS, as described by the IPCC (Grubler et al., 2018; Rogelj et al., 2018), is that of a global society reducing its overall energy demand, demand for greenhouse gas (GHG) intensive consumption goods, and land use. Although possible, even the authors of the study point out the challenges of social and institutional change required, that goes against the historical curve of ever-increasing demand (Grubler et al., 2018).

CCS and CCUS are unavoidable parts of the solution if we are to mitigate global warming, and the larger the implementation gets, the lower the cost of CO_2 capture and storage will get.
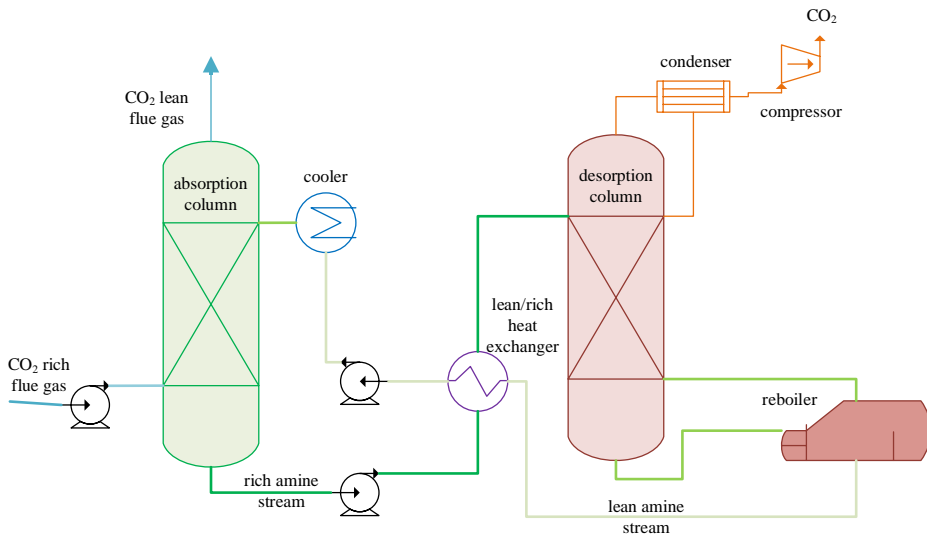
Figure 1.1: Schematics of the post-combustion CO_2 capture process using liquid amine solvents.

1.1.1 Amine scrubbing

When it comes to post-combustion capture of CO_2 (PCCC), no technology has been as thoroughly and successfully tested, nor is on the TRL of chemical absorption with amine solvents (Bui et al., 2018; Rochelle, 2016). The first process using aqueous amines for CO_2 capture was patented already in the 1930s (Kohl and Nielsen, 1997). Amines have the ability to bind CO_2 to form stable, mainly ionic compounds, in a

reaction that can be reversed upon heating. The process typically takes place in a configuration shown simplified in Figure 1.1, by leading pre-treated flue gas, cooled and with prior removal of NO_X, SO_X, and particulate matter, into an absorber column where it travels upward, counter-current to the amine solvent. The absorber column is filled with packing material to increase the rate of flue gas CO_2 binding to the amines. From the bottom of the absorber, often called the "absorber sump", CO_2-rich amine is transported to a desorber column, where a reboiler ensures increased temperature, favouring desorption of CO_2 and regeneration of the amine solvent (Kohl and Nielsen, 1997). This process has the advantage of being possible to retrofit into exciting industrial sources of CO_2, by simply attaching the scrubber unit to the flue gas source. The amine solvents typically consist of a single amine or a mixture of two or more amines in water, although there is also a large research focus on replacing water with other solvents (Wanderley and Knuutila, 2020). One of the most used and studied amine solvents is a 30 wt% ethanolamine (MEA, Figure 1.2) solution in water (Gouedard et al., 2012), which has been employed for about half a century (Kohl and Nielsen, 1997). Other amines that have seen a lot of implementation are diethanolamine (DEA), *N*-methyl diethanolamine (MDEA), piperazine (PZ) and 2-amino-2-methyl-1-propanol (AMP), whereof an aqueous mixture of the latter two has been described as the new benchmark for amine scrubbing (Feron et al., 2020; Gouedard et al., 2012).
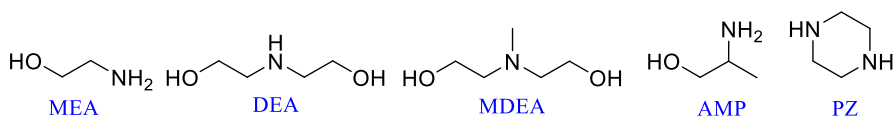
Figure 1.2: Molecular structure of some of the most studied and applied compounds used in conventional amine scrubbing for CO_2 capture.

The amines bind CO_2 in a reversible manner through mainly three mechanisms for primary and secondary amines; carbamate formation (Eq. 1.1), bicarbonate formation (Eq. 1.2) and carbamate reversion (Eq. 1.3) reactions. Tertiary amines primarily bind CO_2 through bicarbonate formation (Eq. 1.4). Some sterically hindered primary and secondary amines such as i.e. AMP can, however, have more similar reaction kinetics to tertiary amines, being less prone to form stable carbamates and also achieving higher CO_2 loadings than a classical primary amine such as MEA.

Eq. 1.1

Eq. 1.2

$$\text{R''R'N-COO}^- + H_2O \;\rightleftharpoons\; \text{R''R'NH} + \;^-O\text{-CO-OH} \qquad \text{Eq. 1.3}$$

$$\text{R''R'N-R'''} + CO_2 + H_2O \;\rightleftharpoons\; \text{R''R'}^+\text{NHR'''} + \;^-O\text{-CO-OH} \qquad \text{Eq. 1.4}$$
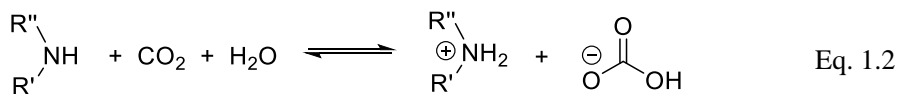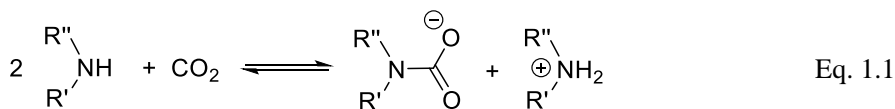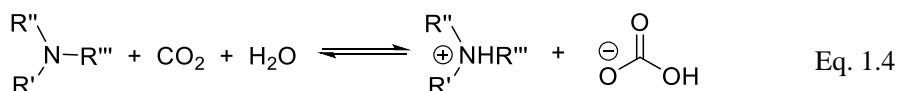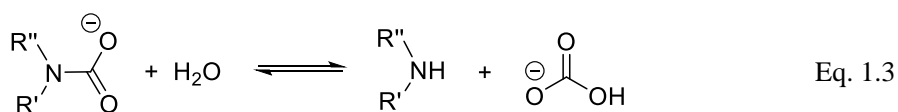
Primary and secondary amines have favourable kinetics and typically undergo a relatively fast CO_2 absorption process compared to tertiary amines, which react slower, but with the advantage of having capacities for absorbing more CO_2 than the primary and secondary amines. Since high CO_2-loadings can be achieved with tertiary amines but these have slow kinetics, a tertiary amine is often combined with a primary amine, to enhance the rate of absorption while keeping the high capacity of the tertiary amine. The primary amine in a blend is often called a "promoter".

The relatively high energy required to reverse the equilibria given in Eq. 1.1-1.4 is one of the largest economic obstacles of amine scrubbing as a means for capturing and storing CO_2. Development of new solvent blends with favourable kinetics, as well as optimising the plant configuration for better heat integration are the main approaches that are being made and are still being addressed to solve this problem. This has resulted in a reduction from around 4 to below 2 GJ $t_{CO_2}^{-1}$ (Abu-Zahra et al., 2016; Oh et al., 2020). The other main, and large, category of improvements for reducing the cost of amine scrubbing for CO_2 capture is issues associated with solvent degradation, which includes solvent loss and replacement, operational issues caused by the changing physical properties of the degrading solvent, corrosion and related issues due to the properties of the formed degradation compounds, and health and environmental concerns raised by the degradation compounds.

1.1.2 Degradation of amines

Amine degradation is an issue that requires monitoring and management in the post-combustion CO_2 capture process. Proper management will reduce the chances of interrupting operation, reduce energy consumption, and cost and decrease the health, safety and environmental (HSE) impact of the amines and their degradation products (Reynolds et al., 2016; Vega et al., 2014). Many degradation compounds are attributed to corrosion of construction material (Fytianos et al., 2014), some increase the overall degradation rate of the solvent, and others are of environmental concern (da Silva et al., 2013). Corrosion and degradation are strongly linked, also because dissolved metals catalyse the degradation reactions (Blachly and Ravner, 1963; Dhingra et al., 2017; Léonard et al., 2014; Nielsen and Rochelle, 2017).

The development of new solvents seeks to combat the degradation issues by designing amines with higher stability, or making blends of readily available amines, which are less prone to degradation than, for example, the conventional ethanolamine

(MEA). Other approaches to reducing the impact of amine degradation on CO_2 capture plant operation are, for example, "feed and bleed", replacement of a fraction of the used solvent with new solvent regularly (Moser et al., 2020), reclaiming technologies for removal of heat-stable salts (HSS), such as flue gas impurities, dissolved metals and degradation compounds from the solvent (Kentish, 2016; Wang et al., 2015), pre-treatment of the flue gas before subjecting it to the amine solvent for CO_2 removal (Meuleman et al., 2016), and in the recent years also oxygen removal from the solvent (Monteiro et al., 2018). Another way of managing the health of the solvent and capture plant, is by using additives, such as degradation or corrosion inhibitors, or anti-foaming agents.

The most dominant mechanisms of degradation in pilot-scale amine scrubbing are: thermal degradation, caused by polymerization reactions, and oxidative degradation, caused by oxidising agents such as dissolved oxygen, SO_X and NO_X, and catalysed by dissolved metals (Reynolds et al., 2016). Both these pathways have been comprehensively studied in literature, resulting in a good understanding of both, but with more open questions when it comes to the mechanisms of oxidative degradation in the large-scale CO_2 capture process than thermal. Although not as rapid as oxidative and thermal degradation in the CO_2 capture process, nitrosamine and nitramine formation are also critical degradation pathways to consider, since their products are highly toxic (de Koeijer et al., 2013; Fostås et al., 2011). All degradation patterns and mechanisms naturally depend on the structure of the amine in use and no amine for PCCC has been as thoroughly studied when it comes to degradation as MEA, so much of the knowledge about amine degradation is based on this amine. An emphasis is therefore also put on MEA in this work.

1.1.3   Environmental impact

CO_2 capture is a technology meant for reducing the anthropogenic footprint on the planet by reducing and removing emissions contributing to climate change. It is therefore also of upmost importance for the technology not to give rise to other issues of environmental concern, neither locally nor globally. To avoid emissions of the solvent itself, choosing a solvent of reasonably low volatility should be considered, as well as implementing a water wash or potentially also an acid wash after the absorber column, to catch remaining amine in the clean flue gas. This will also to a large extent capture and avoid emissions of volatile degradation compounds. To be prepared for any eventuality, such as a liquid or gas leakage from the plant it is still, however, important that neither the amine nor its degradation products cause harm neither to humans operating the plant, nor the environment surrounding it. Both biodegradability and ecotoxicity are important factors to consider when assessing the environmental impact of the solvent and the limits for the two features are normally set by local governing authorities. The study of biodegradability and ecotoxicity has to a large extent been performed for very many amines, but no complete studies investigating the environmental faith of the compounds have been performed, that

look at the pathways of degradation, where it takes place, where the degradation compounds and amines end up and what the impact is on the local ecosystem.

1.2 Scope

The work for this doctoral thesis was performed as a part of the Norwegian CCS Research Centre (NCCS), in the Solvent development task (Task 2), who's purpose it is to address the challenges related to solvent technology, with a focus on environmental aspects.

The overarching goal of the work was to add to the understanding of oxidative amine degradation and by that contribute to finding ways of circumventing it. Laboratory-scale oxidative degradation studies were heavily emphasized, where the impact of the chemical structure of amines impact on stability was studied. Correlations were sought between other amine properties and oxidative degradation, to see whether any could be used for stability predictions. Additionally, an inhibitor for oxidative degradation was identified and studied at laboratory scale to determine if this stable, non-consumable component could enhance the stability of amines under oxidative conditions. The presence of oxygen, dissolved metals, and salts were all investigated in turn. Because of its importance for the oxidative degradation process, oxygen solubility was studied in solvents for CO_2 capture, to better understand and predict the concentrations of oxygen we are dealing with in the CO_2 capture plant. The impact of the amines in the environment was also studied, both in the form of biodegradation studies in seawater, to extend the existing database to all the amines studied in this work, and the impact of simulated amine spills on the environment.

1.3 Layout of the thesis

This first chapter of the thesis contains a brief introduction to the topic and scope of the work, as well as a summary of the publications produced. Following this comes a summary of the current status of knowledge about amine stability, degradation pathways and known stabilising and destabilising effects, mainly under oxidative, but also thermal and biological conditions. After the brief literature review in chapter 2, comes a review paper in chapter 3, that is about the degradation and emissions observed and reported in pilot scale CO_2 capture, that was published in the International Journal of Greenhouse Gas Control. Chapter 4 describes the experimental and analytical procedures utilized in this work. In chapter 5 a manuscript about the measurement of dissolved oxygen and assessment of oxygen solubility in amine solvents is given, which was also published in the International Journal of Greenhouse Gas Control. The manuscript in chapter 6 was published in Industrial & Engineering Research and describes a large study on oxidative stability of structurally varied amines. The stability of the amines is seen in context of other stability properties of the amines. The manuscript in chapter 7 also contains an

oxidative degradation study, this time on ethanolamine in water, and salts were tested as oxidation inhibitors. This paper, which was published in Chemical Engineering Science: X, introduces potassium iodide as an oxidation inhibitor for the tested system. A new approach to testing the environmental impact of ethanolamine is presented in chapter 8, a work that was presented at the TCCS-11 conference in Trondheim. The last chapter contains a summary of the findings and recommendations for future work.

1.4 Papers and presentations

1.4.1 Journal papers

Buvik, Vanja; Bernhardsen, Ida M.; Figueiredo, Roberta V.; Vevelstad, Solrun J.; Goetheer, Earl L.V.; van Os, Peter & Knuutila, Hanna K., *Measurement and prediction of oxygen solubility in post-combustion CO_2 capture solvents*. Int. J. Greenh. Gas Control, Vol 104, 2021, 103205, https://doi.org/10.1016/j.ijggc.2020.103205

Buvik, Vanja; Høisæter, Karen K.; Vevelstad, Solrun J. & Knuutila, Hanna K., *A review of degradation and emissions in post-combustion CO_2 capture pilot plants*. Int. J. Greenh. Gas Control, Vol 106, 2021, 103246, https://doi.org/10.1016/j.ijggc.2020.103246

Buvik, Vanja; Wanderley, Ricardo R. & Knuutila, Hanna K., *Addition of stable salts reduced oxidative degradation of monoethanolamine (MEA)*. Chemical Engineering Science: X, Vol 10, 2021, 100096, https://doi.org/10.1016/j.cesx.2021.100096

Buvik, Vanja; Vevelstad, Solrun J.; Brakstad, Odd G. & Knuutila, Hanna K., *Stability of structurally varied aqueous amines for CO_2 capture*, Ind. Eng. Research Chem., Vol 60, 15, 5627–5638, 2021, https://doi.org/10.1021/acs.iecr.1c00502

1.4.2 Conference proceedings

Buvik, Vanja*; Strimbeck, Richard & Knuutila, Hanna K. *Experimental assessment of the environmental impact of ethanolamine*. SINTEF Conference Proceedings, *accepted* 2021.

Buvik, Vanja*; Thorstad, Silje; Wanderley, Ricardo R. & Knuutila, Hanna K. *Introduction of potassium iodide as an inhibitor for oxidative degradation of amines*. SINTEF Conference Proceedings, *accepted* 2021.

1.4.3 Conference presentations

Buvik, Vanja* & Knuutila, Hanna K. *Review of oxidative degradation of 30 wt. % MEA in pilot campaigns* (30.-31.01.2018), University of Texas 4th Conference on Carbon Capture and Storage UTCCS-4 (online). *Oral presentation.*

Buvik, Vanja*; Vevelstad, Solrun J. & Knuutila & Hanna K. *Comparison of oxidative and biodegradability of aqueous amine solvents for CO_2 capture* (17.-19.06.2019). Trondheim CCS Conference TCCS-10. *Poster presentation.*

Buvik, Vanja*; Vevelstad, Solrun J. & Knuutila, Hanna K. *Oxygen solubility of amine solutions* (17.-20.09.2019). 5th Post Combustion Capture Conference PCCC-5, Kyoto Japan. *Oral presentation.*

Buvik, Vanja*; Vevelstad, Solrun J. & Knuutila, Hanna K. *Oxidative and biological degradability of aqueous amine solvents for CO_2 capture* (28.-29.01.2020). University of Texas 5th Conference on Carbon Capture and Storage, UTCCS-5 (online). *Oral presentation.*

Buvik, Vanja*; Strimbeck, Richard & Knuutila, Hanna K. *Experimental assessment of the environmental impact of ethanolamine* (22.-23.06.2021). Trondheim CCS Conference TCCS-11. *Poster presentation*.

Buvik, Vanja*; Thorstad, Silje; Wanderley, Ricardo R. & Knuutila, Hanna K. *Introduction of potassium iodide as an inhibitor for oxidative degradation of amines* (22.-23.06.2021). Trondheim CCS Conference TCCS-11. *Oral presentation*.

1.4.4 Webinars

* Presenter

Buvik, Vanja* & Knuutila, Hanna K. *Oxygen solubility in selected amine solvents* (21.11.2018). NCCS Webinar.

Wanderley, Ricardo R.*; Buvik, Vanja* & Knuutila, Hanna K. *A look at the state of the art of water-lean solvents* (25.06.2020). NCCS webinar.

Knuutila, Hanna K.* & Buvik, Vanja. *A review of degradation in post-combustion CO_2 capture pilot plants* (15.04.2021). LAUNCH webinar

1.4.5 Popular dissemination

Buvik, Vanja: *Finding the perfect solvent to capture CO_2* (2019), NTNU - NV Faculty blog. https://www.ntnutechzone.no/en/2019/07/finding-the-perfect-solvent-to-capture-co2/

Buvik, Vanja: Oxidative degradation in CO_2 capture and NCCS mobility fund (2019), SINTEF blog. https://blog.sintef.com/sintefenergy/ccs/oxidative-degradation-co2-capture-nccs-mobility-fund/

Buvik, Vanja: *Løsninger for CO₂-fangst*. Presentation at Forsker Grand Prix 24.09.2020. https://youtu.be/mCQ2qgXkQhc [14:13 - 22:18]

Buvik, Vanja: Instagram takeover on the NV Faculty account, 20.11.2020. @ntnurealfag – FGP takeover.

Buvik, Vanja: *Bedre aminer kan hente ut CO₂ mer effektivt* (2020). Podcast episode on Teknisk Sett, https://www.tu.no/artikler/bedre-aminer-kan-hente-ut-co-sub-2-sub-mer-effektivt/502578

Buvik, Vanja & Knuutila, Hanna K.: *When little things have a big impact* (2021), NTNU - NV Faculty blog https://www.ntnu.no/blogger/teknat/en/2021/02/19/when-little-things-have-a-big-impact/

Buvik, Vanja: *Løsninger for CO₂-fangst*. Presentation at Realfagskonferansen 11.05.2021. https://youtu.be/DWSPmzdsAQA

1.5   Author's contribution to the work

Thesis chapter	Publication title	Extent and nature of author's contribution
3	A review of degradation and emissions in post-combustion CO_2 capture pilot plants	The first author contributed to data collection, writing parts of the first draft, revision of the manuscript before and after peer review and editing before resubmission.
5	Measurement and prediction of oxygen solubility in post-combustion CO_2 capture solvents	The first author took part in the conceptualization and planning of the work, performed all the experiments, with the exception of some of the validation of the optical dissolved oxygen sensor, wrote most of the original manuscript, with exception of the description of the optical sensor and the modelling work, and partook in revision and editing of the peer reviewed manuscript.
6	Stability of structurally varied aqueous amines for CO_2 capture	The first author took part in the conceptualization and planning of the work, performed the oxidative degradation experiments and most of the analyses of the degraded solutions, wrote large parts of the original manuscript and partook in revision and editing of the peer reviewed manuscript.

Thesis chapter	Publication title	Extent and nature of author's contribution
7	Addition of stable salts reduced oxidative degradation of monoethanolamine (MEA).	The first author has carried out the oxidative and thermal degradation and chemical analyses and has also written the parts related to thermal and oxidative degradation in the first draft of the paper. The first author also contributed to the revision and editing of the peer reviewed manuscript before publication.
8	Experimental assessment of the environmental impact of ethanolamine	The first author performed the experimental work under guidance of the second author, who also performed the objective observations used for effect quantification. The first author also performed the statistical analyses and wrote the first draft of the original manuscript, as well as revising and editing the peer reviewed manuscript before publication.

1.6 References

Abu-Zahra, M.R.M., El Nasr, A.S., Al Hajaj, A., Goetheer, E.L.V., 2016. Techno-economics of liquid absorbent-based post-combustion CO_2 processes, in: Feron, P.H.M. (Ed.), Absorption-Based Post-combustion Capture of Carbon Dioxide. Woodhead Publishing, pp. 685-710.

Blachly, C., Ravner, H., 1963. The effect of trace amounts of copper on the stability of monoethanolamine scrubber solutions. Naval Research Lab Washington DC.

Bui, M., Adjiman, C.S., Bardow, A., Anthony, E.J., Boston, A., Brown, S., Fennell, P.S., Fuss, S., Galindo, A., Hackett, L.A., Hallett, J.P., Herzog, H.J., Jackson, G., Kemper, J., Krevor, S., Maitland, G.C., Matuszewski, M., Metcalfe, I.S., Petit, C., Puxty, G., Reimer, J., Reiner, D.M., Rubin, E.S., Scott, S.A., Shah, N., Smit, B., Trusler, J.P.M., Webley, P., Wilcox, J., Mac Dowell, N., 2018. Carbon capture and storage (CCS): the way forward. Energy & Environmental Science 11, 1062-1176.

Butler, J.H., Montzka, S.A., 2020. The NOAA annual greenhouse gas index (AGGI), Annual Greenhouse Gas Index (AGGI). NOAA Earth System Research Laboratory.

da Silva, E.F., Kolderup, H., Goetheer, E., Hjarbo, K.W., Huizinga, A., Khakharia, P., Tuinman, I., Mejdell, T., Zahlsen, K., Vernstad, K., Hyldbakk, A., Holten, T., Kvamsdal, H.M., Van Os, P., Einbu, A., 2013. Emission studies from a CO2 capture pilot plant, Energy Procedia. Elsevier Ltd, pp. 778-783.

de Koeijer, G., Talstad, V.R., Nepstad, S., Tønnessen, D., Falk-Pedersen, O., Maree, Y., Nielsen, C., 2013. Health risk analysis for emissions to air from CO2 Technology Centre Mongstad. International Journal of Greenhouse Gas Control 18, 200-207.

Dhingra, S., Khakharia, P., Rieder, A., Cousins, A., Reynolds, A., Knudsen, J., Andersen, J., Irons, R., Mertens, J., Abu Zahra, M., Van Os, P., Goetheer, E., 2017. Understanding and Modelling the Effect of Dissolved Metals on Solvent Degradation in Post Combustion CO2 Capture Based on Pilot Plant Experience. Energies 10.

Etheridge, D.M., Steele, L.P., Langenfelds, R.L., Francey, R.J., Barnola, J.M., Morgan, V.I., 1996. Natural and anthropogenic changes in atmospheric CO2 over the last 1000 years from air in Antarctic ice and firn. Journal of Geophysical Research-Atmospheres 101, 4115-4128.

Feron, P.H.M., Cousins, A., Jiang, K., Zhai, R., Garcia, M., 2020. An update of the benchmark post-combustion CO2-capture technology. Fuel 273, 117776.

Fostås, B., Gangstad, A., Nenseter, B., Pedersen, S., Sjøvoll, M., Sørensen, A.L., 2011. Effects of NOx in the flue gas degradation of MEA. Energy Procedia 4, 1566-1573.

Fytianos, G., Grimstvedt, A.M., Knuutila, H., Svendsen, H.F., 2014. Effect of MEA's degradation products on corrosion at CO2 capture plants.

Gouedard, C., Picq, D., Launay, F., Carrette, P.L., 2012. Amine degradation in CO2 capture. I. A review. International Journal of Greenhouse Gas Control 10, 244-270.

Grubler, A., Wilson, C., Bento, N., Boza-Kiss, B., Krey, V., McCollum, D.L., Rao, N.D., Riahi, K., Rogelj, J., De Stercke, S., Cullen, J., Frank, S., Fricko, O., Guo, F., Gidden, M., Havlík, P., Huppmann, D., Kiesewetter, G., Rafaj, P., Schoepp, W., Valin, H., 2018. A low energy demand scenario for meeting the 1.5 °C target and sustainable development goals without negative emission technologies. Nature Energy 3, 515-527.

IEA, 2020. Energy Technology Perspectives 2020. IEA, Paris.

Kentish, S.E., 2016. Reclaiming of amine-based absorption liquids used in post-combustion capture, Absorption-Based Post-Combustion Capture of Carbon Dioxide, pp. 426-438.

Kohl, A.L., Nielsen, R.B., 1997. Chapter 2 - Alkanolamines for Hydrogen Sulfide and Carbon Dioxide Removal, in: Kohl, A.L., Nielsen, R.B. (Eds.), Gas Purification (Fifth Edition). Gulf Professional Publishing, Houston, pp. 40-186.

Léonard, G., Voice, A., Toye, D., Heyen, G., 2014. Influence of dissolved metals and oxidative degradation inhibitors on the oxidative and thermal degradation of monoethanolamine in postcombustion CO_2 capture. Industrial & Engineering Chemistry Research 53, 18121-18129.

Meuleman, E., Cottrell, A., Ghayur, A., 2016. Treatment of flue-gas impurities for liquid absorbent-based post-combustion CO_2 capture processes, Absorption-Based Post-Combustion Capture of Carbon Dioxide. Woodhead Publishing, pp. 519-551.

Minx, J.C., Lamb, W.F., Callaghan, M.W., Fuss, S., Hilaire, J., Creutzig, F., Amann, T., Beringer, T., de Oliveira Garcia, W., Hartmann, J., 2018. Negative emissions—Part 1: Research landscape and synthesis. Environmental Research Letters 13, 063001.

Monteiro, J., Stellwag, I., Mohana, M., Huizinga, A., Khakharia, P., van Os, P., Goetheer, E., 2018. De-Oxygenation as Countermeasure for the Reduction of Oxidative Degradation of CO_2 Capture Solvents, 14th Greenhouse Gas Control Technologies Conference Melbourne, pp. 21-26.

Moser, P., Wiechers, G., Schmidt, S., Garcia Moretz-Sohn Monteiro, J., Charalambous, C., Garcia, S., Sanchez Fernandez, E., 2020. Results of the 18-month test with MEA at the post-combustion capture pilot plant at Niederaussem – new impetus to solvent management, emissions and dynamic behaviour. International Journal of Greenhouse Gas Control 95, 102945.

Nielsen, P.T., Rochelle, G.T., 2017. Effects of Catalysts, Inhibitors, and Contaminants on Piperazine Oxidation. 114, 1919-1929.

NOAA, 2021. Trends in Atmospheric Carbon Dioxide. NOAA Global Monitoring Laboratory, Mauna Loa, Hawaii, USA.

Oh, H.-T., Ju, Y., Chung, K., Lee, C.-H., 2020. Techno-economic analysis of advanced stripper configurations for post-combustion CO_2 capture amine processes. Energy 206, 118164.

Reynolds, A.J., Verheyen, T.V., Meuleman, E., 2016. Degradation of amine-based solvents, in: Feron, P.H.M. (Ed.), Absorption-Based Post-combustion Capture of Carbon Dioxide. Woodhead Publishing, pp. 399-423.

Rochelle, G.T., 2016. Conventional amine scrubbing for CO2 capture. Elsevier Inc., pp. 35-67.

Rogelj, J., Shindell, D., Jiang, K., Fifita, S., Forster, P., Ginzburg, V., Handa, C., Kheshgi, H., Kobayashi, S., Kriegler, E., Mundaca, L., Séférian, R., Vilariño, M.V., 2018. Mitigation Pathways Compatible with 1.5°C in the Context of Sustainable Development. In: *Global Warming of 1.5°C. An IPCC Special Report on the impacts of global warming of 1.5°C above pre-industrial levels and related global greenhouse gas emission pathways, in the context of strengthening the global response to the threat of climate change, sustainable development, and efforts to eradicate poverty*. IPCC.

UNFCCC, 2015. Adoption of the Paris agreement. United Nations Framework on Climate Change, Paris.

Vega, F., Sanna, A., Navarrete, B., Maroto-Valer, M.M., Cortés, V.J., 2014. Degradation of amine-based solvents in CO2 capture process by chemical absorption. Greenhouse Gases: Science and Technology 4, 707-733.

Wanderley, R.R., Knuutila, H.K., 2020. Mapping Diluents for Water-Lean Solvents: A Parametric Study. Industrial & Engineering Chemistry Research 59, 11656-11680.

Wang, T., Hovland, J., Jens, K.J., 2015. Amine reclaiming technologies in post-combustion carbon dioxide capture. Journal of Environmental Sciences 27, 276-289.

Chapter 2

Literature review

In this chapter a brief summary of the status and knowledge within the field of amine degradation in CO_2 capture applications is given. Since most of the mechanistic studies, and degradation studies in general, have been performed on aqueous ethanolamine (MEA), an emphasis is put on MEA degradation, since much of the knowledge generated on MEA degradation also is applicable to other amines.

2.1 Amine degradation

MEA is no longer the most commonly used amine for CO_2 capture these days, as it has largely been replaced by more stable blends of among others AMP, MDEA and PZ. Much of the data represented in this chapter does, however, originate from MEA studies. All amines degrade to some extent, and MEA doing so more rapidly than most others, having made it easier to gather degradation data on that than many other amines. Other amines seem to follow similar pathways as MEA in terms of primarily forming small, typically acid, alkylamine, ammonia, and aldehyde compounds, and then secondary degradation compounds by further reaction of these, making MEA degradation data useful for studying amine degradation in general. Its fast degradation reactions make it possible to perform a lot of test in laboratory scale under different conditions in a short time. This possibly allows for the discovery of issues that might not be found until a long way into the operation time with other amines. All the experiments presented here are based on enhanced conditions, favouring a rapid breakdown of the amines, much faster than what would take place in an actual CO_2 capture plant.

Many further degradation compounds have been suggested and identified in degraded MEA, that are not represented in the following sections. These tend to occur in lower concentrations than the ones given here or are found for other amines. Many of these compounds are presented in Freeman (2011), Closmann (2011), da Silva et al. (2012), Vevelstad (2013), Voice (2013), Gouedard (2014), Reynolds et al. (2015), Vevelstad et al. (2016), Morken et al. (2017), Thompson et al. (2017), Wang and Jens (2012), and Nielsen (2018).

2.2 Pathways and products of oxidative degradation

formaldehyde   acetaldehyde   oxalaldehyde   methylamine

formic acid   acetic acid   glycolic acid   oxalic acid
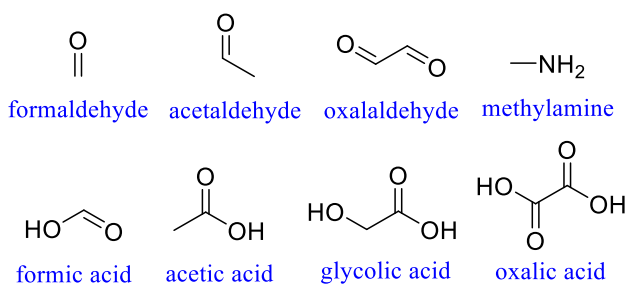
Figure 2.1: Chemical structure of typical primary oxidative degradation products of MEA.

Oxidative degradation takes place, when the amine comes in contact with oxidizing species, such as dissolved O_2, SO_X, or NO_X from the flue gas. Oxidation reactions take place after the amine solution absorbs oxidising species from the flue gas in the absorber column. The initiation step of oxidative degradation reaction is assumed to

take place via a radical mechanism, by either electron abstraction, hydrogen abstraction, or less commonly a reaction between water and aminium (Bedell et al., 2011; Hull et al., 1967; Rooney et al., 1998; Smith and Mann, 1969). The main products of these initial reactions are organic acids, mainly formic, acetic, glycolic, and oxalic acid as well as ammonia (NH_3), aldehydes, and methylamine (Figure 2.1), especially for MEA, but also many other amines (da Silva et al., 2012). The formation of these acids has proven to be catalysed by dissolved metals (Blachly and Ravner, 1963; Goff, 2005; Sexton and Rochelle, 2009). So far, no experimental studies have identified any of the radical intermediates, although many thorough and likely mechanistic predictions have been made.

Formation of all these acids releases ammonia from the organic molecule. The formation of methylamine was hypothesized to take place via a radical mechanism, simultaneously as the acid formation, first by Rooney et al. (1998) and then in a different mechanism by Lepaumier (2008), as show in Figure 2.2. Likely because of the difficulty in setting up mechanistic studies involving radicals, especially in complex mixtures such as CO_2 loaded amine solutions, the exact mechanisms of primary degradation product formation have not been confirmed.
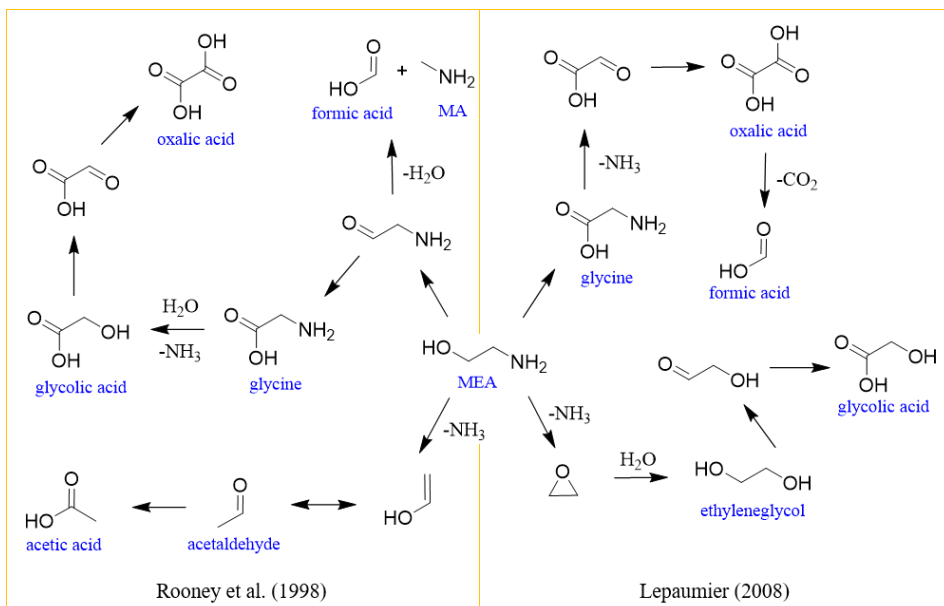
Figure 2.2: Proposed mechanisms of formation of some of the primary degradation products of MEA, by Rooney et al. (1998) and Lepaumier (2008).

Following the formation of the primary degradation compounds; many secondary degradation compounds have been identified. A selection of some of the abundantly studied secondary oxidative degradation compounds can be seen in Table 2.1. Many of these are amides, which may be formed in reactions between the amine and primary

degradation compounds, as shown in Figure 2.3 (da Silva et al., 2012; Lepaumier et al., 2011a; Strazisar et al., 2003). HEA has been shown to form in reaction between MEA and acetic acid, while HEF forms from MEA and formic, or also oxalic acid, (Supap et al., 2011). HHEA is a product from MEA and glycolic acid, while BHEOX is an indirect product formed by reaction of MEA with oxalic acid (Lepaumier et al., 2011a). HEOX is possibly an intermediate, that has only been tentatively identified (Gouedard, 2014; Vevelstad and Svendsen, 2016). HEOX has also been hypothesized to form by hydrolysis of BHEOX (Supap et al., 2011). HEHEAA is suggested to be formed in this manner with either HEA, HEGly or glyoxal, as depicted in Figure 2.4 (da Silva et al., 2012; Gouedard, 2014; Strazisar et al., 2003).

Table 2.1: Names, common abbreviations, CAS number and chemical structure of many of the commonly studied and identified secondary degradation products, mainly of MEA.

Name	Abbreviation	CAS	Structure
N,N'-bis(2-hydroxyethyl)-ethanediamide	BHEOX	1871-89-2	
N-(2-hydroxyethyl)-acetamide	HEA	142-26-7	
N-(2-hydroxyethyl)-formamide	HEF	693-06-1	
N-(2-hydroxyethyl)-glycine	HEGly	5835-28-9	
N-(2-hydroxyethyl)-2-[(2-hydroxyethyl)amino]-acetamide	HEHEAA	144236-39-5	
1H-imidazole-1-ethanol	HEI	1615-14-1	
2-((2-hydroxyethyl)amino)-2-oxoacetic acid	HEOX	5270-73-5	
4-(2-hydroxyethyl)-2-piperazinone	HEPO (4HEPO)	23936-04-1	
1-(2-hydroxyethyl)-2-piperazinone	1HEPO	59702-23-7	
2-hydroxy-N-(2-hydroxyethyl)-acetamide	HHEA	3586-25-2	

One of the big mysteries in oxidative degradation of MEA, is the formation of HEI, being such a dominant degradation product and yet not a direct product of any simple condensation reaction, also being one of few identified aromatic degradation compounds. Patents have suggested that reactions between MEA, glyoxal, formaldehyde and ammonia can produce HEI (Gouedard, 2014; Katsuura and Washio, 2005; Kawasaki et al., 1991), and Vevelstad et al. (2013) proposed a reaction mechanism based on this, shown in Figure 2.4. The fact that the same publication observed that increasing oxygen concentration gives increased HEI production suggests that the formation of HEI is favoured under highly oxidizing conditions, possibly through a radical mechanism.
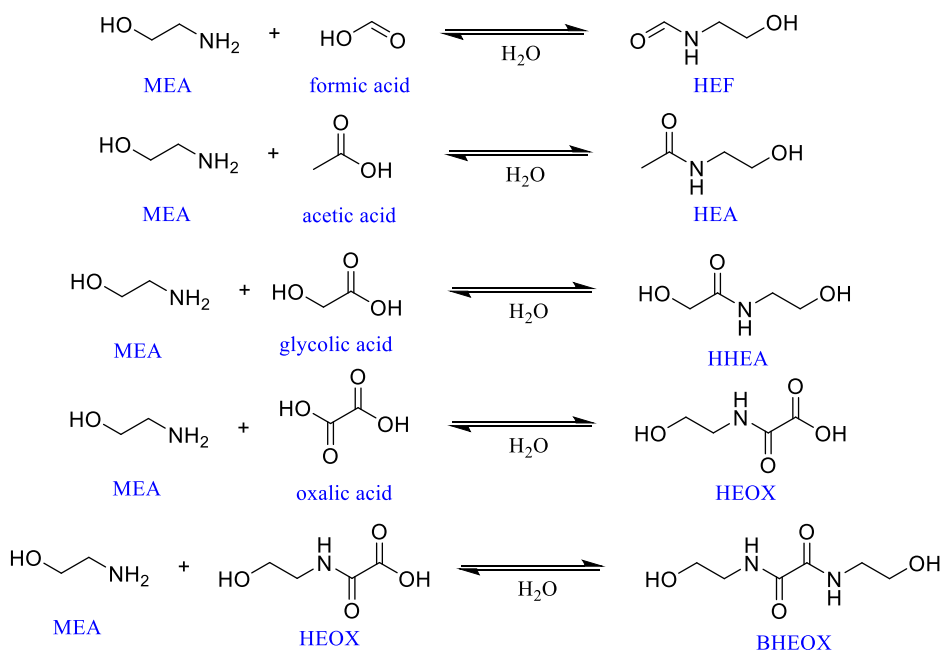
Figure 2.3: Proposed mechanisms of formation of HEF, HEA, HHEA, HEOX, and BHEOX according to da Silva et al. (2012), Lepaumier et al. (2011a), and Strazisar et al. (2003).
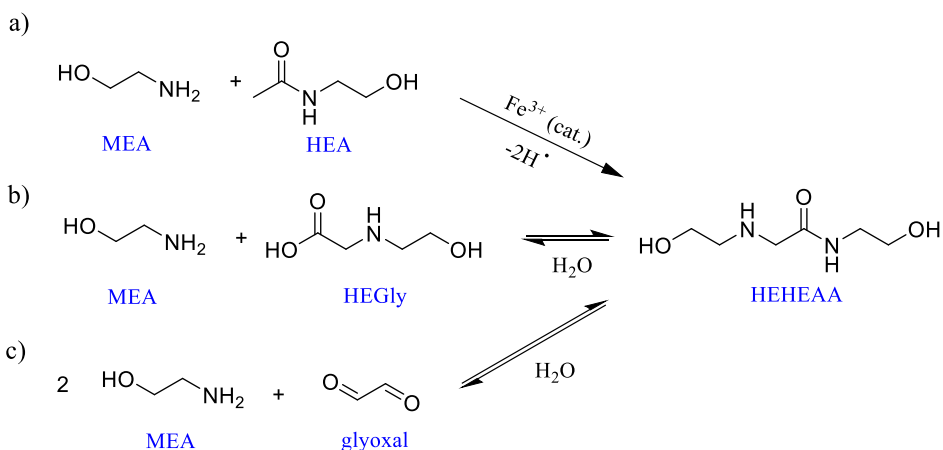
Figure 2.4: Reactions suggested to form HEHEAA, by a) a radical reaction between MEA and HEA, catalysed by ferric (Strazisar et al., 2003), or in condensation reactions between MEA and b) HEGly da Silva et al. (2012), or c) with glyoxal (Gouedard, 2014).
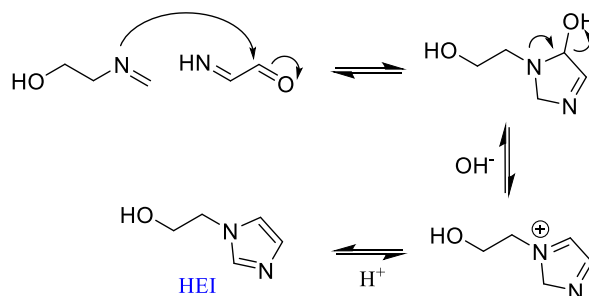
Figure 2.5: Mechanism proposed for the formation of HEI from 2-methyleneamino)ethanol and iminoacetaldehyde, by Vevelstad et al. (2013).

Another unknown is how the dominant degradation product HEGly is formed, which is also present in abundance in degraded MEA, but is not a known condensation product of any two compounds, when tested in laboratory scale. The only mechanisms proposed for HEGly formation were made by Vevelstad et al. (2014) as a condensation reaction between glyoxylic acid and MEA, under dissociation of a CO_2 molecule, as given in Figure 2.6, or from HEHEAA as suggested by Gouedard (2014).
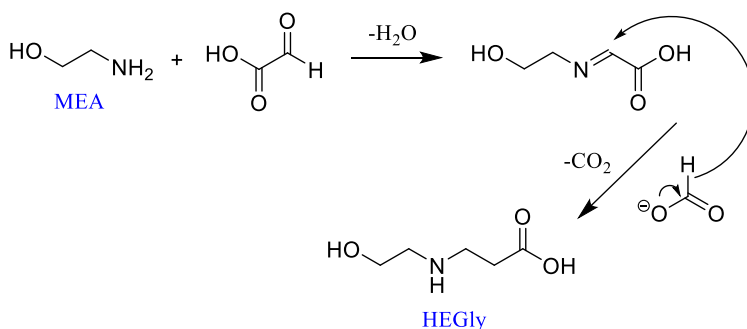
Figure 2.6: Formation mechanism of HEGly from MEA and glyoxylic acid, proposed by Vevelstad et al. (2014).

There also seems to be a disagreement between the ratios of oxidative degradation compounds formed on the pilot scale compared to in laboratory scale oxidative degradation studies. HEPO and HEGly are usually the dominant products observed in pilot scale MEA campaigns (da Silva et al., 2012; Morken et al., 2017), whereas in laboratory scale oxidative degradation experiments at simulates absorber conditions, HEF and HEI have been observed in the largest quantities (Vevelstad et al., 2013). A low concentration of O_2 has, however, proven to give rise to HEGly formation also in laboratory scale (Vevelstad et al., 2013). HEPO on the other hand, is hypothesized to require higher temperatures than given at absorber conditions, or in the studies of purely oxidative conditions, formed by thermal dehydration of HEHEAA, as shown in Figure 2.6. The same studies also saw and suggested an alternative, analogous mechanism for the formation of the less dominant 1HEPO species. Other mechanisms for the formation of HEPO and 1HEPO were also suggested by Gouedard (2014), which can be viewed in Figure 2.8.
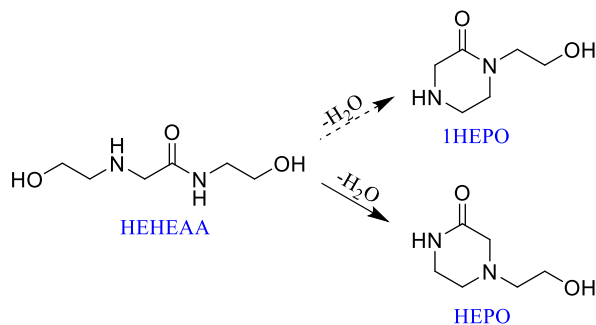
Figure 2.7: Proposed mechanisms of self-condensation of HEHEAA to form HEPO and 1HEPO according to da Silva et al. (2012) and Strazisar et al. (2003).

24
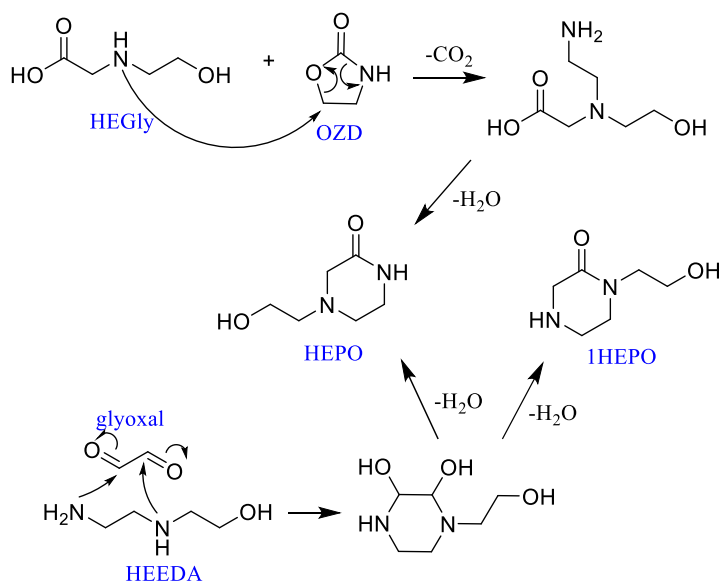
Figure 2.8: Suggested mechanisms for the formation of HEPO and 1HEPO by Gouedard (2014).

Many researchers have previously studied oxidative degradation of amine in laboratory scale, for nearly a century, a selection of which can be seen in Table 2.2. The first of these were comparing different amines and their stabilities, as well as looking for inhibitors and catalysts of degradation. In the past two-three decades a lot of studies have aimed to understand the fundamentals of these reactions on a more mechanistic level, at the same time as studying many different amines, and searching for inhibitors of degradation.

Table 2.2: Research contributions towards understanding oxidative amine degradation.

Group	Amines	Goals	Main findings	References
Standard Oil Company, USA	MEA, TEA, DIPA	Testing resistance of the amine solvents at 85 °C with constant O_2 sparging.	MEA was the most resistant amine towards oxidation, followed by TEA and DIPA.	Gregory and Scharmann (1937)
US Navy	MEA	Stabilising the *aq.* amine solvents used for CO_2 capture in submarines using inhibitors.	Fe and Cu catalyse degradation, while EDTA and Na salt of *N,N*-diethanolglycine act as peroxide scavengers, inhibiting oxidative degradation.	Blachly and Ravner (1963); Blachly and Ravner (1964, 1965, 1966)

Group	Amines	Goals	Main findings	References
Dow Chemical Company	MEA, DEA, MDEA	Study a series of *aq.*, CO_2 free, amines under oxidative conditions.	First proposed mechanism for formation of the primary degradation compounds formic, acetic, oxalic, and glycolic acid	Rooney et al. (1998)
Regina, SK, Canada	MEA	Study oxidative stability of MEA (*aq.*) in the absence of CO_2 in autoclave type reactors at temperatures 120-170 °C and high pressures.	Power-law rate model, able to predict oxidative degradation in their system.	Supap (1999) and Supap et al. (2001)
Regina, SK, Canada	MEA, MDEA and blends of the two	Study oxidative stability in varying concentration, with and without CO_2, $NaVO_3$, in autoclave type reactors at temperatures 55-120 °C and high pressures.	Conclusions about the influence of concentration of amine, O_2, CO_2, temperature, and corrosion inhibitor were made.	Bello and Idem (2006)
University of Texas	MEA	Study stability under typical absorber conditions, investigating the effect of iron and inhibitor concentrations on ammonia evolution	Presence of CO_2 makes a huge difference in the rate of degradation of MEA.	Chi and Rochelle (2002)
US DOE	MEA	Study formation of many of the postulated and identified oxidative degradation products of MEA (*aq.*) were studied in a sample from a CO_2 capture plant.	Many degradation mechanisms were proposed.	Strazisar et al. (2001) and Strazisar et al. (2003)
University of Texas	MEA	Oxidative stability of was tested under a range of varied process parameters: pH, CO_2 loading, and O_2/Fe/Cu /MEA concentrations, inhibitor presence.	Mass transfer of O_2 is the limiting factor for degradation rate of MEA.	Goff and Rochelle (2003), Goff and Rochelle (2004) and Goff (2005)
Université de Savoie/ IFP	12 different amines	Studying degradation of 4 mol kg^{-1} (*aq.*) amine solutions in a pressurised vessel of 2 MPa, with 0.42 MPa O_2, at high temperature (140 °C) in absence of CO_2.	Many oxidative degradation mechanisms were postulated in this work, based on results from GC, GC/MS, NMR, and IC.	Lepaumier et al. (2009b)

Group	Amines	Goals	Main findings	References
University of Texas	MEA, PZ, and MEA/PZ blends	Oxidative amine stability under non-mass transfer limited conditions. Degradation product formation monitored with and without presence of metals or inhibitors.	Studied the catalysts impact on the degradation rate.	Sexton (2008)
NTNU/ SINTEF	MMEA	Degradation at absorber conditions compared to degradation of MEA.	MMEA more unstable than MEA under all tested conditions. Many volatile compounds are formed during degradation of MMEA. Mechanisms were proposed.	Lepaumier et al. (2011b)
University of Texas	MDEA and PZ	Study stability of 7 m MDEA + 2 m PZ with an integrated solvent degradation apparatus (ISDA) for combined oxidative and thermal degradation studies.[1]	Oxidative degradation model made based on the results from the ISDA.	Closmann (2011)
University of Texas	PZ	Study rate of oxidation studied in presence of catalysts.	Fe^{2+}, Ni^{2+} and Cr^{3+} are only weak oxidation catalysts compared to Cu^{2+}.	Freeman (2011)
USN	AMP	Study oxidative degradation of AMP (aq.) in an autoclave type reactor at 100-140 °C.	Degradation rate was found to be mass transfer limited like in Goff and Rochelle (2004).	Wang and Jens (2012)
SINTEF/ NTNU	MEA	Comparison of laboratory scale and pilot scale degradation.	Significant overlap found between degradation products from pilot and laboratory scale. Oxidative degradation more dominant in pilot scale than thermal.	da Silva et al. (2012)

[1] $m = mol_{amine}\ kg^{-1}_{H2O}$.

Group	Amines	Goals	Main findings	References
University of Texas	Mainly MEA and PZ	Achieve a better understanding of the causes and solutions to amine oxidation	Suggested 4 m AMP + 2 m PZ, with a corrosion inhibitor or continuous metal removal as a capture solvent, with process modifications to reduce degradation issues.	Voice (2013)
USN	AMP/ PZ blends	Oxidative stability studied at temperatures between 80 and 140 °C	Degradation rate of PZ increases in blend with AMP, despite of the same compounds detected in the single amine solutions as in the blends.	Wang and Jens (2014)
NTNU	MEA, MMEA, DMMEA, AP, AB, Gly, and Sar	Study oxidative stability in a closed batch system with gas phase recycling.	Temperature and dissolved metals influence degradation and MEA degradation rate.	Vevelstad et al. (2014)
NTNU	MEA, MMEA, AP, AB, and MAPA	Identify the differences between the use of closed, and open batch systems.	Open setup generally gave higher amine losses, with some exceptions where the degradation rate was comparable under both conditions.	Vevelstad et al. (2014)
University of Texas	MEA	Study inhibitors for oxidative degradation of MEA (*aq*.).	Inhibitors that successfully worked under simulated absorber conditions were unsuccessful at hindering degradation under cyclic conditions.	Voice and Rochelle (2014)
SINTEF/ NTNU	MEA	Study oxidative stability of MEA (*aq*.) at different temperatures and pO_2 in an open-batch setup.	Monitored MEA loss and 17 different degradation compounds	Vevelstad et al. (2016)
NTNU	MEA	Studying the influence of degradation and corrosion inhibitors on the oxidative stability of MEA (*aq*.) in open batch reactors	No perfect inhibitor, suitable for both corrosion and degradation inhibition was identified, but inhibitors for each on its own were found.	Fytianos et al. (2016b)

Group	Amines	Goals	Main findings	References
University of Texas	PZ	Study oxidation rates and products in a bench-scale cyclic degradation apparatus. Compared to PZ oxidation from pilot-scale campaigns.	Created a model for degradation and solvent management costs in full-scale.	Nielsen (2018)
University of Texas	PZ	Amine stability was studied under oxidative conditions in an advanced flash stripper.	The stripper configuration seems to reduce PZ degradation.	Wu et al. (2018)
University of Regina	16 alkanol-amines	Study structural effects in amines on oxidative stability. Aqueous amine concentrations of 2 mol kg^{-1} (*aq*.), CO_2 free conditions and an open batch setup.	Results agree with those presented in chapter 6 of this thesis.	Muchan et al. (2021)

As can be understood from the rest of this section, oxidative degradation in very complex and not fully understood, despite of countless researchers giving it their best. To combat degradation in the CO_2 capture process it might, however not, be necessary to understand it to its full extent, so while we are trying to comprehend these mechanisms, we can also focus on solutions for avoiding it. This thesis aims to do just that, not directly contribute to the mechanistic understanding of degradation, but rather to means of avoiding oxidative degradation in the first place.

2.2.1 Oxygen solubility in amine solvents

Not surprisingly, and as seen in laboratory scale experiments, oxygen concentration has an impact on oxidative degradation. The higher the oxygen pressure is, the more oxidation products are observed and the higher the amine loss is (Bello and Idem, 2006; Supap et al., 2001; Vevelstad et al., 2016). The inherent solubility of oxygen gas into water is low, around 40 ppm at atmospheric pressure and room temperature in a 101.3 kPa O_2 atmosphere. CO_2 under the same conditions has a solubility of about 1500 ppm, significantly higher. In the post-combustion CO_2 capture plant, the oxygen concentrations will be much lower than 40 ppm, firstly, because of the lower O_2 pressure (3-16 kPa), secondly, due to the increased temperature, and thirdly because of the electrolytes contained in the solvent, all of which are factors that reduce gas solubility into liquids (Battino and Clever, 1966; Schumpe et al., 1978). The complex process conditions have, however, made it difficult to exactly estimate how low the inherent solubility of the amine solvent is.
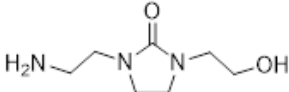
Every solvent has different inherent gas solubility properties (Battino and Clever, 1966), so this is expected also of aqueous amine solvents. A first approach to

understanding the solubility of oxygen in amine solvents was made by Rooney and Daniels (1998), who looked at aqueous solutions of MEA, MDEA, and DGA, at different temperatures, using atmospheric oxygen pressure (21%). They used a commercially available dissolved oxygen (DO) sensor, made for water testing, and determined that the solubility of aqueous amines is comparable to that of water. Later, Wang et al. (2013) studied oxygen solubility in aqueous MEA, with and without CO_2 loading, also using a DO sensor. This study also verified the sensor for use in 30 wt% MEA (*aq.*) without CO_2 loading, by developing an indirect Winkler titration method that deviated 0-11% from the oxygen concentrations measured by the DO sensor. This study observed that the combination of high CO_2 loadings and high temperature (>40 °C) caused the measured oxygen concentrations to drastically drop. No studies looking at oxygen solubility in pure, or diluted amine solvents than those mentioned here have been found. The direct effect of the ionic compounds formed by CO_2 absorption on oxygen solubility has also not been studied in the past.

2.3 Pathways and products of thermal degradation

Thermal degradation has been shown to dominate less in pilot-scale CO_2 capture processes, where typical thermal degradation products that are produced in the lab usually occur only in low concentrations compared to products of oxidative degradation (da Silva et al., 2012; Lepaumier et al., 2011a). Despite of the concentrations being very much lower in pilot than in lab scale, the same compounds seem to be produced in both settings. The most prominent thermal degradation products from MEA, both in laboratory and pilot scale, are HEEDA, HEIA, and OZD (Table 2.3), with HEIA being the most dominant (Davis and Rochelle, 2009; Lepaumier et al., 2011a; Lepaumier et al., 2009a). MEA urea is also expected to be a prominent thermal degradation product on pilot scale, but there is little quantitative data available to evaluate how important it can be (Davis and Rochelle, 2009; Huang et al., 2014). The thermal amine degradation is a result of both a high CO_2 loading and the high temperature in the desorber column and reboiler (Davis and Rochelle, 2009; Lepaumier et al., 2009a). Un-loaded, the reaction pathways are mainly dealkylation, dimerization and cyclisation (Gouedard et al., 2012), reacting from MEA carbamate, however, carbamate polymerization can take place (Lepaumier et al., 2009a).

Table 2.3: Names, common abbreviations, CAS number and chemical structure of many of the commonly studied and identified thermal degradation products, mainly of MEA.

Name	Abbreviation	CAS	Structure
N-(2-aminoethyl)-*N'*-(2-hydroxyethyl)-imidazolidinone	AEHEIA	1402137-23-8	

Name	Abbreviation	CAS	Structure
Diethanolamine	DEA[2]	111-42-2	
2-[(2-aminoethyl) amino]-ethanol	HEEDA[3]	111-41-1	
1-(2-hydroxyethyl)-2-imidazolidinone	HEIA	3699-54-5	
N-(hydroxyethyl) diethylenetriamine	MEA trimer	1965-29-3	
N,*N*'-bis(2-hydroxyethyl) -urea	MEA urea	15438-70-7	
2-oxazolidinone	OZD[4]	497-25-6	
N-[2-[(2-hydroxyethyl) amino]ethyl] imidazolidin-2-one	TriHEIA[5]	1154942-78-5	

OZD is an intermediate product, formed though the cyclisation reaction depicted in Figure 2.9. It should, however, be noted that OZD formation is sensitive to O_2 concentration in laboratory scale oxidative degradation experiment, so the possibility of an oxidative mechanism at lower temperatures should not be excluded (Vevelstad et al., 2013). OZD is reactive and will continue to react, forming i.e. HEEDA, as shown in Figure 2.10. HEIA is energetically favoured compared to HEEDA, and can be formed by HEEDA reacting further in a condensation reaction (Parks et al., 2020). Alternatively, if HEEDA reacts with another OZD molecule, the MEA trimer can be formed (Lepaumier et al., 2009a).
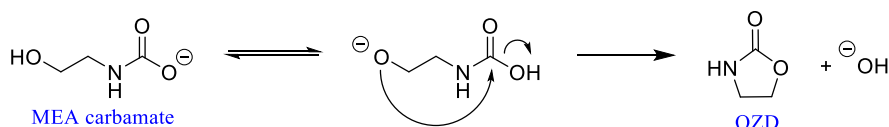
MEA carbamate   OZD

Figure 2.9: The mechanism of OZD formation by MEA carbamate cyclisation. Adapted from Lepaumier et al. (2009a), Davis and Rochelle (2009) and Gouedard et al. (2012).

[2] Has also been proposed to form though reaction between MEA and NO_X (Fostås et al., 2011).
[3] Also sometimes called AEEA
[4] OZD may also be a product of oxidative, lower temperature, degradation.
[5] Also sometimes called HEAEIA
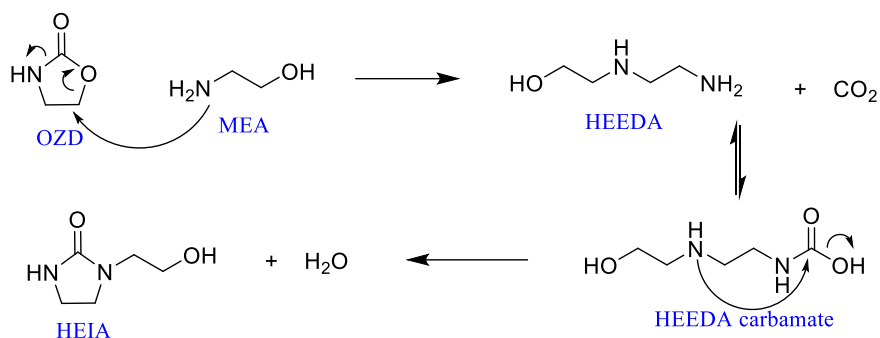
Figure 2.10: OZD is likely to react with a further MEA molecule to form the dimer HEEDA and then HEIA at elevated temperatures (Davis and Rochelle, 2009; Lepaumier et al., 2009a; Parks et al., 2020).

MEA urea formation is suggested to take place by MEA attacking either a MEA carbamate in another condensation reaction, or by nucleophilic substitution on OZD, both shown in Figure 2.11.
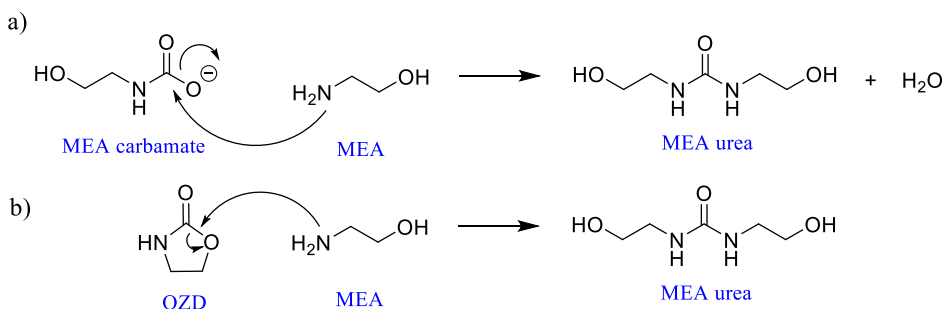
Figure 2.11: Suggested formation mechanism of MEA urea, a) adapted from Davis and Rochelle (2009), and b) from Davis (2009).

The formation of AEHEIA, which was identified as one of the four primary thermal degradation compounds of MEA by Eide-Haugmo et al. (2011a), likely takes place in an intramolecular condensation reaction of the MEA trimer, according to Figure 2.12 (Lepaumier et al., 2009a). This reaction alternatively takes place in the analogous mechanism with the carbamate on the primary amine function, forming TriHEIA, with the same molecular weights as AEHEIA, as reported by Davis (2009).
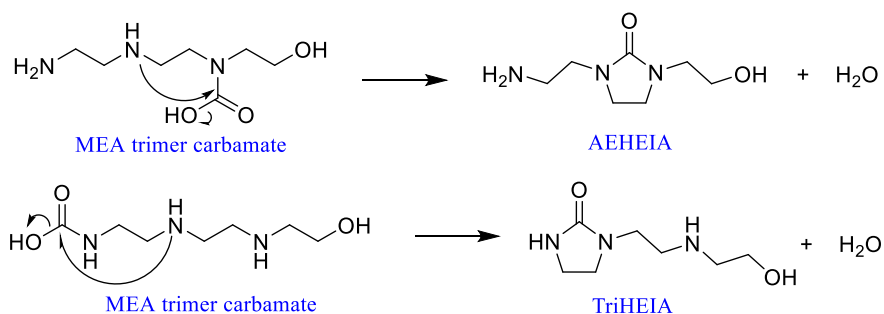
Figure 2.12: Suggested mechanism of formation of the imidazolidinones AEHEIA, by Lepaumier et al. (2009a) and TriHEIA by (Davis, 2009).

Formation of DEA from MEA is hypothesized to take place via the epoxide oxirane (Talzi, 2004), or from HEIA, through the dissociation of first NH_3, then CO_2 (Talzi and Ignashin, 2002). The polymerization reactions taking place during thermal degradation do not necessarily stop at dimers and trimers, such as those represented in Table 2.3, but also form larger amine polymers, many of which have been identified and suggested based on their molecular masses (Davis and Rochelle, 2009; Davis, 2009; Eide-Haugmo et al., 2011a; Eide-Haugmo et al., 2011b; Lepaumier, 2008; Lepaumier et al., 2009a).

2.4 Nitramine and nitrosamine formation
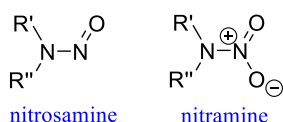
Figure 2.13: General structure of nitrosamines and nitramines, R' and R'' representing arbitrary groups.

The last group of degradation compounds which are commonly monitored in pilot and lab scale oxidative degradation of amines are nitrosamines and nitramines, which are compounds that follow the general structures given in Figure 2.13. A selection of commonly identified nitrosamines in the CO_2 capture plant can be viewed in Table 2.4. These compounds are not found in particularly high concentrations neither in the gas nor in the liquid phase, but their toxicity gives their monitoring high importance. Nitrogen dioxide (NO_2) is prone to undergo nitrosamine formation and nitration reactions with secondary amines. Since secondary amines can be formed though degradation reactions nitrosamines can, therefore, also be formed from primary, tertiary, and even quaternary amines (Fine, 2015; Gouedard et al., 2012). The first time nitrosamines were reported to be found in the context of amine scrubbing was by Strazisar et al. (2003), since then it has been regularly monitored during CO_2 capture plant operation. Nitrosamines are found in approximately one order of

magnitude higher concentrations than nitramines in the CO_2 capture plants where they are measured (Dai and Mitch, 2014; Dai et al., 2012).

Table 2.4: Names, common abbreviations, CAS number and chemical structure of some nitramines and nitrosamines formed by amine degradation.

Name	Abbreviation	CAS	Structure
2-(nitroamino)-ethanol	MEA-NO$_2$	74386-82-6	
N-nitrosodiethanolamine	NDELA	1116-54-7	
N-nitrosodimethylamine	NDMA	62-75-9	
nitroso-(2-hydroxyethyl) glycine	No-HEGly	80556-89-4	

Nitrosamines are highly carcinogenic to humans even at very low concentrations (Fine, 2015; Garcia et al., 1970; Inami et al., 2009) , whereas nitramines are about one order of magnitude less mutagenic (Wagner et al., 2014). On a positive note, nitrosamines are known to degrade rapidly when irradiated with UV-light, such as for example sunlight, reducing the environmental impact of potential nitrosamine emissions (de Koeijer et al., 2013). Nitramines are more stable to photooxidative conditions and are therefore more likely to persist in the environment (Nielsen et al., 2012; Pitts Jr et al., 1978). The main ways of avoiding nitrosamine and nitramine formation in the CO_2 capture plant, is by choosing amines that have low volatility, not employing secondary amines for CO_2 capture, to remove NO_X from the flue gas prior to contact with the amine solvent, or employing a water wash section to capture the degradation products from the cleaned flue gas (Dai and Mitch, 2013, 2014, 2015).

2.5 Degradation inhibitors

Oftentimes an amine solvent or solvent blend contains additives to suppress negative properties like degradation, corrosivity or an inclination to foam. Degradation and corrosion inhibitors can typically be categorised into three overarching types. Either they are *scavengers for removing oxygen or radicals* from the solution, such as quinone, sodium sulphite (Na_2SO_3) or formaldehyde. These react stoichiometrically with dissolved oxygen in the solution and require regular replenishment. Another category is that of *chelating agents* for binding dissolved metal ions and preventing them from catalysing the degradation reactions. Typical chelating agents are ethylenediamine tetra acetic acid (EDTA), sodium phosphate (Na_3PO_4) or sodium

tetra sulphate (Na_2S_4). This category of inhibitors will also require replenishment and possible removal of spent inhibitor species. The last group of degradation inhibitors are *stable inorganic salts,* for which, at least partly, the work mechanism is assumed to be reducing the solubility of oxygen in the solution. (Goff and Rochelle, 2006; Léonard et al., 2014) There are, however, exceptions to this generalisation and as Goff and Rochelle (2006) already have described, namely *reaction inhibitors*. These will influence the degradation mechanism in a way that makes it less favourable, as they describe that their "Inhibitor A" does. A reaction inhibitor for oxidation reaction is iodide (I^-),, according to Altshuller et al. (1959) and Sjostrom et al. (2020), which reversibly forms triiodide (I_3^-) in contact with oxidising agents. I_3^- can easily be reduced back to I^- in the reaction mixture, and then be reused to inhibit further degradation reactions. This is the inhibition mechanism we assume is taking place in the KI salted amine solvent (SAS) presented in Chapter 7. Corrosion inhibitors can also often be oxidation passivators, which promote a film formation on the metal surface, that often consist of heavy metal salts (Fytianos et al., 2016a; Kittel and Gonzalez, 2014; Kohl and Nielsen, 1997).

Ideally, one would find a solvent that works well on its own, without need for additives, as it seems that inhibitors often have a negative side effect that defeat the positive, i.e. that degradation inhibitors can cause foaming (Chen et al., 2011; Thitakamol and Veawab, 2008), that a corrosion inhibitor may increase the degradation rate (Idem et al., 2006), or a degradation inhibitor can increase the corrosivity of the solvent (Palencsár et al., 2019). It has also been seen that an inhibitor can work perfectly for its purpose under one set of conditions, like oxidative, and then fail to do so under a combination of conditions, like cyclic, repeated, absorption and desorption under temperature swing conditions (Nielsen, 2018; Voice and Rochelle, 2014).

2.6   Environmental impact and biodegradation

The study of environmental fate of amines has many aspects. It includes biodegradation and ecotoxicity, which need to be under the limits set by local governance, and it includes the knowledge of the pathways and impacts the compounds themselves, and their degradation products may take in air, water, soil, plants, and animals. Because of this topic's immense complexity, it is usually studied in smaller parts, in studies focusing on one, or some aspects of this in turn.

Among the first targeted biodegradation studies of amines is that of Emtiazi and Knapp (1994), where, among other, MEA, PZ, DGA, DEA, and HEEDA were studied in die-away experiments in soil or sludges. They concluded that all the studied amines were biodegradable, but PZ the least of them. One of the most thorough works performed in regard to the faith of amine compounds in the environment, was done by Eide-Haugmo et al. (2012). They studied the seawater biodegradability and marine

ecotoxicity of 43 amines used, or considered used for CO_2 capture, using internationally acclaimed and standardized tests. They found that 38 of these had low acute toxicity and that more than half of the studied amines were sufficiently biodegradable to be used, according to OECD guideline 306 (OECD, 1992). Henry et al. (2017) performed similar tests in fresh water, where it appears that the amines are slightly more degradable here, than in seawater. Brakstad et al. (2012) additionally screened and studied the biodegradation kinetics of 20 alkanolamines, finding that generally, primary, and secondary alkanolamines are mostly readily biodegradable, tertiary less so, and sterically hindered amines are the least biodegradable. More studies have been performed on single amines, especially on MEA, to determine its biodegradation pathways under aerobic, and anaerobic conditions, in water and soils. these have mostly concluded that MEA is readily degradable (Kim et al., 2010; Mrklas et al., 2004; Ndegwa et al., 2004; Wong et al., 2004).

Gjernes et al. (2013) performed an investigation of the area surrounding a CO_2 capture plant, analysing for amines and degradation compounds in the air, soil, moss, and fresh water nearby, assessing the fate of emissions from the Technology Centre Mongstad (TCM) CO_2 capture plant in the environment. When talking about environmental fate of emissions, nitrosamines is also an important matter that always has to be considered. Due to their fast photoinduced degradation in contact with sunlight, these are, however, more an immediate concern, due to their high carcinogenicity, than a prolonged environmental faith issue (Brakstad et al., 2018; de Koeijer et al., 2013; Fine, 2015). They may however persist if in sufficiently high concentrations and if accumulated in water, in depths where sunlight does not penetrate and should not be ignored (Sørensen et al., 2015). Nitramines are, as mentioned before, more persistent in the environment and more resistant to photooxidation.

That all being said, degradation in general, is also an environmental issue. If one is able to increase overall solvent stability, this will lead to a lower consumption (and need for production) of amine solvent, reduce corrosion, associated operational issues, and save energy in the process, because the capacity of the solvent would not decrease. Reducing the formation of volatile degradation products will also, naturally, reduce the emissions and the need for identifying and assessing the safety of degradation products in the environment.

2.7   Concluding remarks about amine degradation

There have been done a lot of studies to try and fully understand the degradation mechanisms of amines used for CO_2 capture, and this understanding already goes a long way. Many of the mechanisms suggested in literature seem very sensible, although some are missing mechanistic studies to clarify the exact pathways taking

place. To fully comprehend the pathways of the degradation reactions, mechanistic studies would be necessary, but under the conditions and in the complex matrix we find in the CO_2 capture plant these would be hard to perform. Among the largest unknowns are the initiation reactions, that most likely are of radical character. Being able to elucidate these exact pathways would be a very interesting addition to the current knowledge base on amine degradation. A complete understanding of reaction mechanisms may, however, not be the highest priority on the road to achieving more stable amine solvents, as this is tedious work that requires powerful experimental and analytical techniques. Having a fast way of assessing the stability of a potential amine could help make picking novel solvents much easier and add more value to the solvent development field than mechanistic studies. For example, understanding how structural features influence the amine stability under different conditions in a more overarching way can help identify suitable or non-suitable solvents for CO_2 capture, in terms of degradability, more rapidly.

Factors that influence degradation of amines have been thoroughly studied, but some of them are lacking the analytical methods to fully quantify them. This includes measurement techniques for oxygen solubility in amine solutions. No analytical method has so far been validated for amine solutions, although techniques for the removal of oxygen are in development. Development and validation of a technique would aid the understanding on oxygen solubility's impact on oxidative degradation and also be valuable in the dissolved oxygen removal techniques. Something else that's missing, is the understanding of metal solubility in the fresh and dissolved amine solutions. It is often speculated, with good reason, that metals, especially iron become more soluble when the solvent degrades. There is, however, no direct technique to determine this. We know that the presence of metals in the solution play an important role in degradation, but it would also be very interesting to see what role degradation plays on metal solubility. Some degradation compounds are more likely to form complexes with the metal ions, like i.e. oxalic, acetic, or glycolic acid, which have the potential of acting as multidentate ligands.

Because of its complexity, the aspects of amines' environmental faith have been studied independently; biodegradability, ecotoxicity, and environmental pathways. It is of high difficulty to simulate the eventuality of the amine leaking into the environment though emissions or spills, and then recovering it and its degradation products for a holistic understanding. This may be what's missing though.

2.8   References

Altshuller, A.P., Schwab, C.M., Bare, M., 1959. Reactivity of Oxidizing Agents with Potassium Iodide Reagent. Analytical Chemistry 31, 1987-1990.

Battino, R., Clever, H.L., 1966. The solubility of gases in liquids. Chemical Reviews 66, 395-463.

Bedell, S.A., Worley, C.M., Darst, K., Simmons, K., 2011. Thermal and oxidative disproportionation in amine degradation—O2 stoichiometry and mechanistic implications. International Journal of Greenhouse Gas Control 5, 401-404.

Bello, A., Idem, R.O., 2006. Comprehensive study of the kinetics of the oxidative degradation of CO2 loaded and concentrated aqueous monoethanolamine (MEA) with and without sodium metavanadate during CO2 absorption from flue gases. Industrial and Engineering Chemistry Research 45, 2569-2579.

Blachly, C., Ravner, H., 1963. The effect of trace amounts of copper on the stability of monoethanolamine scrubber solutions. Naval Research Lab Washington DC.

Blachly, C.H., Ravner, H., 1964. The stabilization of monoethanolamine solutions for submarine carbon dioxide scrubbers. Naval Research Lab Washington DC, Washington DC.

Blachly, C.H., Ravner, H., 1965. Studies of submarine carbon dioxide scrubber operation: effect of an additive package for the stabilization of monoethanolamine solutions. Naval Research Lab Washington DC.

Blachly, C.H., Ravner, H., 1966. Stabilization of Monoethanolamine Solutions in Carbon Dioxide Scrubbers. Journal of Chemical and Engineering Data 11, 401-403.

Brakstad, O.G., Booth, A., Eide-Haugmo, I., Skjaeran, J.A., Sorheim, K.R., Bonaunet, K., Vang, S.H., da Silva, E.F., 2012. Seawater biodegradation of alkanolamines used for CO2-capture from natural gas. International Journal of Greenhouse Gas Control 10, 271-277.

Brakstad, O.G., Sorensen, L., Zahlsen, K., Bonaunet, K., Hyldbakk, A., Booth, A.M., 2018. Biotransformation in water and soil of nitrosamines and nitramines potentially generated from amine-based CO2 capture technology. International Journal of Greenhouse Gas Control 70, 157-163.

Chen, X., Freeman, S.A., Rochelle, G.T., 2011. Foaming of aqueous piperazine and monoethanolamine for CO2 capture. International Journal of Greenhouse Gas Control 5, 381-386.

Chi, S., Rochelle, G.T., 2002. Oxidative Degradation of Monoethanolamine. Industrial & Engineering Chemistry Research 41, 4178-4186.

Closmann, F.B., 2011. Oxidation and thermal degradation of methyldithanolamine/piperazine in CO_2 capture.

da Silva, E.F., Lepaumier, H., Grimstvedt, A., Vevelstad, S.J., Einbu, A., Vernstad, K., Svendsen, H.F., Zahlsen, K., 2012. Understanding 2-ethanolamine degradation in postcombustion CO_2 capture. Industrial & Engineering Chemistry Research 51, 13329-13338.

Dai, N., Mitch, W.A., 2013. Influence of amine structural characteristics on N-nitrosamine formation potential relevant to postcombustion CO_2 capture systems. Environmental science & technology 47, 13175-13183.

Dai, N., Mitch, W.A., 2014. Effects of flue gas compositions on nitrosamine and nitramine formation in postcombustion CO_2 capture systems. Environmental science & technology 48, 7519-7526.

Dai, N., Mitch, W.A., 2015. Controlling nitrosamines, nitramines, and amines in amine-based CO_2 capture systems with continuous ultraviolet and ozone treatment of washwater. Environmental science & technology 49, 8878-8886.

Dai, N., Shah, A.D., Hu, L., Plewa, M.J., McKague, B., Mitch, W.A., 2012. Measurement of nitrosamine and nitramine formation from NOx reactions with amines during amine-based carbon dioxide capture for postcombustion carbon sequestration. Environmental science & technology 46, 9793-9801.

Davis, J., Rochelle, G., 2009. Thermal degradation of monoethanolamine at stripper conditions, Energy Procedia, pp. 327-333.

Davis, J.D., 2009. Thermal degradation of aqueous amines used for carbon dioxide capture.

de Koeijer, G., Talstad, V.R., Nepstad, S., Tønnessen, D., Falk-Pedersen, O., Maree, Y., Nielsen, C., 2013. Health risk analysis for emissions to air from CO_2 Technology Centre Mongstad. International Journal of Greenhouse Gas Control 18, 200-207.

Eide-Haugmo, I., Brakstad, O.G., Hoff, K.A., da Silva, E.F., Svendsen, H.F., 2012. Marine biodegradability and ecotoxicity of solvents for CO_2-capture of natural gas. International Journal of Greenhouse Gas Control 9, 184-192.

Eide-Haugmo, I., Lepaumier, H., da Silva, E.F., Einbu, A., Vernstad, K., Svendsen, H.F., 2011a. A study of thermal degradation of different amines and their resulting degradation products, 1st Post Combustion Capture Conference, pp. 17-19.

Eide-Haugmo, I., Lepaumier, H., Einbu, A., Vernstad, K., Da Silva, E.F., Svendsen, H.F., 2011b. Chemical stability and biodegradability of new solvents for CO_2 Capture. Energy Procedia 4, 1631-1636.

Emtiazi, G., Knapp, J.S., 1994. The biodegradation of piperazine and structurally-related linear and cyclic amines. Biodegradation 5, 83-92.

Fine, N.A., 2015. Nitrosamine management in aqueous amines for post-combustion carbon capture.

Fostås, B., Gangstad, A., Nenseter, B., Pedersen, S., Sjøvoll, M., Sørensen, A.L., 2011. Effects of NOx in the flue gas degradation of MEA. Energy Procedia 4, 1566-1573.

Freeman, S.A., 2011. Thermal degradation and oxidation of aqueous piperazine for carbon dioxide capture.

Fytianos, G., Ucar, S., Grimstvedt, A., Hyldbakk, A., Svendsen, H.F., Knuutila, H.K., 2016a. Corrosion and degradation in MEA based post-combustion CO_2 capture. International Journal of Greenhouse Gas Control 46, 48-56.

Fytianos, G., Vevelstad, S.J., Knuutila, H.K., 2016b. Degradation and corrosion inhibitors for MEA-based CO_2 capture plants. International Journal of Greenhouse Gas Control 50, 240-247.

Garcia, H., Keefer, L., Lijinsky, W., Wenyon, C.E., 1970. Carcinogenicity of nitrosothiomorpholine and 1-nitrosopiperazine in rats. Zeitschrift für Krebsforschung 74, 179-184.

Gjernes, E., Helgesen, L.I., Maree, Y., 2013. Health and environmental impact of amine based post combustion CO_2 capture. Energy Procedia 37, 735-742.

Goff, G.S., 2005. Oxidative Degradation of Aqueous Monoethanolamine in CO_2 Capture Processes: Iron and Copper Catalysis, Inhibition, and O2 Mass Transfer.

Goff, G.S., Rochelle, G.T., 2003. Oxidative degradation of aqueous monoethanolamine in CO2 capture systems under absorber conditions, Greenhouse Gas Control Technologies-6th International Conference. Elsevier, pp. 115-120.

Goff, G.S., Rochelle, G.T., 2004. Monoethanolamine degradation: O2 mass transfer effects under CO2
 capture conditions. Industrial & Engineering Chemistry Research 43, 6400-6408.

Goff, G.S., Rochelle, G.T., 2006. Oxidation inhibitors for copper and iron catalyzed degradation of monoethanolamine in CO2 capture processes. Industrial & engineering chemistry research 45, 2513-2521.

Gouedard, C., 2014. Novel degradation products of ethanolamine (MEA) in CO2 capture conditions: identification, mechanisms proposal and transposition to other amines. Université Pierre et Marie Curie-Paris VI.

Gouedard, C., Picq, D., Launay, F., Carrette, P.L., 2012. Amine degradation in CO2 capture. I. A review. International Journal of Greenhouse Gas Control 10, 244-270.

Gregory, L., Scharmann, W., 1937. Carbon dioxide scrubbing by amine solutions. Industrial & Engineering Chemistry 29, 514-519.

Henry, I.A., Kowarz, V., Østgaard, K., 2017. Aerobic and anoxic biodegradability of amines applied in CO2-capture. International Journal of Greenhouse Gas Control 58, 266-275.

Huang, Q., Thompson, J., Bhatnagar, S., Chandan, P., Remias, J.E., Selegue, J.P., Liu, K., 2014. Impact of Flue Gas Contaminants on Monoethanolamine Thermal Degradation. Industrial & Engineering Chemistry Research 53, 553-563.

Hull, L., Davis, G., Rosenblatt, D., Williams, H., Weglein, R., 1967. Oxidations of amines. III. Duality of mechanism in the reaction of amines with chlorine dioxide. Journal of the American Chemical Society 89, 1163-1170.

Idem, R., Wilson, M., Tontiwachwuthikul, P., Chakma, A., Veawab, A., Aroonwilas, A., Gelowitz, D., 2006. Pilot Plant Studies of the CO2 Capture Performance of Aqueous MEA and Mixed MEA/MDEA Solvents at the University of Regina CO2 Capture Technology Development Plant and the Boundary Dam CO2 Capture Demonstration Plant. Industrial & Engineering Chemistry Research 45, 2414-2420.

Inami, K., Ishikawa, S., Mochizuki, M., 2009. Activation mechanism of N-nitrosodialkylamines as environmental mutagens and its application to antitumor research. Genes and Environment 31, 97-104.

Katsuura, A., Washio, N., 2005. Preparation of imidazoles from imines and iminoacetaldehydes. JP2005200305A, Japan.

Kawasaki, N., Noguchi, Y., Aoki, H., Fujii, K., 1991. Preparation of 1-substituted imidazoles. JP Patent 03,169,865.

Kim, D.-J., Lim, Y., Cho, D., Rhee, I.H., 2010. Biodegradation of monoethanolamine in aerobic and anoxic conditions. Korean Journal of Chemical Engineering 27, 1521-1526.

Kittel, J., Gonzalez, S., 2014. Corrosion in CO2 post-combustion capture with Alkanolamines–A review. Oil & Gas Science and Technology–Revue d'IFP Energies nouvelles 69, 915-929.

Kohl, A.L., Nielsen, R.B., 1997. Chapter 3 - Mechanical Design and Operation of Alkanolamine Plants, in: Kohl, A.L., Nielsen, R.B. (Eds.), Gas Purification (Fifth Edition). Gulf Professional Publishing, Houston, pp. 187-227.

Léonard, G., Voice, A., Toye, D., Heyen, G., 2014. Influence of dissolved metals and oxidative degradation inhibitors on the oxidative and thermal degradation of monoethanolamine in postcombustion CO2 capture. Industrial & Engineering Chemistry Research 53, 18121-18129.

Lepaumier, H., 2008. Etude des mécanismes de dégradation des amines utilisées pour le captage du CO2 dans les fumées. Chambéry.

Lepaumier, H., da Silva, E.F., Einbu, A., Grimstvedt, A., Knudsen, J.N., Zahlsen, K., Svendsen, H.F., 2011a. Comparison of MEA degradation in pilot-scale with lab-scale experiments. Energy Procedia 4, 1652-1659.

Lepaumier, H., Grimstvedt, A., Vernstad, K., Zahlsen, K., Svendsen, H.F., 2011b. Degradation of MMEA at absorber and stripper conditions. Chemical engineering science 66, 3491-3498.

Lepaumier, H., Picq, D., Carrette, P.L., 2009a. New amines for CO2 Capture. I. Mechanisms of amine degradation in the presence of CO2. Industrial and Engineering Chemistry Research 48, 9061-9067.

Lepaumier, H., Picq, D., Carrette, P.L., 2009b. New amines for CO2 Capture. II. Oxidative degradation mechanisms. Industrial and Engineering Chemistry Research 48, 9068-9075.

Morken, A.K., Pedersen, S., Kleppe, E.R., Wisthaler, A., Vernstad, K., Ullestad, Ø., Flø, N.E., Faramarzi, L., Hamborg, E.S., 2017. Degradation and Emission Results of Amine Plant Operations from MEA Testing at the CO2 Technology Centre Mongstad. Energy Procedia 114, 1245-1262.

Mrklas, O., Chu, A., Lunn, S., Bentley, L.R., 2004. Biodegradation of monoethanolamine, ethylene glycol and triethylene glycol in laboratory bioreactors. Water, air, and soil pollution 159, 249-263.

Muchan, P., Supap, T., Narku-Tetteh, J., Idem, R., 2021. Assessment of the Relationship between Degradation and Emission Activities of Carbon Capture Amines Based on their Chemical Structures, 15th Greenhouse Gas Control Technologies Conference.

Ndegwa, A.W., Wong, R.C., Chu, A., Bentley, L.R., Lunn, S.R., 2004. Degradation of monoethanolamine in soil. Journal of Environmental Engineering and Science 3, 137-145.

Nielsen, C.J., Herrmann, H., Weller, C., 2012. Atmospheric chemistry and environmental impact of the use of amines in carbon capture and storage (CCS). Chemical Society Reviews 41, 6684-6704.

Nielsen, P.T., 2018. Oxidation of Piperazine in Post-Combustion Carbon Capture Austin, TX.

OECD, 1992. Test No. 306: Biodegradability in Seawater.

Palencsár, A., Nyborg, R., Enaasen Flø, N., Iversen, F., Deleneuville, B., Bonis, M., Gregoire, V., 2019. Investigation of Corrosion-related Failure of Reboiler at Technology Centre Mongstad.

Parks, C., Alborzi, E., Akram, M., Pourkashanian, M., 2020. DFT Studies on Thermal and Oxidative Degradation of Monoethanolamine. Industrial & Engineering Chemistry Research 59, 15214-15225.

Pitts Jr, J.N., Grosjean, D., Van Cauwenberghe, K., Schmid, J.P., Fitz, D.R., 1978. Photooxidation of aliphatic amines under simulated atmospheric conditions:

formation of nitrosamines, nitramines, amides, and photochemical oxidant. Environmental Science & Technology 12, 946-953.

Reynolds, A.J., Verheyen, T.V., Adeloju, S.B., Chaffee, A.L., Meuleman, E., 2015. Monoethanolamine Degradation during Pilot-Scale Post-combustion Capture of CO2 from a Brown Coal-Fired Power Station. Energy & Fuels 29, 7441-7455.

Rooney, P., Dupart, M., Bacon, T., 1998. Oxygen's role in alkanolamine degradation. Hydrocarbon processing (International ed.) 77, 109-113.

Rooney, P.C., Daniels, D.D., 1998. Oxygen solubility in various alkanolamine/water mixtures. Petroleum Technology Quarterly, 97-102.

Schumpe, A., Adler, I., Deckwer, W.D., 1978. Solubility of oxygen in electrolyte solutions. Biotechnology Bioengineering 20, 145-150.

Sexton, A.J., 2008. Amine Oxidation in CO2 Capture Processes.

Sexton, A.J., Rochelle, G.T., 2009. Catalysts and inhibitors for oxidative degradation of monoethanolamine. International Journal of Greenhouse Gas Control 3, 704-711.

Sjostrom, S., Baldrey, K.E., Senior, C., 2020. Control of Wet Scrubber Oxidation Inhibitor and Byproduct Recovery.

Smith, P.J., Mann, C.K., 1969. Electrochemical dealkylation of aliphatic amines. The Journal of Organic Chemistry 34, 1821-1826.

Strazisar, B.R., Anderson, R.R., White, C.M., 2001. Degradation of monoethanolamine used in carbon dioxide capture from flue gas of a coal-fired electric power generating station. National Energy Technology Laboratory, Pittsburgh, PA (United States).

Strazisar, B.R., Anderson, R.R., White, C.M., 2003. Degradation pathways for monoethanolamine in a CO2 capture facility. Energy & fuels 17, 1034-1039.

Supap, T., 1999. Kinetic study of oxidative degradation in gas treating unit using aqueous monoethanolamine solution. University of Regina.

Supap, T., Idem, R., Tontiwachwuthikul, P., 2011. Mechanism of formation of heat stable salts (HSSs) and their roles in further degradation of monoethanolamine during CO2 capture from flue gas streams. Energy Procedia 4, 591-598.

Supap, T., Idem, R., Veawab, A., Aroonwilas, A., Tontiwachwuthikul, P., Chakma, A., Kybett, B.D., 2001. Kinetics of the oxidative degradation of aqueous monoethanolamine in a flue gas treating unit. Industrial & engineering chemistry research 40, 3445-3450.

Sørensen, L., Zahlsen, K., Hyldbakk, A., Silva, E.F.d., Booth, A.M., 2015. Photodegradation in natural waters of nitrosamines and nitramines derived from CO2 capture plant operation. International Journal of Greenhouse Gas Control 32, 106-114.

Talzi, V., 2004. NMR determination of the total composition of commercial absorbents based on monoethanolamine. Russian journal of applied chemistry 77, 430-434.

Talzi, V., Ignashin, S., 2002. NMR study of decomposition of monoethanolamine under conditions of industrial gas treatment. Russian journal of applied chemistry 75, 80-85.

Thitakamol, B., Veawab, A., 2008. Foaming behavior in CO2 absorption process using aqueous solutions of single and blended alkanolamines. Industrial & engineering chemistry research 47, 216-225.

Thompson, J.G., Bhatnagar, S., Combs, M., Abad, K., Onneweer, F., Pelgen, J., Link, D., Figueroa, J., Nikolic, H., Liu, K., 2017. Pilot testing of a heat integrated 0.7 MWe CO2 capture system with two-stage air-stripping: Amine degradation and metal accumulation. International Journal of Greenhouse Gas Control 64, 23-33.

Vevelstad, S.J., 2013. CO2 absorbent degradation Department of Chemical Engineering. NTNU, Trondheim.

Vevelstad, S.J., Grimstvedt, A., Elnan, J., da Silva, E.F., Svendsen, H.F., 2013. Oxidative degradation of 2-ethanolamine: The effect of oxygen concentration and temperature on product formation. International Journal of Greenhouse Gas Control 18, 88-100.

Vevelstad, S.J., Grimstvedt, A., Knuutila, H., da Silva, E.F., Svendsen, H.F., 2014. Influence of experimental setup on amine degradation. International Journal of Greenhouse Gas Control 28, 156-167.

Vevelstad, S.J., Johansen, M.T., Knuutila, H., Svendsen, H.F., 2016. Extensive dataset for oxidative degradation of ethanolamine at 55–75° C and oxygen

concentrations from 6 to 98%. International Journal of Greenhouse Gas Control 50, 158-178.

Vevelstad, S.J., Svendsen, H.F., 2016. Challenges related to Analysis of Anions in degraded Samples from Pilot and Lab Experiments.

Voice, A.K., 2013. Amine oxidation in carbon dioxide capture by aqueous scrubbing.

Voice, A.K., Rochelle, G.T., 2014. Inhibitors of monoethanolamine oxidation in CO2 capture processes. Industrial and Engineering Chemistry Research 53, 16222-16228.

Wagner, E.D., Osiol, J., Mitch, W.A., Plewa, M.J., 2014. Comparative in Vitro Toxity of Nitrosamines and Nitramines Associated with Amine-based Carbon Capture and Storage. Environmental Science & Technology 48, 8203-8211.

Wang, M.H., Ledoux, A., Estel, L., 2013. Oxygen solubility measurements in a MEA/H2O/CO2 mixture. Journal of Chemical & Engineering Data 58, 1117-1121.

Wang, T., Jens, K.-J., 2012. Oxidative Degradation of Aqueous 2-Amino-2-methyl-1-propanol Solvent for Postcombustion CO2 Capture. Industrial & Engineering Chemistry Research 51, 6529-6536.

Wang, T., Jens, K.J., 2014. Oxidative degradation of aqueous PZ solution and AMP/PZ blends for post-combustion carbon dioxide capture. International Journal of Greenhouse Gas Control 24, 98-105.

Wong, R.C., Bentley, L., Ndegwa, A., Chu, A., Gharibi, M., Lunn, S.R., 2004. Biodegradation of monoethanolamine in soil monitored by electrical conductivity measurement: an observational approach. Canadian geotechnical journal 41, 1026-1037.

Wu, Y., Nielsen, P.T., Rochelle, G., 2018. Oxidation of Piperazine in the Advanced Flash Stripper, 14th Greenhouse Gas Control Technologies Conference Melbourne.

Chapter 3

A review of degradation and emissions in post-combustion CO₂ capture pilot plants

This chapter comprises a literature review on the published data from pilot scale testing of amine solvents for CO₂ capture in the last decade and was published in the International Journal of Greenhouse Gas Control in January 2021. The goal of this work was to summarize the learnings from individual campaigns and identify common observations and shortcomings. The findings of the paper can be useful for the operation of large-scale amine-based CO₂ capture plants, including both recommendations for monitoring strategies and giving a solid overview of possibilities within analytical equipment.

A review of degradation and emissions in post-combustion CO_2 capture pilot plants

Vanja Buvik[a], Karen K. Høisæter[a], Solrun J. Vevelstad[b], Hanna K. Knuutila[a]*

[a] Department of Chemical Engineering, NTNU, NO-7491 Trondheim, Norway

[b] SINTEF Industry, NO-7465 Trondheim, Norway

[*] Corresponding author: hanna.knuutila@ntnu.no

Abstract

Pilot plant testing of amine solvents for post-combustion CO_2 capture is an essential tool for fully understanding degradation behaviour and emission profiles under realistic process conditions. This review aims to summarise the lessons learned in different pilot campaigns, as well as to give recommendations how solvent stability and emissions can be monitored and assessed. A total of 18 different pilot plants and 29 individual campaigns were studied, of which the majority used ethanolamine and flue gas from coal-fired power plants.

The findings of the review are that solvent stability data from different pilot plants show significantly higher operation time in which the solvent is stable, when extensive flue gas pretreatment is implemented. It was also found that no single degradation compound seems to suffice for the assessment of the degradation of a solvent, even for the widely studied ethanolamine process. Monitoring of the total liquid-phase heat stable salt concentration, as well as gas phase ammonia concentration may, however, give an informative picture of the state and degradation of the solvent. There seems to be a lack of universally applied analytical methods, which makes it difficult to compare one campaign or location to another. The implementation of validated and documented analytical standards in this regard will facilitate production of reproducible, reliable and comparable data for future solvent stability assessment.

_____

Abbreviations

Abs	absolute	LC	liquid chromatography
AMP	2-amino-2- methyl-1-propanol	MEA	monoethanolamine
aq.	aqueous	MDEA	N-methyl diethanolamine
ATR	attenuated total reflectance	MS	mass spectrometry
CHP	combined heat and power	NDIR	non- dispersive infrared
CCS	carbon capture and storage	NG	natural gas
DeSOx	removal of SO_X	OES	optical emission spectroscopy
DeNOx	removal of nitrogen oxides (NO_X)	OPC	optical particle counter
DNPH	2,4- dinitrophenylhydrazine	ppb	parts per billion
ED	electrodialysis	ppm	parts per million
EDX	energy dispersive X-ray microanalysis	PR	particulate removal
ELPI	electrical low pressure impactor	PTR	proton- transfer reaction
ESP	electrostatic precipitator	Pz	piperazine
FGD	flue gas desulphurisation	RFCC	residual fluidised cracker
FMPS	fast mobility particle sizer	SCR	selective catalytic reduction
FT-IR	Fourier- transform infrared spectroscopy	SEM	scanning electron microscope
GC	gas chromatography	TONO	total nitrosamine
HSE	Health, Safety and Environment	VOC	volatile organic compounds
HSS	heat stable salts	WESP	wet electrostatic precipitator
IC	ion chromatography	WFGD	wet flue gas desulphurisation
ICP	inductively coupled plasma	QTOF	quad time of flight

_____

1 Introduction

Removal of CO_2 from gas streams has been performed industrially for almost a century to provide pure CO_2 for industrial purposes, as well as sales-quality natural gas. CO_2 capture and storage is also predicted to be vital for achieving the goals of the Paris agreement and combat anthropogenically caused global warming (Rogelj et al., 2018). In recent years, several new solvents have been developed (Feron et al., 2020) and the interest towards a safe and optimised operation of the plants has increased due to the potential use of the technology for large-scale capture of CO_2 from power plants and other industries. As a consequence of the scaling up, however, various challenges have arisen. In a large-scale plant, solvent degradation, energy consumption, and potential emissions of the solvent or degradation compounds, can have significant environmental and economic consequences. Therefore, to gain a better understanding of the large-scale operation, the process and operating conditions are first studied through a pilot campaign allowing investigation of the effect of flue gas composition, impurities, and solvent performance, including degradation, corrosion, and emissions, on the process performance and costs.

Degradation, as well as corrosion, are considerable challenges in amine-based CO_2 capture. As the degradation increases, the amount of make-up solvent that needs to be added throughout the campaigns increases. Among other, Moser et al. (2020) summarised that solvent-make-up required in 12 campaigns performed with 30wt% (*aq.*) ethanolamine (MEA) varied from 0.3 to 3.6 kg t_{CO2}^{-1}, showing a 10-fold

difference. Furthermore, a feature that is often observed in pilot campaigns using MEA is that after stable operation for a certain amount of time, a sudden and rapid increase in degradation product formation and concentration of dissolved metals occurs (Dhingra et al., 2017; Rieder and Unterberger, 2013). What causes this abrupt spike in degradation rate has not yet been fully understood and prediction of when it will take place is therefore not possible. This effect has also been seen in laboratory-scale studies and it is therefore commonly assumed that dissolved iron and other metals catalyse the oxidative amine degradation in the absorption process also in pilot-scale (Bello and Idem, 2005; Chi and Rochelle, 2002; Léonard et al., 2014; Strazisar et al., 2003). Furthermore, certain degradation products also affect corrosion rates both positively and negatively, as they can act as chelators or inhibit the build-up of a protective film on the metal surface of the plant (Kohl and Nielsen, 1997; Tanthapanichakoon et al., 2006).

The identification of high concentrations of typical primary oxidative degradation products (formed in the first stages of degradation) in solvents used in pilots with real flue gas has shown that oxidative degradation indeed is a dominant degradation mechanism in the absorption process (Vega et al., 2014). Typical concentrations of oxygen in the flue gas is generally between 4 and 15% and lower in flue gases originating from coal-fired power plants than gas-fired power plants. Since the solvent has direct contact with the flue gas oxygen in the absorber and since the solubility of oxygen decreases with increasing temperature, the concentration of dissolved oxygen is the highest in the absorber and the absorber sump. Oxidative degradation is therefore assumed to primarily take place here, although the elevated temperatures in the rich solution also could increase the reactivity despite of low oxygen concentrations (Chi and Rochelle, 2002).

Thermal degradation primarily takes place during the solvent regeneration, at elevated temperatures and in the presence of CO_2 (Davis and Rochelle, 2009). Products of the thermal degradation process, as well as some of the oxidative degradation products, are often more volatile than the amines themselves and are likely to evaporate in the absorber. This increases the chance of emission to the atmosphere together with the purified flue gas, unless emission reduction technologies are in place (Rochelle, 2012).

There are well known methods to reduce degradation. Flue gas pretreatment technologies, removing impurities such as SO_X and NO_X gases, as well as particulate matter such as fly ash are implemented to some extent in most pilot campaigns. Methods such as "Bleed and Feed", removal of a part of the degraded solvent and refilling with fresh solvent throughout the process, have recently been thoroughly tested without success (Moser et al., 2020). Apart from the "Bleed and Feed", solvent reclaiming is often used to limit the amount of makeup solvent and maintaining the operation.

The purpose of this review is to summarise available data from pilot tests using amine solvents for post-combustion CO_2 capture and real flue gas or industrial gases. It covers traditional bench-mark amine 30wt% MEA as well as new amines and amine blends proposed for post-combustion CO_2 capture. The emphasis will be put on solvent stability, emissions and corrosion and how these aspects are monitored, and the three concepts are seen in light of one another. The review aims to be of help for future pilot campaigns and how these concepts can and should be monitored. Although a large number pilots and campaigns for post-combustion capture of CO_2 exist (Idem et al., 2015) and have taken place, those from which reported solvent stability or emission data are not available, are also not included here. Furthermore, most of the data given originates from journal papers and conference proceedings, but to give a complete picture and overview of the pilot plants and campaigns as possible, some of the given data has been found in conference presentations. The campaigns included have also been limited to the latest decade, to provide up-to-date information about current developments and trends.

2 Overview of Pilot plants and campaigns

Table 3.1 lists the pilot plants included in this review. Most of the pilots use a slip-stream of the flue gas from power plants or industrial sources. Furthermore, the table includes only pilot plants where data for emissions or degradation has been published. A more extensive overview of pilots and demonstration plants for post-combustion CO_2 capture can be found elsewhere (Cousins et al., 2016; Idem et al., 2015).

As expected, the CO_2 capture capacity correlates with the absorber diameter, so that the pilot with the smallest absorption capacity (kg CO_2 h^{-1}) also has the smallest absorber diameter. The absorber packing heights vary from 3 meters to 24 meters. Most of the plants have at least one water wash section on the top of the absorber to limit the emissions of volatile solvent components and degradation compounds.

Table 3.2 presents an overview of the gas compositions of the pilot campaigns included in this study. It also shows the gas pretreatment performed before the amine scrubbing. Altogether 19 different flue gas sources were studied, of which 16 originated from coal-fired power plants. The concentrations of CO_2 are between 11 and 14 vol% (dry) for coal-fired power plants, whereas for gas burners, it is typically lower. Pilot campaigns performed in connection to the cement industry have to deal with CO_2 concentrations up to 18 vol%. The pilot plant at Tiller in Norway, receives flue gas from a propane burner, and the gas can be diluted with air or CO_2 to simulate different industrial cases. Technology Centre Mongstad DA (TCM) has a possibility to use a slip-stream from natural gas-fired combined heat and power plant (CHP) or a slip-stream from residual fluidised cracker unit (RFCC). Similarly, the National Carbon Capture Center (NCCC) in Alabama, USA, has two available gas streams for solvent testing, one coal, and one simulated natural gas stream. Therefore, gas streams

of both TCM and NCCC vary in their concentrations of H_2O, CO_2, O_2, NO_X and SO_2, depending on the choice of flue gas source. The Mobile Test Unit (MTU), built and operated by Aker Solutions, has been used at three different test locations in Norway, Scotland and the USA, two with coal-derived flue gas and one time with CHP flue gas at TCM, where degradation data is available from the first two.

In spite of this being a review focusing on pilot scale studies using real flue gas, some additional studies using synthetic flue gas have been included in the evaluation of how amine solvents degrade. These campaigns are given separately in Table 3.11, and have been included because of their extensive analytical work, giving interesting insights on solvent stability, to support trends or shed light on topics included in the discussion.

2.1 Pretreatment technologies

As mentioned in the introduction, removal of contaminants before the CO_2 capture process, limits the possibility of unwanted side reactions of the amine solvent taking place, leading to solvent degradation and deterioration of the overall process performance. The need for pretreatment varies with the type of flue gas, which contaminants it typically contains and in which concentrations they are present, it also depends on the solvent itself. As some of these contaminants are causes of respiratory problems and of environmental concern, systems for removal of these from flue gas have been in use for half a century already. As shown in Table 3.2, in most of the pilot locations at least some pretreatment is used. Here, we separate the contaminants into three categories: particulate matter (ash, soot and catalyst fines), NO_X and SO_2/SO_X, and treatment technologies for each category will be briefly presented below (Meuleman et al., 2016).

Particulate matter is usually removed by wet or dry electrostatic precipitation (ESP). The ESP applies a negative charge to the particulate matter, facilitating their attachment to a positively charge electrode. The dry ESP then removes the particulates from the electrode by mechanical or magnetic impact whereas the wet ESP uses a water wash. It is also possible to apply a filter for the removal of particles. Pressure drops when particulates start accumulating in the filter and this limitation weighs against the otherwise high removal efficiencies (>99.95%) and simplicity of the method (Meuleman et al., 2016; Nicol, 2013).

NO_X gases are typically removed either by selective catalytic reduction (SCR) or a non-catalytic reduction (SNCR), reducing them to N_2 and water, where SCR holds the largest market share. The SCR process takes place at temperatures between 160 and 350 °C, whereas SNCR has a temperature requirement closer to 1000 °C (Meuleman et al., 2016).

Table 3.1: An overview of the dimensions of the different pilot plants studied and compared in this review. Where no numbers are given, the dimensions could not be found in literature.

Pilot plant	CO_2 cap. rate [kg h^{-1}]	Water/acid wash	Abs. diameter [m]	Abs. packed height [m]	Reference(s)
Aioi Works	830	Y	0.85	15	(Nakamura et al., 2013; Nakamura et al., 2014; Okuno et al., 2017)
Brindisi	2500	Y	1.5	22	(Enaasen et al., 2014; Kamijo et al., 2013; Mangiaracina et al., 2014; Rieder et al., 2017)
CAER 0.1 MWth	10		0.1	3.25	(Cousins et al., 2016; Frimpong et al., 2013; Thompson et al., 2014)
CAER 0.7 MWe					(Thompson et al., 2017c)
Changchun	100		0.35	8	(Feron et al., 2014)
Esbjerg	1000	Y	1.1	17	(Knudsen et al., 2009)
Ferrybridge	4167	Y			(Fitzgerald et al., 2014)
Heilbronn	300		0.6	23.9	(Dhingra et al., 2017; Rieder et al., 2017; Rieder and Unterberger, 2013)
Łasziska		Y	0.33	8.4	(Spietz et al., 2018)
Loy Yang	20		0.21	2.7	(Artanto et al., 2012; Dhingra et al., 2017; Reynolds et al., 2015a)
Maasvlakte	250	Y	0.65	8	(Dhingra et al., 2017; Khakharia et al., 2015a; Rieder et al., 2017)
Mikawa	420	Y		15	(Saito et al., 2014; Saito et al., 2015)
MTU	180	Y	0.4	18	(Bade et al., 2014; da Silva et al., 2012; de Koeijer et al., 2011; Morton et al., 2013)
NCCC	various	Y	0.64	6	(Brown et al., 2017; Gao et al., 2019)
Niederaussem	300	Y			(Moser et al., 2011a; Moser et al., 2011b)
Tarong	100		0.35	7.14	(Cousin et al., 2012)
TCM	5200	Y	3.5×2	12-24	(Brigman et al., 2014; de Koeijer et al., 2011; Gorset et al., 2014; Morken et al., 2017)
Tiller	50	Y	0.2	19.5	(Mejdell et al., 2011)

Table 3.2: A summary of the flue gas sources and compositions at different locations, where post-combustion CO_2 capture campaigns have been performed. SR: SO_X removal, NR: NO_X, PR: particle removal. Further details on pretreatment can be found in the appendix, Supplementary table 3.1.

Location	Flue gas source	Pre-treatment	cO_2 (vol%) wet	cO_2 (vol%) dry	cCO_2 (vol%) wet	cCO_2 (vol%) dry	cSO_X ppm	cSO_X mg m$_N^{-3}$	cNO_X ppm	cNO_X mg m$_N^{-3}$	Reference
Aioi Works (IHI), Japan	Coal /propane boiler		-	-	-	-	-	-	-	-	(Nakamura et al., 2013; Nakamura et al., 2014)
Brevik, Norway	Cement		7.5	9.2	17.8	21.8	-	-	-	180-250	(Knudsen et al., 2014)
Brindisi, Italy	Coal	SR, PR, NR	-	6.3-8.2	-	11-13	-	<130	-	-	(Mangiaracina et al., 2014; Rieder et al., 2017)
CAER, 0.1 MWth, USA	Coal	SR, PR	6	-	14	-	17-250	0-20	80-90	-	(Frimpong et al., 2013; Thompson et al., 2014)
CAER, 0.7 MWe, USA	Coal	SR, PR, NR	8	-	10-61	-	<5	-	<50	<160	(Thompson et al., 2017c)
Changchun, China	Coal	SR, PR, NR	5.8	6.4	10.8	12.0	-	-	-	-	(Feron et al., 2014)
Esbjerg, Denmark	Coal	SR, PR, NR	-	5-9	12	-	<10	<50	<65	-	(Knudsen et al., 2009)
Ferrybridge, UK	Coal	SR, PR, NR	-	-	-	-	-	-	-	-	(Fitzgerald et al., 2014)
Heilbronn, Germany	Coal	SR, PR, NR	-	6.4	12-14	-	-	-	-	-	(Dhingra et al., 2017; Mejdell et al., 2017; Rieder et al., 2017)
Łaziska, Poland	Coal	SR	-	-	13.1-13.3	-	-	<10	-	-	(Spietz et al., 2018)
Longannet, Scotland	Coal		~10	-	12	-	-	-	80-170	-	(da Silva et al., 2012; Graff, 2010)
Loy Yang, Australia	Coal	SR, PR, NR	4-5	-	10-11	-	120-200	-	150-250	-	(Artanto et al., 2012; Bui et al., 2016; Dhingra et al., 2017; Reynolds et al., 2015a)
Maasvlakte, The Netherlands	Coal	SR	-	7.4	13	-	-	-	-	-	(Dhingra et al., 2017; Khakharia et al., 2015a; Rieder et al., 2017)
Mikawa, Japan	Coal	SR, PR	-	-	-	12	<5	-	100	-	(Saito et al., 2014; Saito et al., 2015)
Niederaussem, Germany	Coal	SR, PR, NR	-	5.0	-	14.2	-	<1	-	120-200	(Moser et al., 2011a; Moser et al., 2011b; Moser et al., 2020)
Tarong, Australia	Coal	SR, PR	6	-	10	-	200	<1	150	-	(Cousin et al., 2012; Cousins et al., 2016)
TCM, Norway	CPH	SR, PR	14	15	3-6	3.8	<1	-	-	3	(Gorset et al., 2014; Morken et al., 2017; Shah et al., 2018)
	RFCC		3.2	3.3	15	15	5	-	-	60	
Tiller, Norway	Propane burner		<15	-	15	-	very low	very low	-	20	(da Silva et al., 2012; Mejdell et al., 2011)
Wilsonville (NCCC), USA	Coal	SR, PR, NR	-	4.5	4-5-14	14	2.5 (dry)	-	1-3 (dry)	-	(Brown et al., 2017; Bumb et al., 2017; Morton et al., 2013)
	Simulated NG		-	15.9	-	4.5	-	-	-	-	

55

SO_2/SO_X gas is not just a contaminant deriving from the combustion process itself, but is also formed when sulphur components pass through a NO_X-removal unit. It is even occasionally added to the ESP for reducing the resistivity of the fly ash. SO_2/SO_X can be removed in a wet flue gas desulphurisation (WFGD) unit, where the acidic nature of SO_X allows it to be scrubbed out by an alkaline lime stone ($CaCO_3$) solution. There are also dry or semi-dry FGD systems available, relying on dry alkaline sorbents, but the WFGD systems have approximately 84% of the market. The FGD step has the additional benefit of removing chloride from the flue gas, washing it out with the sulphur loaded lime stone (Meuleman et al., 2016; Zhu, 2010).

3. Analytical methods used in pilot campaigns

In amine-based post-combustion CO_2-capture, one of the main challenges is solvent degradation (Rochelle et al., 2001), which requires a reliable solvent monitoring strategy. The main goal of this monitoring is often to quantify the concentration of the intact starting amines. In laboratory scale experiments, knowing the change in amine concentration over time allows assessment of the stability of the solvent system. However, in pilot scale, where the amines chosen are often relatively stable, the amine concentration is also measured to ensure that the amine and water concentrations stay constant. In both cases the analytical method used has to be fast, accurate, and straightforward (Cuccia et al., 2018).

Another target for the monitoring of the solvents is to identify the degradation products of the amines. Degradation products are typically categorised into five main classes: amine derivatives, acids, aldehydes, amides, and nitrosamines. Compared to the analysis of the starting solvent components, the study of degradation compounds is a more challenging endeavour (Cuccia et al., 2018). Firstly, many of them have an unknown structure. Moreover, the high concentration of the starting amine in the solvent can make it hard to detect degradation compounds that are typically present at low levels and even at trace amounts (da Silva et al., 2012). There are multiple analytical methods to choose from when analysing these species, with different advantages and disadvantages. When choosing an analytical method, nature of the compounds, matrix and concentration ranges of the analytes must be regarded. Dissolved metal species can also be found in the solvents and these are measured to monitor corrosion. Lastly, there are many monitoring technologies for gaseous emission (Kolderup et al.). Moreover, a large number of publications studying aerosol formation mechanisms, as well as aerosol reduction technologies, have been published in the last five years using various analytical methods. The most frequently used analytical methods during pilot campaigns are described below and an overview of the methods can be found in Table 3.3.

Titration is a quick tool that can give valuable information of different aspects of a solvent. In CCS, titration is most commonly used to find total alkalinity, the CO_2-

loading and amounts of heat stable salts (HSS). Total alkalinity is a measurement of the total concentration of base in a solution. It is determined by titrating a basic solution with an acid (e.g., sulphuric or hydrochloric) until the equivalence point, at which the base is neutralised, is reached. (Somridhivej and Boyd, 2016)

This method is a quick and inexpensive way of getting an estimate of amine concentration, and thus an easy way of gaining insight into the stability of the amine (Matin et al., 2012). It is, however, important to differentiate between the actual concentration of the starting amine and the total alkalinity as some degradation products are alkaline. Therefore, the result from a total alkalinity measurement incorporates the concentration of the starting amine, as well as possible alkaline degradation products that also have CO_2 binding abilities.

Titration used to find CO_2-loading or HSS concentration works in a similar way as that of the total alkalinity measurements. The difference is that bases are used instead of an acid and the solutions have to be pretreated before the titration. For CO_2-loading measurements, the CO_2 in the solution is first extracted using $BaCl_2$, before titration with NaOH (Hilliard, 2008). To get the HSS concentration, the solution is first treated with a cation exchange resin and then titrated with a base (Aronu et al., 2014; Reynolds et al., 2015a). Both of these methods are more time-consuming than the total alkalinity measurement. Nevertheless, if other, more expensive, analytical techniques are unavailable, these two methods can be a less costly alternative that provide important information.

Liquid Chromatography – Mass Spectroscopy (LC-MS) is an analytical method used to separate molecules based on their chemical and physical properties. The liquid sample passes through an LC-column, and the different species separate as a result of their varying affinity towards a stationary phase in the column. The mass spectrometer ionises the compounds, and a magnetic field separates the ions based on their mass-to-charge ratio (Lundanes et al., 2013). There are multiple additions that can be included, like an additional step for compound separation. An example of this is QTOF (quad time of flight).

LC-MS is a common choice for both quantitative and qualitative analysis of degradation compounds, as this technique can analyse most of the classes of degradation compounds (amine derivatives, acids, amides, and nitrous amines) (Chahen et al., 2016; Cuzuel et al., 2014; Vevelstad et al., 2013). In the quantitative analysis, the remaining concentration of starting amine can be determined with high accuracy using an internal standard. Known degradation compounds can also be quantified, if internal standards are available and their application can also allow for qualitative analysis to identify unknown degradation products (da Silva et al., 2012; Lepaumier et al., 2011). An approach for identifying and semi-quantifying degradation compounds using TOF-MS has been described (Thompson et al., 2017b; Thompson et al., 2017c).

There are some disadvantages to the LC-MS technique. The equipment and maintenance are very costly and require skilled operators. It is, therefore, seldom found on site, which can give rise to challenges regarding the stability of the samples. However, published data on reanalysing samples have shown a good agreement between the analysed samples right after experiments and one month later (Knuutila et al., 2014b). There is also no library with which to compare any unknown peaks (Lepaumier et al., 2011). Identification of unknown peaks in the degraded mixtures will, therefore, start with the prediction of potential degradation compounds based on chemistry, after which deuterated standards will be purchased. These can be expensive, and in some cases, they are even not commercially available (da Silva et al., 2012).

Ion Chromatography (IC) is a sub-category of liquid chromatography, and a useful method for analysing ionic species. Since many degradation products are known to have ionic properties, the IC is well-suited for amine degradation studies (Wang and Jens, 2012). Similar to normal liquid chromatography, the separation of the species occurs due to their different affinity to a stationary phase; in IC this difference is caused by the species different columbic interaction with the ion-exchanger (Lundanes et al., 2013).

There are two types of ion chromatography, namely anion-exchange and cation-exchange (Lundanes et al., 2013). Anion-exchange is commonly used to analyse for degradation products in anionic forms, such as carboxylates, nitrate, and nitrite (Kadnar and Rieder, 1995; Wang and Jens, 2012). It is also one of the most described methods for analysing the total amide content by converting the amides to their corresponding carboxylic acid through amide hydrolysis (Freeman, 2011; Sexton, 2008). The generated carboxylic acids can then be analysed with the anion-exchange, and the surplus of carboxylic acids presents the carbamate concentration. Cation-exchange, on the other hand, is commonly used to quantify solvent amines, as well as to identify and to quantify amine degradation products, like alkyl amines, in the form of heat stable salts (da Silva et al., 2012; Moser et al., 2020; Reynolds et al., 2015b; Thompson et al., 2014). Quantitative IC-analysis requires chemical standards.

IC is a relatively inexpensive analytical method. Compared to LC-MS, the equipment is cheaper and requires less maintenance. Furthermore, the implementation is also somewhat more straightforward, as dilution is the only sample preparation needed (Cuccia et al., 2018). The limitation of the IC method is that non-ionic compounds cannot be analysed. Therefore, IC is often used in combination with other analytical methods. The IC instrumentation requires both regular use and maintenance to deliver reliable results.

Gas Chromatography – Mass Spectroscopy (GC-MS) works similarly as LC-MS, but as the name implies, the analysis occurs in a gas phase. GC-MS can be used both for quantitative analyses as well as to identify some degradation products (Wang and

Jens, 2012). However, only compounds that have boiling points below 300-500 °C, can be analysed. At the same time, the analytes also have to be stable at these high temperatures. This limits the number of degradation compounds that can be analysed.

On the other hand, very high-quality spectra can be achieved as the gaseous eluate allows for the solvent to be removed before entering the MS and as the analytes are easily ionisable in the gas phase. An extensive library of various pure compounds is available, and any unknown spectra can be compared to the library (Lepaumier et al., 2011). The existence of this library is one of the main advantages for this method.

Fourier Transform Infrared Spectroscopy (FT-IR) is a method that utilises molecular bonds' ability to oscillate when exposed to infrared radiation. In principle, FT-IR allows for the simultaneous analysis of up to 50 compounds with a low detection limit (~1 ppm). FT-IR can be used both for analyses of the liquid and gas phases. However, in aqueous solvent solutions, the detection of degradation compounds is challenging, if not impossible, due to low concentrations of degradation compounds, complex chemical matrix, as well as the high concentrations of amine and water (Cuccia et al., 2018; Macbride et al., 1997).

FT-IR is mostly employed as a gas phase on-line analytical method. The method is mostly used to monitor gas effluents, e.g., NO_X, SO_X, CO, and CO_2, and to quantify amines (like Pz, MEA, MDEA and ammonia) present in the gas leaving the absorber/water wash (Bade et al., 2014; Khakharia et al., 2013; Knudsen et al., 2013; Knudsen et al., 2014; Mertens et al., 2012). FT-IR can also be used to quantify aldehydes (formaldehyde and acetaldehydes).The advantage of applying on-line FT-IR is that the only preconditioning needed is heating the gas sample to prevent condensation. However, work should be done to ensure that the heating does not induce further thermal degradation of the amine. The ability to detect aldehydes is an essential advantage for this method, as other analytical methods are often limited in this regard.

FT-IR can also be used to analyse the liquid phase. Here, FT-IR together with Attenuated Total Reflectance (ATR) is typically used to monitor the loading and solvent amine concentrations in the solvent loop. When specific degradation compounds are found in high enough concentrations, they can also be quantified and monitored. The main challenge is that degradation compounds will change the spectra, and the results will become more inaccurate overtime, requiring calibration with degraded solvent (Grimstvedt et al., 2019). In recent years, method, where FT-IR with ATR is used to analyse the speciation in the solvent has also been developed (Diab et al., 2012; Richner and Puxty, 2012).

Proton-Transfer Reaction Mass Spectroscopy (PTR-MS) is a technique used for online measurement of volatile organic compounds (VOCs) in a gas-stream. In the PTR-MS instrument, gas-phase VOCs are ionised as a proton is transferred from an

ion reagent, typically H_3O^+, to the sample molecules. The ionised molecules are then mass analysed in the MS-part of the equipment (Hansel et al., 1995). For the proton transfer to take place, the analysed molecules must have higher proton affinity than water. This gives some restrictions to which compounds can be analysed. To overcome this, instruments have in later years been modified to be able to switch between H_3O+ and for example NO^+ as reagent ions, which has increased the amount of detectable compounds (Jordan et al., 2009).

The PTR-MS can give both quantitative and qualitative measurement results. One of the main advantages of this method is that neither gas standards, nor calibration for different gases, are necessary to get a precise quantification of the different species. Another advantage is the outstanding detection sensitivity of this method. The detection limit varies for different apparatuses, but it is typically in the pptV range (Lindinger et al., 1998). A drawback in this regard is that there is a maximum measurable concentration limit. The equations that are used in the analysis are based on the assumption that the decrease of reagent ions can be neglected. With a concentration at about 10 ppmV and up, this no longer holds and the results will be incorrect. A solution is to dilute the gas with air.

Inductively Coupled Plasma Mass Spectroscopy/Optical Emission Spectroscopy (ICP-MS/-OES) are elemental analytical techniques, which enables detection of most atoms at ppm levels. This is done by atomising and ionising the molecules in the studied mixture by passing it through an inductively heated plasma, often argon (Sheppard et al., 1990). Using an ICP-MS instrument, the atomic ions that are created are then analysed with MS. The ICP-OES uses the fact that some of the atoms/ions that are created are also excited. The intensity of the radiation is proportional with the concentration of each atom, and so this technique can be used for both quantitative and qualitative analysis (Thomas, 2013).

These techniques demand sample preparation, where one usually has to add an internal standard, primarily deionised water with nitric or hydrochloric acid. The drawback is that the equipment is expensive, and the analysis has a high operation cost because it employs argon gas (Todoli and Mermet, 2011). In the field of CCS, this technique is used to monitor the amounts of trace metals in solutions. This give an indication of corrosivity of the studied solvent. It should be noted that the method has not been validated. ICP-MS can also be used for measuring the total amount of carbon in a solution, but this is not widely used in the field of CCS.

Total Organic Carbon (TOC) analyser can measure amounts of carbon in a solution. It has different modes and can also be used for analysis of the total amount of inorganic carbon (IC), total carbon (TC) and total nitrogen (TN). In the field of CCS, it is often used to measure amount of CO_2 in a liquid sample (Bernhardsen et al., 2019; Knudsen et al., 2014).

The analyses happens over three steps, namely acidification, oxidation, and non-dispersive infrared (NDIR) detection. In the acidification step, acid is added, which then converts all bicarbonate and carbonate ions to carbon dioxide. The measurement of the resulting gas gives the amount of IC in the sample, corresponding to the CO_2 loading. Catalytic combustion oxidises all carbon in the sample to CO_2, so that this also can be quantified by NDIR. Other oxidation processes are also available for the quantification of organic carbon (Shimadzu, 2014).

Fast Mobility Particle Sizer (FMPS) is a fast response technique, enabling rapid detection of particle size distribution of aerosols. The gas-streams carrying aerosols is let into the FMPS and through a cyclone that removes particles bigger than 1 µm. The aerosols then continues through a region, in which they are charged with a known charge. The positively charged particles are then separated in an electric field based on their diameter and charge-state. The size distribution is measured in 32 channels, ranging from 5.6 to 560 nm (Jeong and Evans, 2009; Levin et al., 2015). Disadvantages of this technique is that it is not very robust in very demanding industrial surroundings (Kero and Jørgensen, 2016).

Optical Particle Counter (OPC) is an online measuring technique that is used to find aerosol size distribution and total particle number. In the OPC, particles are passed through a laser-light, which results in scattering of this light. The scattering is then classified and this gives a size spectrum (Burkart et al., 2010). OPCs can detect particles as small as 50 nm in diameter, and for smaller particles than this is simply not detected. Particles with a diameter of several hundred µm can also be detected, though not with the same instrument. If the particle size exceeds the detection limit for a certain instrument, it will simply be counted as the maximum diameter (Eliasson et al., 2016; Welker, 2012). A drawback of this method is that properties of the aerosols, such as density, shape, refractive index and absorption, is not accounted for (Welker, 2012).

Scanning Electron Microscope with Energy Dispersive X-ray Microanalysis (SEM/EDX) is an elemental microanalysis technique. The SEM part of the instrument is a microscope that can magnify from about 10 to 3 000 000 times. It is an offline method, so samples must first be collected from for example filters or films (Byers et al., 1971; Li and Shao, 2009). The surface of your sample is scanned with a focused beam of electrons. These electrons react with the atoms in the sample, resulting in various signals. The detection of these by SEM and by EDX can map out both the composition and the topography of the sample surface (Goldstein et al., 2017; Newbury and Ritchie, 2013). The resulting SEM image is quite analogous to normal vision (Byers et al., 1971), and the resulting image can give the structure, the size and the composition of solids in the aerosol particles. It can also be processed with different approaches to give size distribution (Brostrøm et al., 2020; Goldstein et al., 2017; Moser et al., 2017; Sun et al., 2012).

Electron Low Pressure Impactor (ELPI+) is a real-time particle detection technique, which combines electrical detection of charged particles and a 15-stage cascade impactor. When the aerosol enters the ELPI+, a unipolar diffusion charger first charges the particles of the aerosol. The unipolarly charged particles are then deposited in the various impactor stages depending on their aerodynamic size. In the impactor stages, electrometers are used to measure signals from the charged particles, which can then be converted to particle size distribution. In the end, this measurement gives particle number concentration and size distribution in real-time. The particle size distribution ranges from 6 nm to 10 µm (Järvinen et al., 2014; Lamminen, 2011).

Iso-kinetic sampling using impingers is the most common way of manual sampling of emissions (Bade et al., 2014; Gjernes et al., 2017; Lombardo et al., 2017; Mertens et al., 2012; Mertens et al., 2013; Morken et al., 2014; Morken et al., 2017). Typically, multiple impingers are installed in series to avoid breakthrough. The first impinger is often empty, whereas in the following impingers different absorbents, like dilute sulphuric acid or 2,4-dinitrophenylhydrazine (DNPH), are used. Sulphuric acid is often used for collection ammonia and amine samples, while 2,4-dinitrophenylhydrazine is used to sample acetaldehyde and formaldehyde (Bade et al., 2014; Mertens et al., 2012; Mertens et al., 2013). A good overview of standard methods for manual sampling, mainly developed for monitoring of the working environment, can be found elsewhere (Azzi et al., 2010; SEPA, 2015; Wittgens et al., 2010). A disadvantage of the iso-kinetic sampling is that it is a offline method, used periodically. FTIR, discussed earlier, is therefore often used to continuously monitor amine and ammonia emissions in the gas phase.

4 Results

4.1 Solvent Stability and Corrosion

Both oxidative and thermal degradation may take place with the carbamates formed in a reversible reaction between amine and CO_2. In the case of thermal degradation the mechanism often goes through carbamate polymerisation reactions (Davis and Rochelle, 2009; Lepaumier et al., 2009a; Rochelle, 2012). Oxidative degradation mechanisms, which are widely studied but extremely complex and therefore less understood, are assumed to start with radical reactions on the amine or carbamate. Once the reactions have initiated and primary degradation compounds are formed, these can react further with other degradation compounds, carbamates and amine in the solution to form secondary degradation compounds (Bello and Idem, 2005; Eide-Haugmo et al., 2011; Lepaumier et al., 2009a). These reactions are catalysed by the presence of dissolved metals in the aqueous amine solvent (Blachly and Ravner, 1963; Goff, 2005). The chemical structure of some typical degradation compounds identified and/or quantified in pilot plant and lab scale studies can be found in the appendix, in Supplementary table 3.3.

Table 3.3: Summary of the main analytical methods used. *offline measurement

Method	Compounds analysed	Solvent amine	Water wash liquid	Emission	Remarks
LC-MS	Amine and amine degradation products.	x	x	x*	The equipment and maintenance are costly, Requires skilled operator, often off site. However, up-concentration possible and is able to detect compounds in low concentration.
GC-MS	Amine and amine degradation products.	x	x	x*	The compounds need to have boiling point below 300-500 °C and the analytes have to be stable at these high temperatures. High-quality spectra achieved and extensive library of pure compounds available to compare against.
IC	Amine and amine degradation products.	x	x		Relatively inexpensive but requires regular use and maintenance. Only ionic compound could be analysed.
FT-IR	Amine gas effluents e.g. aldehydes, ammonia, water NO_X, SO_X, CO, and CO_2	x	x	x	Online CO_2 analysis possible; both liquid and gas phase analysis possible, often preferred for emission monitoring; Liquid phase analyses more challenging due to degradation; Also used for speciation.
Titration	Total alkalinity in the solvent and in the water wash liquid; the CO_2-loading analyses; heat stable salts (HSS) analyses	x	x		Simple method and inexpensive.
PTR-MS	Amine and volatile organic compounds (VOCs).			x	Gas phase - could be used online; Quantitative data obtained without gas standard and calibration; High detection sensitivity (pptV range)
ICP-MS	Atoms	x			ppm levels can be measured; expensive instrument with high operation cost
TOC/TN	Carbon and nitrogen	x	x		Relatively simple and inexpensive; Could be placed onsite; often used to measure CO_2 in a liquid sample
FMPS	Particle size distribution			x	Fast response; Not robust in demanding industrial surroundings
OPC	Particle size distribution and total particle number			x	Detects particles down to 50 nm in diameter; Properties of aerosol like density and shape not accounted for
SEM/EDX	Particle size distribution and structure, size, and composition of solids in the aerosol particles			x*	Offline method
ELPI+	Particle size distribution and particle number concentration			x	Offline method

A total of 29 individual campaigns in 18 different pilot plants, where solvent degradation was studied, were found. 30wt% MEA (aq.) was used in 19 of these (Table 3.4) and 10 were campaigns testing proprietary or other amine solvents (Table 3.5). A total of about 40 different compounds or compound groups were found measured in the liquid phase of the different campaigns, some just once, while others reoccur in several studies. A summary of the most frequently occurring liquid phase degradation components, as well as in which campaigns they have been analysed, can be found in Table 3.3 for campaigns using 30wt% MEA (aq.) and Table 3.4 for other, including proprietary, solvents.

Despite of pretreating the flue gas to remove reactive contaminants, amine degradation does take place in large scale CO_2 capture. This is sometimes a terminal problem, resulting in the need for solvent replacement and interrupted operation. Some technologies are being studied, to limit degradation after it has began to take place, such as solvent reclaiming, removing irreversibly formed heat stable salts. Reclaiming technologies aim to keep as much of the non-degraded amine as possible and only remove formed contaminants from the solvent. Reclaiming can typically be either thermal, by ion exchange or through electrodialysis and may be performed on- or offline (Kentish, 2016; Wang et al., 2015). The "Bleed and Feed" strategy involves the removal of parts of the degraded solvent and replacing it with fresh solvent (Moser et al., 2020). If any known degradation limiting technologies have been applied throughout the campaign, this is also given in Table 3.4.

Table 3.4: List of all the 30wt% MEA (*aq.*) campaigns studied in this review.

Location	Time [h]	Remarks	Campaign focus	References
Brindisi	550	40 m³ of 30wt% MEA added during campaign. Typically, 1 mg m_N^{-3} of particulate matter at inlet.	Assessment of different operation modes and conditions. Establish guidelines with relevant data on emissions, HSE, and other operability, flexibility, and cost aspects.	Mangiaracina et al. (2014); (Rieder et al., 2017)
CAER 0.1 MWth	100		Comparison of MEA 30wt% and the proprietary solvent CAER B2	(Thompson et al., 2014)
CAER 0.7 MWe	1316	Thermal reclaiming was performed from 880 to 970 hours.	Understand the impact on the solvent of flue gas constituents and potential higher oxygen content in the solvent due to secondary air stripper	(Thompson et al., 2017a; Thompson et al., 2017c; Thompson et al., 2017d)
Changchun	1063		Performance trials; comparison with different solvent blends	(Feron et al., 2015; Feron et al., 2014)

Location	Time [h]	Remarks	Campaign focus	References
Esbjerg (a)	6000	Samples analysed after 500 hours. Solvent partly degraded before start (0.5wt% HSS content). 6 ppm S in flue gas.	Demonstrate the post combustion capture technology in conjunction with a coal-fired power station. Comparison with CASTOR 2, additionally comparing sulphur accumulation properties.	(Dhingra et al., 2017; Knudsen et al., 2009)
Esbjerg (b)	3360	Samples from 1850 hours (11 weeks) studied in degradation study.	Test campaign	(da Silva et al., 2012)
Ferrybridge	>600		Benchmarking with MEA, before testing of a proprietary solvent. Assessment of solvent durability, perform process optimisation and to provide data on plant design and scale-up.	(Fitzgerald et al., 2014)
Heilbronn (a)	1600	Campaign in 2011.	Benchmarking campaign.	(Dhingra et al., 2017; Rieder and Unterberger, 2013)
Heilbronn (b)	1500	760 kg MEA added after 952 hours, water added at end, reducing the MEA concentration to ~25wt%. Concentrations of degradation products given here are from sampling at 535 hours. Campaign took place in 2013/14.	Establish guidelines with relevant data on emissions, HSE, and other operability, flexibility, and cost aspects. ED reclaiming tests performed offline, with degraded solution.	(Bazhenov et al., 2015; Bazhenov et al., 2014; Rieder et al., 2017)
Longannet, MTU	Ca. 4400	Reclaiming after 3 months, total time 6 months		(da Silva et al., 2012)
Loy Yang	834	MEA pre-used 639 or 700 hours, for capture of CO2 from a black coal-fired power plant (Tarong).	Performance trials; comparison with different solvent blends	(Artanto et al., 2012; Dhingra et al., 2017; Reynolds et al., 2015b)
Maasvlakte (a)	3500	Reclaimed after 3000 hours	Study corrosion in relation to solvent degradation and ammonia emissions.	(Dhingra et al., 2017; Khakharia et al., 2015a)
Maasvlakte (b)	890		Establish guidelines with relevant data on emissions, HSE, and other operability, flexibility, and cost aspects.	(Rieder et al., 2017)

Location	Time [h]	Remarks	Campaign focus	References
Niederaussem (a)	5000		Performance validation and investigation of time-dependence of MEA degradation and organic acid formation. Test of optimised process configurations.	(Moser et al., 2011a)
Niederaussem (b)	12 000		Study solvent degradation	(Moser et al., 2018)
Niederaussem (c)	13 000		Study time-dependent degradation products and trace components and how they can act as catalysts for degradation. Confirm threshold concentrations of iron from literature. Testing of "Bleed and Feed" as a degradation management strategy.	(Moser et al., 2020)
TCM (a)	2162	Campaign duration 20.11.13-24.02.14	Verify Aker Solutions' Advanced Carbon Capture® process including two proprietary advanced amine solvents	(Gorset et al., 2014; Morken et al., 2014)
TCM (b)	2000	Reclaimed after 1852 hours	Demonstrate and document the performance of the TCM DA Amine Plant	(Morken et al., 2017)
Tiller	2350		Benchmarking campaign	(da Silva et al., 2012; Mejdell et al., 2011)

Formate, as well as other organic acids, have long been regarded as primary indicators of oxidative degradation in the liquid phase and are therefore among the most reported degradation compounds of MEA degradation. Of the 19 campaigns shown in Table 3.6, formate is quantified in nearly two thirds, and half of the campaigns also analysed for oxalate. These two as well as acetate and glycolate, are formed in the first steps of the degradation process by electron or hydrogen abstraction before they react with the amine or other degradation products to form other degradation compounds (Rooney et al., 1998).

Table 3.5: List of all the campaigns using proprietary or other solvents than MEA 30wt% (*aq.*) studied in this review.

Location	Time [h]	Solvent	Remarks	Reference(s)
Austin		8m PZ		(Nielsen et al., 2013)
CAER 0.1 MWth	185	CAER B2		(Thompson et al., 2014)
Changchun	306	blend 5		(Feron et al., 2014)
Esbjerg	1000	CASTOR 2	Sampling after 500 h, stripper pressure 2.0 bar	(Knudsen et al., 2009)
Ferrybridge	>600	RS-2®		(Fitzgerald et al., 2014)
Łaziska		40wt% AEEA		(Spietz et al., 2018)
Mikawa	840	Solvent A	Sterically hindered, secondary amine	(Saito et al., 2014; Saito et al., 2015)
Mikawa	740	TS-1		(Saito et al., 2014)
TCM	4029	S21	03.10.12-01.04.13, Reclaiming after 3600 hours	(Gorset et al., 2014)
TCM	3507	S26	03.03.14-16.08.14, Reclaiming after 3300 hours	(Gorset et al., 2014)

A summary of reported concentrations of organic acids can be seen in Figure 1, as well as total concentration of other (in some cases unknown) HSS, where that has been reported. One MEA-campaign from the 0.1 MWth CAER pilot (Thompson et al., 2014) of only 100 hours and one campaign from the Esbjerg pilot (Knudsen et al., 2009) of unclear total operation time prior to HSS analysis, were omitted. Figure 1 shows a large span in the concentrations of heat stable salts found in various 30wt% MEA (*aq.*) campaigns when normalised per time in operation. Normalisation of this data does not give a complete picture of the degradation processes and may not be an ideal way of comparing different pilot campaigns and locations to one another, but it gives a visual representation of the degradation compounds observed. Surprisingly, one of the highest HSS concentrations is actually found in the shortest campaigns. A correlation between the amount of pretreatment technologies applied prior to CO_2 removal is apparent, when comparing Figure 1 with Table 2. A summary of the flue gas sources and compositions at different locations, where post-combustion CO_2 capture campaigns have been performed. SR: SO_X removal, NR: NO_X, PR: particle removal. Further details on pretreatment can be found in the appendix, Table S3.1. Esbjerg, Heilbronn and Niederaussem all operate with coal as their flue gas sources and have an extensive pretreatment setup. TCM also observe relatively low

concentrations of HSS. The flue gas originates from sources with less contaminants and the degradation here is comparable to pretreated flues gas from coal-fired power plants.
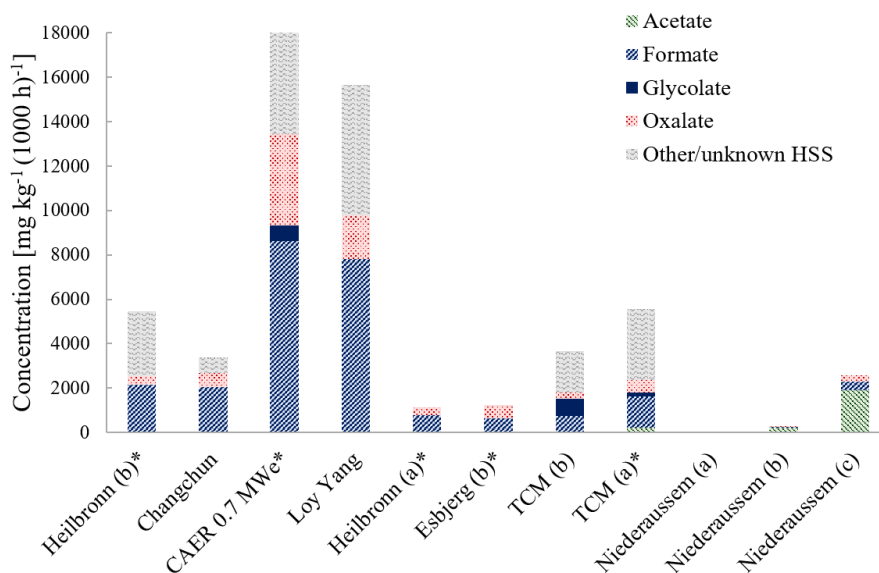
Figure 3.1: Heat stable salt/organic acid concentrations measured in post-combustion CO_2 capture pilot campaigns using 30wt% MEA, at the end of the campaign or right before reclaiming the solvent. Concentrations converted to concentration per 1000 hours, to facilitate comparison of different campaigns and pilots. Keep in mind that where no concentration is given, reported data for the given compounds is not available. All references are given in Table 3.6. *Mass concentration converted to mass fraction under the assumption that $\rho = 1$ kg L^{-1}.

Furthermore, it can be observed that most campaigns see relatively high concentrations of organic acids and HSS at the campaign end, or when samples have been analysed before solvent reclaiming has taken place, but that the ratio between the four organic acids are inconsistent. Acetate and formate are most often the dominant degradation product of those analysed, but it varies which one of the two is found in the highest concentrations. It therefore seems like process conditions play a very important role for which degradation pathways will take place within the solvent. The average concentration of liquid phase formate in Figure 3.1 is 2500 mg kg^{-1} (1000 h)$^{-1}$, whereas acetate, oxalate and glycolate both have an average of 800 and glycolate of 500 mg kg^{-1} (1000 h)$^{-1}$, respectively. All the compounds previously discussed are typical products of oxidative degradation. Thermal degradation products have been reported in many campaigns and include *N*-(2-hydroxyethyl)-2-imidazolidione (HEIA), which is a product of a carbamate polymerization reaction, and 2-(2-hydroxyethylamino)ethanol (HEEDA), which is a product of an addition

reaction. These degradation compounds are typically seen in lower concentrations than the oxidative degradation products. Measured concentrations of thermal (HEIA), as well as secondary oxidative degradation compounds (HEA, HEF, HEI, HEGly, HEPO, OZD, BHEOX) in MEA-campaigns are summarised in Table 3.8, the degradation product bicine is also presented here, assumed to be formed upon oxidation of DEA/MDEA or TEA derivatives (Gouedard et al., 2014; Lepaumier et al., 2009b). It is evident that secondary oxidative degradation compounds, formed when primary degradation compounds proceed to react, also occur in relatively high concentrations, especially HEF, HEGly and HEPO. The average concentrations of both HEGly and HEPO are twice that of formate when considering all campaigns, with about 5000 and 7000 mg kg^{-1} (1000 h)$^{-1}$, respectively. This same trend, of much higher concentrations of HEPO and HEGly in the solvent than formate, is seen also in studies with synthetic flue gas (Chahen et al., 2016; Knuutila et al., 2014b).

Thermal degradation compounds tend, however, to occur in lower concentrations. For example, the concentration of HEEDA are very low and rarely reported, and it has not been included in this table. The highest reported concentration of HEEDA is 246 mg L^{-1}, in one of the MEA 30wt% (*aq.*) pilot campaigns (Thompson et al., 2017a). Some pilot campaigns even observe that the concentrations of some thermal degradation compounds (HEIA and HEEDA) decline after an initial increase, throughout the operation time, making it apparent that they further react, or degrade themselves (Moser et al., 2020; Thompson et al., 2017a). A campaign using synthetic flue gas and 30wt% MEA (*aq.*), also saw OZD reaching a threshold concentration after a certain time of operation, and thereafter no further change, despite of the overall degradation rate sustaining (Chahen et al., 2016). Equally for Pz, thermal degradation products such as ethylenediamine and *N*-(hydroxyethyl)-piperazine have been found to initially increase and then decrease (Nielsen et al., 2013).

Inorganic compounds originating from the flue gas or construction material, like oxidised metal ions and elementary sulphur, are also found in the degraded solvents. Keeping track of dissolved metal concentrations allows for a simple assessment of corrosion of the equipment. The presence of NO_X, SO_2, and chlorine in the flue gas are the reasons why these are found in the solvent. The accumulation of these species is likely to influence degradation rates and mechanisms and therefore give valuable insights about the processes taking place within the degrading solvent. Figure 3.2 shows that there is no immediate correlation between operation time and the accumulation of iron in the MEA solvent.
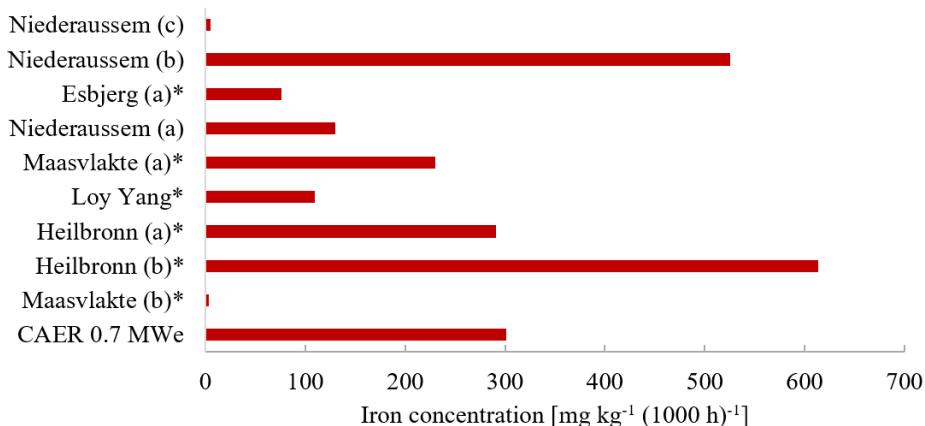
Figure 3.2: Accumulated concentrations of iron during pilot campaigns using MEA 30wt% (*aq.*). All references are given in Table 3.6. *Mass concentration in original publication converted to mass fraction under the assumption that $\rho = 1$ kg L^{-1}.

NO$_X$ are known to form nitrosamines with several amine species. Nitrosamines are toxic already in low concentrations and have therefore been of great concern for the operation of an amine-based CO$_2$ capture process. They are, however, readily degradable in sunlight (de Koeijer et al., 2013). The formation of nitrosamines in pilot plants has been a concern, both with NO$_X$ present in the flue gas and particularly when using secondary amines, which are known to be highly prone to the formation of nitrosamines (Fine, 2015; Knuutila et al., 2014a). A thorough lab-scale pilot test of addition of NO and NO$_2$ to MEA (primary amine) and diethanolamine (DEA; secondary amine) showed this, also testing the UV-radiation as a removal technology (Table 3.11) (Knuutila et al., 2014a; Knuutila et al., 2014b). Where measured, the concentrations of the nitrosamine NDELA is found in Table 3.8. Other nitrosamines, which are quantified less often than NDELA in the liquid phase and gas phase emissions in pilot campaigns are No-HEGly and NDMA. Morken et al. (2014) found 15 times more No-HEGly than NDELA, accounting for about half of the total nitrosamine (TONO) content. This finding indicates that the focus when studying nitrosamines in the amine solutions may not have been on the right compounds. Furthermore, a comparative study quantifying nitrosamines in identical solutions, a large variation in results from different laboratories has been reported (Fraboulet et al., 2016).

Table 3.6: An overview of the campaigns, which have studied degradation in MEA 30wt% (*aq.*) and which degradation product and dissolved inorganic compound concentrations have been reported. x = identified and quantified, nd = not detected, t= tentative

Campaign	Total HSS	Acetate	Formate	Glycolate	Oxalate	HEA	HEI	HEF	HEGly	HEIA	HEPO	BHEOX	OZD	NDELA	HEEDA	Bicine	DEA	Fe	Ni	Cl⁻	SO₄²⁻	NO₃⁻	Reference
Brindisi																		x					(Mangiaracina et al., 2014; Rieder et al., 2017)
CAER 0.1 MWth	x		x																	x	x	x	(Thompson et al., 2014)
CAER 0.7 MWe	x	x	x	x	x	x			x	x			x		x			x	x	x	x	x	(Thompson et al., 2017c; Thompson et al., 2017d)
Changchun	x		x		x																		(Feron et al., 2015; Feron et al., 2014)
Esbjerg (a)	x																	x					(Dhingra et al., 2017; Knudsen et al., 2009)
Esbjerg (b)			x		x	x	x	x	x		x	nd	nd								x		(da Silva et al., 2012)
Heilbronn (a)			x		x													x	x	x		x	(Dhingra et al., 2017; Rieder and Unterberger, 2013)
Heilbronn (b)	x	x	x	x	x													x		x	x	x	(Bazhenov et al., 2015; Rieder et al., 2017)
Longannet, MTU							x	x			x												(da Silva et al., 2012)
Loy Yang	x	x	x		x	x		t	x	t	x	x		nd	x	nd							(Artanto et al., 2012; Dhingra et al., 2017; Reynolds et al., 2015b)
Maasvlakte (a)																		x					(Dhingra et al., 2017; Khakharia et al., 2015a)
Maasvlakte (b)																		x					(Rieder et al., 2017)
Niederaussem (a)		x	x						x									x	x	x			(Moser et al., 2011a)
Niederaussem (b)		x	x															x	x	x	x		(Moser et al., 2018)
Niederaussem (c)		x	x		x				x						x			x	x	x	x	x	(Moser et al., 2020)
TCM (a)	x		x	x	x																		(Gorset et al., 2014; Morken et al., 2014)
TCM (b)	x	x	x	x	x	x	x	x	x	x	x	x	x	x	x	x	x				x	x	(Morken et al., 2017)
Tiller						x	x	x	x		x	x	x	x	x	x	nd						(da Silva et al., 2012; Mejdell et al., 2011)
SUM	8	7	12	4	10	4	7	5	5	5	5	4	7	3	5	3	3	10	5	7	8	7	

Table 3.7: An overview of the campaigns, which have studied degradation in various solvents (*aq.*) and which degradation product and dissolved inorganic compound concentrations have been reported.

Pilot	Solvent	Degradation comp.	Inorganics	Reference(s)
Austin	8m PZ	Formate, acetate, oxalate + more	Cr^{3+}, Fe^{2+}, Ni^{2+}, Cu^{2+}	(Nielsen et al., 2013)
CAER 0.1 MWth	CAER-B2	Total HSS and formate	SO_4^{2-}	(Thompson et al., 2014)
Esbjerg	CASTOR 2	Total HSS	S	(Knudsen et al., 2009)
Changchun	"blend 5"	Formate	SO_4^{2-}	(Feron et al., 2015)
TCM	S21	Total HSS and TONO		(Gorset et al., 2014)
TCM	S26	Total HSS and TONO		(Gorset et al., 2014)
Mikawa	"tertiary solvent A"	Formate, acetate and oxalate		(Saito et al., 2014)
Mikawa	"TS-1"	Formate		(Saito et al., 2014)

Table 3.8: Measured concentrations of degradation compounds in mg L^{-1}, which are not inorganic components nor organic acids, in post-combustion CO_2 capture pilot campaigns using 30wt% MEA, at the end of the campaign or right before reclaiming of the solvent. *Mass fraction in original publication converted to mass concentration under the assumption that $\rho = 1$ kg L^{-1}.

Campaign	HEA	HEF	HEI	HEGly	HEPO	BHEOX	OZD	HEIA	NDELA	Bicine	Reference
CAER 0.7 MWe			4800	1047			< 10	1712			(Thompson et al., 2017c)
Esbjerg (b)	590	440	440	7610	2320						(da Silva et al., 2012)
Longannet		8580	160				23				(da Silva et al., 2012)
Loy Yang			2030*			3400*	350*	960*		270*	(Reynolds et al., 2015b)
Niederaussem (a)								200*			(Moser et al., 2011a)
Niederaussem (c)							96*	380*			(Moser et al., 2020)
TCM (a)	4580	5200	2070	8000	11 140		150		31 µmol L^{-1}		(Morken et al., 2014)
TCM (b)	4963	5062	1826	18 922	18 788	274	82	181	4.9	62	(Morken et al., 2017)
Tiller	731	721	1758	7295	27 691	35.2	8.7		0.536	32.6	(da Silva et al., 2012)
Average/1000 h	1321	1505	839	4821	6940	672	131	435	1	32	

The reported concentrations of inorganic compounds quantified in the solvent during pilot campaigns are summarised in Table 3.6 for MEA and Table 3.7 for other amines and proprietary solvents. Some additional compounds, in addition to those given in Table 3.3 and Table 3.4, can be found quantified for the campaigns described in da

Silva et al. (2012), Morken et al. (2017), Thompson et al. (2014), Reynolds et al. (2015b), Rieder and Unterberger (2013) and Saito et al. (2014). Since these compounds are not widely analysed and thus cannot not be used in search for general trends, they are not given here.

Dhingra et al. (2017) already showed that the concentration of dissolved iron in the 30wt% (*aq.*) solvent tends to reach a sudden spike over a short period of time in four different pilot campaigns. It therefore comes as no surprise, that there is no correlation between operation time and iron concentration in the solvent when studying Figure 3.2. The campaigns at Niederaussem (c) (Moser et al., 2020) and at Maasvlakte (b) (Rieder et al., 2017) have significantly lower iron concentrations compared to the seven other campaigns where data is available, despite of at least the pilots in Maasvlakte, Loy Yang and Esbjerg all being constructed in stainless steel 304/316L (Dhingra et al., 2017). These numbers indicate that no severe corrosion had taken place during the campaign. Comparing the seven campaigns with relatively high iron concentrations, we may still not be able to say much about degradability and corrosivity of the system, since degradation and corrosivity do not increase linearly, instead we can expect a rapid spike after corrosion and solvent degradation have reached a certain level.

Table 3.9: Measured concentrations of inorganic compounds in mg kg^{-1}, including metals, in post-combustion CO_2 capture pilot campaigns using 30wt% MEA as solvent, at the end of the campaign or right before reclaiming of the solvent. *Mass concentration in original publication converted to mass fraction under the assumption that $\rho = 1$ kg L^{-1}.

Campaign	Nitrate (NO$_3^-$)	Sulphate (SO$_4^{2-}$)	Chloride (Cl$^-$)	Nickel (Ni)	Sulphur (S)	Reference(s)
CAER 0.1 MWth	720	3400	40			(Thompson et al., 2014)
CAER 0.7 MWe	1115*	3640*	193*	28		(Thompson et al., 2017c; Thompson et al., 2017d)
Esbjerg (b)		5100*				(da Silva et al., 2012)
Heilbronn (a)	150*	370*	10*	180*		(Rieder and Unterberger, 2013)
Heilbronn (b)	600*	820*	70*			(Bazhenov et al., 2014)
Niederaussem (a)			1800	200	100	(Moser et al., 2011a)
Niederaussem (b)	270	85	8300		20	(Moser et al., 2018)
Niederaussem (c)	2200	800	83	0	200	(Moser et al., 2020)
TCM (b)	1173*	70*				(Morken et al., 2017)

When comparing the degradation of the proprietary solvents in Table 3.10, specific characteristics of the solvent have to be compared to MEA. Formed degradation compounds are solvent specific, making it impossible to compare solvents of unknown amines to any benchmark by comparing single degradation components. However, the formation of HSS over time makes an interesting comparison since total HSS -measurement takes into account all different HSS compounds that are present. For example, HSS formation rate appears to be halved with CAER-B2 compared to 30wt% MEA (*aq.*) under the same conditions in a 0.1 MWth pilot plant (Thompson et al., 2014), whereas when CASTOR-2 is compared to 30wt% MEA (aq.), it is reduced to a fourth (Knudsen et al., 2009). In "Blend 5" tested at Changchun, the HSS formation rate is more or less the same as for 30wt% MEA (*aq.*) (Feron et al., 2015). It should be remembered that comparing total HSS, or solvent make-up-rate, discussed earlier, does not tell anything about the formation of potentially toxic degradation compounds or the formation of volatile degradation products, which can have a huge effect on the design of emission countermeasures and monitoring emissions. A detailed understanding of the degradation compounds formed for all amines is always needed.

Table 3.10: Accumulated concentrations of degradation compounds and sulphate during pilot campaigns using other solvents and blends than MEA 30wt%. *Mass concentration in original publication converted to mass fraction under the assumption that $\rho = 1$ kg L^{-1}. **Sum of formate, oxalate and acetate.

Pilot	Solvent	HSS [mg kg^{-1} (1000 h)$^{-1}$]	Formate [mg kg^{-1}]	Sulfate (SO$_4^{-2}$) [mg kg^{-1}]	Reference(s)
Austin	8m Pz	5648**	3273		(Nielsen et al., 2013)
CAER 0.1 MWth	CAER-B2	22 162	1694	2929	(Thompson et al., 2014)
Changchun	Blend 5	4085	215	980	(Feron et al., 2015)
Esbjerg	CASTOR-2	4000			(Knudsen et al., 2009)
Mikawa	Tertiary solvent A	313*	5*		(Saito et al., 2014)
Mikawa	TS-1	644*			(Saito et al., 2014)
TCM	S21	28 mmol/mg			(Gorset et al., 2014)
TCM	S26	6 mmol/mg			(Gorset et al., 2014)

Table 3.11: An overview of some relevant pilot studies using synthetic flue gas and aqueous amine solutions.

Pilot	Solvent	Time [h]	Compounds studied	Campaign focus	Reference(s)
Austin (SRP)	8m Pz	1350	Formate, oxalate, acetate, Cr^{3+}, Fe^{2+}, Ni^{2+}, Cu^{2+} + more		(Nielsen et al., 2013)
IFPEN	30wt% MEA	1700	Formate, glycolate, acetate, SO_4^{2-}, NO_3^-, NO_2^-, HEGly, DEA, OZD, HEF, HEA, HEI, HEPO + more	Study MEA degradation and predict degradation product emissions.	(Chahen et al., 2016)
Gløshaugen	30wt% MEA	990	Formate, NO_3^-, HEGly, DEA, OZD, HEF, HEPO, HEA, NDELA		(Knuutila et al., 2014a; Knuutila et al., 2014b)
Gløshaugen	50wt% DEA	410	OZD, HEF, HEPO, HEA, HEI, NDELA	Study formation and destruction of nitrosamines.	(Knuutila et al., 2014a; Knuutila et al., 2014b)

4.2 Emissions

In a CO_2 capture plant, it can be distinguished between three different types of emissions; gas-phase (vapour), liquid entrainment, and aerosol/mist emission (Knudsen et al., 2013; Spietz et al., 2018). Factors influencing the gas-phase emission are the volatility of the amine, CO_2 loading, and gas temperature. Often, a well-designed water wash is enough to minimise these emissions. Liquid entrainment emissions are liquid droplets that are carried by the gas flow, however, water wash sections can remove these. Aerosols and mist are small droplets suspended in the gas. The formation of these depend to a large extent on the flue gas composition upstream the CO_2 capture plant and on the capture plant's operation conditions (Mertens et al., 2015) and presence of condensation nuclei (<1 μm) as for example particulate matter, soot, SO_2, SO_3, NO_2 or H_2SO_4 (Mertens et al., 2012; Moser et al., 2015; Spietz et al., 2018). When formed, mist penetrates wash sections and conventional demisters, and therefore, additional mitigation techniques are required.

Several studies have been conducted in the last years to better understand and control emissions and mist/aerosol formation. A summary of the components contained in emissions can be found in Table 3.12. The table shows that the most commonly monitored emission is the solvent amine, followed by ammonia. Ammonia is one of the primary degradation compounds of MEA and is highly volatile. Nitrosamine concentrations are also often monitored due to their harmful nature. Concentration of nitramines in water wash have also been measured, but in both of them the nitramines

were below the detection limit in the water wash water (Khakharia et al., 2014a; Morken et al., 2014). Further volatile degradation compounds, such as allylamines, (form)aldehydes, and some ketones, have been studied only in a few campaigns.

Table 3.12: Emissions monitored at different pilot locations/campaigns. Emission monitoring given here does not necessarily mean that concentrations of emissions are published.

Pilot plant	Solvent amine	NH$_3$	Nitrosamine	Aldehydes	Alkylamine	Nitramine	Ketones	Reference(s)
CAER 0.7 MWe	x	x	x	x			x	(Thompson et al., 2017a; Thompson et al., 2017d)
Esbjerg	x	x		x				(Khakharia et al., 2014b; Mertens et al., 2012; Mertens et al., 2013; Aas and da Silva, 2010)
Ferrybridge	x	x	x					(Fitzgerald et al., 2014)
Łaziska		x		x				(Spietz et al., 2018)
Maasvlakte	x	x	x			x		(da Silva et al., 2013; Khakharia et al., 2014a)
Mitsubishi		x						(Kamijo et al., 2013)
MTU - Brevik	x	x	x					(Knudsen et al., 2014)
MTU - Longannet	x							(Graff, 2010)
MTU - NCCC	x	x			x			(Knudsen et al., 2013)
NCCC	x	x	x	x	x			(Dahlin et al., 2013)
Niederaussem	x							(Moser et al., 2014; Moser et al., 2013; Moser et al., 2017)
TCM	x	x	x	x		x	x	(Bade et al., 2014; Gorset et al., 2014; Lombardo et al., 2017; Morken et al., 2014; Morken et al., 2017)
Tiller	x	x	x		x			(Mejdell et al., 2011)
Toshiba	x							(Fujita et al., 2013)

The concentrations of the main degradation species detected in the gas phase can be found in Table 3.13, where it can be observed that there is no universal standard for the reporting of concentrations of compounds in emissions. Variation in practice, insufficient information and the different units makes it challenging to compare the results in detail. The MEA emissions are below one ppm in three out of the six campaigns. In the pilot campaigns with high MEA emissions, the emissions are

measured after the absorber and no water wash sections are used. For proprietary solvents, the solvent emissions are, in all cases, lower compared to those of MEA campaigns. This could mean that the proprietary solvent components are less volatile than MEA, or well-designed emission mitigation methods are used.

Ammonia emissions, as seen in Table 3.13, are larger than MEA emissions due to the high volatility of ammonia. Also ammonia emissions can be controlled with water wash systems, partly explaining the lower emissions at TCM, Tiller, Maasvlakte and Mitsubishi compared to CAER. Furthermore, as the ammonia concentrations are often at ppm-levels in the gas phase, it is an attractive compound to monitor as a sign of degradation. Proprietary solvents seem to degrade less to ammonia as, in all cases, the ammonia emissions are significantly lower than those of MEA. However, since ammonia is highly volatile, the ammonia emissions are very dependent on the operating time, temperatures in the water wash sections and process conditions. The solvent degradation also influences emissions. As solvent degradation increases, the emission of ammonia has been reported to increase in MEA (Mertens et al., 2012; Mertens et al., 2013). However, no dedicated studies were found looking at the effect of degradation on emissions.

As seen in Table 3.13, nitrosamines are generally observed only in the lower ppm to ppb range. The same is true for aldehydes with one exception: a laboratory pilot study by Chahen et al. using 30wt% MEA (*aq.*) and a synthetic flue gas. In this study, acetaldehyde was measured in the range of 1 mg m^{-3}. This is a nearly 80 times higher concentration than formaldehyde in this particular study. This study also found relatively high concentrations of ethylene glycol and the nitrosamine NDMA, but these in the range of <0.5 mg m^{-3} (Chahen et al., 2016).

Based on the pilot results it is clear that for MEA, the wash water section can limit the MEA emission to a few hundred ppb, ammonia in the low ppm range, methylamine at low ppb range in case no mist is present (Gjernes et al., 2017; Lombardo et al., 2017; Morken et al., 2017). Furthermore, in these cases, there is no observation of nitrosamine and nitramine emissions over the detection limit. The solvent emissions of the tested proprietary solvents can be controlled to similar levels as seen with 30wt% MEA (*aq.*). This is in line with reported numbers for commercially available proprietary solvents (Feron et al., 2020; Singh and Stéphenne, 2014).

Table 3.13: Concentrations of emissions in different campaigns and locations, where given in literature. *Reclaiming was, or may have been performed in the duration of the campaign. [a] Reduced after water wash and BDU. [b] Reduced with ACC™ emission control system. [c] Reduced by cooling lean temperature. [d] Reduced by higher lean temperature and two-stage water wash [e] μmol m_N^{-3} nd = not detected.

Pilot plant	Solvent	Solvent amine	NH$_3$	TONO	Formaldehyde	Reference(s)
Mitsubishi [ppm]	MEA		14			(Kamijo et al., 2013)
TCM [ppm]	MEA	<1	20	$<8\times10^{-8}$		(Morken et al., 2014)
Tiller [ppm]	MEA	<0.4	20	[d]		(Mejdell et al., 2011)
CAER 0.7 MWe* [ppmV]	MEA	5-1385	12-282	< LOQ	35-73	(Thompson et al., 2017a; Thompson et al., 2017d)
MTU - NCCC [ppmV]	MEA	10-50 / 0[b]	10-40			(Knudsen et al., 2013)
NCCC [ppmV]	MEA (water wash)	2.13	1.74		0.0031	(Dahlin et al., 2013)
NCCC [ppmV]	MEA (acid wash)	3.02	4.75		0.0020	(Dahlin et al., 2013)
Ferrybridge* [mg m_N^{-3}]	MEA			0.020		(Fitzgerald et al., 2014)
Maasvlakte [mg m_N^{-3}]	MEA	250 / 1[a]	10-70	(5 to 75)$\times10^{-6}$		(da Silva et al., 2013; Khakharia et al., 2014a)
MTU - Longannet* [mg m_N^{-3}]	MEA	<4	50-80			(Graff, 2010)
Łaziska [ppm]	AEEA		27-50		0.11	(Spietz et al., 2018)
Mitsubishi [ppm]	KS-1		<1.5			(Kamijo et al., 2013)
MTU - NCCC [ppmV]	ACC novel solvent	20 / 0[b]	1-4			(Knudsen et al., 2013)
Toshiba [ppmV]	TS-1		18 / 5.6[c]			(Fujita et al., 2013)
Esbjerg [mg m_N^{-3}]	CASTOR/CESAR	0.02-0.7			0.059-1.1	(Khakharia et al., 2014b; Mertens et al., 2012; Aas and da Silva, 2010)
MTU - Breivik [mg m_N^{-3}]	S26	<0.46[b]	<4.0[b]	<0.03[b,d]		(Knudsen et al., 2014)
MTU - TCM* [mg m_N^{-3}]	S21	0.031	0.14	<0.83[e]		(Gorset et al., 2014)o
MTU - TCM* [mg m_N^{-3}]	S26	0.09[b]	0.01[b]	<0.05[e]		(Gorset et al., 2014)o
NCCC [ppm]	Pz	<1[d]	3.1	<0.34[e]		(Akinpelumi et al., 2019)
TCM* [mg m_N^{-3}]	S21	0.5	3.1	<0.34[e]		(Gorset et al., 2014)o
TCM* [mg m_N^{-3}]	S26	1.8 / 0.09[b]	1.9 / 0.01[b]	<0.02[e]		(Gorset et al., 2014)o

As mentioned earlier, the presence of mist can increase the emissions significantly and thus, extensive work has been conducted to study aerosol emissions, their formation, mechanisms, and countermeasures. Mist can be formed via two different nucleation mechanisms, homogeneous and heterogeneous (Kolderup et al.) and both mechanisms are important. Avoiding homogeneous nucleation by removing SO_3 and avoiding H_2SO_4 will not entirely eliminate aerosol formation, since heterogeneous nucleation and growth by condensation have been reported to be the main mechanisms leading to aerosol-based emissions in a CO_2 capture column (Khakharia et al., 2015a; Kolderup et al.; Moser et al., 2011b; Moser et al., 2014). Also, both the concentration of particles and sulphuric acid has an impact on the formation of aerosol emissions (Khakharia et al., 2015a; Khakharia et al., 2013). For cases with low particle numbers before the absorber, typically seen for natural gas-fired power plants, mist is often not detected (Morken et al., 2017). For TCM, a 500 000 particles cm^{-3} was deemed acceptable to stay below the local emission permit (Lombardo et al., 2017). Several publications discuss the influence of flue gas cleaning before the absorption column (Khakharia et al., 2013; Knudsen et al., 2013) and different process changes (Khakharia et al., 2015a; Khakharia et al., 2013; Khakharia et al., 2014b; Moser et al., 2011b; Moser et al., 2014; Moser et al., 2013) as the flue gas composition and operational settings influence the particle number, size, size distribution, composition, and physical/chemical properties of the mist

Effects of water wash temperature, acid wash, dry bed, flue gas pretreatment, and wet electric precipitator have been tested alone or in coupled operation. They all showed a reduction up to an order of magnitude of amine emission (Moser et al., 2014). A wet electrostatic precipitator (WESP), often seen as an option to avoid mist formation, could also cause aerosol formation by increasing the number concentration of ultra-fine particles or droplets in the flue gas (Moser et al., 2015). A gas-gas heater installed up- or downstream of the wet flue gas desulphurisation (WFGD) prevents amine mist formation inside the absorber (Harsha et al., 2019; Khakharia et al., 2015b; Khakharia et al., 2014b; Lombardo et al., 2017; Majeed et al., 2017; Mertens et al., 2015).

Having a dry bed between the absorber and the water wash reduces the emission of amine compounds (Moser et al., 2014). Furthermore, lean MEA inlet temperature to the absorber influencing the absorber temperature profile and flue gas temperature at the top of the absorber, flue gas temperature difference over the washing section, flow rate of water in wash sections as well as the amount of make-up water to these sections have a significant impact on the amine and ammonia emissions (Akinpelumi et al., 2019; Lombardo et al., 2017; Spietz et al., 2018). Demisters are an efficient way to reduce amine emissions when mist is present, and further testing of impaction candles and high efficiency demisters is proposed to identify options with low pressure drop and high efficiency (Lombardo et al., 2017). Finally, proprietary emission control concept (ACC), combining a novel absorber design to prevent amine mist formation and a final pH-controlled wash stage is reported to reduce the emission

of alkylamines, ammonia and solvent amine(s) (Bade et al., 2014; Knudsen et al., 2013).

4.3 Analytical Methods

For the monitoring of both the solvent degradation and the emissions in the pilot plants, many different analytical methods are being deployed. The amount of information given about these, however, is varying. How much information is given can for example be dependent on the purpose of the given paper/report, if the analysis is done internally or externally, or if the specific method used is disclosed or not. In this section, the analytical methods that are most frequently deployed in the pilots and how they are used will be presented. These include FT-IR, LC-MS, GC-MS, IC, titration, PTR-MS and ICP-MS/-OES. Note that results from papers that only reports their findings, without stating which analytical method is being used, are not included.

When monitoring the emissions from the pilot plants, online FT-IR is often the preferred method (Artanto et al., 2012; Bade et al., 2014; de Koeijer et al., 2011; Fitzgerald et al., 2014; Khakharia et al., 2013; Khakharia et al., 2014a; Knudsen et al., 2013; Knudsen et al., 2014; Mertens et al., 2012; Moser et al., 2018; Thompson et al., 2017a). Here, the FT-IR is used to analyse the emissions from the absorber, and can detect and quantify various amines and aldehydes, water content, as well as standard inorganic components such as NH_3, SO_2, NO_X, etc.. The detection limit is usually 1 ppmv. When the solvent amine emission concentration dips below this limit, manual sampling campaigns have been conducted (Gorset et al., 2014).

LC-MS has also been frequently used to monitor emissions in many of the pilot plants (Bade et al., 2014; da Silva et al., 2012; Fujita et al., 2013; Khakharia et al., 2014a; Knudsen et al., 2013; Knudsen et al., 2014). This is however not done online, but through absorption in impingers. Different absorption medias are utilised, but sulphuric and sulfamic acid are the most common. At Norcem, DNPH cartridges was also used (Knudsen et al., 2014). These can capture condensate and aldehydes/ketones which is not captured in the acid absorbers. Sampling in the impingers are usually done for 1-2 hours. The impinger methods used are often well documented in the publications. The LC-MS results are, also, often used to verify FT-IR results. As manual sampling combined with LC-MS analyses is based on up-concentrating the degradation compounds into the impingers, it can be used to detect compounds present in low concentrations, and can therefore give a more overall picture of the composition of the emissions. LC-MS is also used to study the solvent degradation and quantify degradation components (Knuutila et al., 2014a; Moser et al., 2020; Thompson et al., 2017c). Unfortunately, in general very little information is given about the LC-MS methods used by the pilot plants.

Like LC-MS, GC-MS is also used to monitor both the emissions and the solvent degradation in various pilots (Artanto et al., 2012; da Silva et al., 2012; Fujita et al., 2013; Knudsen et al., 2013; Knudsen et al., 2009; Moser et al., 2011b; Thompson et al., 2017c). The samples are often the same as the ones analysed with LC-MS, and so these two methods combined gives a comprehensive overview of the sample composition. But like with LC-MS, the methods used is in most cases under reported or not reported at all. There are however exceptions, where the method used is thoroughly rendered (Reynolds et al., 2015b).

Compared to the methods mentioned above, the information gained from IC is restricted to ionic species. This results in that that its use varies a lot in the different pilot plants. In some cases, it is used to analyse HSS in the solvent samples (da Silva et al., 2012; Fitzgerald et al., 2014; Moser et al., 2020; Reynolds et al., 2015b; Thompson et al., 2017c; Thompson et al., 2017d; Thompson et al., 2014), while in some cases only inorganic anions such as sulphate is analysed (Knuutila et al., 2014a; Mertens et al., 2015; Moser et al., 2020). How well the methods are rendered seems to depend on where the analysis has been conducted. For the ones performed in-house, the method is described well, while when external laboratories have been used it is usually not described.

Titration is a quick and cheap method, but is nevertheless not extensively used in the pilots. Under titration measurements of total amine concentration (total alkalinity), masurement of the CO_2-loading, or measurement of HSS is included. When titration is used to analyse samples from the pilots, many or all of these are usually performed (Fitzgerald et al., 2014; Knudsen et al., 2014; Knudsen et al., 2009; Moser et al., 2011a).

The last two analytical methods included is PTR-MS and ICP-MS/-OES. PTR-MS is used in some of the plants as an online analysis tool for amine concentration and volatile components (Bumb et al., 2017; Moser et al., 2014). In these cases, it is often used to study volatile degradation products in the emission stream (Fujita et al., 2013). ICP-MS/-OES is an offline method, and is used by some pilots to detect and quantify metals and trace elements in a solution (Knudsen et al., 2014; Moser et al., 2020; Thompson et al., 2017c). Little information is shared about the instruments or methods being used for both these analyses.

5 Discussion and Recommendations

Most of the pilots are not in continuous operation. Furthermore, the different campaigns typically focus on various aspects of the process to reduce risk, costs, and close knowledge gaps. As the pilot campaigns are costly, data on a lot of different aspects of the process is collected simultaneously. The campaign's focus may be on process performance of a promising solvent or solvent blend, and large changes in the process parameters are done throughout the campaign duration. At the same time

as the process itself is optimised, data related to solvent degradation can be collected for stability assessment. These different focus points of the different campaigns make it more challenging to compare them to one another, when it comes to degradation and emission. Degradation depends on many factors as well as process parameters, including flue gas composition, temperatures in the absorber and desorber, construction material of the plant, and the solvent residence times in the absorber and desorber. This means that for a clear and unambiguous comparison, all these factors need to be taken into consideration, when they mostly are reported in varying detail, depending on the campaign emphasis. Finally, the reported degradation, the analytical methods, sampling frequency and type of compounds analysed, also vary a lot from campaigns to campaign. All these factors lead to a situation, where a comparison of degradation in different campaigns, even when operated with the same solvent, is intricate. The gathered learning from all these campaigns together does, however, give an overall picture of the degradation that has been and can be observed when operating a post-combustion CO_2 capture plant using MEA.

Below, the main findings related to flue gas treatment, degradation and emission are discussed.

Flue gas pretreatment. Sufficient flue gas pretreatment before entering the absorber column plays a vital role in the solvent stability in connection with coal-fired power plants. For example, the pilot plants in Niederaussem, Esbjerg and Heilbronn, which have extensive setups for pretreatment, have much lower formation rates of HSS than those, like Loy Yang and the 0.1 MWth CAER pilot, where more limited flue gas pretreatment is performed. There is a good agreement that removing SO_X, NO_X and particulates from the flue gas a positive effect on solvent degradation and therefore emissions of degradation compounds.

Solvent degradation. When reading the summaries of degradation and corrosion products quantified in Table 3.6 to Table 3.10 it is important to keep in mind that a plethora of process conditions may play decisive roles in the degradation mechanisms and rates that take place. Usually, limited information is reported when it comes to changes in process conditions during the campaign, and detailed process design, like residence time of the solvent in the absorber sump. Knowledge of these details could give additional insights on what influences solvent stability.

Organic acids have often been used as an indication of MEA degradation, but no studies have yet found a direct correlation between their concentration and the total degradation in an arbitrary MEA campaign. In addition to the organic acids being precursors for the formation of other degradation compounds, HEF being formed from formic acid, HEA from acetic acid etc., different campaigns have showed different acids as primary degradation products. At the pilot plant in Niederaussem, acetate is measured in higher concentrations than formate (Moser et al., 2011a; Moser et al., 2018; Moser et al., 2020), but in the Loy Yang and TCM pilots the opposite is

seen (Morken et al., 2017; Reynolds et al., 2015b) (Figure 3.1). Furthermore, as some (thermal) degradation compounds tend to increase in concentration in the beginning of a campaign and then steadily decrease later in the campaign (Moser et al., 2020), reacting to further degradation compounds or decomposing, it is important to be aware of what one is measuring. These compounds should therefore not be used for assessing the state of the amine solvent.

Because organic acids react further to form other degradation compounds throughout the operation time, their concentrations do not always increase linearly. It is less common to quantify other degradation compounds, since they typically require more complicated analytical methods, which are time-consuming and costly. Based on the results of the studied pilot campaigns, there doesn't seem to be any single degradation product that quantitatively correlates with the overall amine degradation. Despite of some of the HSS being of inorganic origin, coming from the flue gas itself (SO_4^{2-}, Cl^-, NO_3^-, etc.) and some from the degradation of the amine, it is still an important parameter so consider when assessing the state of the solvent. It has been seen that despite of extensive flue gas pretreatment, remaining concentrations of inorganic contaminants increases steadily with operation time (Thompson et al., 2017c). However, in several cases the total amount of heat stable salts (HSS) in the solvent increases nearly linearly throughout the operation time, regardless of other process parameters and this might give a good indication of the solvent degradation rate (Feron et al., 2015; Reynolds et al., 2015b; Thompson et al., 2014). The total amount of HSS is often not given in articles describing pilot campaigns and instead, the monitoring focuses on selected organic acids. In these cases, knowing how well the monitored compounds describe the solvent's degree of degradation can be challenging. If one still wants to study single organic acids, an assessment should probably still be made to the total amount of HSS.

Also, although organic acids are some of the typical main degradation products of MEA, this is most likely not the same for other amines. Despite of these products often being denominated as *primary* degradation products, this does not state anything about their importance, merely the order in which they are formed. Using an organic acid, such as i.e. formic acid as a proxy to assess overall degradation should therefore be done with caution, regardless of which amine is studied. Nevertheless, the concentrations of heat stable salts and inorganics from the flue gas and corrosion can still indicate the properties and stability of the different solvents. Iron is a frequently monitored inorganic species in the solvent and a correlation between ammonia formation and iron concentration in the solvent has been clearly observed (Dhingra et al., 2017). Despite of this correlation, it is not clear which effects cause this, whether it is the increasing corrosivity with increasing degradation or an increased iron solubility caused by pH changes (Nordstrom and Alpers, 1997) or iron complex formation with a more degraded solution. A combination of these explanations is also likely. An explanation for the rapid spike observed both for

ammonia formation and iron concentration has not been found. Further and thorough analytical work will be needed to fully understand these phenomena in degraded amine solvents.

Most studies choose a factor to compare a new solvent blend to benchmark 30wt% MEA (*aq.*), like total concentration of HSS or total concentration of nitrosamines in the solvent (TONO). These give insights about specific degradation properties of the solvent and is useful for solvent stability assessment. Comparing single property of solvent, like TONO-concentration can be a way to address specific issues, like safety of the operators. However, it does not say anything about the overall solvent stability. Comparing the amount of dissolved inorganic components in the same pilot but for different solvent systems may indicate the suitability of a certain solvent in certain application (Feron et al., 2015; Thompson et al., 2014).

There is no guideline for how to monitor amine degradation in a carbon capture plant. This has resulted in the use of various methods in different pilot campaigns, with no common consensus in terms of what compounds to analyse for and how this is done. A determining factor in the choice of analytical method is often the availability and cost of the analytical methods. Some methods might be more readily available but give less information, for example total alkalinity, while others are very costly and unavailable, and might therefore not be chosen, like for example LC-MS.

Combination of measurement of NH_3 by FT-IR combined with determination of NH_3 concentrating in the water wash, as well as total HSS concentration in the liquid solvent could be a relatively easy and solvent independent way of monitoring the state of degradation in the plant. It should be remembered, that specific analyses should be performed to monitor the accumulation of toxic and harmful degradation compounds in the solvent loop. Additionally, specific methods to monitor the emission of volatile degradation compounds and solvent amine will always be needed.

Analytical methods. Few of the analytical methods applied in monitoring the amine degradation have been sufficiently validated. Validation of a method ensures that the analytical system used is suitable for its purpose and that it provides legitimate data. Ideally, an analytical method should be validated against another method, which is independent of its measurement principle. For instance, the quantification of MEA by LC-MS should agree with the concentration measured by cation IC, as these methods depend on entirely different measurement principles.

Furthermore, in many cases, very little information has been published regarding the parameters of the analytical methods used, e.g. flow rate and retention time, in the chromatographic methods. This is unfortunate, as it makes it impossible for others to validate the reliability of the claims given regarding the results of these analyses. In combination with, and maybe as a result of, the restricted information given about the analytical methods is the under-reporting of uncertainties and detection limits. Both

of these parameters are important in handling the data given, and the lack thereof therefore impairs the results.

It is widely seen that some external laboratories are processing the samples from different campaigns and pilots. In these cases, accredited, validated methods for the specific compounds in question are crucial. Use of round robin tests could be an effective way to ensure the consistence of the reported analyses of degradation compounds. Published round robin tests have, for example, highlighted the challenges in analyses of nitrosamines (Fraboulet et al., 2016).

Emissions. As emissions are site and solvent specific, direct comparison of actual emissions from different pilot plants is therefore not an option. The emission of highly volatile degradation compounds, like ammonia, can usually be controlled with water or acid wash (Knudsen et al., 2013; Mertens et al., 2013). The same applies to many solvent compounds, as long as the aerosol formation is limited. For example, the gaseous MEA emission could be abated by single well-designed water wash (Mertens et al., 2012; Mertens et al., 2013). In the presence of aerosol, the solvent emissions can be significant, and aerosol mitigation techniques are needed to reduce the emissions to acceptable levels. The emissions through aerosol particles can be reduced by eliminating the mist precursors upstream from the absorber, or by controlling the growth of the aerosol particles in the absorber. The proposed ways to control the aerosol growth, are reducing the temperature gradients in the absorber or accelerating the particle growth to form large, easily removable aerosols (Knudsen et al., 2013; Mertens et al., 2013; Moser et al., 2014). Operation of the presence of some upstream equipment like wet flue gas desulphurisation unit, gas heater, and wet electrostatic precipitator can have a crucial influence on the aerosol formation (Mertens et al., 2015; Moser et al., 2015). In general, the installation of a Brownian demister unit reduces the aerosol emissions (Bade et al., 2014; Khakharia et al., 2014a; Lombardo et al., 2017).

Emissions of both the solvent itself and its degradation products has to be considered and monitored, but the available information about the pilots and performed campaigns varies. For example, data related to solvent emissions and descriptions of emission reduction technologies are often missing. Besides, the emission reduction technologies used are sometimes proprietary, and details are therefore not given in the publication. A reliable monitoring strategy is required to keep track of the degradation and emission in pilot-plants. There is, however, no set standard to follow. Instead, multiple analytical methods are being used, and this choice is often dependent on the desired information, available resources and know-how as well as the availability of equipment.

Finally, all full-scale plants will need an emission permit, and these depend on local regulations where the plant is located. In Norway, for example, the emission permit for TCM regulates the emission levels for solvent amine, alkylamines aldehydes and

ammonia (Morken et al., 2014). The regulation also includes nitrosamine and nitramine.

The following take-home-messages and trends summarise the main findings:

- Flue gas pretreatment including SO_X, NO_X and particle removal significantly increases solvent stability. Pilot plants containing an excessive flue gas pretreatment system tend to experience significantly less degradation than those with a limited or no such system. However, the type of flue gas pretreatment also impacts the emissions, as some flue gas pretreatments can increase the risk of amine mist formation by increasing the presence of nuclei in the flue gas.
- Monitoring of any single known degradation compound is not a universal way of assessing solvent stability, not even for the comprehensively studied MEA. The organic compounds formate and acetate, for example, seem to vary in their relative abundance in different pilot plants and campaigns. Some compounds even decrease in concentration after a certain time of operation and therefore, the monitoring of single compounds should be done with caution and this knowledge in mind.
- A relatively simple, and to some extent, solvent independent method to monitor solvent degradation could be a combination of measurement of gas-phase NH_3 by FT-IR with total HSS concentration in the liquid solvent. However, monitoring of NH_3 or the total HSS concentration is not always the best solution. But for solvents that produce NH_3 and HSS as one of their primary degradation compounds,such as MEA, this is a straight-forward and informative monitoring approach. Knowledge of the main degradation compounds are therefore always needed.
- There is no universal standard for measurement of emission from large-scale capture plant. An international standard is also lacking for sampling, conditioning, and analysis of volatile trace elements in flue gas, leaving the CO_2 capture plant (Moser et al., 2013). These issues should be addressed in future works and development of such a standard would enhance the comparability and certainty in the measurements on site.
- There is a general lack in reporting of analytical methods and their uncertainties, when emission and degradation data is published. To facilitate reproducible and comparable results, documented methods should be applied for the quantification of species both in gas and liquid phase, including all parameters for chromatographic analyses.

Acknowledgement

References

Akinpelumi, K., Saha, C., Rochelle, G.T., 2019. Piperazine aerosol mitigation for post-combustion carbon capture. International Journal of Greenhouse Gas Control 91, 102845.

Aronu, U.E., Lauritsen, K.G., Grimstvedt, A., Mejdell, T., 2014. Impact of heat stable salts on equilibrium CO_2 absorption, Energy Procedia. Elsevier Ltd, pp. 1781-1794.

Artanto, Y., Jansen, J., Pearson, P., Do, T., Cottrell, A., Meuleman, E., Feron, P., 2012. Performance of MEA and amine-blends in the CSIRO PCC pilot plant at Loy Yang Power in Australia. Fuel 101, 264-275.

Azzi, M., Day, S., French, D., Halliburton, B., Jackson, P., Lavrencic, S., Riley, K., Tibbett, A., 2010. CO_2 Capture Mongstad-Project A-Establishing sampling and analytical procedures for potentially harmful components from post-combustion amine based CO_2 capture Task 2: Procedures for Manual Sampling.

Bade, O.M., Knudsen, J.N., Gorset, O., Askestad, I., 2014. Controlling amine mist formation in CO_2 capture from Residual Catalytic Cracker (RCC) flue gas, Energy Procedia. Elsevier Ltd, pp. 884-892.

Bazhenov, S., Rieder, A., Schallert, B., Vasilevsky, V., Unterberger, S., Grushevenko, E., Volkov, V., Volkov, A., 2015. Reclaiming of degraded MEA solutions by electrodialysis: Results of ED pilot campaign at post-combustion CO_2 capture pilot plant. International Journal of Greenhouse Gas Control 42, 593-601.

Bazhenov, S., Vasilevsky, V., Rieder, A., Unterberger, S., Grushevenko, E., Volkov, V., Schallert, B., Volkov, A., 2014. Heat Stable Salts (HSS) Removal by Electrodialysis: Reclaiming of MEA Used in Post-combustion CO_2-Capture. Energy Procedia 63, 6349-6356.

Bello, A., Idem, R.O., 2005. Pathways for the formation of products of the oxidative degradation of CO2-loaded concentrated aqueous monoethanolamine solutions during CO2 absorption from flue gases. Industrial & engineering chemistry research 44, 945-969.

Bernhardsen, I.M., Trollebø, A.A., Perinu, C., Knuutila, H.K., 2019. Vapour-liquid equilibrium study of tertiary amines, single and in blend with 3-(methylamino) propylamine, for post-combustion CO2 capture. The Journal of Chemical Thermodynamics 138, 211-228.

Blachly, C., Ravner, H., 1963. The effect of trace amounts of copper on the stability of monoethanolamine scrubber solutions. Naval Research Lab Washington DC.

Brigman, N., Shah, M.I., Falk-Pedersen, O., Cents, T., Smith, V., De Cazenove, T., Morken, A.K., Hvidsten, O.A., Chhaganlal, M., Feste, J.K., Lombardo, G., Bade, O.M., Knudsen, J., Subramoney, S.C., Fostås, B.F., de Koeijer, G., Hamborg, E.S., 2014. Results of Amine Plant Operations from 30 wt% and 40 wt% Aqueous MEA Testing at the CO2 Technology Centre Mongstad. Energy Procedia 63, 6012-6022.

Brostrøm, A., Kling, K.I., Hougaard, K.S., Mølhave, K., 2020. Complex Aerosol Characterization by Scanning Electron Microscopy Coupled with Energy Dispersive X-ray Spectroscopy.

Brown, N., Heller, G., Staab, G., Silverman, T., Kupfer, R., Brown, R., Brown, A., 2017. Novel Advanced Solvent-based Carbon Capture Pilot Demonstration at the National Carbon Capture Center. Energy Procedia 114, 1075-1086.

Bui, M., Gunawan, I., Verheyen, V., Feron, P., Meuleman, E., 2016. Flexible operation of CSIRO's post-combustion CO2 capture pilot plant at the AGL Loy Yang power station. International Journal of Greenhouse Gas Control 48, 188-203.

Bumb, P., Patkar, P.E.A., Mather, R., Kumar, R., Hall, J., Morton, F., Anthony, J., 2017. Field Demonstration of Advanced CDRMax Solvent at the US-DOE's National Carbon Capture Centre and the CO2 Technology Centre Mongstad DA, Norway, Energy Procedia. Elsevier Ltd, pp. 1087-1099.

Burkart, J., Steiner, G., Reischl, G., Moshammer, H., Neuberger, M., Hitzenberger, R., 2010. Characterizing the performance of two optical particle counters (Grimm OPC1.108 and OPC1.109) under urban aerosol conditions. Journal of Aerosol Science 41, 953-962.

Byers, R.L., Davis, J.W., White, E.W., McMillan, R.E., 1971. Computerized method for size characterization of atmospheric aerosols by the scanning electron microscope. Environmental Science & Technology 5, 517-521.

Chahen, L., Huard, T., Cuccia, L., Cuzuel, V., Dugay, J., Pichon, V., Vial, J., Gouedard, C., Bonnard, L., Cellier, N., Carrette, P.-L., 2016. Comprehensive monitoring of MEA degradation in a post-combustion CO_2 capture pilot plant with identification of novel degradation products in gaseous effluents. International Journal of Greenhouse Gas Control 51, 305-316.

Chi, S., Rochelle, G.T., 2002. Oxidative Degradation of Monoethanolamine. Industrial & Engineering Chemistry Research 41, 4178-4186.

Cousin, A., Cottrell, A., Huang, S., Feron, P.H.M., Lawson, A., 2012. Tarong CO_2 capture pilot plant. Energy Generation, 16-17.

Cousins, A., Wardhaugh, L., Cottrell, A., 2016. Pilot plant operation for liquid absorption-based post-combustion CO_2 capture. Elsevier Inc.

Cuccia, L., Dugay, J., Bontemps, D., Louis-Louisy, M., Vial, J., 2018. Analytical methods for the monitoring of post-combustion CO_2 capture process using amine solvents: A review. International Journal of Greenhouse Gas Control 72, 138-151.

Cuzuel, V., Brunet, J., Rey, A., Dugay, J., Vial, J., Pichon, V., Carrette, P.-L., 2014. Validation of a liquid chromatography tandem mass spectrometry method for targeted degradation compounds of ethanolamine used in CO_2 capture: application to real samples. Oil & Gas Science and Technology–Revue d'IFP Energies nouvelles 69, 821-832.

da Silva, E.F., Kolderup, H., Goetheer, E., Hjarbo, K.W., Huizinga, A., Khakharia, P., Tuinman, I., Mejdell, T., Zahlsen, K., Vernstad, K., Hyldbakk, A., Holten, T., Kvamsdal, H.M., Van Os, P., Einbu, A., 2013. Emission studies from a CO_2 capture pilot plant, Energy Procedia. Elsevier Ltd, pp. 778-783.

da Silva, E.F., Lepaumier, H., Grimstvedt, A., Vevelstad, S.J., Einbu, A., Vernstad, K., Svendsen, H.F., Zahlsen, K., 2012. Understanding 2-ethanolamine degradation in postcombustion CO_2 capture. Industrial & Engineering Chemistry Research 51, 13329-13338.

Dahlin, R.S., Landham, E.C., Kelinske, M.L., Wheeldon, J.M., Love, D.H., 2013. Amine Losses and Formation of Degradation Products in Post-Combustion CO_2

Capture, 38th International Technical Conference on Clean Coal & Fuel Systems 2013: The Clearwater Clean Coal Conference.

Davis, J., Rochelle, G., 2009. Thermal degradation of monoethanolamine at stripper conditions, Energy Procedia, pp. 327-333.

de Koeijer, G., Enge, Y., Sanden, K., Graff, O.F., Falk-Pedersen, O., Amundsen, T., Overå, S., 2011. CO2 Technology Centre Mongstad–Design, functionality and emissions of the amine plant. Energy Procedia 4, 1207-1213.

de Koeijer, G., Talstad, V.R., Nepstad, S., Tønnessen, D., Falk-Pedersen, O., Maree, Y., Nielsen, C., 2013. Health risk analysis for emissions to air from CO2 Technology Centre Mongstad. International Journal of Greenhouse Gas Control 18, 200-207.

Dhingra, S., Khakharia, P., Rieder, A., Cousins, A., Reynolds, A., Knudsen, J., Andersen, J., Irons, R., Mertens, J., Abu Zahra, M., Van Os, P., Goetheer, E., 2017. Understanding and Modelling the Effect of Dissolved Metals on Solvent Degradation in Post Combustion CO2 Capture Based on Pilot Plant Experience. Energies 10.

Diab, F., Provost, E., Laloué, N., Alix, P., Souchon, V., Delpoux, O., Fürst, W., 2012. Quantitative analysis of the liquid phase by FT-IR spectroscopy in the system CO2/diethanolamine (DEA)/H2O. Fluid Phase Equilibria 325, 90-99.

Eide-Haugmo, I., Lepaumier, H., da Silva, E.F., Einbu, A., Vernstad, K., Svendsen, H.F., 2011. A study of thermal degradation of different amines and their resulting degradation products, 1st Post Combustion Capture Conference, pp. 17-19.

Eliasson, J., Watson, I.M., Weber, K., 2016. Chapter 5 - In Situ Observations of Airborne Ash From Manned Aircraft, in: Mackie, S., Cashman, K., Ricketts, H., Rust, A., Watson, M. (Eds.), Volcanic Ash. Elsevier, pp. 89-98.

Enaasen, N., Zangrilli, L., Mangiaracina, A., Mejdell, T., Kvamsdal, H.M., Hillestad, M., 2014. Validation of a dynamic model of the brindisi pilot plant, Energy Procedia. Elsevier, pp. 1040-1054.

Feron, P., Conway, W., Puxty, G., Wardhaugh, L., Green, P., Maher, D., Fernandes, D., Cousins, A., Cottrell, A., Li, K., Shiwang, G., Lianbo, L., Hongwei, N., Hang, S., Jinyi, W., Shiqing, W., Dongfang, G., Maeder, M., Clifford, S., 2015. Comparative evaluation of a new liquid absorbent in a PCC pilot plant in China, PCCC3, Regina SK, Canada.

Feron, P., Conway, W., Puxty, G., Wardhaugh, L., Green, P., Maher, D., Fernandes, D., Cousins, A., Gao, S.W., Liu, L.B., Niu, H.W., Shang, H., 2014. Amine based post-combustion capture technology advancement for application in Chinese coal fired power stations. 12th International Conference on Greenhouse Gas Control Technologies, Ghgt-12 63, 1399-1406.

Feron, P.H.M., Cousins, A., Jiang, K., Zhai, R., Garcia, M., 2020. An update of the benchmark post-combustion CO_2-capture technology. Fuel 273, 117776.

Fine, N.A., 2015. Nitrosamine management in aqueous amines for post-combustion carbon capture.

Fitzgerald, F.D., Hume, S.A., McGough, G., Damen, K., 2014. Ferrybridge CCPilot100+ operating experience and final test results, Energy Procedia. Elsevier Ltd, pp. 6239-6251.

Fraboulet, I., Chahen, L., Lestremau, F., Grimstvedt, A., Schallert, B., Moeller, B.C., Järvinen, E., 2016. Round robin tests on nitrosamines analysis in the effluents of a CO_2 capture pilot plant, Energy Procedia. Elsevier Ltd, pp. 252-261.

Freeman, S.A., 2011. Thermal degradation and oxidation of aqueous piperazine for carbon dioxide capture, Energy Procedia.

Frimpong, R.A., Johnson, D., Richburg, L., Hogston, B., Remias, J.E., Neathery, J.K., Liu, K., 2013. Comparison of solvent performance for CO_2 capture from coal-derived flue gas: A pilot scale study. Chemical Engineering Research and Design 91, 963-969.

Fujita, K., Muraoka, D., Ogawa, T., Kitamura, H., Suzuki, K., Saito, S., 2013. Evaluation of amine emissions from the post-combustion CO_2 capture pilot plant, Energy Procedia. Elsevier Ltd, pp. 727-734.

Gao, T., Selinger, J.L., Rochelle, G.T., 2019. Demonstration of 99% CO_2 removal from coal flue gas by amine scrubbing. International Journal of Greenhouse Gas Control 83, 236-244.

Gjernes, E., Pedersen, S., Cents, T., Watson, G., Fostås, B.F., Shah, M.I., Lombardo, G., Desvignes, C., Flø, N.E., Morken, A.K., De Cazenove, T., Faramarzi, L., Hamborg, E.S., 2017. Results from 30 wt% MEA Performance Testing at the CO_2 Technology Centre Mongstad, Energy Procedia. Elsevier Ltd, pp. 1146-1157.

Goff, G.S., 2005. Oxidative Degradation of Aqueous Monoethanolamine in CO2 Capture Processes: Iron and Copper Catalysis, Inhibition, and O2 Mass Transfer.

Goldstein, J.I., Newbury, D.E., Michael, J.R., Ritchie, N.W., Scott, J.H.J., Joy, D.C., 2017. Scanning electron microscopy and X-ray microanalysis. Springer.

Gorset, O., Knudsen, J.N., Bade, O.M., Askestad, I., 2014. Results from testing of Aker Solutions advanced amine solvents at CO2 Technology Centre Mongstad, Energy Procedia. Elsevier Ltd, pp. 6267-6280.

Gouedard, C., Rey, A., Cuzuel, V., Brunet, J., Delfort, B., Picq, D., Dugay, J., Vial, J., Pichon, V., Launay, F., 2014. Amine degradation in CO2 capture. 3. New degradation products of MEA in liquid phase: amides and nitrogenous heterocycles. International Journal of Greenhouse Gas Control 29, 61-69.

Graff, O.F., 2010. Advanced CO2 capture with Bio Aker Clean Carbon-Emission measurement and analysis from Mobile Carbon Capture Test Facility.

Grimstvedt, A., Wiig, M., Einbu, A., Vevelstad, S.J., 2019. Multi-component analysis of monethanolamine solvent samples by FTIR. International Journal of Greenhouse Gas Control 83, 293-307.

Hansel, A., Jordan, A., Holzinger, R., Prazeller, P., Vogel, W., Lindinger, W., 1995. Proton transfer reaction mass spectrometry: on-line trace gas analysis at the ppb level. International Journal of Mass Spectrometry and Ion Processes 149-150, 609-619.

Harsha, S., Khakharia, P., Huizinga, A., Monteiro, J., Goetheer, E., Vlugt, T.J.H., 2019. In-situ experimental investigation on the growth of aerosols along the absorption column in post combustion carbon capture. International Journal of Greenhouse Gas Control 85, 86-99.

Hilliard, M.D., 2008. A Predictive Thermodynamic Model for an Aqueous Blend of Potassium Carbonate, Piperazine, and Monoethanolamine for Carbon Dioxide Capture from Flue Gas.

Idem, R., Supap, T., Shi, H., Gelowitz, D., Ball, M., Campbell, C., Tontiwachwuthikul, P., 2015. Practical experience in post-combustion CO2 capture using reactive solvents in large pilot and demonstration plants. International Journal of Greenhouse Gas Control 40, 6-25.

Jeong, C.-H., Evans, G.J., 2009. Inter-Comparison of a Fast Mobility Particle Sizer and a Scanning Mobility Particle Sizer Incorporating an Ultrafine Water-Based Condensation Particle Counter. Aerosol Science and Technology 43, 364-373.

Jordan, A., Haidacher, S., Hanel, G., Hartungen, E., Herbig, J., Märk, L., Schottkowsky, R., Seehauser, H., Sulzer, P., Märk, T.D., 2009. An online ultra-high sensitivity Proton-transfer-reaction mass-spectrometer combined with switchable reagent ion capability (PTR+SRI−MS). International Journal of Mass Spectrometry 286, 32-38.

Järvinen, A., Aitomaa, M., Rostedt, A., Keskinen, J., Yli-Ojanperä, J., 2014. Calibration of the new electrical low pressure impactor (ELPI+). Journal of Aerosol Science 69, 150-159.

Kadnar, R., Rieder, J., 1995. Determination of anions in amine solutions for sour gas treatment. Journal of Chromatography A 706, 339-343.

Kamijo, T., Sorimachi, Y., Shimada, D., Miyamoto, O., Endo, T., Nagayasu, H., Mangiaracina, A., 2013. Result of the 60 tpd CO2 capture pilot plant in European coal power plant with KS-1™ solvent, Energy Procedia. Elsevier Ltd, pp. 813-816.

Kentish, S.E., 2016. Reclaiming of amine-based absorption liquids used in post-combustion capture, Absorption-Based Post-Combustion Capture of Carbon Dioxide, pp. 426-438.

Kero, I.T., Jørgensen, R.B., 2016. Comparison of Three Real-Time Measurement Methods for Airborne Ultrafine Particles in the Silicon Alloy Industry. International Journal of Environmental Research and Public Health 13.

Khakharia, P., Brachert, L., Mertens, J., Anderlohr, C., Huizinga, A., Fernandez, E.S., Schallert, B., Schaber, K., Vlugt, T.J.H., Goetheer, E., 2015a. Understanding aerosol based emissions in a Post Combustion CO2 Capture process: Parameter testing and mechanisms. International Journal of Greenhouse Gas Control 34, 63-74.

Khakharia, P., Brachert, L., Mertens, J., Huizinga, A., Schallert, B., Schaber, K., Vlugt, T.J.H., Goetheer, E., 2013. Investigation of aerosol based emission of MEA due to sulphuric acid aerosol and soot in a Post Combustion CO2 Capture process. International Journal of Greenhouse Gas Control 19, 138-144.

Khakharia, P., Kvamsdal, H.M., Da Silva, E.F., Vlugt, T.J.H., Goetheer, E., 2014a. Field study of a Brownian Demister Unit to reduce aerosol based emission from a

Post Combustion CO2 Capture plant. International Journal of Greenhouse Gas Control 28, 57-64.

Khakharia, P., Mertens, J., Huizinga, A., De Vroey, S., Sanchez Fernandez, E., Srinivasan, S., Vlugt, T.J.H., Goetheer, E., 2015b. Online corrosion monitoring in a postcombustion CO2 capture pilot plant and its relation to solvent degradation and ammonia emissions. Industrial and Engineering Chemistry Research 54, 5336-5344.

Khakharia, P., Mertens, J., Vlugt, T.J.H., Goetheer, E., 2014b. Predicting aerosol based emissions in a post combustion CO2 capture process using an aspen plus model, Energy Procedia. Elsevier Ltd, pp. 911-925.

Knudsen, J.N., Bade, O.M., Anheden, M., Bjorklund, R., Gorset, O., Woodhouse, S., 2013. Novel concept for emission control in post combustion capture, Energy Procedia. Elsevier Ltd, pp. 1804-1813.

Knudsen, J.N., Bade, O.M., Askestad, I., Gorset, O., Mejdell, T., 2014. Pilot plant demonstration of CO2 capture from cement plant with advanced amine technology, Energy Procedia. Elsevier Ltd, pp. 6464-6475.

Knudsen, J.N., Jensen, J.N., Vilhelmsen, P.-J., Biede, O., 2009. Experience with CO2 capture from coal flue gas in pilot-scale: Testing of different amine solvents, Energy Procedia, pp. 783-790.

Knuutila, H., Asif, N., Vevelstad, S.J., Svendsen, H.F., 2014a. Formation and Destruction of NDELA in 30 wt% MEA (Monoethanolamine) and 50 wt% DEA (Diethanolamine) Solutions. Oil & Gas Science and Technology–Revue d'IFP Energies nouvelles 69, 805-820.

Knuutila, H., Svendsen, H.F., Asif, N., 2014b. Decomposition of nitrosamines in aqueous monoethanolamine (MEA) and diethanolamine (DEA) solutions with UV-radiation. International Journal of Greenhouse Gas Control 31, 182-191.

Kohl, A.L., Nielsen, R.B., 1997. Chapter 3 - Mechanical Design and Operation of Alkanolamine Plants, in: Kohl, A.L., Nielsen, R.B. (Eds.), Gas Purification (Fifth Edition). Gulf Professional Publishing, Houston, pp. 187-227.

Kolderup, H., da Silva, E., Mejdell, T., Tobiesen, A., Haugen, G., Hoff, K.A., Josefsen, K., Strøm, T., Furuseth, O., Hanssen, K.F., Myhrvold, T., Johnsen, K., SINTEF REPORT Emission Reducing Technologies H&ETQP Amine6 SINTEF Materials and Chemistry.

Lamminen, E., 2011. Accurate measurement of nanoparticle charge, number and size with the ELPI+™ instrument, Journal of Physics: Conference Series. IOP Publishing, p. 012064.

Léonard, G., Voice, A., Toye, D., Heyen, G., 2014. Influence of dissolved metals and oxidative degradation inhibitors on the oxidative and thermal degradation of monoethanolamine in postcombustion CO_2 capture. Industrial & Engineering Chemistry Research 53, 18121-18129.

Lepaumier, H., Grimstvedt, A., Vernstad, K., Zahlsen, K., Svendsen, H.F., 2011. Degradation of MMEA at absorber and stripper conditions. Chemical engineering science 66, 3491-3498.

Lepaumier, H., Picq, D., Carrette, P.L., 2009a. New amines for CO_2 Capture. I. Mechanisms of amine degradation in the presence of CO_2. Industrial and Engineering Chemistry Research 48, 9061-9067.

Lepaumier, H., Picq, D., Carrette, P.L., 2009b. New amines for CO_2 Capture. II. Oxidative degradation mechanisms. Industrial and Engineering Chemistry Research 48, 9068-9075.

Levin, M., Gudmundsson, A., Pagels, J.H., Fierz, M., Mølhave, K., Löndahl, J., Jensen, K.A., Koponen, I.K., 2015. Limitations in the Use of Unipolar Charging for Electrical Mobility Sizing Instruments: A Study of the Fast Mobility Particle Sizer. Aerosol Science and Technology 49, 556-565.

Li, W., Shao, L., 2009. Transmission electron microscopy study of aerosol particles from the brown hazes in northern China. Journal of Geophysical Research Atmospheres 114.

Lindinger, W., Hansel, A., Jordan, A., 1998. On-line monitoring of volatile organic compounds at pptv levels by means of proton-transfer-reaction mass spectrometry (PTR-MS) medical applications, food control and environmental research. International Journal of Mass Spectrometry and Ion Processes 173, 191-241.

Lombardo, G., Fostås, B.F., Shah, M.I., Morken, A.K., Hvidsten, O.A., Mertens, J., Hamborg, E.S., 2017. Results from Aerosol Measurement in Amine Plant Treating Gas Turbine and Residue Fluidized Catalytic Cracker Flue Gases at the CO_2 Technology Centre Mongstad, Energy Procedia. Elsevier Ltd, pp. 1210-1230.

Lundanes, E., Reubsaet, L., Greibrokk, T., 2013. Chromatography: basic principles, sample preparations and related methods. John Wiley & Sons.

Macbride, D.M., Malone, C.G., Hebb, J.P., Cravalho, E.G., 1997. Effect of Temperature Variation on FT-IR Spectrometer Stability, APPLIED SPECTROSCOPY.

Majeed, H., Knuutila, H., Hillestad, M., Svendsen, H.F., 2017. Effect of Amine Volatility on Aerosol Droplet Development in Absorption Columns, Energy Procedia. Elsevier Ltd, pp. 977-986.

Mangiaracina, A., Zangrilli, L., Robinson, L., Kvamsdal, H.M., Os, P.V., 2014. OCTAVIUS: Evaluation of flexibility and operability of amine based post combustion CO2 capture at the Brindisi Pilot Plant, Energy Procedia. Elsevier Ltd, pp. 1617-1636.

Matin, N.S., Remias, J.E., Neathery, J.K., Liu, K., 2012. Facile Method for Determination of Amine Speciation in CO2 Capture Solutions. Industrial & Engineering Chemistry Research 51, 6613-6618.

Mejdell, T., Haugen, G., Rieder, A., Kvamsdal, H.M., 2017. Dynamic and Control of an Absorber - Desorber Plant at Heilbronn, Energy Procedia, pp. 1231-1244.

Mejdell, T., Vassbotn, T., Juliussen, O., Tobiesen, A., Einbu, A., Knuutila, H., Hoff, K.A., Andersson, V., Svendsen, H.F., 2011. Novel full height pilot plant for solvent development and model validation, Energy Procedia. Elsevier Ltd, pp. 1753-1760.

Mertens, J., Bruns, R., Schallert, B., Faniel, N., Khakharia, P., Albrecht, W., Goetheer, E., Blondeau, J., Schaber, K., 2015. Effect of a gas-gas-heater on H2SO4 aerosol formation: Implications for mist formation in amine based carbon capture. International Journal of Greenhouse Gas Control 39, 470-477.

Mertens, J., Knudsen, J., Thielens, M.L., Andersen, J., 2012. On-line monitoring and controlling emissions in amine post combustion carbon capture: A field test. International Journal of Greenhouse Gas Control 6, 2-11.

Mertens, J., Lepaumier, H., Desagher, D., Thielens, M.L., 2013. Understanding ethanolamine (MEA) and ammonia emissions from amine based post combustion carbon capture: Lessons learned from field tests. International Journal of Greenhouse Gas Control 13, 72-77.

Meuleman, E., Cottrell, A., Ghayur, A., 2016. Treatment of flue-gas impurities for liquid absorbent-based post-combustion CO2 capture processes, Absorption-Based Post-Combustion Capture of Carbon Dioxide. Woodhead Publishing, pp. 519-551.

Morken, A.K., Nenseter, B., Pedersen, S., Chhaganlal, M., Feste, J.K., Tyborgnes, R.B., Ullestad, Ø., Ulvatn, H., Zhu, L., Mikoviny, T., Wisthaler, A., Cents, T., Bade, O.M., Knudsen, J., De Koeijer, G., Falk-Pedersen, O., Hamborg, E.S., 2014. Emission results of amine plant operations from MEA testing at the CO2 Technology Centre Mongstad, Energy Procedia. Elsevier Ltd, pp. 6023-6038.

Morken, A.K., Pedersen, S., Kleppe, E.R., Wisthaler, A., Vernstad, K., Ullestad, Ø., Flø, N.E., Faramarzi, L., Hamborg, E.S., 2017. Degradation and Emission Results of Amine Plant Operations from MEA Testing at the CO2 Technology Centre Mongstad. Energy Procedia 114, 1245-1262.

Morton, F., Laird, R., Northington, J., 2013. The National Carbon Capture Center: Cost-effective test bed for carbon capture R&D. Energy Procedia 37, 525-539.

Moser, P., Schmidt, S., Sieder, G., Garcia, H., Stoffregen, T., 2011a. Performance of MEA in a long-term test at the post-combustion capture pilot plant in Niederaussem. International Journal of Greenhouse Gas Control 5, 620-627.

Moser, P., Schmidt, S., Sieder, G., Garcia, H., Stoffregen, T., Stamatov, V., 2011b. The post-combustion capture pilot plant Niederaussem–results of the first half of the testing programme. Energy Procedia 4, 1310-1316.

Moser, P., Schmidt, S., Stahl, K., Vorberg, G., Lozano, G.A., Stoffregen, T., Richter, T., 2015. The wet electrostatic precipitator as a cause of mist formation-Results from the amine-based post-combustion capture pilot plant at Niederaussem. International Journal of Greenhouse Gas Control 41, 229-238.

Moser, P., Schmidt, S., Stahl, K., Vorberg, G., Lozano, G.A., Stoffregen, T., Rösler, F., 2014. Demonstrating emission reduction - Results from the post-combustion capture pilot plant at niederaussem, Energy Procedia. Elsevier Ltd, pp. 902-910.

Moser, P., Schmidt, S., Wallus, S., Ginsberg, T., Sieder, G., Clausen, I., Palacios, J.G., Stoffregen, T., Mihailowitsch, D., 2013. Enhancement and long-term testing of optimised post-combustion capture technology - Results of the second phase of the testing programme at the Niederaussem pilot plant, Energy Procedia. Elsevier Ltd, pp. 2377-2388.

Moser, P., Wiechers, G., Schmidt, S., Elsen, R., Khakharia, P., Garcia, J., Monteiro, M.-S., Jens, K.-J., Solli, K.-A., Sanchez Fernandez, E., Garcia, S., Maroto-Valer, M., Barrio, J., Kvamsdal, M., 2018. MEA consumption-ALIGN-CCUS: Comparative long-term testing to answer the open questions, GHGT-14, Melbourne, Australia.

Moser, P., Wiechers, G., Schmidt, S., Garcia Moretz-Sohn Monteiro, J., Charalambous, C., Garcia, S., Sanchez Fernandez, E., 2020. Results of the 18-month test with MEA at the post-combustion capture pilot plant at Niederaussem – new impetus to solvent management, emissions and dynamic behaviour. International Journal of Greenhouse Gas Control 95, 102945.

Moser, P., Wiechers, G., Stahl, K., Stoffregen, T., Vorberg, G., Lozano, G.A., 2017. Solid Particles as Nuclei for Aerosol Formation and Cause of Emissions - Results from the Post-combustion Capture Pilot Plant at Niederaussem, Energy Procedia. Elsevier Ltd, pp. 1000-1016.

Nakamura, S., Yamanaka, Y., Matsuyama, T., Okuno, S., Sato, H., 2013. IHI s Amine-Based CO2 Capture Technology for Coal Fired Power Plant. Energy Procedia 37, 1897-1903.

Nakamura, S., Yamanaka, Y., Matsuyama, T., Okuno, S., Sato, H., Iso, Y., Huang, J., 2014. Effect of Combinations of Novel Amine Solvents, Processes and Packing at IHI's Aioi Pilot Plant. Energy Procedia 63, 687-692.

Newbury, D.E., Ritchie, N.W.M., 2013. Is Scanning Electron Microscopy/Energy Dispersive X-ray Spectrometry (SEM/EDS) Quantitative? Scanning 35, 141-168.

Nicol, K., 2013. Recent developments in particulate control, pp. 1-54.

Nielsen, P.T., Li, L., Rochelle, G.T., 2013. Piperazine degradation in pilot plants, Energy Procedia. Elsevier Ltd, pp. 1912-1923.

Nordstrom, D.K., Alpers, C.N., 1997. The environmental geochemistry of mineral deposits. Reviews in economic geology 6A, 133-160.

Okuno, S., Nakamura, S., Yamanaka, Y., Matsuyama, T., Sato, H., Ikeda, R., 2017. Demonstration Results on Advanced Amine Solvents, Packings and Process at IHI's AIOI PILOT PLANT, Energy Procedia. Elsevier Ltd, pp. 1282-1287.

Reynolds, A.J., Verheyen, T.V., Adeloju, S.B., Chaffee, A.L., Meuleman, E., 2015a. Evaluation of methods for monitoring MEA degradation during pilot scale post-combustion capture of CO2. International Journal of Greenhouse Gas Control 39, 407-419.

Reynolds, A.J., Verheyen, T.V., Adeloju, S.B., Chaffee, A.L., Meuleman, E., 2015b. Monoethanolamine Degradation during Pilot-Scale Post-combustion Capture of CO2 from a Brown Coal-Fired Power Station. Energy & Fuels 29, 7441-7455.

Richner, G., Puxty, G., 2012. Assessing the Chemical Speciation during CO2 Absorption by Aqueous Amines Using in Situ FTIR. Industrial & Engineering Chemistry Research 51, 14317-14324.

Rieder, A., Dhingra, S., Khakharia, P., Zangrilli, L., Schallert, B., Irons, R., Unterberger, S., van Os, P., Goetheer, E., 2017. Understanding solvent degradation: A study from three different pilot plants within the OCTAVIUS project. Energy Procedia 114, 1195-1209.

Rieder, A., Unterberger, S., 2013. EnBW's Post-Combustion Capture Pilot Plant at Heilbronn–Results of the First Year's Testing Programme. Energy Procedia 37, 6464-6472.

Rochelle, G., Bishnoi, S., Chi, S., Dang, H., Santos, J., 2001. Research needs for CO2 capture from flue gas by aqueous absorption/stripping, Research Report for P.O.: No. DE-AF26-99FT01029 of U.S. Department of Energy.

Rochelle, G.T., 2012. Thermal degradation of amines for CO2 capture. Current Opinion in Chemical Engineering 1, 183-190.

Rogelj, J., Shindell, D., Jiang, K., Fifita, S., Forster, P., Ginzburg, V., Handa, C., Kheshgi, H., Kobayashi, S., Kriegler, E., Mundaca, L., Séférian, R., Vilariño, M.V., 2018. Mitigation Pathways Compatible with 1.5°C in the Context of Sustainable Development. In: *Global Warming of 1.5°C. An IPCC Special Report on the impacts of global warming of 1.5°C above pre-industrial levels and related global greenhouse gas emission pathways, in the context of strengthening the global response to the threat of climate change, sustainable development, and efforts to eradicate poverty.* IPCC.

Rooney, P., Dupart, M., Bacon, T., 1998. Oxygen's role in alkanolamine degradation. Hydrocarbon processing (International ed.) 77, 109-113.

Saito, S., Udatsu, M., Kitamura, H., Murai, S., Kato, Y., Maezawa, Y., Watando, H., 2014. Development and Evaluation of a New Amine Solvent at the Mikawa CO2 Capture Pilot Plant. Energy Procedia 51, 176-183.

Saito, S., Udatsu, M., Kitamuraa, H., Murai, S., 2015. Absorption-Based Post-Combustion Capture of Carbon Dioxide, PCCC-3. IEAGHG, Regina SK, Canada.

SEPA, 2015. Review of amine emissions from carbon capture systems, Version 2.01.

Sexton, A.J., 2008. Amine Oxidation in CO2 Capture Processes.

Shah, M.I., Lombardo, G., Fostås, B., Benquet, C., Kolstad Morken, A., De Cazenove, T., 2018. CO2 capture from RFCC flue gas with 30 wt% MEA at Technology Centre Mongstad, process optimization and performance comparison, 14th International Conference on Greenhouse Gas Control Technologies, GHGT-14.

Sheppard, B.S., Shen, W.-L., Davidson, T.M., Caruso, J.A., 1990. Helium-argon inductively coupled plasma for plasma source mass spectrometry. Journal of Analytical Atomic Spectrometry 5, 697-700.

Shimadzu, 2014. Manual TOC Shimadzu.

Singh, A., Stéphenne, K., 2014. Shell Cansolv CO2 capture technology: Achievement from first commercial plant, Energy Procedia. Elsevier B.V., pp. 1678-1685.

Somridhivej, B., Boyd, C.E., 2016. An assessment of factors affecting the reliability of total alkalinity measurements. Aquaculture 459, 99-109.

Spietz, T., Chwoła, T., Krótki, A., Tatarczuk, A., Więcław-Solny, L., Wilk, A., 2018. Ammonia emission from CO2 capture pilot plant using aminoethylethanolamine. International Journal of Environmental Science and Technology 15, 1085-1092.

Strazisar, B.R., Anderson, R.R., White, C.M., 2003. Degradation pathways for monoethanolamine in a CO2 capture facility. Energy & fuels 17, 1034-1039.

Sun, K., Lu, L., Jiang, H., 2012. Experimental study of aerosol distribution and concentration variation through curved ducts. Thermal Science 16, 1437-1441.

Tanthapanichakoon, W., Veawab, A., McGarvey, B., 2006. Electrochemical Investigation on the Effect of Heat-stable Salts on Corrosion in CO2 Capture Plants Using Aqueous Solution of MEA. Industrial & Engineering Chemistry Research 45, 2586-2593.

Thomas, R., 2013. Practical guide to ICP-MS: a tutorial for beginners.

Thompson, J., Nikolic, H., Combs, M., Bhatnagar, S., Pelgen, J., Abad, K., Liu, K., 2017a. Solvent Degradation and Emissions from a 0.7MWe Pilot CO2 Capture System with Two-stage Stripping. Energy Procedia 114, 1297-1306.

Thompson, J., Richburg, H., Liu, K., 2017b. Thermal Degradation Pathways of Aqueous Diamine CO2 Capture Solvents. Energy Procedia 114, 2030-2038.

Thompson, J.G., Bhatnagar, S., Combs, M., Abad, K., Onneweer, F., Pelgen, J., Link, D., Figueroa, J., Nikolic, H., Liu, K., 2017c. Pilot testing of a heat integrated 0.7 MWe CO2 capture system with two-stage air-stripping: Amine degradation and metal accumulation. International Journal of Greenhouse Gas Control 64, 23-33.

Thompson, J.G., Combs, M., Abad, K., Bhatnagar, S., Pelgen, J., Beaudry, M., Rochelle, G., Hume, S., Link, D., Figueroa, J., 2017d. Pilot testing of a heat integrated 0.7 MWe CO2 capture system with two-stage air-stripping: Emission. International Journal of Greenhouse Gas Control 64, 267-275.

Thompson, J.G., Frimpong, R., Remias, J.E., Neathery, J.K., Liu, K., 2014. Heat stable salt accumulation and solvent degradation in a pilot-scale CO2 capture process using coal combustion flue gas. Aerosol and Air Quality Research 14, 550-558.

Todoli, J.-L., Mermet, J.-M., 2011. Liquid sample introduction in ICP spectrometry: A practical guide. Elsevier.

Vega, F., Sanna, A., Navarrete, B., Maroto-Valer, M.M., Cortés, V.J., 2014. Degradation of amine-based solvents in CO2 capture process by chemical absorption. Greenhouse Gases: Science and Technology 4, 707-733.

Vevelstad, S.J., Grimstvedt, A., Elnan, J., da Silva, E.F., Svendsen, H.F., 2013. Oxidative degradation of 2-ethanolamine: The effect of oxygen concentration and temperature on product formation. International Journal of Greenhouse Gas Control 18, 88-100.

Wang, T., Hovland, J., Jens, K.J., 2015. Amine reclaiming technologies in post-combustion carbon dioxide capture. Journal of Environmental Sciences 27, 276-289.

Wang, T., Jens, K.-J., 2012. Oxidative Degradation of Aqueous 2-Amino-2-methyl-1-propanol Solvent for Postcombustion CO2 Capture. Industrial & Engineering Chemistry Research 51, 6529-6536.

Welker, R.W., 2012. Chapter 4 - Size Analysis and Identification of Particles, in: Kohli, R., Mittal, K.L. (Eds.), Developments in Surface Contamination and Cleaning. William Andrew Publishing, Oxford, pp. 179-213.

Wittgens, B., Einbu, A., Brunsvik, A., Zahlsen, K., 2010. H&E TQP 1D1: Establish sampling and analytical procedures for potentially harmful components post combustion amine based CO2 capture. Subtask 3: Online sampling and analysis. FM07-AJZ00-Z-RA-0002-03.

Zhu, Q., 2010. Non-calcium desulphurisation technologies, pp. 1-42.

Aas, N., da Silva, E.F., 2010. Emission measurements at Dong's Emission measurements at Dong s pilot plant for CO2 capture in Esbjerg, Oslo.

A review of degradation and emissions in post-combustion CO_2 capture pilot plants

Vanja Buvik[a], Karen K. Høisæter[a], Solrun J. Vevelstad[b], Hanna K. Knuutila[a]*

[a] Department of Chemical Engineering, NTNU, NO-7491 Trondheim, Norway

[b] SINTEF Industry, NO-7465 Trondheim, Norway

* Corresponding author: hanna.knuutila@ntnu.no

Appendix

Supplementary table 3.1: A more detailed summary of the different pretreatment technologies applied at the different pilot campaign locations.

Location	Pretreatment
Austin, Texas	SCR, FGD
Brindisi, Italy	deNOx, WESP/ESP/FF, deSOx
CAER 0.1 MWth, USA	WFGD, high-temperature cyclone, knock-out
CAER 0.7 MWe, USA	WFGD, low NO_X, ESP
Changchun, China	PR, FGD, SCR, denitrification
Esbjerg, Denmark	SCR, deNOx, ESP, FGD
Ferrybridge, UK	FGD, in-furnace NO_X reduction
Heilbronn, Germany	deep SO_2 removal, pre-scrubber, deNOx, ESP
Łaziska, Poland	Water scrubber, FGD
Loy Yang, Australia	knock-out drum, caustic wash
Maasvlakte, The Netherlands	BDU, FGD, caustic wash
Mikawa, Japan	ESP, FGD
Niederaussem, Germany	FGD, SCR, caustic wash
Tarong, Australia	PR, caustic wash
TCM, Norway	FGD, BD filter
Tiller, Norway	water scrubber
Wilsonville, USA	particulate filter, SCR, ESP, WFGD
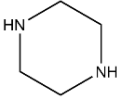
Supplementary table 3.2: Measured concentrations of total amount of heat stable salts (HSS) and organic acids in post-combustion CO_2 capture pilot campaigns using 30wt% MEA as their solvent, at the end of the campaign of right before reclaiming the solvent, in mg kg^{-1}. Hours of operation given in table indicates the time of sampling. *Mass concentration in original publication converted to mass fraction under the assumption that $\rho = 1$ kg L^{-1}.

Campaign	HSS	Acetate	Formate	Glycolate	Oxalate
Niederaussem (a)			200		
Niederaussem (b)		2500	530		240
Niederaussem (c)		25 000	5000		2700
CAER 0.1 MWth	4700		799		
CAER 0.7 MWe	17 677*	884*	7583*	619*	3643*
Loy Yang	24 000	5000	12 000		3000
Esbjerg (a)	13 000				
Esbjerg (b)			1200*		1100*
Heilbronn (a)			1260*		560*
Heilbronn (c)*	3482	350	1160	205	270
Changchun	3590		2160		700
TCM (a)	12 000	500*	3000*	400*	1200*
TCM (b)	6785 (0.12 mol kg^{-1})		1400	1440	520

Supplementary table 3.3: Chemical structures of compounds, which have been quantified in pilot campaigns. [a]Thermal degradation compounds, [b]Primary and [c]Secondary oxidative degradation compounds.

IUPAC name	Abbreviation	CAS-number	Chemical structure
Acetate	[b]	71-50-1	
N-(2-Aminoethyl)-N'(2-hydroxyethl)-imidazolidione	AEHEIA	no CAS	
N,N'-Bis(2-hydroxy-ethyl)oxamide	BHEOX[c]	1871-89-2	
Bicine		150-25-4	
Diethanolamine	DEA[a]	109-89-7	
Ethylamine	EA[b]	75-04-7	
Formate	[b]	71-47-6	
Glycolate	[b]	79-14-1	
N-(2-Hydroxyethyl)-acetamide	HEA[c]	142-26-7	
2-(2-Hydroxyethylamino)-ethanol	HEEDA[a] or AEEA	111-41-1	
N-(2-Hydroxyethyl)-formamide	HEF[c]	693-06-1	
N-(2-Hydroxyethyl)-glycine	HEGly[c]	5835-28-9	

IUPAC name	Abbreviation	CAS-number	Chemical structure
(N-(2-Hydroxyethyl)-(hydroxyethyl)-amino)acetamide	HEHEAA[c]	144236-39-5	
N-(2-Hydroxyethyl)-imidazole	HEI[c]	1615-14-1	
N-(2-Hydroxyethyl)-2-imidazolidione	HEIA[a]	3699-54-5	
4-(2-Hydroxyethyl)-2-piperazinone	HEPO[c]	23936-04-1	
Monoethanolamine	MEA	141-43-5	
2-(Nitroamino)-ethanol	MEA-NO$_2$	74386-82-6	
N-Nitrosodiethanolamine	NDELA	1116-54-7	
N-Nitrosodimethylamine	NDMA	62-75-9	
Nitroso-(2-hydroxy ethyl)-glycine	No-HEGly	80556-89-4	
Oxalate	b	338-70-5	
2-Oxazolidinone	OZD[c]	497-25-6	

IUPAC name	Abbreviation	CAS-number	Chemical structure
Piperazine	Pz	110-85-0	

Chapter 4

Materials and methods

This chapter aims to give a more in-depth description of the experimental and analytical methodology used in this PhD. Recommendations for future operators will be included here to a larger extent than in the published papers. This chapter also includes some results from validation experiments, that may help other researchers in setting up their experiments.

4.1.   Oxidative degradation setup 1

The setup used for most of the oxidative degradation experiments performed in the scope of his work, was an open-batch setup and based on the work of Vevelstad (2013) and Fytianos (2016). First, one setup of three parallel reactors was built and after that was successfully in use another, identical setup was made. This allowed for six parallel reactions to run at the same time.
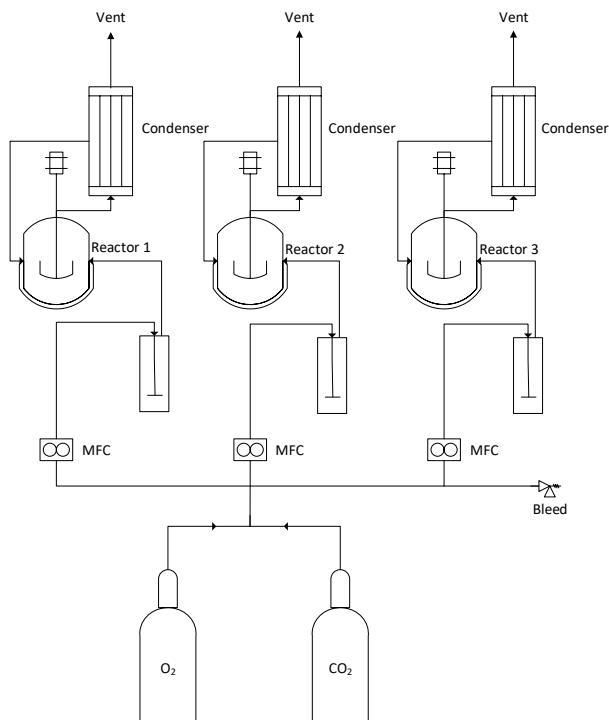
Figure 4.1: Schematic of oxidative degradation setup 1, of which there were two.

The experimental conditions were meant to simulate absorber conditions, so the temperature was kept constant at 60 °C throughout every experiment. Temperature control was ensured by making the reactors of double-jacketed glass, meaning that there is a large contact area between the heating liquid, which was water provided by a circulating heating bath. The temperature of the Graham condensers was kept constant by using a circulating cooling bath with water kept at 5 °C. Each reactor has a total volume of ~275 mL and a liquid volume of ~200 mL was used during the experiments. The gas mixture was provided though five Alicat mass flow controllers (MFC), two regulating the pressure of CO_2 and O_2, and three MFCs connected after the two gases had been mixed, providing an equal gas flow to each reactor. A bleed valve coupled in parallel with the three MFCs going into the reactors, ensured release of excess gas mixture. The gas is passed through an empty gas wash bottle and

111

through a Pyrex® gas dispersion tube (GDT) of porosity grade 1 into the liquid, to increase mass transfer from the gas to the liquid phase. The GDTs were either new, or thoroughly cleaned with sulphuric acid (H_2SO_4), and deionized water between experiments. Magnetic stirring was maintained constant throughout every experiment at a rate of ~200 rpm. Each reactor has three openings, one at the top, for the condenser, one on the side, where a thermometer adapter ensured a tight fit around the GDT going into the reactor and a third opening covered with a screw cap with septum, for sampling.
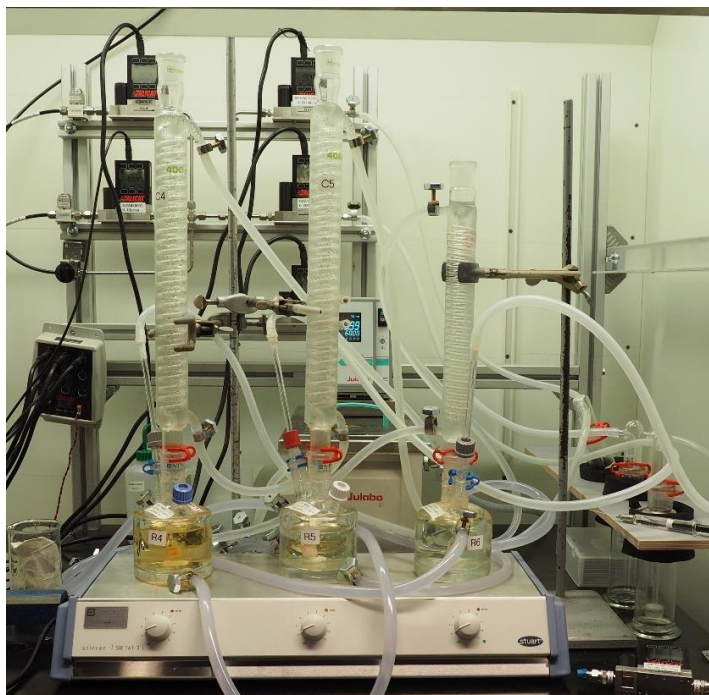
Figure 4.2: Photo of oxidative degradation setup 1. Photo: Per Henning, NTNU.

Each experiment started with adding ~200 mL of an accurately weighed amine solution, which was typically pre-loaded with CO_2 and contained 0.5 mM of iron sulphate heptahydrate ($FeSO_4 \cdot 7H_2O$), into pre-heated reactors with the cooling system on. The GDT was already secured and connected and as soon as the sample was added to the reactor, the septum-containing cap was put in place. Magnetic stirring and gas flow were commenced as soon as all reactors were filled. Sampling was performed regularly through the septum, using a syringe with a needle. Each sampling removed 2-3 mL of the liquid and every sample was accurately weighed, to ensure knowledge of the mass balance throughout the experiment. The typical duration of an experiment was 21 days, with sampling two times per week.

The following subchapters contain results from two different method validation experiments, that are not included in the published papers.

4.1.1 Catalysis of oxidative MEA degradation

One experiment testing the catalytic effect of copper was performed in three parallel reactors in Setup 1. The experimental procedure given in section 4.1 was followed, with the exception of 0.5 mM $CuSO_4$ addition instead of $FeSO_4 \cdot 7H_2O$. the experiment was performed in 30 wt% MEA (*aq*.) with a loading kept at approximately 0.4 mol_{CO2} mol_{MEA}^{-1}. The gas mixture sparged into each reactor consisted of 98% O_2 and 2% CO_2, and the gas flow rate was kept at 60 mL min^{-1}.
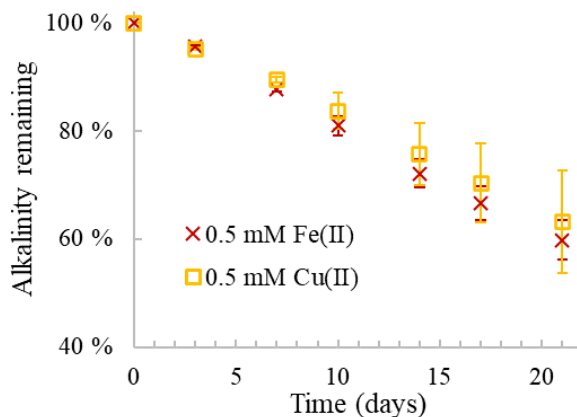
Figure 4.3: Relative alkalinity remaining in the 30 wt% MEA (*aq*.) solution throughout three weeks under oxidising conditions when added Fe^{2+} or Cu^{2+}.

As can be seen in Figure 4.3, the rate of copper-catalysed oxidative degradation of 30 wt% MEA (*aq*.) is comparable to that of iron-catalysed degradation. The data for MEA 30 wt% with Fe^{2+} is from the publication printed in chapter 7, the data for the copper-catalysed experiments is found in Table 4.1. The alkalinity show in the figure was measured by titration, then corrected to CO_2-free concentration, and under the assumption that water loss is linear, corrected for loss of mass (water) throughout the experiment.

Table 4.1: Measured concentrations of alkalinity (section 4.4.1) and CO_2 (section 4.6.1) for oxidative degradation of 30 wt% MEA (aq.) with 0.5 mM $CuSO_4$ in three parallel reactors (a, b, and c).

Day	Alkalinity (w/ CO_2) [mol kg^{-1}]	CO_2 concentration [g kg^{-1}]	Loading [mol_{CO2} mol_{MEA}^{-1}]	Alkalinity (w/o CO_2) [mol kg^{-1}]	Alkalinity (corrected) [mol kg^{-1}]
0	4.511	85.81	0.43	4.898	4.898
3a	4.340	83.31	0.44	4.701	4.659
3b	4.349	-	-	4.715	4.674
3c	4.345	-	-	4.710	4.653

Day	Alkalinity (w/ CO_2) [mol kg^{-1}]	CO_2 concentration [g kg^{-1}]	Loading [mol$_{CO2}$ mol$_{MEA}$$^{-1}$]	Alkalinity (w/o CO_2) [mol kg^{-1}]	Alkalinity (corrected) [mol kg^{-1}]
7a	4.127	81.17	0.45	4.462	4.369
7b	4.164	82.47	0.45	4.507	4.416
7c	4.152	82.21	0.45	4.493	4.367
10a	3.765	71.42	0.43	4.034	3.913
10b	4.043	-	-	4.355	4.228
10c	4.016	-	-	4.320	4.147
14a	3.337	60.86	0.41	3.540	3.391
14b	3.831	71.86	0.43	4.107	3.940
14c	3.753	69.06	0.42	4.012	3.787
17a	3.042	53.52	0.40	3.205	3.041
17b	3.663	-	-	3.908	3.715
17c	3.609	-	-	3.842	3.581
21a	2.619	45.09	0.39	2.737	2.565
21b	3.443	61.90	0.41	3.656	3.434
21c	3.376	59.98	0.40	3.578	3.278

4.1.2   Oxidative degradation with 1% vs 98% O_2

To test whether degradation takes place also with very low pO_2, an experiment was run replacing pure O_2, with a mixture of 99% N_2 and 1% O_2 in 30 wt% MEA (*aq.*). The instructions in section 4.1 were otherwise followed, resulting in a 60 mL min^{-1} flow rate of approximately 1% O_2, 2% CO_2 and 97% N_2 into each reactor. The solution contained 0.5 mM FeSO$_4$·7H$_2$O to catalyse the reaction.

Figure 4.4: Oxidative stability of 30 wt% MEA (*aq.*) with high and low pO_2.

In Figure 4.4 the loss of alkalinity for MEA sparged with 1% O_2 is compared to that of 98% O_2 (the same data as in Figure 4.3). In the figure, alkalinity of the CO_2-free

solution is given, corrected for water loss throughout the experiment. It can be seen that the loss of amine is negligible in this case, that more oxygen is required to induce a significant loss of alkalinity in the three weeks the experiments take. The measured concentrations of amine and CO_2 are given in Table 4.2.

Table 4.2: Measured concentrations of alkalinity (section 4.4.1) and CO_2 (section 4.6.1) for oxidative degradation of 30 wt% MEA (aq.) with 1% O_2 in three parallel reactors (a, b, and c).

Day	Alkalinity (w/ CO_2)	CO_2 concentration	Loading	Alkalinity (w/o CO_2)	Alkalinity (corrected)
	[mol kg^{-1}]	[g kg^{-1}]	[mol$_{CO2}$ mol$_{MEA}$$^{-1}$]	[mol kg^{-1}]	[mol kg^{-1}]
0	4.514	81.33	0.41	4.881	4.881
3a	4.548	83.37	0.42	4.928	4.883
3b	4.541	-	-	4.929	4.887
3c	4.511	-	-	4.919	4.882
7a	4.558	84.10	0.42	4.942	4.838
7b	4.597	89.34	0.44	5.008	4.910
7c	4.577	99.78	0.50	5.034	4.946
10a	4.620	84.82	0.42	5.012	4.862
10b	4.595	84.29	0.42	4.983	4.843
10c	4.615	84.32	0.42	5.004	4.879
14a	4.667	89.75	0.44	5.086	4.872
14b	4.646	89.77	0.44	5.063	4.864
14c	4.641	90.22	0.44	5.060	4.883
17a	4.672	90.97	0.44	5.097	4.837
17b	4.695	90.14	0.44	5.118	4.875
17c	4.650	91.30	0.45	5.075	4.859
21a	4.690	92.69	0.45	5.125	4.802
21b	4.669	92.93	0.45	5.103	4.803
21c	4.700	91.74	0.44	5.131	4.861

4.2 Oxidative degradation setup 2

One oxidative degradation experiment was also performed in an open batch degradation rig at SINTEF. This setup is described in detail in Vevelstad et al. (2016). The principle of this setup is the same as for setup 1, only with a larger reactor volume and higher gas flow (357.5 mL min^{-1}), including a pump recycling the gas phase into the liquid by vigorous sparging (50 L h^{-1}). It is also equipped with two 50 cm water-cooled Graham condensers and the fresh gas (98% O_2, 2% CO_2) is pre-saturated with water through a gas wash bottle.

This setup offers an increased mass transfer from the gas to the liquid phase than setup 1 and was therefore used to validate the results of the KI SAS solution, verifying its inhibition effect on oxidative degradation of MEA.
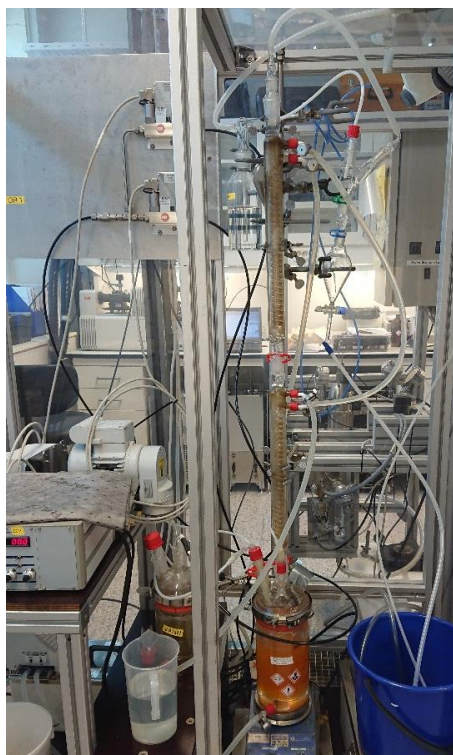
Figure 4.5: Photo of oxidative degradation setup 2 (belongs to SINTEF Industry).

4.3 Thermal degradation experiments

The thermal degradation experiments performed in the scope of this work were performed in accordance with Eide-Haugmo et al. (2011). Approximately 8 mL of solvent was filled in stainless steel 316 cylinders with diameters of 0.5 inch and volumes of approximately 11 mL, equipped with Swagelok® end caps. The weight of the solvent and cylinder were accurately noted prior to starting the experiment. The cylinders were then kept at 135 °C for up to five weeks. Each sampling involved the removal of two metal cylinders per experiment and the analyses of their contents, meaning i.e. that the sample taken after two weeks was kept at 135 °C for two weeks.

For the experiments performed in conjunction with the investigation of stable salts as degradation inhibitors, the cylinders were washed with sulfuric acid (H_2SO_4, 0.1 M) to remove iron carbamate ($FeCO_3$) and other corrosion products. The weighing of the cylinders and caps was then performed on a Mettler-Toledo ME204 analytical scale (taring range 0-220 g and readability 0.0001 g) to determine loss of mass due to corrosion, throughout the experiment.

4.3.1　Influence of O_2 on thermal stability of MEA

In conjunction with the investigations of oxygen solubility and the impact of oxygen on chemical stability of amines, a set of thermal degradation experiments was performed with MEA as described in the first paragraph in section 4.3. Four cylinders containing 8 mL of 30wt% MEA (*aq.*) was prepared for each sampling, whereof two of the cylinders were sparged with N_2, to remove all O_2 from the solution and head space, before closing the caps and two with O_2, to saturate the liquid phase and head space with O_2. The results of these experiments are given in Figure 4.4 in the form of total alkalinity determined by titration with H_2SO_4, where it can be observed that the presence of these amounts of O_2 does not play a significant role in the thermal degradation of MEA. These results were the reasoning for not removing head or liquid space O_2 prior to closing the cylinders during thermal degradation experiments.
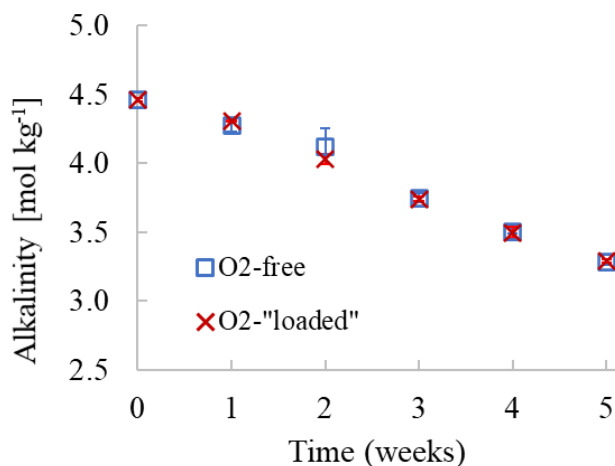
Figure 4.6: Thermal stability of 30wt% MEA (*aq.*) in O_2-"loaded" and O_2 free conditions.

4.4　Biodegradation experiments in soil

To study the effect of small concentrations of amine in a plant-soil system, six plant pots of equal size (cubical, 8·8·8 cm) were used for each treatment (treatment = concentration/amount of amine). This study had a total of 36 pots, with some reserve pots in case any system looked different from the other at the time of treatment start, so that these may be replaced. Each pot was filled with approximately 400 mL of soil, its surface wetted and grass seeds were sowed. The grass was allowed to grow until a height of approximately 5-8 cm at conditions of growth light and regular watering (every 2nd day), to make sure that a solid system of roots had developed in each pot. This took ~1.5 months.

The pots were systematically numbered for the sake of logging the results throughout the experiment. When the grass was deemed healthy and strong, treatments with

MEA was conducted by giving each plant-soil system a one-one treatment. The pots were divided into sets of 6 (because there were 6 individual treatments), resulting in 6 sets of 6 pots. Prior to the treatment, an objective observer assessed the health of each plant-soil systems, by giving each individual system a score between 0 and 5, where 0 represented 0% brown leaves, 1: 1-10%, 2: 11-20%, 3: 31-60%, 4: 61-90%, and 5 91-100% brown leaves. Every plant-soil system was then given the same *volume* of treatment, but each treatment contained different *concentrations* of MEA. Within each set of six, every pot then received a different treatment, in a randomized order. The number of the pot and the treatment given was systematically logged.

After the treatment, the plant-soil systems were all kept at conditions of growth light and regular watering, as before the treatment, but every 3-4 days the score was logged anew by the same objective observer. The observer was unaware of which treatment each plant-soil system had received. Scoring was continued for three weeks in this work, but for future studies and deeper insight it would be recommended to continue for a while longer. Longer intervals between scorings can be used.

The statistical relevance of the results was assessed, both to verify significant differences between treatments over all scoring times by using a Friedman test, and at any given time, by using a Kruskal-Wallis test. The effect size was determined using Kendall's *W* and Cohen's interpretation. P-values were adjusted with Bonferroni correction method.

4.2.   Titration

Titration methods were used both for quantification of alkalinity, heat stable salts (HSSs) and dissolved oxygen, and each methodology is found described in the following sections.

4.4.1   Amine quantification

Amine concentrations were primarily quantified indirectly, by titration with sulfuric acid (H_2SO_4) to find total alkalinity of the solutions. Total alkalinity does not necessarily describe the total concentration of one given amine species but will indiscriminately quantify all alkaline species. Alkaline degradation products will therefore be included in the total amine concentration in this way. The method bases on the description found in Ma'mun et al. (2006).

0.2 g of the sample is added to 50 mL deionized water and its mass exactly noted down. The sample is then titrated using a Metrohm 702 SM Titrino automatic titrator and 0.1 M H_2SO_4 until the end point around pH 4-5. The concentration of alkaline species is calculated from the amount of acid used to titrate.

$$c_{\text{amine}} = \frac{2 \cdot c_{\text{H}_2\text{SO}_4} \cdot V_{\text{H}_2\text{SO}_4}}{m_{\text{sample}}}$$

<div align="right">Eq. 4.1</div>

Analysis of samples of known concentrations gave maximum deviations of ± 2%. All samples were analysed in 2 parallels and the average of these are given as the result. The maximum deviation between the two parallel analyses should not exceed 2%.

4.4.2 Heat stable salt analysis

Heat stable salt (HSS) is a collective term for all ionic species, which can be found in the amine solution, that can withstand elevated temperatures over time. The temperature elevation removes the reversibly formed carbonate, carbamate and bicarbonate species and effectively strips the solution of CO_2. The method described in this section is based on that described in Reynolds et al. (2015) as well as method developed by SINTEF Industry.

Dowex 50W-X8 anion exchange resin (CAS: 69011-20-7) was used in this procedure, which was activated with hydrochloric acid (HCl) prior to use. The activation was performed by magnetically stirring two volumetric parts resin with one-part HCl (10%) for 10 min before letting the solution settle and then decanting off the acidic supernatant. The resin is then rinsed with deionized water by filling the container, stirring the solution for a few minutes, letting it settle and discarding the supernatant. The rinsing step is repeated until the supernatant has the pH of deionized water. The resin is now activated and should not dry out. The activated resin needs to be stored in deionized water until it is in use.

The HSS analysis is performed by adding 2 g of the sample to 40 mL of activated resin and 40 mL deionized water, noting the exact mass of the sample. The beaker is partly covered with i.e. parafilm or a watch glass and is magnetically stirred at 70 °C for 1 h. After the solution has cooled down and the resin settled at the bottom of the glass, the supernatant is carefully poured through a frit, to avoid resin particles in the liquid, and into another beaker. 40 mL deionized water is added to the resin and stirred for a couple of minutes before allowing the resin to settle again. This supernatant is also gently decanted through the frit and into the same beaker as the previous supernatant. This rinsing step is repeated until the supernatant has the pH of deionized water, normally 3-4 times, combining all the supernatants. The combined supernatants are then titrated with 0.05 M sodium hydroxide (NaOH) using a Metrohm 702 SM Titrino automatic titrator until the end point of pH 5-6. The concentration of HSS is calculated from the amount of NaOH used to reach end point, using Eq. 4.2. All samples were analysed in 2 parallels and the average of these are given as the result. The maximum deviation between the two parallel analyses should not exceed 5%. Blank samples should be analysed regularly.

$$c_{HSS} = \frac{V_{NaOH} \cdot c_{NaOH}}{m_{sample}}$$

Eq. 4.2

The anion exchange resin can be regenerated by covering it with HCl (10%) and stirring it, partly covered, at 70 °C for 1 h. The solution is allowed to settle and cool before the acid is gently decanted and the resin repeatedly rinsed with deionized water until the liquid shows the pH of deionized water.

To validate the HSS analysis, "artificially degraded" samples of MEA were analysed as unknowns. These were made by adding known concentrations of formic, acetic, oxalic and/or glycolic acid to a 30wt% (*aq*.) solution of MEA. The analysis of these artificially degraded samples gave a maximum deviation of $\pm$ 0.007 mol kg^{-1} or $\pm$ 7%.

4.4.3 Winkler titration

The Winkler method is a colorimetric titration technique for the determination of dissolved oxygen in aqueous solutions (Winkler, 1888). The dissolved oxygen is bound by divalent manganese (Mn^{2+}) in a manganese chloride ($MnCl_2$) or sulphate ($MnSO_4$) solution, forming a white manganese(IV)oxide (MnO_2) precipitate. Upon hydration, brown $MnO(OH)_2$ is formed.

$$2Mn^{2+} + O_2 + 2OH^- \rightarrow 2MnO_2 + 2H_2O \rightarrow 2MnO(OH)_2$$

Eq. 4.3
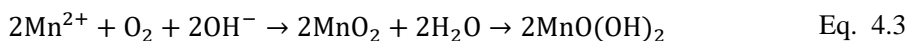
Potassium iodide (KI) and sulfuric acid (H_2SO_4) are then added to the solution, forming iodine (I_2) in equal proportion to the amount of dissolved oxygen in the initial solution.

$$2MnO(OH)_2 + 2I^- + 4H^+ \rightarrow 2Mn^{2+} + I_2 + 3H_2O$$

Eq. 4.4
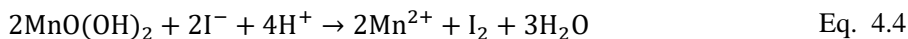
A starch indicator is then used to recognize the equivalence point in a titration with thiosulfate solution ($Na_2S_2O_3$), which gives a characteristic dark purple colouration of the solution with I_3^- (formed from I^- + I_2), but not with I^-, giving a loss of colour when all I_2 is consumed.

$$I_2 + 2S_2O_3^{2-} \rightarrow 2S_4O_6^{2-} + 2I^-$$

Eq. 4.5

It is of upmost importance to maintain the bottle where the reactions take place out of contact with air during the titration, as oxygen from the air influences the result of the titration. All Winkler titrations in this work were performed using a commercially available test kit purchased from Hanna Instruments (HI-3810).

Since the second step of the Winkler method (Eq. 4.4) depends on acidification with a strong acid to form highly volatile I_2, the direct Winkler titration method is not suitable for determination of dissolved oxygen in alkaline solutions. Wang et al. (2013) therefore developed an indirect Winkler titration method for alkaline solutions, which includes adding thiosulfate before the acidification, and titration with a potassium iodate (KIO_3) solution to determine the amount of excess thiosulfate. This method was not used in this thesis.

4.5 Chromatography

Chromatography methods allow the separation of components from a mixture where they are dissolved in a mobile phase (liquid or gas), and passed through a solid phase, where they are separated based on their properties. Chromatography coupled with a detection method therefore allows for single components to be identified and quantified. One gas chromatography (GC) method and two liquid chromatography (LC) techniques were used in this work.

4.5.1 Gas chromatography

Gas chromatography (GC) was performed on an Agilent 7890A GC-MS system according to the description found in chapter 5.

4.5.2 Liquid chromatography

Quantification of ethanolamine (MEA) and some degradation products was performed by LC-MS/MS as SINTEF using the method shortly described in chapter 6.

4.5.3 Ion chromatography

Ion chromatography (IC) is a subcategory of liquid chromatography, where ionic components, dissolved in water, are separated based on their affinity to a solid phase. Anion and cation chromatography with conductivity detection were used for quantifying both single amines and anionic degradation compounds. The ion chromatograph is an instrument that is very sensitive to change and requires a lot of maintenance. Ideally, the instrument should be in continuous operation, with a constant solvent flow through the column. Vevelstad et al. (2012) discussed the challenges with using IC as an analytical tool for degraded amine solvents, addressing matrix effects, and separation challenges. These challenges were also observed in the scope of this work.

4.5.3.1 Cation chromatography

Single amine compounds can be separated by cation chromatography, due to their ability to get protonated in presence of an acidic eluent. The method used is based on that developed by Fytianos et al. (2015). The eluent used for separating the amines was in this case a 15 mM methanesulfonic acid (MSA), prepared freshly once a week with water from an ICW-3000 Millipore purification system. The instrument used was a Thermo Scientific™ Dionex™ ICS-5000 system, with a Thermo Scientific Dionex IonPac™ CS19 analytical column (2 mm · 250 mm) and a CG19 guard column (2 · 50 mm). An eluent flow of 0.300 mL min^{-1} was used, the temperature of the column compartment was 30 °C and the cell compartment 25 °C. A 20 min method sufficed to elute all the studied amines, although for smaller amines like MEA

15 min sufficed. A suppressor current of 11 mA was used to suppress the background noise of the conductivity detection.

Not all amines were quantified in this manner due to a series of problems with the instrument, not allowing further analysis on the cationic system despite of replacing almost every replaceable component of it.

4.5.3.2 Anion chromatography

In an opposite manner to cation chromatography, anion chromatography is based on the detection of negatively charged species, that i.e. get deprotonated in the alkaline eluent. Acetate, formate and oxalate were quantified using a Thermo Scientific™ Dionex™ ICS-5000 system located at USN Porsgrunn, with a Dionex™ AG11-HC RFIC™ analytical (4 · 250 mm) and guard column (2 · 50 mm) and conductivity detection. The column compartment was kept at 35 °C and the cell temperature at 30 °C. A gradient of potassium hydroxide (KOH), generated by an eluent generation (EG) system, was used as the eluent, with the program given in Table 4.1. Standards of the organic acids were prepared in the concentration range from 1 to 30 ppm and the degraded amine samples were diluted between 1:100 and 1:350 with deionised water, depending on their known total content of heat stable salts (HSS). All standards and samples were filtered from any remaining particulate matter before analysis and peak areas were used for calculating the concentrations of the anions.

Table 4.3: KOH gradient used in the anion IC analysis of formate, acetate and oxalate in degraded amine samples

Time	$C_{KOH,start}$ [mM]	$C_{KOH,stop}$ [mM]
0-30	3	3
30-32	3	30
32-52	30	30
52-54	30	60
54-64	60	60
64-66	60	3
66-74	3	3

The anion chromatographic system at NTNU, Thermo Scientific™ Dionex™ ICS-5000 IC system, connected to an ICW-3000 Millipore water purification system and equipped with an ASRS300 suppressor (2mm), a carbonate removal device and conductivity detection was used to quantify iodide in the oxidatively degraded KI SAS solutions. The column was a 15IonPac 2×250mm with an AG15 guard column 2×50mm and column temperature 30 °C. An eluent generator provided the gradient given in Table 4.2. Quantification of iodide concentrations were performed based on calibration in a concentration range of 0–116 ppm of iodide in the form of KI and

dilution of the fresh and degraded samples to the corresponding concentration range. Peak areas were used for calculating iodide concentration.

Table 4.4: KOH gradient used in the anion IC analysis of iodide in the KI SAS solutions.

Time	$C_{KOH,start}$ [mM]	$C_{KOH,stop}$ [mM]
0-10	13	13
10-15	13	45
15-49	45	45
49-60	13	13

4.6 TOC/TIC/TN

CO_2 concentrations and CO_2 loadings of amine solutions were determined by total inorganic carbon (TIC) analysis on a Shimadzu TOC-L$_{CPH}$ instrument. Total nitrogen (TN) analyses were also performed on the same instrument, on its TN-unit. The total organic carbon (TOC) instrument can quantify total carbon (TC), TIC content as well as indirectly by performing both these analyses, TOC.
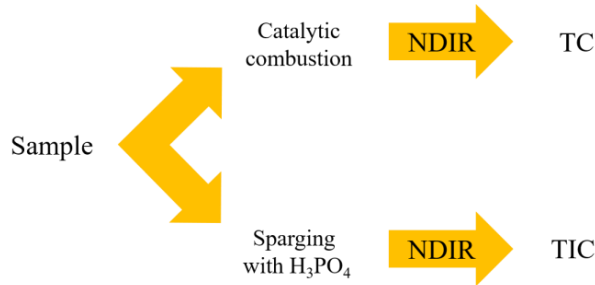
Figure 4.7: Schematic of the TC and TIC analysis on the Shimadzu TOC-L$_{CPH}$ analyzer.

The sample is diluted in purified water to contain a concentration of TIC, TC or TN >500 ppm prior to analysis. As shown in Figure 4.5, TC is quantified by combustion of the sample over a platinum (Pt) catalyst at 680 °C and in the presence of air, prior to nondispersive infrared detection (NDIR) of carbon in the form of CO_2. TIC analysis is performed by sparging the sample in phosphoric acid (H_3PO_4) to release all inorganic carbon as CO_2, which is also quantified by NDIR.

TN analysis is performed by catalytic combustion of the sample over the same Pt catalyst as the TC analysis, at 720 °C. All bound nitrogen is converted to nitrogen oxide (NO) which is added ozone (O_3) to form excited nitrogen dioxide (NO$_2$*) according to Eq. 4.6.

$$NO + O_3 \rightarrow NO_2^* + O_2 \qquad\qquad \text{Eq. 4.6}$$

TN is then quantified in a chemiluminescence detector, based on the specific relaxation energy (hv) of NO_2^* as shown in Eq. 4.7.

$$NO_2^* \rightarrow NO_2 + hv$$

<div align="right">Eq. 4.7</div>

4.6.1 TIC analysis

The amine samples were usually diluted 1:100 in Millipore water, as their original concentration of around 2-5 mol_{amine} kg^{-1} solution ensured a TIC concentration < 500 ppm. The method parameters for the TIC analysis were an injection volume of 50 µL and triplicate analyses. Limitations for the method to give a result was that either SD < 1 or CV < 2% for the average of the three injections. The method was set to replace the H_3PO_4 for each sample. Standards of known concentration of TIC were always run alongside with the unknown samples and the deviation from known concentrations were always below ± 3%. Calibrations were performed regularly, at the latest when the deviation between known and measured concentrations in standard solutions exceeded 3%.

4.2.1. TN analysis

For the TN analysis, the amine samples were diluted between 1:500 in Millipore water, as their original concentration of around 2-5 mol_{amine} kg^{-1} solution ensured a TN concentration < 500 ppm. The method parameters for the TIC analysis were an injection volume of 40 µL and triplicate analyses and the oven temperature was set to 720 °C. Limitations for the method to give a result was that either SD < 1 or CV < 2% for the average of the three injections. Standards of known concentration of TN were always run alongside with the unknown samples and the deviation from known concentrations were always below ± 3%. Calibrations were performed regularly, at the latest when the deviation between known and measured concentrations in standard solutions exceeded 3%.

4.2.2. Calibration of TN and TIC

For all analyses at least two calibration ranges are recommended, to achieve higher accuracy. The approach that has been used in this work is calibration from 0 to 150 ppm and 150 to 500 ppm for the TIC analysis and 0-200 ppm and 200-500 ppm in the TN analysis. Calibration standards for the TIC analysis are prepared from sodium bicarbonate ($NaHCO_3$) and TN potassium nitrate (KNO_3) for unknown nitrogen species, although calibration with the amine species to be analysed for gives the highest accuracy (Laukvik and Laukvik, 2019). Typical calibrations for TIC analysis were 0, 25, 50, 100 and 150 ppm TIC standards for the lower range and 150, 200, 300, 400 and 500 ppm TIC for the higher concentration range. The peak areas

resulting from the analysis of the calibration standards correlated linearly with the concentrations with $R^2 > 0.999$.

4.3.   References

Fytianos, G., 2016. Corrosion and degradation in amine based post-combustion CO_2 capture, in: Norges teknisk-naturvitenskapelige universitet Institutt for kjemisk, p. (Ed.). Norwegian University of Science and Technology, Faculty of Natural Sciences and Technology, Department of Chemical Engineering, Trondheim.

Fytianos, G., Callot, R., Svendsen, H.F., Knuutila, H.K., 2015. Quantitative determination of amines used in post-combustion CO2 capture process by ion chromatography. International Journal of Greenhouse Gas Control 42, 372-378.

Laukvik, M., Laukvik, T., 2019. Kvantitering av nitrogenholdige degraderingsprodukter i aminløsninger, Institutt for bioingeriørvitenskap. NTNU, Trondheim, p. 86.

Ma'mun, S., Jakobsen, J.P., Svendsen, H.F., Juliussen, O., 2006. Experimental and modeling study of the solubility of carbon dioxide in aqueous 30 mass% 2-((2-aminoethyl) amino) ethanol solution. Industrial & engineering chemistry research 45, 2505-2512.

Reynolds, A.J., Verheyen, T.V., Adeloju, S.B., Chaffee, A.L., Meuleman, E., 2015. Evaluation of methods for monitoring MEA degradation during pilot scale post-combustion capture of CO2. International Journal of Greenhouse Gas Control 39, 407-419.

Vevelstad, S.J., 2013. CO2 absorbent degradation Department of Chemical Engineering. NTNU, Trondheim.

Vevelstad, S.J., Grimstvedt, A., Lepaumier, H., Zahlsen, K., Kjos, M.S., Knudsen, J.N., Svendsen, H.F., 2012. Identification and Quantification of Degradation Products by Ion Chromatography, Recent Advances in Post-Combustion CO2 Capture Chemistry. American Chemical Society, pp. 239-247.

Vevelstad, S.J., Johansen, M.T., Knuutila, H., Svendsen, H.F., 2016. Extensive dataset for oxidative degradation of ethanolamine at 55–75° C and oxygen concentrations from 6 to 98%. International Journal of Greenhouse Gas Control 50, 158-178.

Wang, M.H., Ledoux, A., Estel, L., 2013. Oxygen solubility measurements in a MEA/H2O/CO2 mixture. Journal of Chemical & Engineering Data 58, 1117-1121.

Winkler, L.W., 1888. Die bestimmung des im wasser gelösten sauerstoffes. European Journal of Inorganic Chemistry 21, 2843-2854.

Chapter 5

Measurement and prediction of oxygen solubility in post-combustion CO₂ capture solvents

This chapter contains a paper about measurement and prediction of oxygen solubility, published in the International Journal of Greenhouse Gas Control, January 2021. It comprises both experimental and modelling approaches to the topic and fills a gap in the understanding of the presence, concentrations, and impact of oxygen in amine solvents. The results imply that mass transfer of oxygen may be the limiting factor for oxidative degradation of unstable amines such as MEA. This is an important factor to consider in the development of oxygen removal technologies if they are intended for use in rapidly degrading amine solvents.

Measurement and prediction of oxygen solubility in post-combustion CO_2 capture solvents

Vanja Buvik[a], Ida M. Bernhardsen[a], Roberta V. Figueiredo[b], Solrun J. Vevelstad[c], Earl Goetheer[b], Peter van Os[b] and Hanna K. Knuutila[a*]

[a] Department of Chemical Engineering, Norwegian University of Science and Technology (NTNU), NO-7491 Trondheim, Norway

[b] TNO, Leeghwaterstraat 44, 2628 CA Delft, The Netherlands

[c] SINTEF Industry, NO-7465 Trondheim, Norway

[*] Corresponding author: hanna.knuutila@ntnu.no

Abstract

This work aims to understand oxygen solubility in pure and aqueous amine solvents for CO_2 capture. Commercially available dissolved oxygen sensors were studied to evaluate whether these can be used for measuring oxygen solubility in the carbon capture processes. It also aims to understand the possible discrepancies from realistic concentrations of oxygen when using a dissolved oxygen sensor. Two independent measurement principles were used for this purpose, both electrochemical and optical. Furthermore, a Winkler titration method was used to aid the validation of the sensors as well as understanding salting-out effects. A simple model for predicting oxygen solubility in CO_2-loaded ethanolamine solutions was made, which also has potential for predicting oxygen solubility in other loaded amine solutions.

The results of the study show that dissolved oxygen sensors may be applied for measurement of oxygen concentrations in amine solutions and that the different amines and different concentrations in water only show small variations in oxygen solubility. The sensors may also be used in CO_2-loaded amine solutions, but here the increased conductivity of the solution may give a higher measured concentration of oxygen, than it is in reality. In ethanolamine, the consumption of oxygen is faster than the mass transfer of oxygen from gas to liquid phase, giving lower concentrations of oxygen than it should be in absence of a chemical reaction between oxygen and amine.

Keywords

5.1   Introduction

The capture and storage of CO_2 from large emission sources (CCS) has to play a key role for reaching the target of not exceeding 1.5 °C increase of global average temperatures, concludes the Intergovernmental Panel on Climate Change (IPCC) in their report from 2017 (Rogelj et al., 2018). CCS allows for carbon (in form of CO_2), that would otherwise be released to the atmosphere and contribute to global warming, to be returned underground to safe and permanent storage. There are many studied technologies for CO_2 capture and of those, flue gas scrubbing with liquid amine solvents is one of the most mature technologies. (Kohl and Nielsen, 1997; Leung et al., 2014; Rochelle, 2009). Liquids have inherent gas absorption properties and can physically absorb gases to some extent (Battino and Clever, 1966). Solvents with amine functions are, however, also chemically reacting with some gases, among these CO_2. The amines can more selectively, and in higher concentrations than physical gas absorption, bind the gas molecules. In this process, a solvent reversibly binds CO_2 at low temperatures in an absorber column and is released at high temperatures in a desorber column.

Because the reaction is reversible, the amine solution is circulated and reused continuously. The harsh operational conditions to which the solution is subjected, contact time with all flue gas components and construction material, as well as high temperatures in the desorber, can lead to amine degradation over time (Gouedard et al., 2012; Mazari et al., 2015; Meisen and Shuai, 1997; Reynolds et al., 2016). Oxidative degradation, the degradation that occurs in the presence of oxygen is a complex problem that can lead to corrosion, solvent and equipment replacement costs, and interruption of operation time (Dhingra et al., 2017; Goff and Rochelle, 2004; Rieder et al., 2017). For oxidative degradation reactions to take place they require presence of oxygen (O_2), and the main source for oxygen is the gas phase molecular oxygen present in the surrounding air or in the flue gas. It is commonly assumed that most of the oxidative degradation reactions take place in the absorber column where the oxygen concentration is the highest, because this is where the solvent is in contact with the flue gas and the temperature is the lowest in the process (da Silva et al., 2012).

Laboratory experiments, where oxygen rich gas has been bubbled through aqueous amine solutions, have shown that there is a correlation between the amount of oxygen and the amount of oxidative degradation observed; increasing the oxygen pressure leads to increased rate of oxidative degradation (Supap et al., 2001; Vevelstad et al.,

2016). Further, post combustion CO_2 capture pilot studies have shown that the loss of amine, caused by degradation into other compounds, increases linearly with the concentration of oxygen in the treated flue gas (Léonard et al., 2015). As a means of avoiding or limiting the extent of oxidative degradation, addition of oxygen scavenging compounds is a proven and commercially available method of reducing oxidative degradation in carbon capture plants (Fytianos et al., 2016; Léonard et al., 2014; Supap et al., 2011; Veldman and Trahan, 1997). These scavengers react stoichiometrically with dissolved oxygen and reduce the occurrence of oxidative degradation in the amine solution. However, another issue arises when the scavenger molecules are used up and removal of used-up scavenger, as well as addition of fresh scavenger has to be performed (Léonard et al., 2014). Together with this, undesired side effects such as foaming and cross-reactions with the solvent or other products can also occur with the direct contact of the solvent with the scavenger, as has been observed with corrosion inhibitors and other additives (Chen et al., 2011; Thitakamol and Veawab, 2008). To simplify operation of the carbon capture plant, a simpler way of eliminating molecular oxygen and thereby avoiding oxidative degradation would be preferred.

Because experimental observations show that oxygen pressure plays an important role in degradation, oxygen solubility is, also, a parameter in models attempting to predict oxidative solvent degradation (Pinto et al., 2014) under the assumption that its solubility in amines is similar to that of water.

The solubility of oxygen and other gases in non-reactive liquids is an inherent property and it depends on partial pressure of the gas and the temperature, as described by Henry's law given in equation 1

$$H^{cp} = \frac{C_l \cdot R \cdot T}{C_g} \tag{1}$$

where Henry's law constant (H^{cp}) is correlated to the liquid-phase (C_l) and gas phase concentrations (C_g) of the gas component (in this case O_2), as well as the ideal gas constant (R) and temperature (T) (Henry, 1832).

$$O_2(g) \rightleftarrows O_2(aq) \tag{2}$$

$$CO_2(g) \rightleftarrows CO_2(aq) \tag{3}$$

$$CO_2(aq) + H_2O(l) + MEA(aq) \rightleftarrows HCO_3^-(aq) + MEAH^+(aq) \tag{4}$$

$$HCO_3^-(aq) + MEA\ (aq) \rightleftarrows MEACO_2^-(aq) + H_2O(l) \tag{5}$$
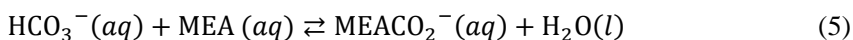
In addition to the physical solubility of gases (Eq. 2 and 3), CO_2 will chemically react with the amine in the solution. Depending on the type of amine, different reaction products are formed. For instance, a primary amine like ethanolamine (MEA) forms carbamate and protonated MEA ($MEACO_2^-$ and $MEAH^+$, Eq. 4 and 5) when reacting

with CO_2, while a. tertiary amines form (bi)carbonate and protonated amine species (Danckwerts, 1979; Puxty and Maeder, 2016). Bicarbonate (HCO_3^-, Eq. 4) is also formed in reaction with water. Carbamates, as well as bicarbonate, are ionic species which will change the ionic strength of the solution when formed from non-ionic compounds, a factor that influences oxygen solubility, known as a "salting in" or "salting out" effect (Schumpe et al., 1978).

The existing techniques for the quantification of dissolved oxygen include Winkler titration (Montgomery et al., 1964; Winkler, 1888), by means of gas chromatography in a molecular sieve column with thermal conductivity detection (GC-TCD) (Park and Catalfomo, 1964) and using electrochemical (polarographic) dissolved oxygen sensors. The titration method described by Winkler in 1888 is very accurate for aqueous samples with low or no alkalinity but is not directly applicable for the titration of amines. Quantification using an electrochemical sensor is a highly desirable method for industrial applications (Rooney and Daniels, 1998; Wang et al., 2013); it offers a fast, cheap and direct measurement that can easily be coupled online in a gas sweetening process. One of the challenges of the dissolved oxygen sensors is however the ionic strength of the solutions, which increases the conductivity and thereby enhances the electrochemical signal which is perceived by the sensor. The effect that the increased ionic strength has on the dissolved oxygen sensors is experimentally investigated in this work and compared to the predictions of the Schumpe model for gas solubility in aqueous electrolytes. Membrane transport of liquid or gas phase oxygen to the electrode of the sensor through the oxygen selective membrane of the electrochemical sensor is also studied in this work, to see if the presence of CO_2 impedes oxygen transport to the electrodes, as this type of membrane also is permeable to other small gas molecules (Bhattacharya and Hwang, 1997).

There are three main types of dissolved oxygen sensors, all designed for quantification of dissolved oxygen in water: polarographic, galvanic and optical. Polarographic, or "Clark" sensors (Clark, 1959), based on the same working principle as galvanic dissolved oxygen sensors, being selective reduction of O_2, but the galvanic type has a faster response time. The third type of dissolved oxygen sensors is optical, which relies on an oxygen-sensitive fluorescent dye, a light emitting diode and a photodetector to measure oxygen concentration in the solution. In this study sensors both the galvanic, electrochemical and the optical type have been used and compared.
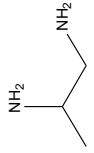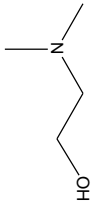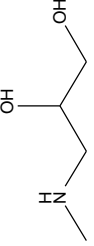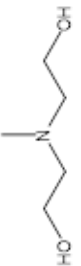
The need for quantifying dissolved oxygen is not solely interesting for degradation modelling purposes mentioned above, but also for the development of oxygen removal technologies (Monteiro et al., 2018), where oxygen concentration needs to be quantified both before and after removal. The ideal analysis method should be direct (no sample processing), as this evades the issue of taking a sample for further processing, both decreasing the amount of work and sources of error. As already described, the solubility of oxygen is dependent of partial pressure and temperature,

so that even small changes in either of these parameters, which is likely to happen during sample processing, could influence the measurement greatly. A further challenge for the measurements is the very low concentration range in which oxygen can be present. Any measurement method for dissolved oxygen needs to be sensitive enough to detect and quantify concentrations of oxygen in the low ppm-range (< 8 ppm).

This work has studied if different parameters, such as amine structure and concentration, as well as CO_2 loading, influence oxygen solubility. The methodological emphasis in this work was on electrochemical and optical dissolved oxygen sensors, because of their simple operation and potential for online measurements. Additionally, a promising modelling approach was used to predict oxygen solubility in CO_2 loaded amine solutions. The results of this study deepen the understanding of the extend of oxygen solubility in CO_2 loaded and unloaded amine solutions and how oxygen concentrations can be measured. The results also indicate that oxygen mass transfer is a limiting factor in the oxidative degradation of amines. The results of the study are an addition to the current understanding of oxidative degradation in amine-based CO_2-removal, as well as giving valuable information to those wanting to measure and understand oxygen solubility in the process.

5.2 Materials and methods

Table 5.1: Short and trivial name, as well as structure, CAS number and key features of the chemicals used in the experiments.

IUPAC name	Abbreviation	Chemical structure	CAS	Purity	Supplier	Features
phenylmethylamine	benzylamine		100-46-9	99%	Aldrich	Primary aromatic amine
1,2-diaminopropane	1,2-DAP		78-90-0	99%	Aldrich	Diamine
2-(2-aminoethoxy) ethanol	DGA		929-06-6	98%	Acros Organics	Ether of a primary alkanolamine
2-(dimethylamino) ethanol	DMMEA		108-01-0	$\geq$99.5%	Aldrich	Tertiary alkanolamine
3-methylamino-1,2-propanediol	MAPD		40137-22-2	97%	Aldrich	Secondary alkane-diolamine
N-methyl-diethanolamine	MDEA		105-59-9	$\geq$99%	Aldrich	Tertiary alkanolamine
2-aminoethan-1-ol	MEA		141-43-5	$\geq$99%	Sigma-Aldrich	Primary alkanolamine
ethane-1,2-diol	MEG		107-1-1	$\geq$99.8%	Sigma-Aldrich	Diol
2-methyl-aminoethanol	MMEA		109-83-1	$\geq$98%	Aldrich	Secondary alkanolamine

5.2.1 Chemicals

Pure oxygen (O_2, N5.0) and carbon dioxide (CO_2, N5.0) gas were obtained from AGA and Linde Gas and compressed air from in-house air compression systems at NTNU and TNO. Deionized water was obtained from local water deionization systems at NTNU and TNO. Further chemicals and abbreviations used can be found in Table 5.1. All solutions were prepared gravimetrically.

5.2.2 Dissolved oxygen (DO) sensors

The solubility of oxygen was measured using two different electrochemical dissolved oxygen sensors and one optical oxygen sensor, all designed for measurement of oxygen concentrations in water. The electrochemical dissolved oxygen sensors used are based on galvanic probes that give a measurable current proportional to the chemical reduction of O_2 on a cathode. The two different electrochemical sensors were used in this work were a HI-5421 Dissolved Oxygen and BOD Meter from Hanna Instruments, with a HI76483 Clark-Type polarographic probe and a handheld pHenomenal® OX 4100 H dissolved oxygen meter with a pHenomenal® OXY-11 polarographic probe, from VWR. A redox reaction gives a measurable current which directly correlates to the oxygen concentration in the solution. Effectively, the dissolved oxygen sensors measure the activity of O_2 in the solution which in ion-free conditions is the same as the concentration of O_2. Since salinity influences the activity coefficient of O_2, the sensors are provided with a correction for sodium chloride (NaCl) salinity. This correction factor is not applicable for other salts, as all ions have different salting-in or -out effects (Schumpe et al., 1978).

The optical dissolved oxygen sensor was a Memosens COS81D from Endress+Hauser. This was mainly used to validate the galvanic sensor working principle (electrochemical), to prove that a different principle (fluorescence quenching) also measures the same concentrations of oxygen. Each experimental section specifies which sensors have been used for the measurement and further details on their working principles are given in the appendix.

5.2.3 Methods

Schematics of the experimental setups used in the various experiments are depicted in Figure 5.1.
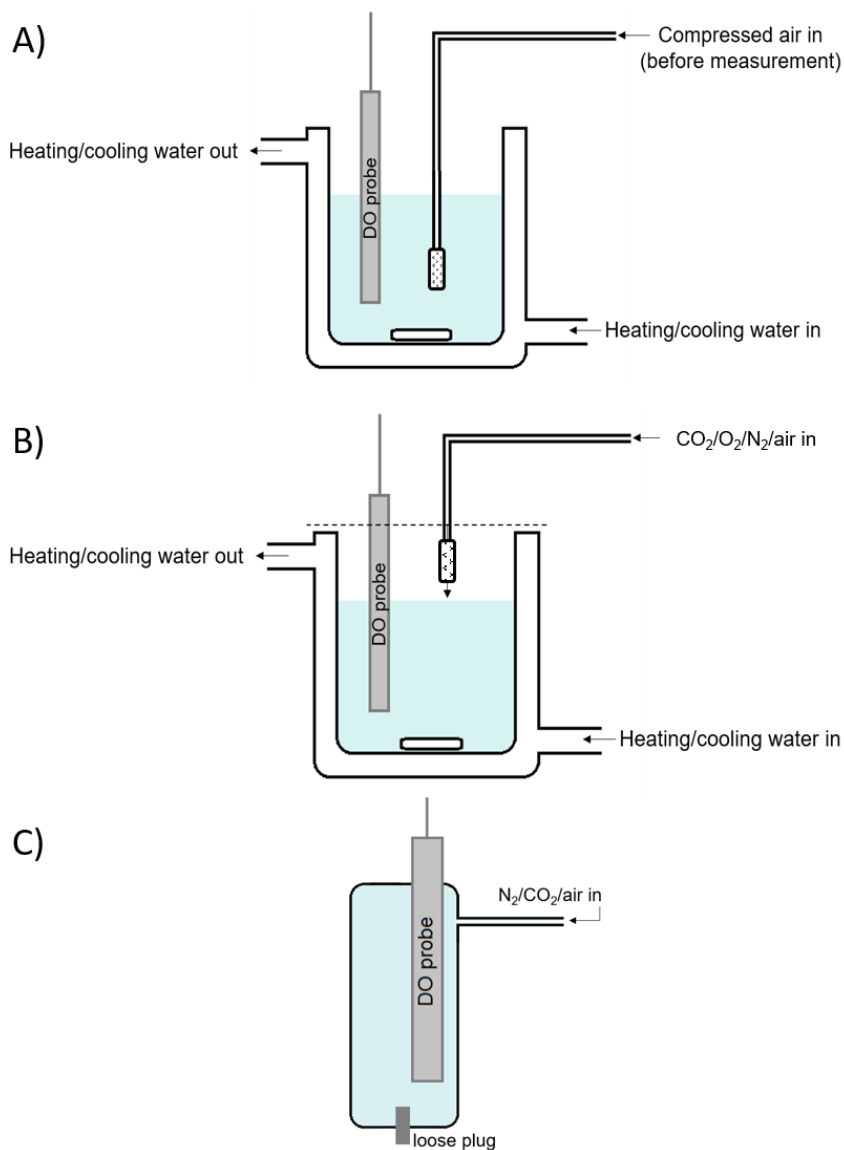
Figure 5.1: Scheme for experimental setups A, B and C. Setup A and B are temperature controlled in a double-jacketed reactor, whereas C is only operated at room temperature. The gas distribution tube in setup B is moveable and maintained over the liquid surface during the measurment. Both setup A and B use magntic stirring for mixing, whilst setup C relies on a constant flow of gas though the reactor, eliminating the need for futher agitation.

5.2.3.1 Experimental setup A: Oxygen solubility at ambient O_2 partial pressure

A 300 mL double-jacketed glass reactor (Figure 5.1A), which was connected to a circulating combined heating and cooling bath, was filled with approximately 200 mL of the solution, which was cooled or heated to the experiments' starting temperature. When the desired temperature was achieved, compressed air was bubbled through the solution through a sintered gas dispersion tube, under magnetic stirring for at least 10 minutes. The gas dispersion tube was thereafter removed, for gas bubbles not to disturb the measurement. The magnetic stirring was maintained throughout the experiment, to ensure circulation of the liquid, maintaining the measured concentration around the probe head constant. The concentration of dissolved oxygen was recorded after the temperature stabilisation for each measurement point. Further measurements of dissolved oxygen were made at stable temperatures up to the upper operational temperature of the sensors.

5.2.3.2 Experimental setup B: Influence of CO_2 loading on oxygen solubility

A 300 mL double-jacketed glass reactor (Figure 5.1B), connected to a circulating combined heating and cooling bath, was filled with approximately 200 mL of the solvent. Centrally supplied CO_2 and O_2 gas added through two mass flow controllers and subsequently mixed in a stainless-steel tube, was suspended over the surface of the solution. A thermometer was inserted into the solution and the water bath adjusted to the desired temperature and temperature stability was awaited under a pure O_2 atmosphere, which was added through the gas tube suspended over the liquid surface. Once temperature stability in the liquid was reached, the dissolved oxygen sensor(s) was (were) inserted to the solution. A liquid sample for total inorganic carbon (TIC) analysis (section 5.2.8) was taken and simultaneously the first measurement of dissolved oxygen is recorded. The gas flow from the tube above the liquid surface was adjusted to contain the desired ratios of CO_2 and O_2 and was kept constant throughout the whole experiment. A layer of parafilm was used to make a partial cover of the reactor, to assure that the gas phase over the liquid surface always contained the desired partial pressures of CO_2 and O_2. Liquid samples for TIC analysis were taken simultaneously as oxygen concentration recordings were made, approximately every 20 or 30 minutes.

5.2.4 Comparison of a galvanic and an optical dissolved oxygen sensor

Experimental setup A (Figure 5.1A) was used for the following experiments with MEA, where oxygen solubility was measured with the galvanic VWR pHenomenal® and the optical Endress+Hauser COS81D dissolved oxygen sensors at room temperature with low loadings of 0.03 and 0.1 mol_{CO2} mol_{MEA}^{-1}. The solutions were sparged with compressed air before commencing the measurement of their oxygen

concentrations, for reaching oxygen saturation at ambient pressure faster. Since MEA is commonly known as an unstable amine which degrades rapidly oxidatively, a very stable tertiary amine, MDEA, was also investigated. This was to see if a polarization of the oxygen selective membrane to inhibit oxygen permeation could occur with CO_2, which would be an operational problem with CO_2 present in the solutions. This experiment would also show if degradation rates can be assessed with the commercial sensors. A solution of 30wt% MDEA (*aq.*) with a loading of 0.4 mol of CO_2 per mol MDEA was studied using experimental setup A (section 5.2.3.1). The solution was sparged with compressed air for 15 minutes after reaching temperature stability at 20 °C. Before measuring the oxygen concentration, the gas dispersion tube was removed, and the two sensors and a thermometer were inserted into the liquid. Temperature and oxygen concentration stability was awaited, before the first concentration and temperature point were noted. The liquid was slowly heated up and temperature and oxygen concentration measured by the two individual sensors were recorded regularly. Because of the high oxygen consumption rate, the same experiment could not be performed with MEA with CO_2 loading.

5.2.5 Study of possible CO_2 effects on dissolved oxygen sensors

5.2.6 Solubility of oxygen in water using three different gas phase compositions

Experimental setup B (Figure 5.1B) was filled with deionized water and partly closed using parafilm. The water was then sparged with a specific gas composition, provided by two mass flow controllers, for 10-15 minutes at 20 °C, the temperature being kept constant at 20 °C using the combined heating and cooling bath. The gas distribution tube was then placed above the liquid surface with gas still being distributed into the gas phase of the partly closed system and the Endress+Hauser COS81D dissolved oxygen sensor submerged in the liquid. Stability of the signal was awaited for 10-15 minutes and the temperature and concentration of oxygen measurement was noted. Three gas mixtures were studied using this setup: N_2 with air, CO_2 with air and pure air.

5.2.7 Gas phase oxygen measurement with the optical sensor

In experimental setup C (Figure 5.1C), a 1.3 L glass reactor was added gas mixtures of different compositions, which were investigated using the Endress+Hauser COS81D dissolved oxygen sensor. Gas flows were controlled using two Bronkhorst® mass flow controllers, which supplied the gas at the top of the reactor and could escape through a small opening in the bottom of the reactor. The constant flow of the gas through the reactor ensured agitation around the sensor head, ensuring reliable oxygen solubility measurements. Stability of the signal was awaited for 10-15 minutes and the temperature and concentration of oxygen measurement was noted.

Three compositions of air, CO_2 and N_2 were investigated, all at a room temperature of about 20 °C.

5.2.8   Analytical methods

A Shimadzu TOC-L$_{CPH}$ in Total Inorganic Carbon (TIC) mode was used for the determination of the amount of CO_2 (as the only inorganic carbon species) in the solution. Amine titration with H_2SO_4 determined the exact amine concentration and from this, the exact CO_2 loading (α) of the solution was determined (Ma'mun et al., 2006). All samples were analysed twice, yielding a relative deviation of ≤2% for both methods, both comparing two parallel analyses and when analysing standards of known concentrations.

Winkler titrations were performed using a HI-3810 Chemical test Dissolved Oxygen kit from Hanna Instruments. The quantification of dissolved oxygen relies on the reactions given in Equations 6, 7 and 8.

$$2Mn^{2+} + O_2 + 4OH^- \rightarrow 2MnO_2 \downarrow +2H_2O \rightarrow 2MnO(OH)_2 \qquad (6)$$

$$MnO(OH)_2 + 2I^- + 4H^+ \rightarrow I_2 + Mn^{2+} + 3H_2O \qquad (7)$$

$$I_2 + 2S_3O_3^{2-} \rightarrow 2S_4O_6^{2-} + 2I^- \qquad (8)$$
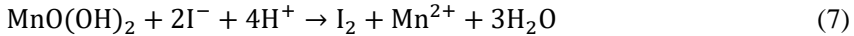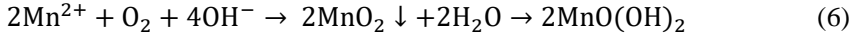
An Agilent 7890A GC-MS was used in Electron Spray Impact ionization mode (ESI) with an *Equity^{TM} – 1701 Fused silica capillary column* (30 m × 0.25 mm film thickness) and helium as the carrier gas. The quantification of dissolved oxygen was performed by a triple quadrupole mass spectrometer, by Single Ion Monitoring (SIM) of the fragment and molecular ions of oxygen, $m/z = 16$ and $m/z = 32$. These ions appear in the very start of the chromatogram before any other compounds elute.

5.2.9   Modelling

The solubility of O_2 in CO_2 loaded and unloaded 30 wt% MEA solutions and concentrated NaCl solutions was estimated using the model of Weisenberger and Schumpe (1996). The model is suitable for predicting gas solubility into electrolyte solutions with concentrations up to 2 – 5 m^3 kmol^{-1} and has been widely used in the literature. (Chatenet et al., 2000; Haug et al., 2017; Knuutila et al., 2010). The model expression is given in Equation 9.

$$\log\left(\frac{C_{G,0}}{C_G}\right) = \Sigma(h_i + h_G)c_i \qquad (9)$$

In the equation $C_{G,0}$ and C_G are the gas solubility in water and in the electrolyte solution, respectively, h_i is the ion-specific parameter, h_G is the gas-specific parameter and c_i is the concentration the ion. The temperature dependence of the gas-specific parameter is given in Equation 10.

$$h_G = h_{G,0} + h_T(T - 298.15 \text{ K}) \tag{10}$$

here $h_{G,0}$ is a gas-specific parameter, h_T is a gas-specific parameter for the temperature effect and T is temperature.

In this work, the solubility of O_2 in water, $C_{O_2,0}$ with unit mol dm^{-3}, was determined using the correlation given in Equation 11 proposed by Xing et al. (2014). In the equation p_{O_2} is the partial pressure of O_2 above the solution,

$$C_{O_2,0} = \frac{55.56 p_{O_2}}{\exp\left(3.71814 + \dfrac{5596.17}{T} - \dfrac{1049668}{T^2}\right) - p_{O_2}} \tag{11}$$

The ion concentrations in CO_2 loaded 30wt% MEA (*aq.*) solutions were determined from NMR speciation data reported by Böttinger et al. (2008) and density data needed to convert mole fractions to molar concentrations were taken from Hartono et al. (2014).

The gas-specific parameter for oxygen in Equation 9 are reported in literature. However, since the ion-specific parameters for protonated MEA (h_{MEAH^+}) and carbamate (h_{MEACOO^-}) were unknown, they were determined by fitting Equation 9 to experimental N_2O solubility data for CO_2 loaded 30wt% MEA (*aq.*) solutions at 40 °C reported by Hartono et al. (2014). Since N_2O does not react chemically with the amine, it offers data for only the physical absorption in the liquid phase, which is then used to calculate the ion specific parameters. The Henry's law constant for N_2O in water was determined using the correlation given in Equation 12, provided by Penttilä et al. (2011), and the partition coefficient expressed in Equation 13 was calculated to be used as the $C_{G,0}$ value for N_2O at 40 °C.

$$H_{N_2O,W} = \exp\left(158.245 - \frac{9048.596}{T} - 20.860\ln T - 0.00252\,T\right) \tag{12}$$

$$m = \frac{RT}{H} \tag{13}$$

5.3 Results and discussion

5.3.1 Schumpe model and parameter fitting for estimation of oxygen solubility

The Schumpe model was used to represent the solubility of oxygen into water and salt solutions using parameters from literature. However, the model can also be used

to predict oxygen solubility of aqueous amine solutions, if data for physical solubility of N_2O and speciation in CO_2 loaded solution is available. A theoretical prediction of oxygen solubility in loaded amine solutions, based on the effects of the ionic species in the solution has not yet been made for MEA. Using the literature and fitted ion specific constants given in Table 5.2, the predicted shown in Figure 5.2 were calculated, proving that the model can accurately represent the N_2O solubility in loaded 30wt% MEA. The constants needed for calculating the O_2 and N_2O solubility into CO_2 loaded 30wt% MEA (*aq.*) solutions and in concentrated NaCl solutions are given in Figure 5.2. The performance of the model to predict O_2-solubility using the fitted parameters will be discussed in section 5.3.4.3 and Figure 5.6.

Table 5.2: Parameters for Equation 1 and 2. The $h_{T,i}$ value for O_2 is valid from 273 K to 353 K and that of N_2O is valid from 273 K to 313 K.

Parameter	Unit	Value	Reference
h_{MEAH^+}	m³ kmol⁻¹	0.0133	This work
h_{MEACOO^-}	m³ kmol⁻¹	0.1284	This work
$h_{HCO_3^-}$	m³ kmol⁻¹	0.0967	(Weisenberger and Schumpe, 1996)
h_{Na^+}	m³ kmol⁻¹	0.1143	(Weisenberger and Schumpe, 1996)
h_{Cl^-}	m³ kmol⁻¹	0.0318	(Weisenberger and Schumpe, 1996)
h_{G,o,N_2O}	m³ kmol⁻¹	-0.0085	(Weisenberger and Schumpe, 1996)
h_{G,o,O_2}	m³ kmol⁻¹	0	(Weisenberger and Schumpe, 1996)
h_{T,O_2}	m³ kmol⁻¹ K⁻¹	-0.000334	(Weisenberger and Schumpe, 1996)
h_{T,N_2O}	m³ kmol⁻¹ K⁻¹	-0.000479	(Weisenberger and Schumpe, 1996)
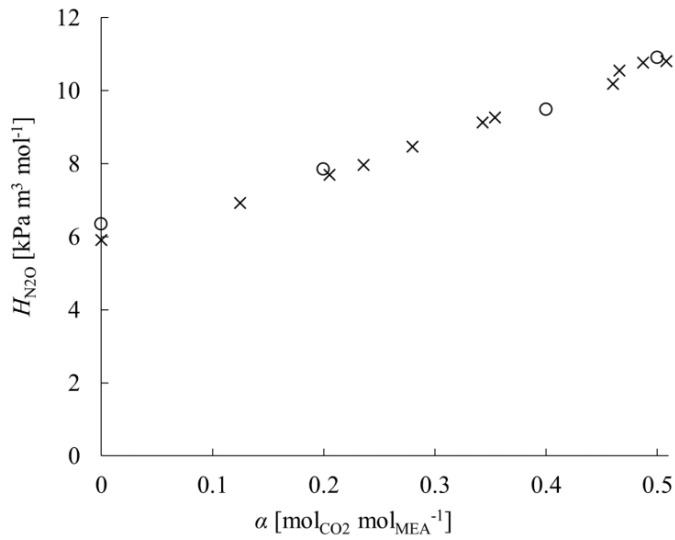
Figure 5.2: The Henry's law constant for N_2O at 40 °C in MEA 30wt% (*aq.*) solutions at different loadings. (○) Hartono et al. (2014) and (x) the model of Weisenberger and Schumpe (1996).
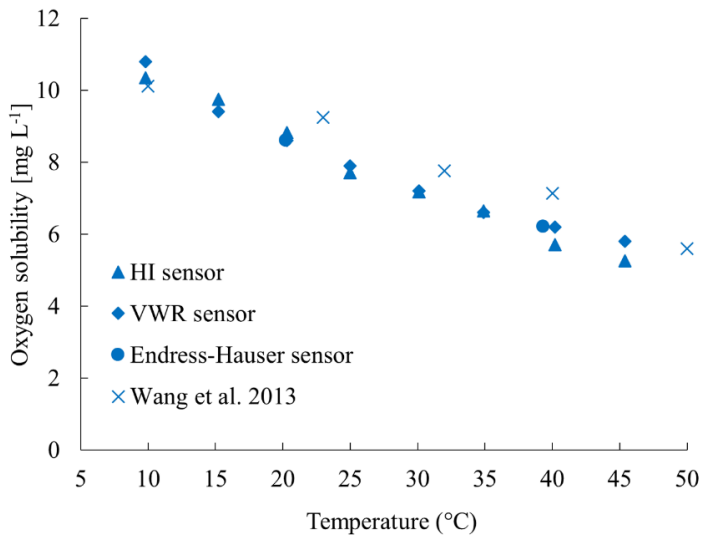
Figure 5.3: Oxygen solubility of 30wt% (*aq.*) MEA measured with three different dissolved oxygen sensors and compared to data from Wang et al. (2013). Solubility measured at $p_{O2} = 0.21$ atm.

5.3.2 Validation of the oxygen sensors with CO_2 unloaded solutions

Solubility of oxygen was measured in water (results in the appendix) and in 30wt% (*aq.*) MEA by the three dissolved oxygen sensors was compared to available literature data. The results of this validation experiment can be found in Figure 5.3. In MEA 30wt% (*aq.*), the maximum absolute deviation between the dissolved oxygen sensors in this work was ± 0.6 mg L^{-1} (13%, in the higher temperature range) and the maximum absolute deviation comparing the measured oxygen solubility to literature values from Wang et al. was 1.4 mg L^{-1} (13%, in the higher temperature range). It should be noted that Rooney and Daniels (1998) and Wang et al. (2013) used polarographic dissolved oxygen probes for their dissolved oxygen measurements. Polarographic dissolved oxygen sensors use the same principle of detection as galvanic probes; therefore, the same oxygen selective cathode reactions apply.

All oxygen selective membranes are also selective towards carbon dioxide, , the effect of varying the gas phase composition between O_2, N_2 and CO_2 was studied in both water (described in section 5.2.6, results in Supplementary table 4) and gas phase (described in section 5.2.7, results in Supplementary table 5). No significant difference could be observed between measurements in mixtures of air and N_2, and air and CO_2. Replacing half the air with either of the two other gases, gave half the concentration of oxygen measured with only air, although a small difference can be seen in the gas phase experiment, which can potentially be explained either by the sensor being slightly less accurate in air, or the experimental setup not being ideal for this type of experiment. Either way, dissolved or chemically bound CO_2 does not appear to influence the dissolved oxygen sensor.

Overall, the validation experiments and comparison with literature data for oxygen solubility in amine solutions and water, measured with comparable sensors, show a good agreement. This means that the sensors can be assumed to work in the same manner as other sensors from other brands and with slightly different working principles.

5.3.3 Winkler titration and GC-MS analyses

Oxygen solubility in selected solutions was also measured using Winkler titration. The quantification principles of dissolved oxygen using an electrochemical sensor and by performing a Winkler titration are different, but both are species-specific for measuring only dissolved oxygen. The electrochemical sensor gives a signal based on the current created from the cathodic reduction of O_2 to H_2O., while the titration relies on reduction of O_2 to form a MnO_2 salt. These independent methods show the same concentration of oxygen in pure water, but upon addition of salt, they deviate from one another. As Winkler titration method is not suitable for measuring the concentration of oxygen in amine solutions with a high pH, only aqueous solutions with NaCl or MEG because of their neutral pH, were analysed. Other disadvantages of a titration method in this case are the challenges related to sampling. Sampling will

involve change of temperature and oxygen pressure, which in turn influences the oxygen solubility of the sample, additionally the amine solutions used for CO_2 capture are alkaline, a trait that is not compatible with the necessary acidification of the sample. All in all, these disadvantages make Winkler titration a bad alternative in industrial applications.

Further, as an attempt to find an additional independent validation method, a GC-MS study was performed for pure amine solutions, saturated with oxygen at normal atmospheric oxygen pressure ($p_{O2} \approx 0.21$ atm) by sparging with air. The possibility of using a GC-MS quantifying the molecule ions with m/z 16 and 32 in the pre-elution peak of a fused silica capillary column, was also tested in this work. Since the dissolved gas molecules are not retained in the column, the assumption that all the gas would elute before the rest of the sample was made, and indeed a pre-chromatogram peak containing only the m/z 14 and 28 (N^+ and N_2^+) in addition to 16 and 32 (O^+ and O_2^+) was seen. In different solvents, this peak's size varied, sometimes in orders of magnitude, in different amines and solvents and the reproducibility was poor (repeated analyses gave standard deviations >30%). This validation attempt was therefore abandoned. A MS method for oxygen quantification could maybe become useful if it would be possible to retain the analytes in the chromatographic column in the future. If a GC method should be used, the results suggest that a molecular sieve (for gas separation) with a pre-column (for removal of solvent/liquid) GC-TCD method (Park and Catalfomo, 1964) would be recommended, although this equipment is not very common. Because of this, we were not able to access an instrument for testing the GC-TCD method in this work. It is also unsure whether this detection method would be able to quantify such low concentrations of oxygen.

5.3.4 Oxygen solubility in amine solutions

5.3.4.1 Oxygen solubility in different concentration of MEA (*aq.*)

The concentration of amine in water changes the physical properties of the liquid like viscosity and density. To study whether varying the concentration of amine also influences the oxygen solubility of the solvent, aqueous solutions of ethanolamine (MEA) were prepared and their oxygen solubility measured at different temperatures and compared to pure MEA and water.
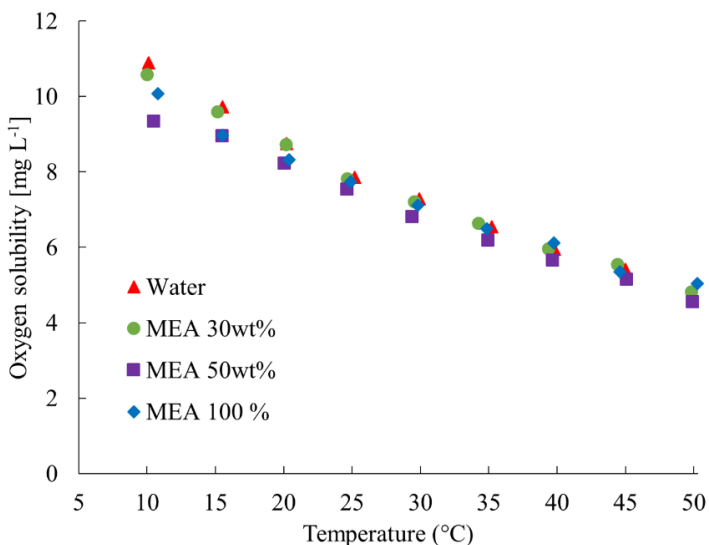
Figure 5.4: Oxygen solubility in various concentrations of MEA at varying temperatures at $p_{O2} = 0.21$ atm. The shown oxygen solubility is the average of the measured solubility from the two different probes.

The experiments were performed using the two electrochemical dissolved oxygen sensors and experimental setup A (section 5.2.3.1). The results given in Figure 5.4 show a small deviation (17% deviation and ± 1.6 mg L^{-1} in the lower temperature range, 11% and 0.6 mg L^{-1} above 20 °C) from the oxygen solubility in water. These observations agree with those of Wang et al. (2013), who concluded that the presence of MEA in an aqueous solutions does not significantly influence the concentration of dissolved oxygen compared to pure water. For further comparison, Henry's law constant (H^{cp}) was calculated from the measured solubility and pressure and these results show no significant difference from the Henry's law constants of water reported in literature (can be found in the supporting information).
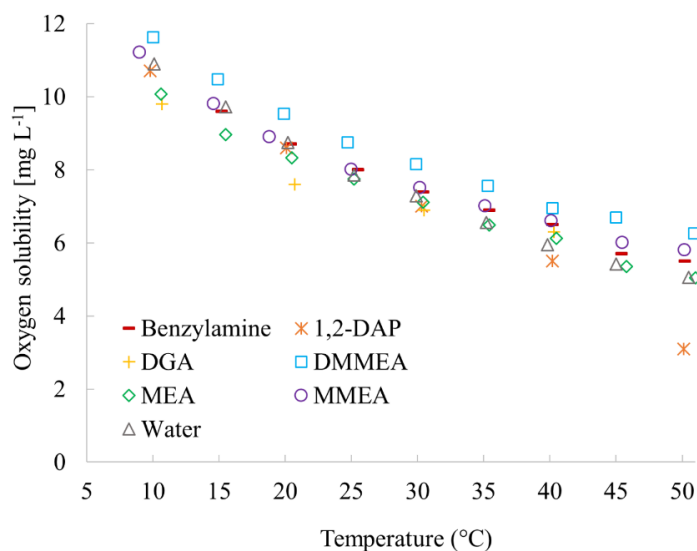
Figure 5.5: Oxygen solubility of pure solvents as a function of temperature, all measured at $p_{O2} = 0.21$ atm.

5.3.4.2 Oxygen solubility in pure amine solvents

The structural variations in different amines, suggest that the oxygen solubility could vary, as other chemical and physical properties of the solvents do. For the purpose of investigating this, amines with a relatively wide array of structural variation were subjected to the same conditions.

Oxygen solubility was measured and compared in structurally different amines at varying temperatures, using experimental setup A (5.2.3.1) and both electrochemical dissolved oxygen sensors. A primary (MEA), a secondary (*2-methylaminoethanol*, MMEA) and a tertiary alkanolamine (*2-(dimethylamino) ethanol*, DMMEA), as well as an aromatic amine (benzylamine), a diamine (*1,2-diaminopropane*, 1,2-DAP) and an ether of a primary alkanolamine (*2-(2-aminoethoxy) ethanol*, DGA) were studied, and the measured oxygen solubility of the amines are shown in Figure 5.5. Pure amine solutions also show a very similar oxygen solubility to water, with very little variation. A study of amine viscosity and density showed that for alkanolamines, the oxygen solubility seems to decrease with increasing viscosity and density, an effect that could be related to the strength of hydrogen bonding in the solution. Detailed information about this can been found in the appendix.

5.3.4.3 Influence of CO_2 loading on oxygen solubility

An increase in ionic strength, such as achieved by loading an amine with CO_2, leads to decreasing oxygen solubility. This effect is described by the ability of the ionic species to influence the dissolved oxygen activity coefficient and is commonly known

as the "salting out effect", vice versa, ions that decrease the dissolved gas' activity coefficient can cause a "salting in effect" (Battino and Clever, 1966).

When an amine is used for CO_2 capture, the solution always contains CO_2, even at "lean" loadings. Therefore, experiments with pre-loaded solutions of MEA were studied at different temperatures. Aqueous solutions of MEA were loaded with pure CO_2 to obtain loadings in the range of 0.07-0.4 mol CO_2 per mol amine. The amine and CO_2 concentrations were determined by amine titration and TIC analysis (section 5.2.8). The ability of the solutions to dissolve oxygen was investigated at different temperatures using experimental setup A (section 5.2.3.1) and both electrochemical dissolved oxygen sensors. The results given in Figure 5.6 show decreasing oxygen solubility with increasing concentration of CO_2 in the solution. Oxygen concentration was also measured at the temperatures 30, 35 and 45 °C and these follow the same trend. For illustrational purposes, only the data for the temperatures which have been modelled are depicted in Figure 5.6, whereas the other datasets are given in Supplementary figure 5.5. The oxygen concentration reaches a similar sudden drop in the data series recorded at 35 and 45 °C. Whether a drop or a linear decay in oxygen concentration is taking place already at 30 °C is unclear. These findings do, however, indicate that at realistic process conditions, which are above 35 °C, the oxygen concentration is likely to be severely influenced by rapid oxidative degradation of MEA already at typical lean loadings. While the modelling approach predicts the oxygen solubility into a MEA solutions, what is measured here, is not representative of the physical solubility of the solvent because oxygen is being chemically consumed through degradation reactions with loaded MEA. It can be assumed that oxidative degradation already takes place at lower loadings, but that it seems that the degradation reactions are slow enough for the measured dissolved O_2 and the model predictions to be close to each other.
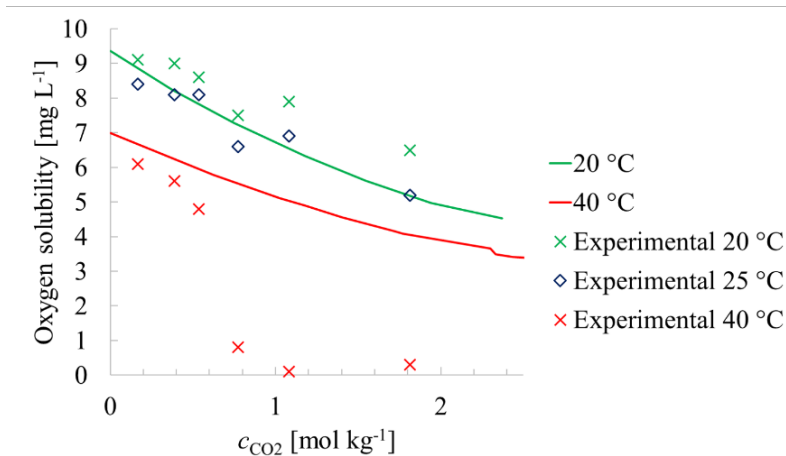
Figure 5.6: With the adjusted ion parameters for MEAH$^+$ and MEACOO$^-$, as well as known values from (Weisenberger and Schumpe, 1996), the solubility oxygen in loaded MEA-solutions were predicted. The predicted solubilities are here compared to the measured solubilities at different temperatures, using the VWR pHenomenal® dissolved oxygen sensor.

After observing the drastic drops in oxygen solubility with increasing CO_2 loading, a series of experiments where oxygen partial pressure was varied were performed. MEA solutions of 30wt% (*aq.*) were subjected to an O_2/CO_2 atmosphere of different, but in each experiment constant, ratios of the two gases, using experimental setup B (Figure 5.1B and section 5.2.3.2) and the VWR pHenomenal® sensor. This led to the CO_2 loading increasing over time. All mixing ratios of O_2 and CO_2 gave a decreasing measured oxygen solubility in the amine solution with increasing loading (and time). Figure 5.7 shows how the amount of oxygen in the surrounding atmosphere directly influences the solubility of oxygen in the solutions, but with increasing CO_2 loading the oxygen concentration in all cases suddenly drops. This drop indicates the point at which chemical reaction between amine and oxygen takes place faster than oxygen is transferred from the gas to the liquid phase.
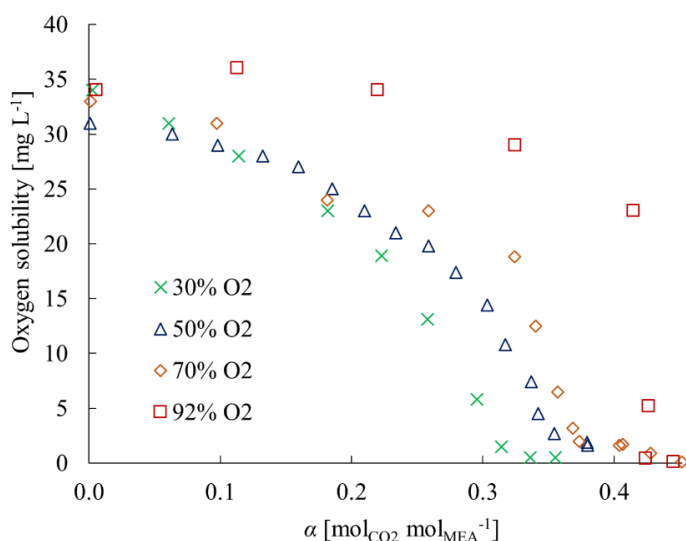
Figure 5.7: The solubility of oxygen decreasing with increasing CO_2 loading, when left in a gas atmosphere containing solely O_2 and CO_2 vol%) at 30 °C and 1 atm.

Finally, to better understand the results, the concentrations of dissolved oxygen was measured in unloaded and loaded MDEA. The results are presented in Figure 5.8 and in Supplementary table 13Supplementary table 5.13. When compared to data presented in Figures 8 and 9 for MEA loaded with CO_2, the same unexpected drop at higher loading was not seen in MDEA. Instead the apparent oxygen solubility increases from 7.6 mg L^{-1} in CO_2 free MDEA to 8.0 mg L^{-1} when the solution was

loaded to 0.4 mol CO_2 per mol MDEA at 20 °C. The same behaviour was seen with both the optical and a galvanic sensor.
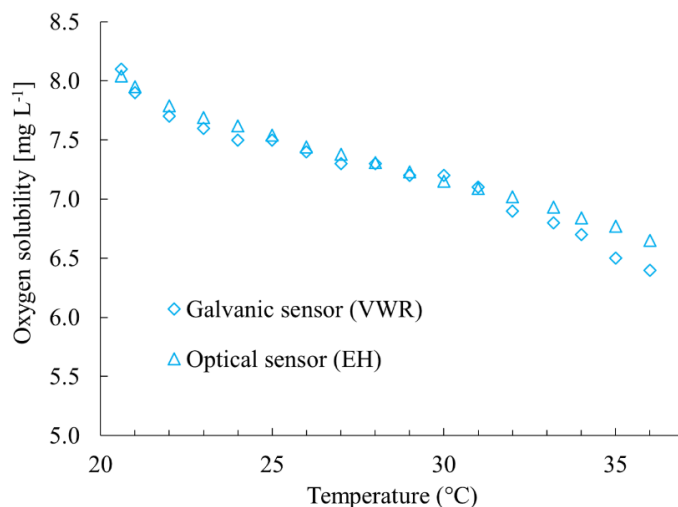
Figure 5.8: The oxygen solubility of a solution of aqueous 30wt% MDEA (*aq.*) with 0.4 mol of CO_2 per mol MDEA, measured with VWR pHenomenal® galvanic and the Endress+Hauser optical dissolved oxygen sensor at different temperatures.

The fact that CO_2 loaded MDEA shows a measurable concentration of oxygen and loaded MEA not, supports the explanation of rapid consumption of dissolved oxygen in rapidly degrading amine solutions such as MEA. It can be assumed that dissolved oxygen sensors are able to give information about oxygen consumption rates, which again could give indications about the amines' oxidative degradation rates. For this to be fully understood, mass transfer rates of oxygen from gas to liquid phase must be known.

Furthermore, the solubility of oxygen in loaded MDEA is comparable to that of water or unloaded MEA. Since the dissolved oxygen sensor also measures the same concentration of oxygen regardless of N_2 or CO_2 being present in the gas phase in addition to O_2, it can be clear that CO_2 does not influence the measurement or causes membrane concentration polarization. As both the electrochemical and optical sensor measure the same oxygen concentrations in loaded solutions, we regard that both sensors are free from influence of other gases.

Finally, Figure 5.6 also shows the modelling results based on the measured physical solubility of inert N_2O in loaded solutions of MEA by Hartono et al. (2014) and NMR speciation data of loaded MEA solutions (Böttinger et al., 2008). The oxygen solubility of solutions of MEA with CO_2 loading could be predicted using the model parameters given in Table 5.2 and equations 9, 10 and 11. As it can be seen in Figure

5.6, where oxygen concentrations at different temperatures and CO_2 concentrations are compared to the concentrations predicted by the model, a slight deviation is observed for temperatures at 20 °C, where the measured concentration of oxygen is slightly higher than predicted. This effect can be explained by the increased conductivity and therefore amplification of the probe signal. At 40 °C, the deviation is however high, due to rapid oxygen consumption at this temperature.

Despite the signal being influenced by the ionic strength of the solution, the dissolved oxygen sensor method for determining oxygen concentrations of the amine solutions is the simplest, and only direct, of the tested methods. Of the few other existing options, the Winkler titration method is not suitable for use in alkaline solutions in addition to being indirect and involving sampling, and equilibrium cell experiments for measurement of dissolved oxygen requires high pressure, due to the low solubility of O_2. If the amines degrade rapidly in the presence of oxygen, the dissolved oxygen sensors do not actually measure the solubility of oxygen in the solution, as it is limited by the mass transfer from gas to liquid phase and the degradation rate of the amine. This goes especially for CO_2-loaded solutions of degradable amines like MEA and puts a large limitation to the applicability of dissolved oxygen sensors for determining the presence of liquid phase oxygen. Considering the results of this study, MEA appears to consume oxygen faster than fresh oxygen dissolves from the gas to the liquid phase, so although there is a physically inherent property of oxygen solubility in the solution, this is not measurable. This is not due to the measurement principle, but rather MEA's fast degradation or reaction rate in the presence of oxygen.

5.3.4.4 O_2 solubility in a degraded amine solution

A degraded amine solution contains a mixture which can contain alkaline amine, acidic and alkaline degradation products, heat stable salts, carbamate, dissolved metals, and other ionic components. To study the effect of degradation products on oxygen solubility in an amine solution, a highly degraded amine solution was studied in the same manner as lean and loaded amines were studied in experimental section 5.3.4.1 to 5.3.4.3, with varying temperature of the solution. The degraded solution which was studied had been submitted to a three-week campaign of laboratory scale oxidative degradation and contained less than 1% of the original alkalinity (amine concentration). The degraded solution contained a total anionic HSS concentration of 0.75 mol/kg.

The oxygen solubility in 30wt% (*aq.*) MAPD (CO_2 free) was measured with the VWR pHenomenal® dissolved oxygen sensor in experimental setup A (5.2.3.1) before and after strong oxidative degradation (CO_2 concentration < 1 g/kg). A complete loss of amine was found in the degraded solution, meaning that the solution primarily consisted of water and degradation compounds. The measurement results in Table 5.3 oxygen solubility neither increases nor decreases significantly with amine loss and increased concentration of degradation products.

Since there is no significant difference in the concentration of an unloaded (CO_2-free) amine solution and a highly degraded solution (also as good as CO_2-free), it can be speculated that the presence of degradation compounds in the form of heat stable salts have much less influence on the oxygen solubility than carbamate and protonated amine formation.

Table 5.3: Oxygen solubility of 3-methylamino-1,2-propanediol (MAPD, α = 0) before and after laboratory scale oxidative degradation over a three-week period. Oxygen solubility was measured at pO_2 = 0.21 atm.

MAPD 30wt% (aq.)		MAPD 30wt% (aq.) degraded	
Amine conc. [mol kg⁻¹]	2.85	Amine conc. [mol kg⁻¹]	0.0161
T (°C)	c_{O2} [mg L⁻¹]	T (°C)	c_{O2} [mg L⁻¹]
11.0	10.3	10.4	10.3
20.4	7.8	20.5	8.2
30.3	6.7	30.3	6.8
39.8	5.7	39.8	5.7
49.2	4.5	49.8	4.8

5.3.5   Significance of the results for the capture process

In an absorber column where CO_2 is absorbed from a flue gas, the liquid temperatures typically vary from 40 to 80°C and as the solvent absorbs CO_2, the ionic strength of the solution increases. Furthermore, typical flue gas contains generally between 5 and 14 mol% oxygen (Feron et al., 2014; Hjelmaas et al., 2017; Lombardo et al., 2014; Moser et al., 2011a; Moser et al., 2011b; Rieder et al., 2017). These factors lead to lower oxygen concentrations compared to those seen in this study, making the quantification of dissolved oxygen challenging, both because of upper operating temperature limits of the sensors and their limits of detection and quantification. The use of commercially available dissolved oxygen sensors made for water testing purposes can, however, be considered in industrial applications in amine solutions, if it has a relatively low oxygen consumption rate and the measurement takes place below the upper operating temperature of the sensor. Of the tested sensors, the optical dissolved oxygen sensor seems more capable of withstanding the alkalinity of the amine solutions than the other two, not suffering from neither corrosion nor other damage in the process, and may therefore be more suitable for dissolved oxygen measurements in a carbon capture facility.

Technologies for oxygen removal and oxidation inhibition in the amine solvent are being developed, to reduce the problems and costs related to oxidative degradation in amine scrubbers. These techniques generally base on oxygen removal by addition of oxygen scavengers, either by direct addition to the amine solution or indirect contact through a membrane barrier (Monteiro et al., 2018; Supap et al., 2011; Veldman and Trahan, 1997). Additionally a "salting out" method could potentially be applied,

where an intentional increase of ionic strength of a solution is performed by addition of salts to decrease the overall oxygen solubility (Léonard et al., 2014). This approach will need careful testing, as the increase of salinity also may influence other solvent properties, like corrosivity, viscosity, density, cyclic capacity, and heat of absorption.

Regardless of which of these techniques are being investigated or applied in industry, there is a need for a reliable method for quantifying the amount of oxygen in the solution before and after the removal operation, to evaluate the efficiency of the technology and to detect operational problems in the removal process if they occur. Ideally, the means of measurement should be direct, and preferably also online, to avoid unnecessary amounts of work and errors during sampling, in addition to giving a possibility for automated analyses. A dissolved oxygen sensor would be an ideal solution for direct measurement, but it would require the amine solution of choice to not consume dissolved oxygen faster than it is being transferred from the gas to the liquid phase, to make any sense to measure at all. It also requires a sufficiently low detection and quantification limit of the sensor. Oxygen concentrations expected to be found in an amine scrubbing facility, where the temperature generally is high and the pressure of flue gas oxygen is low, are in the lower ppm range (at least <6 ppm, probably lower) and if the solvent is readily degradable, maybe even in the ppb-range. Since the apparent solubility given by the dissolved oxygen sensors are higher than reality, given the increased conductivity of the solution, it is possible that the sensor's sensitivity is increased and may be used in lower concentration ranges than expected. This effect will, however, need to be further studied and understood.

5.4   Conclusions

The results of the study show that commercially available dissolved oxygen sensors may be used to measure oxygen concentrations in amine solutions both in the presence and absence of CO_2. The increased conductivity of the solution when the amine has chemically bonded CO_2 gives a slight amplification of the signal, which means that the actual concentration of oxygen is lower than measured. Oxygen solubility does not vary much in different solutions with and without amines. The factors influencing oxygen solubility the most are temperature, oxygen pressure and also the CO_2 loading. Amines with rapid oxidative degradation rates, such as ethanolamine, will consume oxygen from the solution faster than the oxygen transfer rate from gas to liquid phase. Measurement of oxygen concentrations in rapidly degrading amine solutions is therefore not useful. The actual oxygen concentration in these solvents will be very low, likely below the detection limit of any commercially available dissolved oxygen sensors (<<1 ppm). For amines which are stable under oxidative conditions, the sensors are fit for the purpose of measuring their oxygen concentrations.

The tested modelling approach seems both promising and realistic. However, for adjusting the Schumpe model, data on physical solubility of CO_2 in loaded solutions as well as ionic speciation are needed. Comparing model predictions to measured oxygen concentrations in solutions give indications of the solvent's degradation rate. The modelling approach can be a helpful tool when using oxygen solubility as a parameter for degradation modelling or when experimental determination is not possible.

The commercially available dissolved oxygen sensors may find an application as a fast screening method for the evaluation of oxidative stability of novel solvents, in addition to measurement of dissolved oxygen concentrations in chemically stable solvents.

Acknowledgements

References

Battino, R., Clever, H.L., 1966. The solubility of gases in liquids. Chemical Reviews 66, 395-463.

Bhattacharya, S., Hwang, S.-T., 1997. Concentration polarization, separation factor, and Peclet number in membrane processes. Journal of membrane science 132, 73-90.

Böttinger, W., Maiwald, M., Hasse, H., 2008. Online NMR spectroscopic study of species distribution in MEA–H2O–CO2 and DEA–H2O–CO2. Fluid Phase Equilibria 263, 131-143.

Chatenet, M., Aurousseau, M., Durand, R., 2000. Comparative Methods for Gas Diffusivity and Solubility Determination in Extreme Media: Application to

Molecular Oxygen in an Industrial Chlorine–Soda Electrolyte. Industrial & Engineering Chemistry Research 39, 3083-3089.

Chen, X., Freeman, S.A., Rochelle, G.T., 2011. Foaming of aqueous piperazine and monoethanolamine for CO2 capture. International Journal of Greenhouse Gas Control 5, 381-386.

Clark, L.C., 1959. Electrochemical device for chemical analysis. Google Patents.

da Silva, E.F., Lepaumier, H., Grimstvedt, A., Vevelstad, S.J., Einbu, A., Vernstad, K., Svendsen, H.F., Zahlsen, K., 2012. Understanding 2-ethanolamine degradation in postcombustion CO2 capture. Industrial & Engineering Chemistry Research 51, 13329-13338.

Danckwerts, P., 1979. The reaction of CO2 with ethanolamines. Chemical Engineering Science 34, 443-446.

Dhingra, S., Khakharia, P., Rieder, A., Cousins, A., Reynolds, A., Knudsen, J., Andersen, J., Irons, R., Mertens, J., Abu Zahra, M., Van Os, P., Goetheer, E., 2017. Understanding and Modelling the Effect of Dissolved Metals on Solvent Degradation in Post Combustion CO2 Capture Based on Pilot Plant Experience. Energies 10.

Feron, P., Conway, W., Puxty, G., Wardhaugh, L., Green, P., Maher, D., Fernandes, D., Cousins, A., Gao, S.W., Liu, L.B., Niu, H.W., Shang, H., 2014. Amine based post-combustion capture technology advancement for application in Chinese coal fired power stations. 12th International Conference on Greenhouse Gas Control Technologies, Ghgt-12 63, 1399-1406.

Fytianos, G., Vevelstad, S.J., Knuutila, H.K., 2016. Degradation and corrosion inhibitors for MEA-based CO2 capture plants. International Journal of Greenhouse Gas Control 50, 240-247.

Goff, G.S., Rochelle, G.T., 2004. Monoethanolamine degradation: O2 mass transfer effects under CO2
 capture conditions. Industrial & Engineering Chemistry Research 43, 6400-6408.

Gouedard, C., Picq, D., Launay, F., Carrette, P.L., 2012. Amine degradation in CO2 capture. I. A review. International Journal of Greenhouse Gas Control 10, 244-270.

Hartono, A., Mba, E.O., Svendsen, H.F., 2014. Physical properties of partially CO2 loaded aqueous monoethanolamine (MEA). Journal of Chemical & Engineering Data 59, 1808-1816.

Haug, P., Koj, M., Turek, T., 2017. Influence of process conditions on gas purity in alkaline water electrolysis. International Journal of Hydrogen Energy 42, 9406-9418.

Henry, W., 1832. Experiments on the quantity of gases absorbed by water, at different temperatures, and under different pressures, Abstracts of the Papers Printed in the Philosophical Transactions of the Royal Society of London. The Royal Society London, pp. 103-104.

Hjelmaas, S., Storheim, E., Flø, N.E., Thorjussen, E.S., Morken, A.K., Faramarzi, L., de Cazenove, T., Hamborg, E.S., 2017. Results from MEA amine plant corrosion processes at the CO2 Technology Centre Mongstad. Energy Procedia 114, 1166-1178.

Knuutila, H., Juliussen, O., Svendsen, H.F., 2010. Density and N2O solubility of sodium and potassium carbonate solutions in the temperature range 25 to 80°C. Chemical Engineering Science 65, 2177-2182.

Kohl, A.L., Nielsen, R.B., 1997. Chapter 2 - Alkanolamines for Hydrogen Sulfide and Carbon Dioxide Removal, in: Kohl, A.L., Nielsen, R.B. (Eds.), Gas Purification (Fifth Edition). Gulf Professional Publishing, Houston, pp. 40-186.

Léonard, G., Crosset, C., Toye, D., Heyen, G., 2015. Influence of process operating conditions on solvent thermal and oxidative degradation in post-combustion CO2 capture. Computers & Chemical Engineering 83, 121-130.

Léonard, G., Voice, A., Toye, D., Heyen, G., 2014. Influence of dissolved metals and oxidative degradation inhibitors on the oxidative and thermal degradation of monoethanolamine in postcombustion CO2 capture. Industrial & Engineering Chemistry Research 53, 18121-18129.

Leung, D.Y., Caramanna, G., Maroto-Valer, M.M., 2014. An overview of current status of carbon dioxide capture and storage technologies. Renewable and Sustainable Energy Reviews 39, 426-443.

Lombardo, G., Agarwal, R., Askander, J., 2014. Chilled Ammonia Process at Technology Center Mongstad–First Results, Energy Procedia, pp. 31-39.

Ma'mun, S., Jakobsen, J.P., Svendsen, H.F., Juliussen, O., 2006. Experimental and modeling study of the solubility of carbon dioxide in aqueous 30 mass% 2-((2-aminoethyl) amino) ethanol solution. Industrial & engineering chemistry research 45, 2505-2512.

Mazari, S.A., Ali, B.S., Jan, B.M., Saeed, I.M., Nizamuddin, S., 2015. An overview of solvent management and emissions of amine-based CO2 capture technology. International Journal of Greenhouse Gas Control 34, 129-140.

Meisen, A., Shuai, X., 1997. Research and development issues in CO2 capture. Energy Conversion and Management 38, S37-S42.

Monteiro, J., Stellwag, I., Mohana, M., Huizinga, A., Khakharia, P., van Os, P., Goetheer, E., 2018. De-Oxygenation as Countermeasure for the Reduction of Oxidative Degradation of CO2 Capture Solvents, 14th Greenhouse Gas Control Technologies Conference Melbourne, pp. 21-26.

Montgomery, H., Thom, N., Cockburn, A., 1964. Determination of dissolved oxygen by the Winkler method and the solubility of oxygen in pure water and sea water. Journal of Chemical Technology and Biotechnology 14, 280-296.

Moser, P., Schmidt, S., Sieder, G., Garcia, H., Stoffregen, T., 2011a. Performance of MEA in a long-term test at the post-combustion capture pilot plant in Niederaussem. International Journal of Greenhouse Gas Control 5, 620-627.

Moser, P., Schmidt, S., Sieder, G., Garcia, H., Stoffregen, T., Stamatov, V., 2011b. The post-combustion capture pilot plant Niederaussem–results of the first half of the testing programme. Energy Procedia 4, 1310-1316.

Park, K., Catalfomo, M., 1964. Gas chromatographic determination of dissolved oxygen in sea water using argon as carrier gas, Deep Sea Research and Oceanographic Abstracts. Elsevier, pp. 917-920.

Penttilä, A., Dell'Era, C., Uusi-Kyyny, P., Alopaeus, V., 2011. The Henry's law constant of N2O and CO2 in aqueous binary and ternary amine solutions (MEA, DEA, DIPA, MDEA, and AMP). Fluid Phase Equilibria 311, 59-66.

Pinto, D.D., Brodtkorb, T.W., Vevelstad, S.J., Knuutila, H., Svendsen, H.F., 2014. Modeling of oxidative MEA degradation. Energy Procedia 63, 940-950.

Puxty, G., Maeder, M., 2016. The fundamentals of postcombustion capture, in: Feron, P.H.M. (Ed.), Absorption-Based Post-Combustion Capture of Carbon Dioxide. Woodhead Publishing.

Reynolds, A.J., Verheyen, T.V., Meuleman, E., 2016. Degradation of amine-based solvents, in: Feron, P.H.M. (Ed.), Absorption-Based Post-combustion Capture of Carbon Dioxide. Woodhead Publishing, pp. 399-423.

Rieder, A., Dhingra, S., Khakharia, P., Zangrilli, L., Schallert, B., Irons, R., Unterberger, S., van Os, P., Goetheer, E., 2017. Understanding solvent degradation: A study from three different pilot plants within the OCTAVIUS project. Energy Procedia 114, 1195-1209.

Rochelle, G.T., 2009. Amine scrubbing for CO2 capture. Science 325, 1652-1654.

Rogelj, J., Shindell, D., Jiang, K., Fifita, S., Forster, P., Ginzburg, V., Handa, C., Kheshgi, H., Kobayashi, S., Kriegler, E., Mundaca, L., Séférian, R., Vilariño, M.V., 2018. Mitigation Pathways Compatible with 1.5°C in the Context of Sustainable Development. In: *Global Warming of 1.5°C. An IPCC Special Report on the impacts of global warming of 1.5°C above pre-industrial levels and related global greenhouse gas emission pathways, in the context of strengthening the global response to the threat of climate change, sustainable development, and efforts to eradicate poverty*. IPCC.

Rooney, P.C., Daniels, D.D., 1998. Oxygen solubility in various alkanolamine/water mixtures. Petroleum Technology Quarterly, 97-102.

Schumpe, A., Adler, I., Deckwer, W.D., 1978. Solubility of oxygen in electrolyte solutions. Biotechnology Bioengineering 20, 145-150.

Supap, T., Idem, R., Tontiwachwuthikul, P., Saiwan, C., 2011. Investigation of degradation inhibitors on CO_2 capture process. Energy Procedia 4, 583-590.

Supap, T., Idem, R., Veawab, A., Aroonwilas, A., Tontiwachwuthikul, P., Chakma, A., Kybett, B.D., 2001. Kinetics of the oxidative degradation of aqueous monoethanolamine in a flue gas treating unit. Industrial & engineering chemistry research 40, 3445-3450.

Thitakamol, B., Veawab, A., 2008. Foaming behavior in CO2 absorption process using aqueous solutions of single and blended alkanolamines. Industrial & engineering chemistry research 47, 216-225.

Veldman, R.R., Trahan, D., 1997. Oxygen scavenging solutions for reducing corrosion by heat stable amine salts. Google Patents.

Vevelstad, S.J., Johansen, M.T., Knuutila, H., Svendsen, H.F., 2016. Extensive dataset for oxidative degradation of ethanolamine at 55–75° C and oxygen concentrations from 6 to 98%. International Journal of Greenhouse Gas Control 50, 158-178.

Wang, M.H., Ledoux, A., Estel, L., 2013. Oxygen solubility measurements in a MEA/H2O/CO2 mixture. Journal of Chemical & Engineering Data 58, 1117-1121.

Weisenberger, S., Schumpe, A., 1996. Estimation of gas solubilities in salt solutions at temperatures from 273 K to 363 K. AIChE Journal 42, 298-300.

Winkler, L.W., 1888. Die bestimmung des im wasser gelösten sauerstoffes. European Journal of Inorganic Chemistry 21, 2843-2854.

Xing, W., Yin, M., Lv, Q., Hu, Y., Liu, C., Zhang, J., 2014. 1 - Oxygen Solubility, Diffusion Coefficient, and Solution Viscosity, in: Xing, W., Yin, G., Zhang, J. (Eds.), Rotating Electrode Methods and Oxygen Reduction Electrocatalysts. Elsevier, Amsterdam, pp. 1-31.

Measurement and prediction of oxygen solubility in post-combustion CO$_2$ capture solvents

Vanja Buvik[a], Ida M. Bernhardsen[a], Roberta V. Figueiredo[b], Solrun J. Vevelstad[c], Earl Goetheer[b], Peter van Os[b] and Hanna K. Knuutila[a*]

[a] Department of Chemical Engineering, Norwegian University of Science and Technology (NTNU), NO-7491 Trondheim, Norway

[b] TNO, Leeghwaterstraat 44, 2628 CA Delft, The Netherlands

[c] SINTEF Industry, NO-7465 Trondheim, Norway

[*] Corresponding author: hanna.knuutila@ntnu.no

Appendix

Dissolved oxygen sensors

The two different electrochemical sensors were used in this work were a HI-5421 Dissolved Oxygen and BOD Meter from Hanna Instruments, with a HI76483 Clark-Type polarographic probe and a handheld pHenomenal® OX 4100 H dissolved oxygen meter with a pHenomenal® OXY-11 polarographic probe, from VWR. The first sensor was calibrated using a HI-7040L Zero Oxygen Solution and water-saturated air (suspended directly above the water surface, as described in the sensor manual) and the second was calibrated using an OxiCal®-SL calibration vessel from VWR, using water-saturated air. The cathode material of the Hanna Instrument sensor is platinum and the anode material silver, while the cathode material in the VWR sensor is of gold and the anode of led. In both probes, the electrodes and electrolyte solutions are separated from the solution, in which the concentration of dissolved oxygen is measured, by an oxygen permeable membrane (further details about the probes can be found in Supporting Information 1).

$$\frac{1}{2} O_2 + 2e^- + 2H^+ \rightarrow H_2O, \qquad E^0 = +1,23 \text{ V} \qquad (14)$$
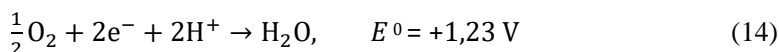
Both probes have a temperature range from 0 °C up to 50 °C and rely on the same cathode reaction (Equation 6), although the cathode material differs.

$$Ag \rightarrow Ag^+ + e^-, \qquad\qquad E^0 = -0,80 \text{ V} \qquad (15)$$

$$Pb \rightarrow Pb^{2+} + 2e^-, \qquad\qquad E^0 = +0,126 \text{ V} \qquad (16)$$
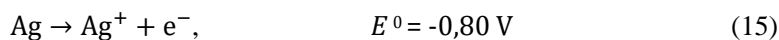
The anode reactions of the two sensors are described in equation 7 for HI76483 and equation 8 for the OXY-11 polarographic probe. The redox reactions give a measurable current which is translated to oxygen concentration by the sensor. Effectively, the dissolved oxygen sensors measure the activity of O_2 in the solution which in ion-free conditions is the same as the concentration of O_2. Since salinity influences the activity coefficient of O_2, the sensors are provided with a correction for sodium chloride (NaCl) salinity. This correction factor is not applicable for other salts (Battino and Clever, 1966; Schumpe et al., 1978). Both galvanic sensors also have thermometers incorporated in the probe.

The optical dissolved oxygen sensor was a Memosens COS81D from Endress+Hauser. The optical dissolved oxygen sensors are sturdier and is less impacted by the alkaline conditions in the amine solutions over time and can measure oxygen concentrations both in liquid and gas phase. While the electrochemical sensor undergoes a chemical reaction with dissolved oxygen, the optical sensor enables the analysis via an inductive signal transmission. The sensor is not directly in contact with the liquid phase, as three layers are present on the active sensor tip: a fluorescence layer, an optical insulating layer, and a cover layer. As soon as an equilibrium is achieved between the oxygen partial pressure in the medium and in the fluorescent layer in which an oxygen-sensitive fluorophore is present, stable measurement can be obtained. Depending on the oxygen concentration, the intensity of the signal and the signal decay time will change as the properties of the fluorophore changes with the presence of oxygen. The oxygen concentration is then calculated from the Stern-Volmer equation (Cammack et al., 2008). The sensor corrects the measured values according to the current temperature and air pressure. The data was acquired via the transmitter that is coupled to the sensor. The optical DO sensor was calibrated with pure nitrogen and air, for the gas phase (zero and maximum, respectively), and with a saturated sodium bisulphite solution as zero for the liquid phase. The sensor can only be utilized with solutions that do not contain halogens, ketones, and toluene. (Endress+Hauser)

Density and viscosity of structurally varied amines in correlation with oxygen solubility

To investigate whether any specific physical properties of a solvent can correlate with its oxygen solubility, densities, and viscosities of all the (amine) solvents were measured and compared to oxygen solubility. In Supplementary figure 5.1 no direct correlation could be observed for all amines, but a correlation between measured oxygen solubility and density for the alkanolamines, meaning all amines with an alcohol and an amine functionality, where oxygen solubility increases with decreasing density at 25 °C. With some deviation from a linear trend it can also be seen that, for most of the studied solvents, lower viscosities give higher oxygen solubility as seen in Supplementary figure 5.2. Again, there is a nearly linear correlation between viscosity and oxygen solubility for alkanolamines, with only 1,2-DAP, benzylamine and water not fitting on a linear trendline. The correlations between alkanolamine oxygen solubility and their density and viscosity are likely due to hydrogen bonding effects within the solutions.
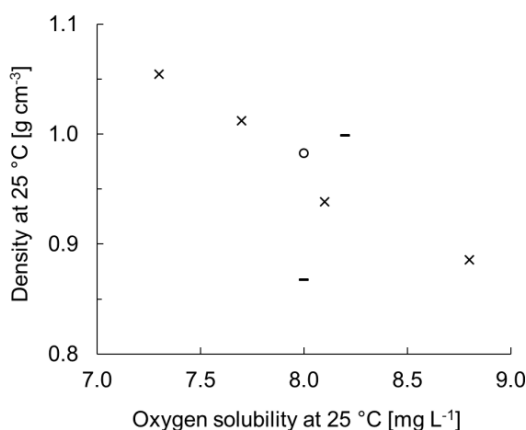
Supplementary figure 5.1: Density of pure amines and water compared to oxygen solubility at 25 °C. Densities measured with an Anton Paar DMA™ 4500 density meter. Density of MEA not measured in this work, but on the same instrumentation by (Amundsen et al., 2009). (x representing alkanolamines, ○ water and ─ non-alkanolamines.)
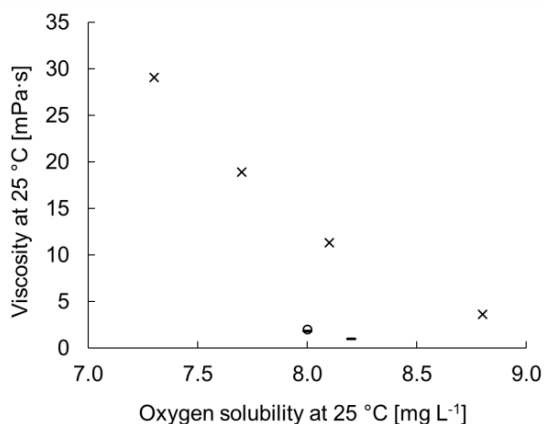
Supplementary figure 5.2: Dynamic viscosities of amines at 25 °C, measured with an Anton Paar Lovis 2000 ME viscosity meter, all except for the viscosity of MEA from this work, dynamic viscosity of MEA from Arachchige et al. (2013), which measured using a MCR 101 Anton Paar double-gap rheometer. (x representing alkanolamines, ○ water and ─ non-alkanolamines.)

Validation with water
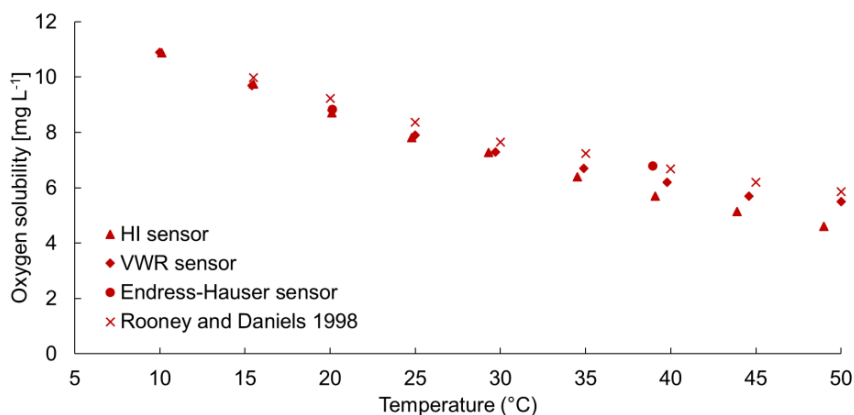
Supplementary figure 5.3: Oxygen solubility of deionized water measured with two different dissolved oxygen sensors and compared with oxygen solubility data compared to data from Rooney and Daniels (1998). Solubility measured at $p_{O2} = 0.21$ atm.

The three sensors used in this study were validated against literature data for the solubility of oxygen in water for which data is abundant (experimental setup described in section 5.2.3.1). The results of this validation experiment are given in Supplementary figure 5.3. In deionized water the maximum absolute deviation when comparing the three different dissolved oxygen sensors applied in this work was ± 0.9 mg L^{-1} (20%, in the higher temperature range) and between the sensors and

literature data ± 1.3 mg L^{-1} (27%, in the higher temperature range) (Rooney and Daniels, 1998).

Electrochemical sensor validation with ethylene glycol and literature data

Solutions of different mixing ratios of monoethylene glycol (MEG) and water were studied using experimental setup A. The dissolved oxygen measurements were performed with the pHenomenal® VWR dissolved oxygen sensor and by Winkler titration. The obtained data was compared to literature values measured in an equilibrium cell (Yamamoto and Tokunaga, 1994) and another dataset where the methodology used has not been specified (Joosten et al., 2007).
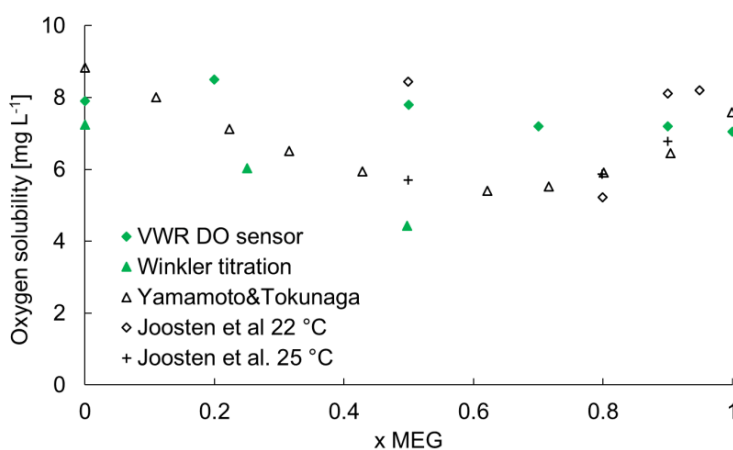
Supplementary figure 5.4: Oxygen solubility in mixtures of MEG and water (in wt%).

The standard deviation within the parallel solubility measurements in the literature are up to 32% of the mean oxygen solubility at a given temperature. Mean oxygen solubility measured by the dissolved oxygen sensor in this work deviates up to 37% from the literature mean solubility at a given temperature given by Joosten et al. (2007), which in absolute numbers equals a maximum deviation of ± 2.4 mg L^{-1} (depicted in Supplementary figure 5.4).

The literature data from Yamamoto and Tokunaga (1994) at 22 °C deviates at the most by 30% from the measured oxygen solubility in this work at 20 °C, which also equals a maximum absolute deviation of ± 2.4 mg L^{-1}. At 25 °C the maximum absolute deviation was 23% and 1.7 mg L^{-1}. Comparing the data points with the same conditions (composition and temperature) from the two sources, the maximum deviation is 20% or 1.7 mg L^{-1}.If the equilibrium cell experiments yield a more

realistic oxygen concentration than the sensors, the signal is amplified by the sensors. This could be because the dissolved oxygen sensors do not directly measure the physical solubility of oxygen, but its activity in the solutions. Considering the purpose for which the sensor is meant in this case, measurement of oxygen concentration in solvent solutions for CO_2 capture, as well as the general lack of data and documented measurement methods of oxygen solubility in similar solutions, the uncertainties in the measurements described in this section may be acceptable.

Influence of CO_2 loading and temperature on oxygen solubility

Additional data for oxygen solubility in loaded aqueous MEA solutions at 30, 35 and 45 °C is given in Supplementary figure 5.5, as an extension to the data shown in Figure 5.6. These results are discussed further in section 5.3.4.3.
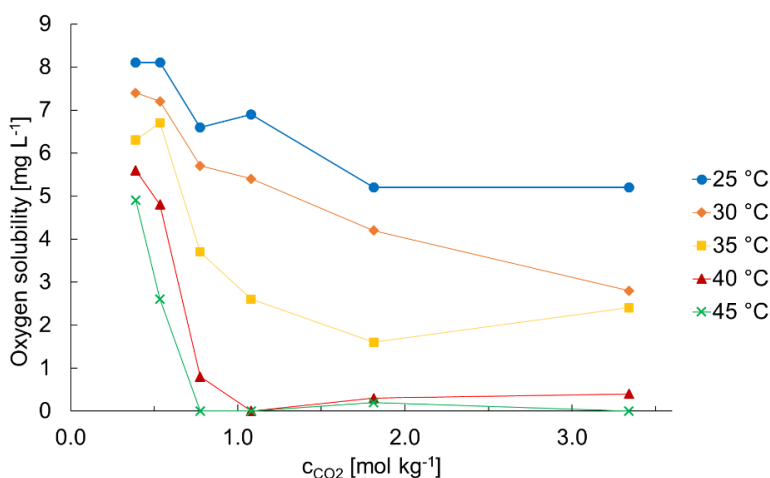
Supplementary figure 5.5: Oxygen solubility in aqueous MEA solutions of varying carbamate (loaded carbon dioxide) concentration at different temperatures, only taking the amount of CO_2 loaded to the solution into account, disregarding the concentration of MEA, at $pO_2 = 0.21$ atm. Lines have been added for illustrational purposes and do not represent actual data points.

References

Amundsen, T.G., Øi, L.E., Eimer, D.A., 2009. Density and Viscosity of Monoethanolamine + Water + Carbon Dioxide from (25 to 80) °C. Journal of Chemical & Engineering Data 54, 3096-3100.

Arachchige, U., Aryal, N., Eimer, D.A., Melaaen, M.C., 2013. Viscosities of pure and aqueous solutions of monoethanolamine (MEA), diethanolamine (DEA) and N-

methyldiethanolamine (MDEA). Annual Transactions of the Nordic Rheology Society 21, 299.

Joosten, M.W., Tier, B., Seiersten, M., Wintermark, C., 2007. Materials considerations for MEG (mono ethylene glycol) reclamation Systems, CORROSION 2007. NACE International.

Rooney, P.C., Daniels, D.D., 1998. Oxygen solubility in various alkanolamine/water mixtures. Petroleum Technology Quarterly, 97-102.

Yamamoto, H., Tokunaga, J., 1994. Solubilities of Nitrogen and Oxygen in 1,2-Ethanediol + Water at 298.15 K and 101.33 kPa. Journal of Chemical Engineering Data 39, 544-547.

Measurement and prediction of oxygen solubility in post-combustion CO₂ capture solvents

Vanja Buvik[a], Ida M. Bernhardsen[a], Roberta V. Figueiredo[b], Solrun J. Vevelstad[c], Earl Goetheer[b], Peter van Os[b] and Hanna K. Knuutila[a*]

[a] Department of Chemical Engineering, Norwegian University of Science and Technology (NTNU), NO-7491 Trondheim, Norway

[b] TNO, Leeghwaterstraat 44, 2628 CA Delft, The Netherlands

[c] SINTEF Industry, NO-7465 Trondheim, Norway

* Corresponding author: hanna.knuutila@ntnu.no

Supporting Information

Tables and figures

Supplementary table 5.1: Dissolved oxygen sensor specifications.

Sensor	VWR OXY-11	HI76483
Anode material	Pb	Ag
Cathode material	Au	Pt
Electrolyte solution	"ELY-G" solution	KCl (aq)
Membrane material	Fluorinated ethylene propylene (FEP)	Polytetrafluorethylene (PTFE)
Temperature range	0-40 °C (but measures T up to 50 °C)	0-50 °C
Measuring range at 20 °C	0.0-50 mg L^{-1}	0.00 to 90.00 mg L^{-1}
Consumption of oxygen at 20 °C	0.006 µg h^{-1}	N/G
Precision of temperature measurement	± 0.2 K	± 0.2 K

Sensor	Endress+Hauser COS81D
Measurement range (liquid phase)	4 µg L^{-1} to 30 mg L^{-1} 0.05 to 300% SAT
Measurement range (gas phase)	0.1 to 700 hPa

Supplementary table 5.2: Measured oxygen concentrations (DO), ambient pressure and temperature of deionized water, as well as the literature values for oxygen solubility in water used in Supplementary figure 5.3.

	HI sensor			VWR sensor		Rooney and Daniels (1998)		Endress-Hauser sensor	
	c_{O_2} [mg L⁻¹]	p [atm]	$T_{reactor}$ (°C)	c_{O_2} [mg L⁻¹]	$T_{reactor}$ (°C)	c_{O_2} [mg L⁻¹]	$T_{reactor}$ (°C)	c_{O_2} [mg L⁻¹]	$T_{reactor}$ (°C)
	10.88	0.979	10.1	10.9	10.0				
	9.74	0.979	15.5	9.7	15.4	9.98	15.5		
	8.70	0.979	20.1	8.8	20.1	9.23	20	8.85	20.1
	7.82	0.979	24.8	7.9	25.0	8.37	25		
	7.27	0.984	29.3	7.3	29.7	7.65	30		
	6.40	0.985	34.5	6.7	34.9	7.24	35		
	5.70	0.986	39.1	6.2	39.8	6.68	40	6.80	38.9
	5.14	0.986	43.9	5.7	44.6	6.20	45		
	4.60	0.987	49.0	5.5	50.0	5.86	50		

Supplementary table 5.3: Measured oxygen concentrations, ambient pressure and temperature of 30wt% $(aq.)$ ethanolamine (MEA), as well as the literature values for oxygen solubility in water used in section 5.3.2, Figure 5.3.

	HI-sensor			VWR sensor			(Wang et al., 2013)		Endress-Hauser sensor	
	c_{O_2} [mg L⁻¹]	p [atm]	T (°C)	c_{O_2} [mg L⁻¹]	T (°C)	Dev. from HI [mg L⁻¹]	c_{O_2} [mg L⁻¹]	T (°C)	c_{O_2} [mg L⁻¹]	T (°C)
	10.34	1.003	10.3	10.8	9.8	0.5	10.11	10		
	9.75	1.003	15.2	9.4	15.2	-0.4	9.24	23		
	8.82	1.003	20.2	8.6	20.2	-0.2	7.76	32	8.61	20.2
	7.70	1.003	24.6	7.9	24.8	0.2	7.13	40		
	7.18	1.003	29.4	7.2	29.8	0.0	5.60	50		
	6.64	1.003	34.0	6.6	34.6	0.0	3.65	60		
	5.70	1.003	38.9	6.2	39.9	0.5			6.22	39.3
	5.26	1.004	43.9	5.8	45.0	0.5				
	4.50	1.004	49.4	5.1	50.3	0.6				

168

Supplementary table 5.4: Oxygen solubility in deionized water with different gas phase compositions, measured by the Endress+Hauser optical dissolved oxygen sensor as described in section 5.3.2.

c_{Air} (vol%)	c_{CO2} (vol %)	c_{N2} (vol %)	$c_{O2,meas.}$ [mg L^{-1}]	T (°C)
100	0	0	8.47	20.0
50	50	0	4.16	20.1
50	0	50	4.16	20.0

Supplementary table 5.5: Oxygen solubility in gas phase with different gas phase compositions, measured by the Endress+Hauser optical dissolved oxygen sensor as described in section 5.3.2.

c_{Air} (vol %)	c_{CO2} (vol %)	c_{N2} (vol %)	$c_{O2,meas.}$ [mg L^{-1}]	T (°C)
100	0	0	8.48	21.6
50	50	0	4.11	21.8
50	0	50	4.25	21.1

Supplementary table 5.6: Measured oxygen concentration (DO) and temperature in the liquid phase as an average of the inbuilt thermometer of the DO sensors, and calculated Henry's law constants (H^{cp}) used in section 5.3.4.1 and Supplementary figure 5.6.

Water			MEA 30wt% (aq.)			MEA 50wt% (aq.)			MEA 100 %		
c_{O2} [mg L^{-1}]	Avg. T(°C)	H^{cp} [mol m^{-3} Pa^{-1}]	c_{O2} [mg L^{-1}]	Avg. T(°C)	H^{cp} [mol m^{-3} Pa^{-1}]	c_{O2} [mg L^{-1}]	Avg. T(°C)	H^{cp} [mol m^{-3} Pa^{-1}]	c_{O2} [mg L^{-1}]	Avg. T(°C)	H^{cp} [mol m^{-3} Pa^{-1}]
10.9	10.1	1.64E-05	10.6	10.1	1.55E-05	9.3	10.5	1.36E-05	10.1	10.8	1.5E-05
9.7	15.5	1.46E-05	9.6	15.2	1.41E-05	9.0	15.5	1.3E-05	9.0	15.5	1.32E-05
8.8	20.2	1.32E-05	8.7	20.2	1.28E-05	8.2	20.1	1.2E-05	8.3	20.4	1.24E-05
7.9	25.2	1.18E-05	7.8	24.7	1.14E-05	7.5	24.7	1.1E-05	7.7	24.9	1.15E-05
7.3	29.9	1.09E-05	7.2	29.6	1.06E-05	6.8	29.4	9.89E-06	7.1	29.8	1.06E-05
6.6	35.2	9.79E-06	6.6	34.3	9.72E-06	6.2	35.0	9.01E-06	6.5	34.9	9.63E-06
6.0	39.8	8.88E-06	6.0	39.4	8.73E-06	5.7	39.7	8.22E-06	6.1	39.8	9.06E-06
5.4	45.0	8.09E-06	5.5	44.5	8.11E-06	5.2	45.1	7.5E-06	5.4	44.6	7.93E-06
5.1	50.5	7.53E-06	4.8	49.9	7.04E-06	4.6	50.0	6.63E-06	5.0	50.3	7.48E-06

Supplementary table 5.7: Measured oxygen solubility (DO) and temperature in water, pure MEA, DMMEA and MMEA, used in section 5.3.4.2, Figure 5.5.

Water		MEA		DMMEA		MMEA	
T (°C)	c_{O_2} [mg L^{-1}]	T (°C)	c_{O_2} [mg L^{-1}]	T (°C)	c_{O_2} [mg L^{-1}]	c_{O_2} [mg L^{-1}]	T (°C)
10.1	10.9	10.6	10.1	10.0	11.6	11.2	9.0
15.5	9.7	15.5	9.0	14.9	10.5	9.8	14.6
20.2	8.8	20.5	8.3	19.9	9.5	8.9	18.8
25.2	7.9	25.2	7.7	24.7	8.8	8.0	25.0
29.9	7.3	30.4	7.1	29.9	8.2	7.5	30.2
35.2	6.6	35.4	6.5	35.3	7.6	7.0	35.1
39.8	6.0	40.5	6.1	40.2	7.0	6.6	40.1
45.0	5.4	45.8	5.4	45.0	6.7	6.0	45.5
50.5	5.1	51.0	5.0	50.9	6.3	5.8	50.2

Supplementary table 5.8: Measured oxygen solubility (DO) and temperature in pure 1,2-DAP, Benzylamine and DGA, used in section 5.3.4.2, Figure 5.5.

1,2-DAP		Benzylamine		DGA	
c_{O_2} [mg L^{-1}]	T (°C)	c_{O_2} [mg L^{-1}]	T (°C)	c_{O_2} [mg L^{-1}]	T (°C)
10.7	9.8	9.6	15.2	9.8	10.7
8.6	20.1	8.7	20.4	7.6	20.7
7.0	30.3	8.0	25.5	6.9	30.5
5.5	40.2	7.4	30.4	6.3	40.3
3.1	50.1	6.9	35.4	5.6	50.1
		6.5	40.2		
		5.7	45.4		
		5.5	50.2		

Supplementary table 5.9: Viscosity (η) and density (ρ) of pure amine solutions and water measured at 25 °C with an Anton Paar density meter DMA™ 4500 and an Anton Paar Lovis 2000 ME viscosity meter, except MEA which was measured by Dynamic viscosity was measured using MCR 101 Anton Paar double-gap rheometer (Amundsen et al., 2009; Arachchige et al., 2013). All measurements were performed in 2 parallels, except water which was measured 12 times. Depicted in Supplementary figure 5.1 and Supplementary figure 5.2.

Chemical	η [mPa s]	Std. dev. Viscosity [mPa s]	ρ [g mL⁻¹]	Std. dev. Density [g mL⁻¹]	Oxygen solubility [mg L⁻¹]
Water	0.9302	$4.570 \cdot 10^{-4}$	0.99833	$7.8881 \cdot 10^{-6}$	8,2
Benzylamine	1.8534	$2.5456 \cdot 10^{-3}$	0.98263	$7.0711 \cdot 10^{-6}$	8,0
MEA	18.924 (Arachchige et al., 2013)	-	1.0123 (Amundsen et al., 2009)	-	7,7
MMEA	11.308	$5.6569 \cdot 10^{-3}$	0.93823	$7.0711 \cdot 10^{-6}$	8.1
1,2-DAP	1.7774	$1.2728 \cdot 10^{-3}$	0.86708	$1.4142 \cdot 10^{-5}$	8.0
DMMEA	3.6061	$3.2527 \cdot 10^{-3}$	0.88585	$1.4142 \cdot 10^{-5}$	8.8
DGA	29.053	$6.3640 \cdot 10^{-2}$	1.05464	$7.0711 \cdot 10^{-6}$	7.3

Supplementary table 5.10: Oxygen solubility in solutions of MEA of different concentrations and CO_2 loadings. Data used in section 5.3.4.3 and Figure 5.6.

MEA 51% 0.40 n_{CO2}/n_{MEA}		MEA 41% 0.27 n_{CO2}/n_{MEA}		MEA 43% 0.11 n_{CO2}/n_{MEA}		MEA 44% 0.15 n_{CO2}/n_{MEA}		MEA 34% 0.07 n_{CO2}/n_{MEA}		MEA 43% 0.08 n_{CO2}/n_{MEA}	
c_{O2} [mg L⁻¹]	T(°C)	c_{O2} [mg L⁻¹]	T(°C)	c_{O2} [mg L⁻¹]	T(°C)	c_{O2} [mg L⁻¹]	T(°C)	c_{O2} [mg L⁻¹]	T(°C)	c_{O2} [mg L⁻¹]	T(°C)
7.8	10.6	9.1	10.5	9.1	10.6	9.1	10.9	10.7	10.7	9.8	10.8
7.2	15.6	8.3	15.5	8.5	15.3	8.6	15.5	9.7	15.0	9.4	15.0
6.4	20.3	6.5	20.4	7.5	20.4	7.9	20.0	9.0	20.0	8.6	20.2
5.2	25.2	5.2	25.2	6.6	25.1	6.9	25.1	8.1	25.0	8.1	25.0
4.2	30.1	2.8	30.0	5.7	29.8	5.4	29.9	7.4	30.0	7.2	30.0
2.4	34.9	1.6	34.8	3.7	34.8	2.6	35.0	6.3	35.1	6.7	35.0
0.4	39.9	0.3	39.8	0.8	39.8	0.0	39.9	5.6	40.0	4.8	40.0
0.2	44.8	0.0	44.6	0.0	44.5			4.9	44.8	2.6	44.9
0.1	49.4							4.2	49.8	0.3	49.9

Supplementary table 5.11: Measured oxygen solubility of 30wt% (*aq.*) MEA, measured with a pHenomenal® dissolved oxygen sensor at varying oxygen partial pressure (p_{total} = 1 atm) with increasing CO_2 loading (α, quanitified by Shimadzu TOC-L$_{CPH}$ and amine titration). Showed in Figure 5.7, section 5.3.4.3.

30% O$_2$		50% O$_2$		70% O$_2$		85% O$_2$		92% O$_2$	
c_{O2} [mg L^{-1}]	α [c_{CO2}/c_{MEA}]	c_{O2} [mg L^{-1}]	α [c_{CO2}/c_{MEA}]	c_{O2} [mg L^{-1}]	α [c_{CO2}/c_{MEA}]	c_{O2} [mg L^{-1}]	α [c_{CO2}/c_{MEA}]	c_{O2} [mg L^{-1}]	α [c_{CO2}/c_{MEA}]
34	0.003	31	0.001	33	0.001	26	0.088	34	0.006
31	0.06	30	0.064	31	0.097	26	0.13	36	0.11
28	0.1	29	0.098	24	0.182	26	0.18	34	0.22
23	0.2	28	0.13	23	0.259	23	0.24	29	0.32
18.9	0.2	27	0.16	18.8	0.324	11.3	0.28	23	0.41
13.1	0.3	25	0.19	12.5	0.340	2.5	0.31	5.2	0.43
5.8	0.3	23	0.21	6.5	0.357	2.5	0.34	0.4	0.42
1.5	0.3	21	0.23	3.2	0.369	1.7	0.37	0.1	0.45
0.5	0.3	19.8	0.26	2.0	0.373	1.7	0.40		
0.5	0.4	17.4	0.28	1.7	0.407	0.5	0.42		
		14.4	0.30	1.6	0.404	0.4	0.43		
		10.8	0.32	0.9	0.428				
		7.4	0.34	0.1	0.452				
		4.5	0.34						
		2.7	0.35						
		1.9	0.38						
		1.6	0.38						

Supplementary table 5.12: The oxygen concentrations of MDEA 30wt% ($aq.$) loaded with 0.4 mol CO2 per mol MDEA measured at different temperatures, presented in section 1465.3.4.3, Figure 5.8.

T (°C)	$c_{O2,\text{galvanic}}$ [mg L^{-1}]	$c_{O2,\text{optical}}$ [mg L^{-1}]
20.6	8.1	8.04
21.0	7.9	7.95
22.0	7.7	7.79
23.0	7.6	7.69
24.0	7.5	7.62
25.0	7.5	7.54
26.0	7.4	7.44
27.0	7.3	7.38
28.0	7.3	7.31
29.0	7.2	7.23
30.0	7.2	7.15
31.0	7.1	7.09
32.0	6.9	7.02
33.2	6.8	6.93
34.0	6.7	6.84
35.0	6.5	6.77
36.0	6.4	6.65

Supplementary table 5.13: Measured oxygen concentration in a 30wt% MDEA ($aq.$) solution, with a constant loading of 0.4 mol$_{CO2}$/mol$_{MDEA}$, while heating. Comparison of an optical and galvanic sensor. Data used in Figure 5.7.

T (°C)	VWR sensor c_{O2} [mg L^{-1}]	Endress+Hauser sensor c_{O2} [mg L^{-1}]
20.6	8.1	8.04
21.0	7.9	7.95
22.0	7.7	7.79
23.0	7.6	7.69
24.0	7.5	7.62
25.0	7.5	7.54
26.0	7.4	7.44
27.0	7.3	7.38
28.0	7.3	7.31
29.0	7.2	7.23
30.0	7.2	7.15
31.0	7.1	7.09
32.0	6.9	7.02
33.2	6.8	6.93
34.0	6.7	6.84
35.0	6.5	6.77
36.0	6.4	6.65
37.0	7.1	6.44

Supplementary table 5.14: Measured concentrations of oxygen in mixtures of varying weight fractions (x) of water and MEG used in Supplementary figure 5.4.

Supplementary table 5.15: Mole fractions of oxygen, calculated from the oxygen solubily given in Supplementary table 5.14, for different compositions of MEG in water (weight fractions, wt%) and different temperatures.

Oxygen solubility [mg L⁻¹]

xMEG\T	20 °C	25 °C	30 °C	40 °C	50 °C
0,2	8.8	8.5	7.9	6.8	6.0
0,5	8.5	7.8	7.4	6.3	5.4
0,7	7.9	7.2	6.6	5.8	5.3
0,9	7.9	7.2	6.5	5.6	5.2
1,0	7.7	7.1	6.5	5.7	5.4

x O_2 (mol%)

T\xMEG	0.0	0.2	0.5	0.7	0.9	1.0
20 °C	5.0E-06	5.9E-06	7.5E-06	8.6E-06	1.1E-05	1.3E-05
25 °C	4.5E-06	5.5E-06	6.7E-06	7.7E-06	1.0E-05	1.2E-05
30 °C	4.1E-06	5.3E-06	6.5E-06	7.2E-06	9.5E-06	1.1E-05
40 °C	3.5E-06	4.6E-06	5.6E-06	6.4E-06	8.2E-06	1.0E-05
50 °C	3.1E-06	4.1E-06	4.8E-06	5.9E-06	7.7E-06	9.7E-06

Supplementary table 5.16: Data used in Supplementary figure 5.4 from Joosten et al. (2007). Data points extracted with https://automeris.io/WebPlotDigitizer/ and compared to dissolved oxygen data from this work in mixtures of MEG and water. Standard deviation (Stdev.S) given as maximum deviation from data mean.

T	x MEG (wt%)	#points	Joosten et al. (2007) mol% O_2	Stdev.S	std.dev%	This work mol% O_2	Deviation from Joosten et al.
22 °C	0.50	2	7.20E-06	5.00E-08	1 %	-	-
	0.80	2	8.16E-06	2.60E-06	32 %	-	-
	0.90	2	1.23E-05	4.61E-07	4 %	-	-
	0.95	2	1.30E-05	6.19E-08	0 %	-	-
25 °C	0.50	3	4.87E-06	4.01E-07	8 %	6.7E-06	37 %
	0.80	2	7.22E-06	1.69E-07	2 %	-	-
	0.90	2	9.79E-06	6.50E-07	7 %	1.0E-05	6 %
30 °C	0.50	2	6.62E-06	6.69E-08	1 %	6.3E-06	4 %
	0.80	3	7.99E-06	1.93E-06	24 %	-	-
	0.90	2	1.09E-05	5.68E-08	1 %	9.4E-06	13 %
	0.95	2	1.10E-05	3.11E-08	0 %	-	-
40 °C	0.50	2	6.04E-06	8.40E-08	1 %	5.4E-06	10 %
	0.80	2	8.06E-06	5.34E-07	7 %	7.2E-06	10 %
	0.90	4	1.16E-05	2.23E-06	19 %	8.2E-06	30 %
	0.95	3	1.24E-05	3.53E-06	28 %	-	-
60 °C	0.50	2	3.98E-06	2.04E-07	5 %	-	-
	0.70	2	6.02E-06	1.93E-07	3 %	-	-
	0.99	1	1.47E-05	-	-	-	-

Supplementary table 5.17: Data extracted from Joosten et al. (2007) who were converted from measured Ostwald coefficient at 22 °C from Yamamoto and Tokunaga (1994) to ppm and used in Supplementary figure 5.4. The data points were extracted using https://automeris.io/WebPlotDigitizer/.

		Yamamoto and Tokunaga (1994)		
wt% MEG	x MEG	c_{O2} [ppm]	c_{O2} [mmol L^{-1}]	mol% O_2
0.0	0.0	8.8	0.28	5.0E-06
11.0	0.1	8.0	0.25	5.7E-06
22.3	0.2	7.1	0.22	4.7E-06
31.5	0.3	6.5	0.20	4.6E-06
42.9	0.4	5.9	0.19	3.4E-06
62.2	0.6	5.4	0.17	3.1E-06
71.6	0.7	5.5	0.17	5.9E-06
80.1	0.8	5.9	0.18	7.3E-06
90.4	0.9	6.4	0.20	9.3E-06
99.9	1.0	7.6	0.24	1.3E-05

Supplementary table 5.18: Comparison of oxygen solubility from this work and literature data (Yamamoto and Tokunaga, 1994). Standard deviations as maximum deviation from mean.

	This work: 20 °C			
x MEG	c_{O2} [mmol L^{-1}]	c_{O2} Std. dev. [mmol L^{-1}]	c_{O2} Std. dev. [mg L^{-1}]	Std. deviation
0.0	0.25	0.03	0.92	12 %
0.2	0.27	0.04	1.37	16 %
0.7	0.23	0.05	1.68	23 %
0.9	0.23	0.02	0.75	10 %
1.0	0.22	0.02	0.48	7 %

	This work: 25 °C			
x MEG	c_{O2} [mmol L^{-1}]	c_{O2} Std. dev. [mmol L^{-1}]	c_{O2} Std. dev. [mg L^{-1}]	Std. deviation
0.0	0.28	0.00	0.02	0 %
0.2	0.28	0.05	1.68	19 %
0.7	0.25	0.07	2.38	30 %
0.9	0.25	0.05	1.45	18 %
1.0	0.24	0.00	0.12	2 %
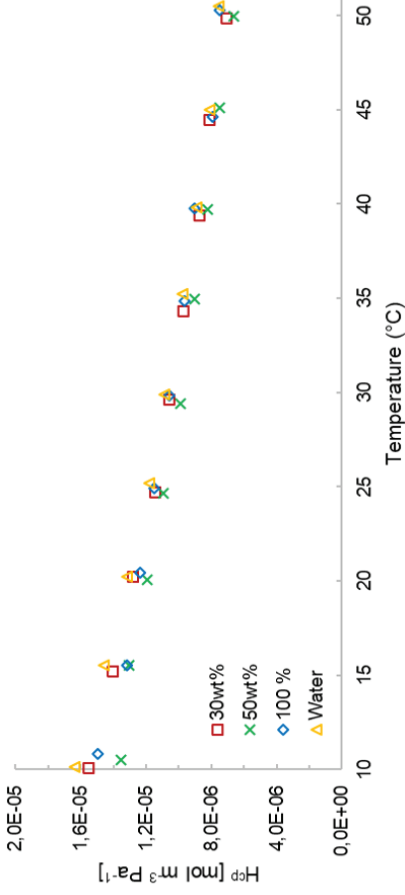
Supplementary figure 5.6: Henry's law constants as a function of temperature for various concentrations of MEA at $pO_2 = 0.21$ atm. The constants were calculated using the oxygen solubility depicted in Figure 5.4.

References

Amundsen, T.G., Øi, L.E., Eimer, D.A., 2009. Density and Viscosity of Monoethanolamine + Water + Carbon Dioxide from (25 to 80) °C. Journal of Chemical & Engineering Data 54, 3096-3100.

Arachchige, U., Aryal, N., Eimer, D.A., Melaaen, M.C., 2013. Viscosities of pure and aqueous solutions of monoethanolamine (MEA), diethanolamine (DEA) and N-methyldiethanolamine (MDEA). Annual Transactions of the Nordic Rheology Society 21, 299.

Joosten, M.W., Tier, B., Seiersten, M., Wintermark, C., 2007. Materials considerations for MEG (mono ethylene glycol) reclamation Systems, CORROSION 2007. NACE International.

Rooney, P.C., Daniels, D.D., 1998. Oxygen solubility in various alkanolamine/water mixtures. Petroleum Technology Quarterly, 97-102.

Wang, M.H., Ledoux, A., Estel, L., 2013. Oxygen solubility measurements in a MEA/H2O/CO2 mixture. Journal of Chemical & Engineering Data 58, 1117-1121.

Yamamoto, H., Tokunaga, J., 1994. Solubilities of Nitrogen and Oxygen in 1,2-Ethanediol + Water at 298.15 K and 101.33 kPa. Journal of Chemical Engineering Data 39, 544-547.

Chapter 6

Stability of structurally varied aqueous amines for CO$_2$ capture

This chapter contains a journal paper published in the Industrial & Engineering Chemistry Research journal in March 2021, where the stability of a series of amine of different chemical structures are studied under mainly oxidative conditions, but also biological. The experimental results are then compared to literature data for biological and thermal stability, as well as ecotoxicity of the same amines. The goal of this study was to see if the identification of any features of the amine could help predict other important features.

Stability of structurally varied aqueous amines for CO$_2$ capture

Vanja Buvik [a], Solrun J. Vevelstad [b], Odd G. Brakstad [c] and Hanna K. Knuutila [a][6]

[a] Department of Chemical Engineering, Norwegian University of Science and Technology (NTNU), NO-7491 Trondheim, Norway

[b] SINTEF Industry, NO-7465 Trondheim, Norway

[c] SINTEF Ocean, NO-7465 Trondheim, Norway.

Abstract

Eighteen structurally varied amines were subjected to harsh oxidative conditions and their stability assessed and seen in the context of biological and thermal stability. Steric effects play a large role in the stabilization of the amines under oxidative conditions and presence of carbon dioxide plays a vital part in the degradation pathway of ethanolamine (MEA). Tertiary amines are generally very stable, and these are all known to not form carbamate to any large extent. Many steric effects play a vital role in stabilization, such as chain length, substituents both close and farther from the nitrogen and bond strain. A correlation is seen between biodegradability and oxidative degradability, giving similar degradability in both cases. There are, however, promising exceptions to this, such as 3-(dimethylamino)-1-propylamine (DMAPA) and 2-dimethylaminoethanol (DMMEA), which are stable under oxidative conditions, but also biodegradable. Direct correlations between oxidative stability and ecotoxicity or thermal stability are not seen.

Keywords

CCS, oxidative degradation, amine scrubbing, post-combustion CO$_2$ capture, biodegradation

---

[6] Corresponding author: hanna.knuutila@ntnu.no

1. Introduction

The increasing concentrations of atmospheric carbon dioxide (CO_2) due to anthropogenic industrial emissions are leading to dramatic and irreversible changes in the global climate. Capture of CO_2 from large emission points, such as cement and steel production, waste incineration or energy production, on the way to a global society relying on renewable energy, should be implemented immediately. Already in 2014, the Intergovernmental Panel on Climate Change (IPCC) stated that any climate change mitigation strategy not containing carbon capture and storage (CCS) would be more expensive than one where it is included (IPCC, 2014). According to more recent reports and studies, carbon capture, utilisation and storage (CCUS) is needed to avoid the global average temperatures from rising more than 2 °C before 2050 (Bui et al., 2018; Rogelj et al., 2018) and to achieve zero emissions (IEA, 2020).

CO_2 capture using liquid amine solvents has been performed for nearly a century and is already considered a mature technology as well as a viable and attractive option for large scale CO_2 removal from large flue gas emission sources (Bui et al., 2018; Rochelle, 2009). Amines chemically bind CO_2 at low temperature or increased pressure, mainly forming carbamates, bicarbonate, or carbonate, in a reaction that can be reversed either by increasing temperature or decreasing pressure. One of the main reasons why the implementation still is limited, is the cost of operation, both because of the energy intensity of the regeneration step and because of degradation issues, leading to unpredictable replacements costs and potential interruption of operation. Despite this, amine scrubbing is still the least expensive means of large-scale post-combustion CO_2 capture (Leung et al., 2014). Development of novel amine solvents or solvent blends aims to combat these challenges. While amine degradation has been thoroughly studied over the last decades, many aspects of the complex degradation processes are yet to be explained (Reynolds et al., 2016; Rieder et al., 2017).

Flue gas contains a range of components that impact the stability and degradability of the amines. Firstly CO_2 plays a major role in thermal degradation, where studies show a huge significance of CO_2 loading of the amines (Lepaumier et al., 2009b). Secondly the presence of oxygen gives rise to oxidative degradation. Furthermore, the presence of inorganic species originating from flue gas or construction materials also impact both the degree and pathways of solvent degradation (Blachly and Ravner, 1963; Blachly and Ravner, 1966; Chi and Rochelle, 2002; Knuutila et al., 2014). Degradation patterns and the type of compounds formed during oxidative degradation varies a lot from one amine to another, as well as depending the overall process conditions. A considerable amount of knowledge about degradation is available for compounds formed during MEA degradation (Gouedard et al., 2014; Vevelstad et al., 2013b; Vevelstad et al., 2016) as well as also for some other amines (Fredriksen and Jens, 2013; Lepaumier et al., 2009c). Oxidative degradation reactions typically form among other formic, acetic and oxalic acid in the initial degradation steps, which are attributed to the rise of corrosion and fouling in the capture plants

(Rooney et al., 1996; Rooney et al., 1997). The initiation step of the oxidative degradation pathways is not fully understood, but most studies point towards an electron abstraction mechanism (Rosenblatt et al., 1967; Smith and Mann, 1969), although hydrogen abstraction and the less commonly assumed reaction between amine radicals (aminium) and water are also described as possible pathways. Following these primary degradation compounds are a range of secondary products, formed by reaction between these and the amines (da Silva et al., 2012; Lepaumier et al., 2011; Lepaumier et al., 2009c; Strazisar et al., 2003; Supap et al., 2011). Thermal degradation pathways also occur due to the elevated temperatures in the desorber column. These pathways seem to be better understood than oxidative degradation pathways (Davis, 2009; Lepaumier et al., 2009a; Martin et al., 2012; Rochelle, 2012).

This work does not attempt to fully understand the degradation mechanisms of every single amine compound studied, but rather aims to identify features that can allow a fast assessment of the amine's stability under oxidative conditions. Despite of the harsh degradation conditions in these experiments, including higher concentrations of oxygen and dissolved iron than can be expected in reality, an overall picture of degradability can still be formed. Stability of the amine is a critical aspect to consider before moving towards large-scale testing or implementation of a novel amine. It is also potentially a showstopper for up-scaling, and therefore oxidative and thermal stability should be considered in an early stage of solvent development.

When upscaling amine-based CO_2 removal to industrial level, potential environmental impacts must, also, be considered. Environmental persistence of emitted compounds may result in potential long-term effects and accumulation in the biota. Thus, ensuring that that organic solvents enzymatically decompose by microbial digestion (often called biodegradation), is essential.

This study can be divided into three main parts:

- First the oxidative degradability at absorber conditions of a series of structurally different amines is measured under identical conditions. Also, the influence of the presence of CO_2 on oxidative stability is assessed in ethanolamine (MEA).

- Secondly, the biodegradability of some new amines is studied and compared to literature data for amine biodegradation in seawater (Eide-Haugmo et al., 2012).

- Finally, the oxidative degradation results are compared to literature data for biological and thermal stability to discuss whether oxidative degradability can be used to assess these key properties of the amines and vice versa.

Titration, ion chromatography, total nitrogen, and total inorganic carbon analysis as well as liquid chromatography coupled with mass spectrometry have been used as means of detection and quantification of the degraded amines.
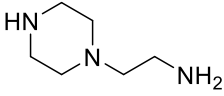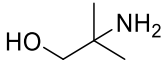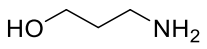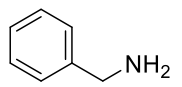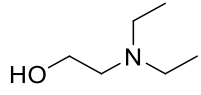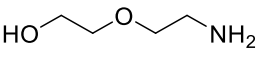
Mechanisms and pathways of oxidative degradation has been studied for many years but has yet to be completely understood. This work contributes to the existing knowledge base about the oxidative degradation reactions of amines but does not contain mechanistic studies to conclude on the pathways of the reactions. The results do, however, point out reasons for i.e. considering the carbamate route to have a higher significance in these reactions than earlier assumed.

2. Materials and methods

2.1. Chemicals

All solutions were prepared gravimetrically using deionized water from an in-house purification system at NTNU unless otherwise specified. Oxygen (O_2) and carbon dioxide (CO_2) gas were purchased from AGA in N5.0 purity. Millipore water for analytical use was obtained from a Dionex™ ICW-3000 water purification system from Merck Millipore and methanesulfonic acid (MSA, CAS: 75-75-2, ≥99.0%) for cation ion chromatography (IC) was purchased from Merck Life Science/Sigma Aldrich Norway. Supplier and purity information about the tested amines can be found in Table 6.1. Analytical standards for the anion IC analyses were prepared from sodium formate (CHO_2Na, ≥99.0%, CAS: 141-53-7) and sodium oxalate ($C_2O_4Na_2$, ≥99.5%, CAS: 62-76-0) from Sigma-Aldrich and sodium acetate ($C_2H_3O_2Na$, ≥99.0%, CAS: 127-09-3) from Merck. The potassium hydroxide (EGC III KOH, CAS: 1310-58-3) was purchased from Thermo Scientific in eluent generator cartridges.

Table 6.1: List of the amines studied, their structure as well as their purity. Chemicals were purchased from [a] Sigma Aldrich Norway AS/Merck Life Sciences, [b] ACROS Organics™.

Compound	Abbreviation	Structure	CAS-number	Purity
1-(2-Aminoethyl)piperazine [a]	AEP		140-31-8	99%
2-Amino-2-methyl-1-propanol [b]	AMP		124-68-5	99%
3-Aminopropanol [a]	AP		156-87-6	99%
Benzylamine [a]	BzA		100-46-9	99%
2-(Diethylamino)-ethanol [a]	DEEA		100-37-8	≥ 99.5%
2-(2-Aminoethoxy)ethanol (Diglycolamine®) [b]	DGA		929-06-6	98%

Compound	Abbreviation	Structure	CAS-number	Purity
3-(Dimethylamino)-1-propylamine [b]	DMAPA		109-55-7	99%
2-(Dimethylamino)-ethanol [a]	DMMEA		108-01-0	$\geq$ 99.5%
3-(Dimethylamino)-1-propanol [b]	DMPA		3179-63-3	99%
1-(Dimethylamino)-2-propanol [a]	1DMA2P		108-16-7	$\geq$ 99%
2-(Ethylamino)ethanol [a]	EAE		110-73-6	$\geq$ 98%
1-(2-Hydroxyethyl)piperidine [a]	1-(2HE)PP		3040-44-6	99%
3-(Methylamino)propylamine [a]	MAPA		6291-84-5	$\geq$ 97.0%
N-Methyldiethanolamine [a]	MDEA		105-59-9	$\geq$ 99%
Ethanolamine [a]	MEA		141-43-5	$\geq$ 99.0%
($\pm$)-1-Amino-2-propanol [b]	MIPA		78-96-6	$\geq$ 99%
N-(Methylamino)-ethanol [a]	MMEA		109-83-1	$\geq$ 98%
Piperazine [a]	PZ		110-85-0	99%
Triethanolamine [a]	TEA		102-71-6	> 99%

2.2. Oxidative degradation experiments

Oxidative degradation experiments were performed at simulated absorber conditions in custom made open, water bath-heated, double-jacketed glass reactors with magnetic stirring (approximately 250 mL) as shown in Figure 6.1. The reactor

temperature was maintained at 60 °C and the water bath-cooled Graham condensers at 5 °C. Each reactor was filled with 200 mL of the gravimetrically prepared 30 wt% (*aq.*) amine solvent mixture, which was pre-loaded to 0.4 mol of CO_2 per mol amine and contained 0.5 mM iron sulfate ($FeSO_4 \cdot 7H_2O$). A mixture of O_2 and CO_2 gas was sparged through the solutions from Alicat mass flow controllers (MFC) and through Pyrex® glass gas distribution tubes of porosity grade 1, under constant magnetic stirring for the total experimental time of three weeks. Empty gas wash bottles were used as safety solvent traps between the mass flow controllers and the gas distribution tubes in case of power outage. Sampling from the liquid phase was performed regularly through a septum on top of each reactor. Each experiment was performed in two or three parallels, and the data presented in this work is given as the average values, with the standard deviation of the sample average given as the uncertainty. Uncertainty within each analytical method is given in the description of each method and is additional to the standard deviation of the sample average.
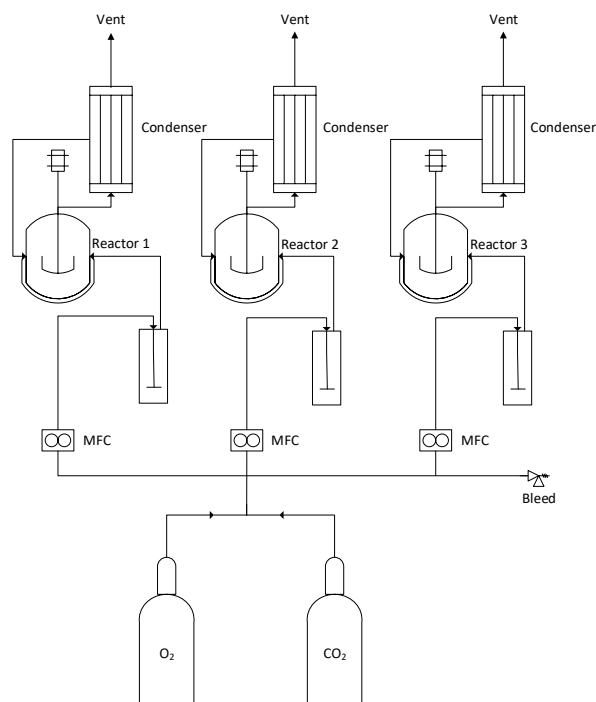
Figure 6.1: Schematic of the oxidative degradation setup.

The initial experimental procedure was designed for maintaining the loading of the primary amines at 0.4 mol CO_2 per mol amine. For this, a total of 60 mL min^{-1} of gas was used, containing 2% CO_2 and 98% O_2. This CO_2 pressure was not high enough to maintain the loading of 0.4 of the tertiary amines, and the tertiary amines and as a result, the first experiments conducted with tertiary amines had a lower CO_2 loading.

Some experiments were, therefore, run with a total of 60 mL min^{-1} gas flow containing 16.5% CO_2 and 83.5% O_2 to keep the loading constant. Finally, the oxidative degradation of tertiary amines was performed using a higher total flow of gas. In these experiments, the same O_2 flow as for primary and secondary amines (58.8 mL min^{-1}) was used, but the CO_2 flow was increased to achieve the required CO_2 partial pressure to maintain a loading of 0.4 mol CO_2 per mol amine, resulting in a higher flow. No significant difference in degradation could be seen in the tertiary amines tested using the different conditions, so some of these experiments were not repeated.

2.3. Marine biodegradability tests

Closed bottle biodegradation tests of amines were performed by SINTEF Ocean, according to the OECD guideline 306 "Biodegradability in seawater" (OECD, 1992). Natural seawater was collected from a local Norwegian fjord (Trondheimsfjorden; 63°26′N, 10°24′E). The seawater is transported to the laboratory of SINTEF Ocean though a polyethylene pipeline system from a depth of 80 m, well below the thermocline, and securing stable temperatures the year around. The seawater has a salinity of 34‰, and the water source is considered to be non-polluted. The seawater was filtered (50 µm), acclimated (20°C) for 5 days, aerated for 20 min (bubbling of sterile-filtered air), and amended with inorganic nutrients (N-, P-, Ca-, Mg-, and Fe-sources) (OECD, 1992). Biological oxygen demand (BOD) bottles (275 ml) were completely filled (no headspace) with acclimated, filtered and nutrient-amended seawater with 2 mg L^{-1} test substances or aniline (positive control), or nutrient-amended seawater without test- or control substance (seawater blank). Test solutions biocide (50 mg L^{-1} $HgCl_2$) were included to determine potential abiotic degradation. The solutions were incubated at 20 °C for up to 28 days, and bottles were sacrificed for dissolved oxygen (DO) analyses on days 0, 7, 14 and 28 (duplicate samples except on day 0) The BOD of each substrate was determined by calculating the differences between DO-concentrations in blank and test solutions. The ultimate biodegradability of each substance was determined as the percentage of its theoretical oxygen demand (ThOD). ThOD was calculated assuming complete mineralisation to CO_2 of the test substance and release of nitrogen in the form of ammonia (NH_3) or nitrogen dioxide (NO_2) (OECD, 1992). NO_2 is formed in the further reaction of NH_3 with oxygen, resulting in ThOD-NH_3 being lower than ThOD-NO_2.

2.4. Analytical methods

The concentration of amine in the solutions was determined by titration with sulfuric acid (H_2SO_4, 0.2 N) according to Ma'mun et al. (2006), a procedure with an uncertainty of $\leq 2\%$. For all the samples, the concentration of amine is back calculated to the solution without CO_2 and corrected for evaporation of water and degradation products, assuming a linear loss throughout the experiment, as the total mass of the solution is only known for the start and end solutions.

The total concentration of heat stable salts (HSS) was determined according to a method described by Reynolds et al. (2015), by adding approximately 2 g of the sample to 40 mL activated Dowex 50W-X8 ion exchange resin (Merck, CAS: 69011-20-7) and 40 mL deionized water. The mixture was partly covered and heated to 70 °C under magnetic stirring for an hour, then left to cool down to room temperature and settle. The supernatant was carefully transferred to another container through a frit and the ion exchange resin extracted repeatedly by addition of 40 mL water, stirring for 1 minute, leaving the resin to settle and combining the resulting supernatant by filtering, until the supernatant showed the pH of deionized water. The combined supernatants were titrated with 0.05 M sodium hydroxide (NaOH, CAS: 1310-73-2) to determine the molar concentration of cationic species. Analysis of 30 wt% (*aq.*) MEA with known concentrations of oxalic, formic, and acetic acid gave deviations of $\pm$ 0.007 mol kg^{-1} (max. 7%).

Quantification of amine concentrations by ion chromatography (IC) was performed on a Thermo Scientific™ Dionex™ ICS-5000 system, using a Thermo Scientific Dionex IonPac™ CS19 analytical column (2 mm · 250 mm), with a CG19 guard column (2 · 50 mm) and an eluent consisting of 15 mM methanesulfonic acid (MSA) in ultrapure water from an ICW-3000 Millipore purification system. Calibration was performed with each compound for every analysis and all data was processed using the chromatography processing software Chromeleon® 7. The method used for cation chromatography was based on that developed and used by Fytianos et al. (2015). Standard solutions of concentrations between 10 and 100 ppm of the compound (amine) to be quantified were prepared and analysed along with the diluted samples. The standards were used to make a calibration curve for each individual amine and each individual analytical procedure, and their conductivity signals (peak areas) were used to calculate the concentration of the original samples.

Acetate, formate and oxalate were quantified using a Thermo Scientific™ Dionex™ ICS-5000 system located at USN Porsgrunn, with a Dionex™ AG11-HC RFIC™ analytical (4 · 250 mm) and guard column (2 · 50 mm) and conductivity detection. The column compartment was kept at 35 °C and the cell temperature at 30 °C. A gradient of potassium hydroxide (KOH), generated by an eluent generation (EG) system, was used as the eluent, with the program given in Table 6.2. Standards of the organic acids were prepared in the concentration range from 1 to 30 ppm and the degraded amine samples were diluted between 1:100 and 1:350 with deionised water, depending on their known total content of heat stable salts (HSS). All standards and samples were filtered from any remaining particulate matter before analysis.

Table 6.2: KOH eluent gradient used for anion separation in IC.

Time (min)	$c_{KOHstart}$ [mM]	$c_{KOHstop}$ [mM]
0-30	3	3
30-32	3	30
32-52	30	30
52-54	30	60
54-64	60	60
64-66	60	3
66-74	3	3

Quantification of some alkanolamine concentration was performed by liquid chromatography coupled with mass spectrometry (LC-MSMS), performed by SINTEF Industry on a UHPLC Agilent 1290 Infinity System with an Agilent 6490 Triple Quadrupole detector. An Ascentis® Express Phenyl-Hexyl, 2.7 µm HPLC Column as well as a Discovery® HS F5 HPLC Column, both from Sigma-Aldrich Co. LLC, were used for analyte separation. MEA and MMEA were quantified using an isotope labelled internal standard and the results have a typical uncertainty of 3%. Quantification of MAPA and DMPA in samples analysed without isotope labelled standards has an uncertainty of 5%.

A Shimadzu TOC-L$_{CPH}$ analyzer equipped with a TN-unit and auto sample injector (ASI) was used for the quantification of CO_2 loading as total inorganic carbon (TIC) and total nitrogen (TN). The instrument was calibrated with sodium bicarbonate (NaHCO$_3$) for the CO_2 analysis, and potassium nitrate (KNO$_3$) for the nitrogen analysis. The uncertainty of the CO_2 quantification is $\leq 2\%$, when used in the range of 10-500 ppm carbon. The TN analysis was only used to compare the nitrogen content of the start and end sample, as matrix effects have proven to impact the ability of the method to quantify different amines with a universal calibration. Both the TIC and TN analysis were used in the range of < 500 ppm N, to avoid saturating the detector signal. The principle of quantification for inorganic carbon in the sample is based on acidification with phosphoric acid (H$_3$PO$_4$, 25wt%), releasing the inorganic carbon, including that bound as carbamate, as CO_2. The detection is then made with a nondispersive infrared detector (NDIR), selectively measuring at the wavelength of bond vibrations in the CO_2 molecule. Nitrogen can be combusted over a platinum catalyst at 720 °C and fully converted to NO$_2$, which is detected and quantified by a chemiluminescence detector.

3. Results and Discussion
3.1. Oxidative degradation
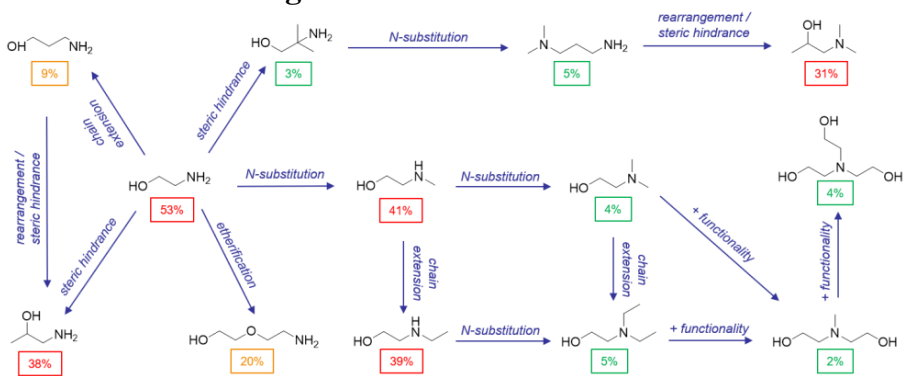
Figure 6.2: Amine loss after 21 days under oxidative conditions in relation to their structural characteristics for non-cyclic alkanol monoamines.
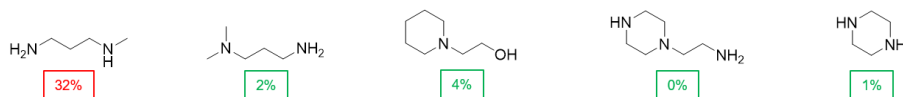
Figure 6.3: Amine loss after 21 days under oxidative conditions in relation to their structural characteristics for diamines, cyclic amines and a triamine.

Oxidative degradation of amines was primarily quantified as the loss of alkalinity throughout the experiments, as this reflects the CO_2 capture efficiency of the solvent. TN analysis, IC and LC-MS were used both for validation and for supporting information about the degradation patterns of the amines. The effect of amine structure on oxidative stability is showed in Figure 6.2 and Figure 6.3. Overall, the trend shows that all tertiary amines generally are stable under oxidative conditions, secondary and primary less so, in agreement with the studies of Lepaumier et al. (2009c), Voice and Rochelle (2011) and Voice et al. (2013). This is, however, only true if no additional steric hindrance is present in the proximity of the nitrogen group(s), such as Lepaumier et al. (2009c) postulated for AMP. If the oxidative degradation mechanisms mainly take place via carbamates and not pure amines reacting with the oxidant, this pattern can partly be explained by the lack of carbamate formation from tertiary amines. The most stable primary amine studied in this work, the sterically hindered AMP, is also known for forming bicarbonate over carbamate in aqueous solutions (Ciftja et al., 2014). Next, a more detailed discussion is given.

As mentioned earlier (section 2.2), the experimental conditions needed adjustment to the vapour-liquid equilibrium properties of the tertiary amines, and several tests with five different amines barely gave significant differences in degradability regardless of CO_2 or O_2 concentrations and end loading of CO_2. A comparison of the different tested experimental conditions can be seen in Table 6.3, where each given amine was subjected to the oxidative degradation conditions for three weeks, with two different

compositions of the gas phase or different total gas flows. The table shows the total loss of amine at the end of the experiment. All experiments had loading of 0.4 mol CO_2 per mol amine at the start of the experiment. As shown in Table 3, all tertiary amines tested, except for 1DMA2P, had losses of < 5% alkalinity during three weeks under highly oxidizing conditions.

Table 6.3: The influence of CO_2 and O_2 concentration on end loading and degradability of tertiary amines given in total amine loss after three weeks. *This experiment was run with two different solutions/concentrations of DEEA, so the uncertainty is here given as the deviation from the average of the two, not the standard error of the parallels. **Only one parallel was studied, hence, no uncertainty apart from that of the analytical methods can be given.

Amine	% CO_2	F_{total} [mL min^{-1}]	α_{end} [mol$_{CO_2}$ mol^{-1}]	Amine loss (%)
DEEA	16.5	60	0.7	1 ± 2*
	3.5	60	0.4	4 ± 0.4
DMMEA	16.5	70.4	0.7	3 ± 1
	2.0	60	0.2	4 ± 0.4
DMPA	16.5	60	0.5	3**
	3.5	60	0.2	5 ± 1
MDEA	16.5	70.4	0.5	2 ± 1
	2.0	60	0.1	3 ± 0.2
TEA	16.5	60	0.3	3 ± 1
	3.5	60	0.04	3 ± 0.2
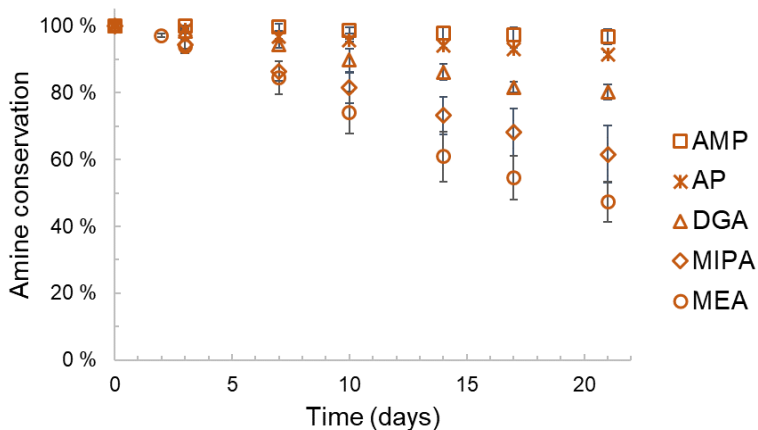
Figure 6.4: Normalized amine concentration of primary amines throughout the 21-day oxidative degradation experiments. Quantification made by amine titration and corrected to CO_2 free solution and corrected for water loss.

If the compounds studied have comparable structures, apart from a small substituent on the nitrogen atom, increasing the order of the amine, a general increase of stability can be seen with increasing order. This can be seen when the three amines in the centre of Figure 6.2, MEA, MMEA and DMMEA. The only structural feature differing is the substitution of hydrogen by methyl groups on the nitrogen atom, which increases the stability from 53% amine loss (MEA), through 41% (MMEA) to only 4% (DMMEA). A similar trend can be observed when comparing EAE and DEEA. A combination of the carbamate formation reaction of tertiary amines and an exposed amine group can make the primary amines more prone to degrade oxidatively than amines of higher substitution. Moreover, other structural features also increase oxidative stability. Figure 6.4 shows the degradation of a selection of primary amines over time and shows that all amines with more complexity degrade slower than MEA. Addition of steric hindrance in β-position relative to the amine group, such as in MIPA increases oxidative stability. Increasing steric hindrance by addition on the α-position, such as in AMP, increases the oxidative stability of a primary amine to the range of tertiary amines in this study. Even just extending the chain length relative to MEA, looking at the primary amine AP and DGA increases the stability significantly. The results of this study suggest that the carbamate of the amine may play a more significant role in the oxidative degradation pathways than previously assumed. This assumption is further supported by an oxidative degradation experiment with MEA, identical with the other experiments, but without addition of CO_2. In this case, the amines loss is only $3 \pm 1\%$, as can be seen in Figure 6.5. At the same time, carbamate forming AP (Zhang et al., 2017) is more stable than MEA. Thus, the results are not conclusive and more mechanistic studies are needed to fully understand the role carbamate may play in the degradation mechanisms of amines.
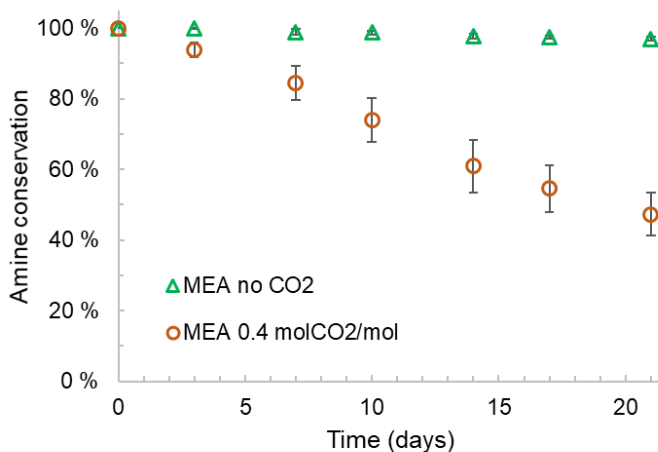
Figure 6.5: Oxidative degradation of MEA in the absence and in the presence of CO_2.

Figure 6.6 shows that also secondary amines can be relatively unstable under oxidative conditions, both MMEA and EAE as well as MAPA, a diamine with one secondary and one primary amine group, gave a high relative amine loss after 21 days under oxidative conditions. However, the diamine PZ containing two secondary amine groups is very stable throughout the whole experiment. With its cyclic form, the lower flexibility of the C-N bond compared to MMEA, EAE and MAPA can explain this stabilising effect. The step in a radical reaction where electron transfer can take place requires the reactants to arrange the position of its atoms to the configuration of the products, since this reaction is very fast (Marcus et al., 1954). This means that certain flexibility within the bonds of molecules being oxidized is required for the oxidation to occur. The rigidity of the C-N bonds in PZ may be less likely to enter a configuration where the radical oxidation reaction can take place. The high oxidative stability observed for PZ in this work is in agreement with that of Voice and Rochelle (2011).
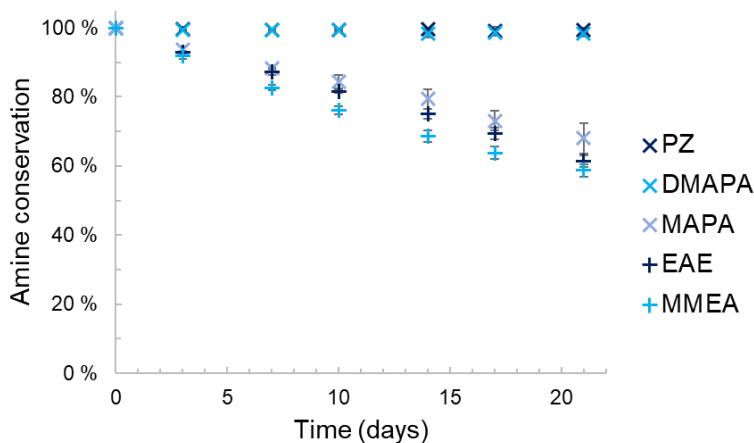
Figure 6.6: Normalized amine concentration of secondary (+) and diamines (x) throughout the 21-day oxidative degradation experiments. Quantification made by amine titration and corrected to CO_2 free solution and corrected for water loss.

As discussed earlier, most of the studied tertiary amines showed amine losses <5% after three weeks under oxidative conditions. Even the diamine DMAPA, which contains a primary amine functionality, and the cyclic AEP, containing both a primary and a secondary amine function. In the case of AEP, the secondary amine group is incorporated in the cyclic structure, like PZ, so this group is protected by the rigidity of the ring structure. The primary groups of DMAPA and AEP are likely shielded by steric effects, that protect the molecules from attack or constructing a lower compatibility with the radical donor, potentially favouring termination rather than propagation. A sterically hindered molecule has less bond flexibility and less possibility to exist in many configurations, such as for example resonance forms and rotational isomerism. 1DMA2P presented itself as an outlier among the tertiary amines, with a total loss of amine of 31% after 21 days under oxidative conditions. Despite of being tertiary, this amine behaves more like the structurally similar, although primary, MIPA. It can be speculated whether a hydroxy substituent in β-position to the nitrogen on a secondary carbon, may be unfavourable for stability, allowing for the mechanism given in Figure 6.7 to take place. In this suggested mechanism, both amines form acetone, additionally 1DMA2P forms dimethylamine and MIPA ammonia, all volatile degradation compounds. This may be the predominant degradation mechanism for 1DMA2P, but in MIPA the content of non-alkaline nitrogen, as seen in Figure 6.8 indicates that other pathways may be more or as dominant.
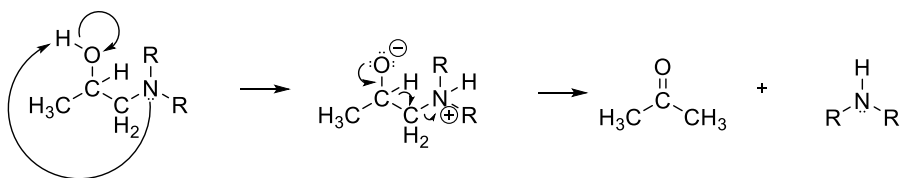
Figure 6.7: Suggested mechanism for the formation of acetone and dimethylamine/ammonia during 1DMA2P (R = CH$_3$) and MIPA (R = H) degradation.

To introduce further structural variance to the study, we wanted to see the effect of adding an aromatic functionality to the amine. Therefore, the aromatic amine benzylamine (BzA) was attempted studied under oxidative conditions, both in 30 wt% and 15 wt% concentration. In both cases, phase separation occurred before a week had passed. A thick, viscous, and dark organic phase with a higher density than water formed, and no alkalinity could be detected in the aqueous phase anymore. At 60 °C the benzylamine carbamate was soluble in water, although it precipitated at room temperature, as reported in Richner et al. (2015). Therefore, the attempt to study BzA, an aromatic amine, under these conditions was abandoned.
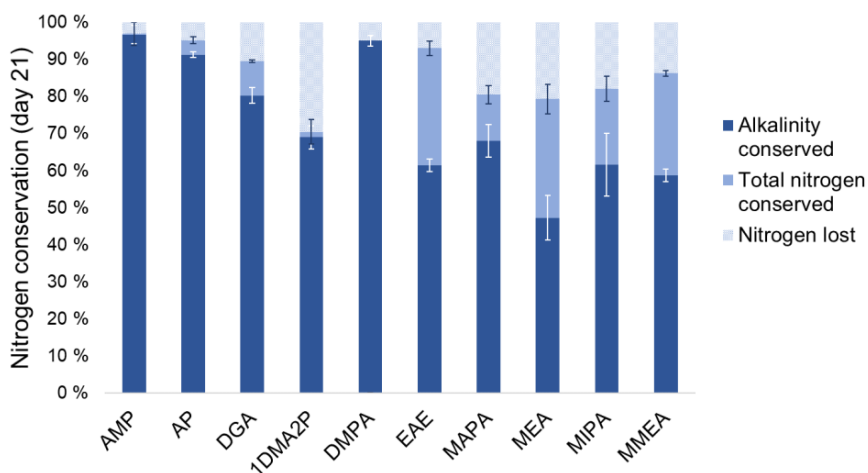
Figure 6.8: Loss of alkalinity and total nitrogen after 21 days under oxidative conditions for primary, secondary and diamines. Analysed by amine titration, TIC and TN.

The analysis of total nitrogen content after three weeks of oxidative degradation, compared to the start, as well as comparing it to the remaining alkalinity of the solutions, gives an impression of the type of degradation compounds formed, as shown in Figure 6.8. It is evident that volatile nitrogen-containing degradation compounds, such as ammonia (NH$_3$), have been formed where the nitrogen content of the initial solution has not been conserved throughout the experiment. This approach does not identify the volatile, nor the less volatile degradation compounds, but it allows an assessment of the amount of emissions which can expected from a given amine. The primary amines form a more or less equal amount of volatile and

195

less volatile nitrogen containing degradation products. This is probably mostly due to the cleavage of the C-N bond forming NH_3 that escapes the liquid phase. Secondary amines like MMEA and EAE are known to form volatile alkylamines (Vevelstad et al., 2013a), so at least for these, we can assume that a significant part of the nitrogen lost is not in the form of NH_3. For the secondary amines, more of the nitrogen is contained in the liquid phase in the form of non-alkaline degradation products. No correlation between nitrogen loss and amine volatility could be found when looking at the respective boiling points. This can be seen illustrated in the Supporting information, in Figure S1. The high loss of nitrogen from MAPA correlates with what was observed by Vevelstad et al. (2014) when using a similar open-batch oxidative degradation setup.

3.2. Comparison of different methods of amine analysis

For control and comparison, the concentration of amine was measured by cation ion chromatography (IC) in addition to amine titration to validate the results obtained by the titration by an independent method. IC separates ionic components based on their charge density and affinity to the mobile and stationary phases of the chromatographic system. The signal obtained from each component in the form of a peak, which can be integrated and quantified by comparison to a calibration curve, is characteristic for the amine, but can also overlap with other compounds of similar charge densities. Other compounds can also falsify the titration results, as all alkaline components will give the same signal. Comparing results from the two methods increases the certainty of the measured concentrations originating from the desired compound.

For four amines, a time series was also sent for LC-MS analysis at an external laboratory, for further validation and comparison. A visual representation of the results from the three different analytical methods are shown in Figure 6.9. The different methods show some deviations from one another, but overall, the same trends. Throughout the experimental period, the remaining alkalinity measured by titration in MAPA is higher than the amount of MAPA quantified by cation IC and LC-MS, although the standard error of the average of the two parallel experiments overlap. MAPA with its two amine functionalities is likely to degrade on just one of them and remain active or alkaline despite of being degraded. A deviation between titration and IC/LC-MS is therefore expected in this case. The relative large deviation between LC-MS and IC/titration for DMPA may origin from the lack of and internal deuterated standard of DMPA, also yielding a higher uncertainty for this amine and MAPA, than for MEA and MMEA, where internal standards were used for quantification.
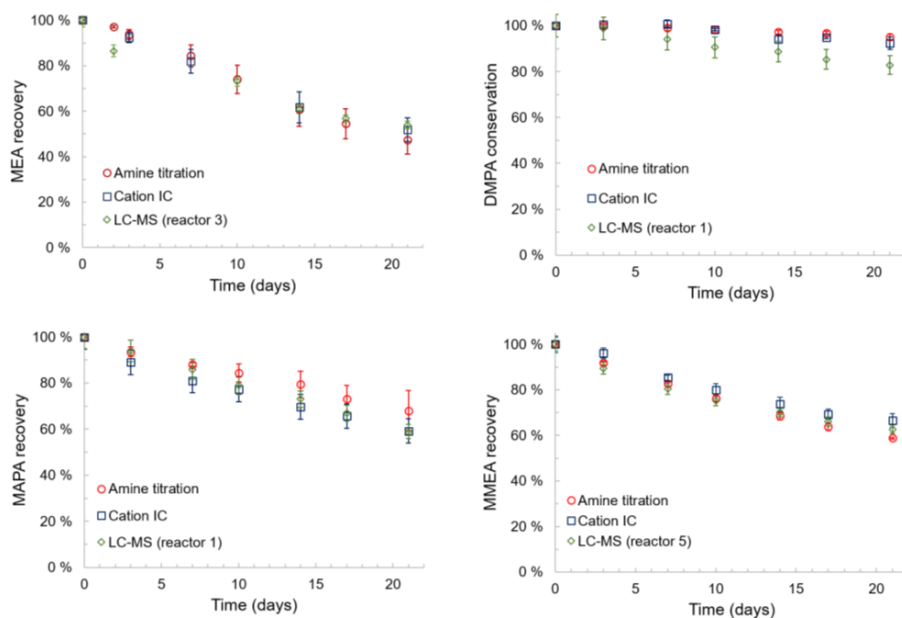
Figure 6.9: Normalized amine concentration measured by amine titration and cation chromatography from the same samples and experiments. Error bars for titration and IC represent the standard error between the parallel reactors and the data points the average value of the 2 or 3 parallels, for LC-MS they represent the uncertainty of the method. MMEA recovery given from experiment with 17 °C condenser temperature.

3.3. Heat stable salts

Anion IC analyses were performed on the end samples after 21 days of oxidative degradation of the amines. Formate, acetate and oxalate were measured in diluted samples of all amines, and Figure 6.10 shows the concentrations of these in the amines where a quantifiable amount of at least one of the acids were found.
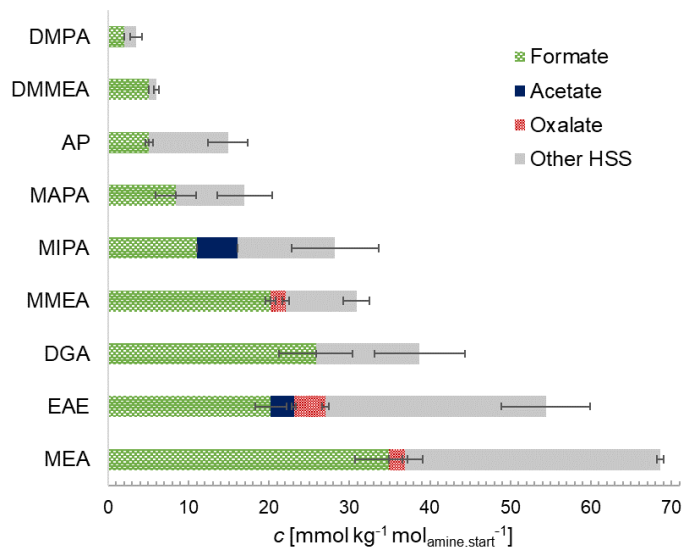
Figure 6.10: Concentrations of HSS quantified in end samples of oxidative degradation experiments. Error bars represent the standard deviation of the average of parallels.

Formate could be quantified in all of the amine samples that degraded significantly during the three-week experiments and in DMMEA and DMPA, which both had low relative amine losses. Since most of the amines which are unstable under oxidative conditions also are carbamate-forming amines, it seems likely that carbamate plays a more significant role than it has in the earlier suggested degradation mechanisms. The possibility of formate originating from the carbonyl group of the amine carbamate, as illustrated in Figure 6.11, should therefore be considered.
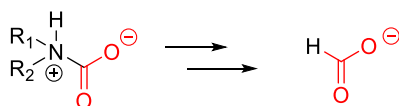
Figure 6.11: Formate may be formed through a direct redox reaction on carbamate.

Acetate was only found in concentrations above the quantification limit in two of the degraded solutions, EAE and MIPA, and oxalate in three, EAE, MEA and MMEA. Acetate and formate have both been observed to be formed in other oxidation studies of MIPA (Hutchinson et al., 1984). EAE or similar structures have not been seen to be particularly prone to form acetate under oxidative conditions, but we suggest that the reaction may take place as depicted in Figure 6.12, where the positively charged nitrogen in EAE allows for attack by an oxygen radical or a superoxide ion formed in the solution. Following an analogous mechanism, DMPA, MAPA and MMEA would form formate.
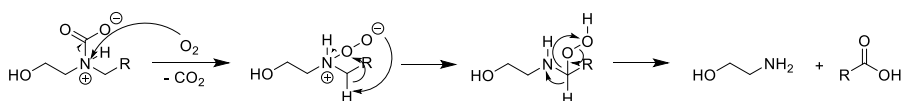
Figure 6.12: Suggested mechanism for the degradation of MMEA- (R = H) or EAE-carbamate (R = CH₃) to MEA and formic (R = H) or acetic acid (R = CH₃).

The total heat stable salt analysis shows that there are other ionizable degradation products present than the three which were quantified by ion chromatography, some of which could also be observed in the anion chromatograms, although not identified. The ion chromatogram of degraded MEA can be found in the Supporting information, depicted in Figure S2.

3.3. Biodegradation

Since alkanolamines may not evaporate in the environment and have poor affinities for soil (Davis and Carpenter, 1997), these compounds may end up in aquatic systems and eventually in seawater. Since biodegradation of several alkanolamines was faster in fresh water than in seawater (Brakstad et al., 2012; Eide-Haugmo et al., 2012; Henry et al., 2017; Price et al., 1974), biodegradability in seawater may also be used as a good representation of biodegradability limitations of amines in this work.

Table 6.4 Biodegradability measured according to OECD guideline 306 under the assumption that nitrogen digestion forms ammonia (NH₃) or nitrogen dioxide (NO₂) after 28 days of incubation. The amines are also characterised as natural products or not.(DNP, 2020)

Amine	Biodegradability (% of ThOD-NH₃)	Biodegradability (% of ThOD-NO₂)	Natural product
AEP	12.5 ± 0.2	7.8 ± 0.2	No
DMMEA	98.7 ± 1.3	77.6 ± 1.0	Yes
DMAPA	96.7 ± 0.0	67.7 ± 0.0	Yes
1DMA2P	5.2 ± 1.7	4.3 ± 1.4	No
1-(2HE)PP	3.4 ± 2.8	2.9 ± 2.4	No
Aniline (reference)	100.8 ± 2.0	83.0 ± 1.7	Yes

Five amines were tested for ultimate biodegradation in seawater, and the results are presented in Table 6.4, where the amines are also classified as natural or synthetic The results show that 1-(2HE)PP, 1DMA2P and AEP, have low marine biodegradability, below 20%, whereas DMMEA and DMAPA are highly biodegradable. As expected, and also seen in observed in previous studies, the naturally occurring amines have a higher biodegradability than synthetic amines. In addition to the results given here, abiotic tests were performed for all amines, all showing that they do not degrade in the absence of microbes under the given conditions (results given in Table S8).

The piperazine and piperidine (AEP and 1-(2HE)PP) showed poor degradability, as previously seen with some other cyclic amines (Eide-Haugmo et al., 2012). The two degradable amines (DMMEA and DMAPA) were associated with terminal alcohol or amine groups, typically subject to enzymatic attack during amine biodegradation (Brakstad et al., 2018; Cerniglia and Perry, 1975).

3.4. Comparison of oxidative, thermal and biodegradation

Since one of the most common pathways of biological amine degradation reactions occurs through catalysis by the *monoamine oxidase* enzymes (Silverman, 1995), it is not unexpected to find a correlation between oxidative and aerobic biological degradability (Figure 6.13). Most of the amines that were unstable under oxidative conditions in the experiments performed in this work also showed a high biodegradability when compared to the results of marine biodegradability studied both in this work and in previous studies (Eide-Haugmo et al., 2012). There are, however, some amines which are stable under oxidative conditions and still have a high biodegradability, properties that are favourable from a combined industrial and environmental perspective. Another observed trend in Figure 6.13 is that most of the highly degradable amines are of natural origin and the ones showing low degradability are of synthetic origin. In the case of biodegradability, this makes sense, as there is a compatibility between natural compounds and enzymes, but it can interestingly also be seen as a trend for oxidative degradability in the absence of microorganisms. Ideally, one would want an amine for use industrially to be stable under oxidative conditions but biologically unstable so that it can degrade in nature in case of a spill. This is the case for two of the tested amines, DMMEA (94% of ThOD) and DMAPA (55% of ThOD). DMMEA was pointed out as a promising solvent by Eide-Haugmo (2011) because of it is seen that it has relatively high thermal stability and biodegradability, which can be seen in Figure 6.13. All compounds with a biodegradability above 60% of ThOD are considered readily biodegradable .

BIOLOGICAL DEGRADABILITY

> 60%

DMMEA
DMMEA*
DMAPA*

MEA   MAPA
MMEA   EAE

20-60%

DMAPA
TEA

MIPA

< 20%

DEEA   1-(2HE)PP*
MDEA   AEP*
DMPA   AMP
PZ

DGA
AP

1DMA2P*

< 6%   6-20%   > 20%

OXIDATIVE DEGRADABILITY
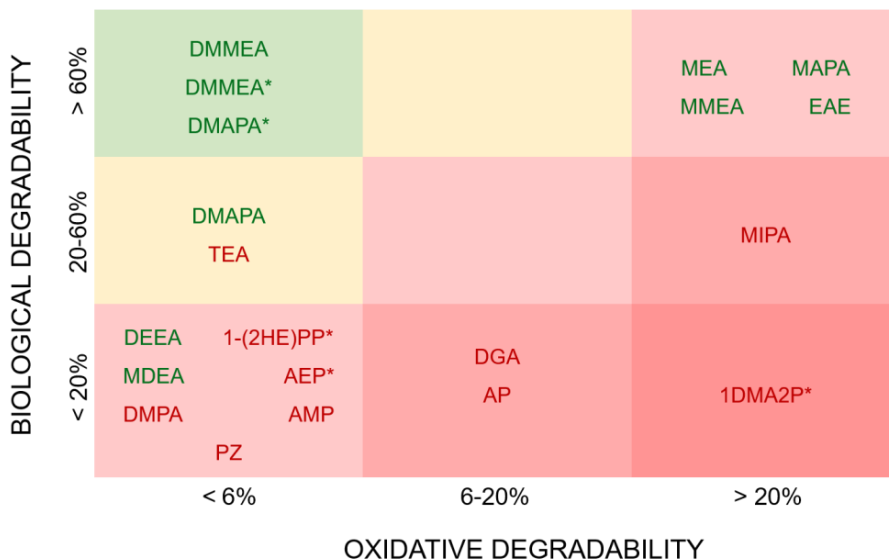
Figure 6.13: Marine biodegradability (% of ThOD-NH$_3$) of amines from Eide-Haugmo et al. (2012)Eide-Haugmo et al. (2012) and this work (*) categorized according to their biological and oxidative degradability. Oxidative degradability given as alkalinity lost after 3 weeks under oxidative conditions. Natural (green) amines are generally more biodegradable than non-natural amines (red).

The knowledge of biological degradability is insufficient for assessing the total impact of an amine in case of a spill in nature. Ecotoxicity tests provide additional information that allows assessing the amines potential effect on the local environment if leaked. Eide-Haugmo et al. (2012) also studied this in a marine environment and the ecotoxicity is tested according to ISO/DIS guideline 10253, with the marine diatom *Skeletonema Costatum* (ISO, 1999). There is no visible correlation between biological degradability and ecotoxicity in this case. None of the amines from this study were deemed acutely toxic to marine life, but many of them fall into the category of "slightly toxic".
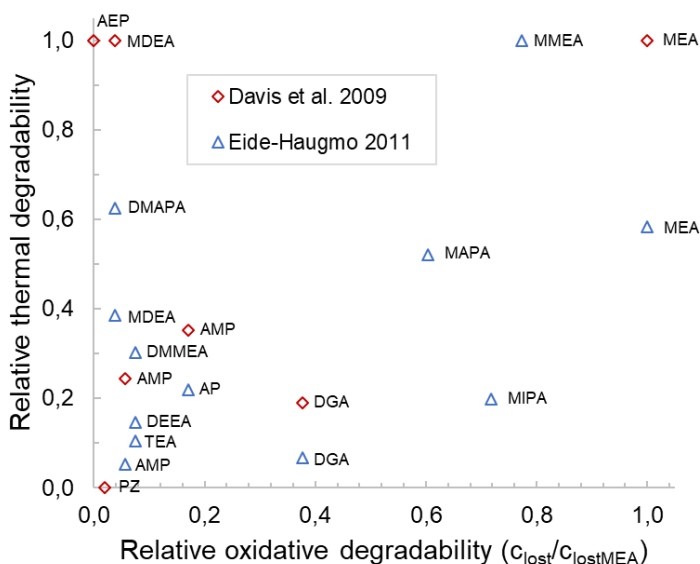
Figure 6.14: Comparison of the relative oxidative and thermal degradability of 14 of the studied amines. Davis et al. (2009) (Davis, 2009) studied degradability with 0.4 mol CO_2 per mol amine and amine concentration of 3.5-8.4 mol/kg (40wt%) for 4 weeks and Eide-Haugmo et al. (2011) (Eide-Haugmo, 2011) with 0.5 mol CO_2 per mol amine and amine concentration 2.1-4.6 mol/L (30wt%) for 5 weeks, both in stainless steel cylinders at 135 °C.

In addition to the conditions with high oxygen availability and relatively low temperatures, as simulated in these oxidative degradation experiments, thermally aggravating conditions are met in the desorber and reboiler of a CO_2 capture plant. To assess the overall stability of the amines tested, a comparison with thermal degradation data from Davis (2009) and Eide-Haugmo (2011) is given in this section. Because the experiments were performed under slightly different conditions, the degradability is normalized in regard to the amine with the highest amine loss at the end of the experiment in Figure 6.14, which was MEA in the study of Davis (2009) and MMEA in Eide-Haugmo (2011), since small differences in experimental conditions make a direct comparison and visualization difficult. The oxidative degradability has also been normalized in relation to the amine loss of MEA. Exact amine losses can be found in Table S5. The comparison shows that oxidative stability not necessarily means thermal stability, as AEP, MDEA and DMAPA all seem very promising after studying their stability under oxidative conditions but have proven to have a low relative thermal stability.

4. Conclusions

After nearly three decades of studies focusing on mechanistic understanding of oxidative degradation of amines, there are still many unknowns when it comes to its reaction pathways. This work contributes to the existing knowledge with some new insights from laboratory scale degradation experiments.

Ethanolamine (MEA) has a high oxidative stability in the absence of CO_2, indicating that MEA carbamate partakes in the initiation step of the oxidative degradation reaction. In contrast, 2-amino-2-methyl-1-propanol (AMP), which is a similar but sterically hindered primary amine known to form bicarbonate over carbamate in reaction with CO_2, hardly degrades at all under oxidative conditions. This does, however not, explain the full extent of degradability of amines, as some typical carbamate-forming amines, such as 3-aminopropanol (AP) have higher stability than MEA. Further mechanistic studies are recommended to determine the role of carbamate in the degradation mechanisms of amines.

Eight of the nine studied tertiary amines show high oxidative stability under the experimental conditions and had losses of alkalinity ≤ 5% after three weeks subjected to 98% O_2, CO_2-loading, iron and 60 °C.

Steric hindrance and high substitution can give oxidative stability to amines, regardless of the number of substituents on the nitrogen atom. In addition to AMP, other primary amines such as 3-aminopropanol (AP), amino-2-propanol (MIPA) and 2-(2-aminoethoxy)ethanol (DGA) have a higher oxidative stability than MEA, likely due to steric effects.

Secondary amines, such as *N*-methylaminoethanol (MMEA) and 2-(ethylamino)ethanol (EAE), are generally unstable, but even for here, steric constraint around the nitrogen atom, such as in the ring structure of piperazine (PZ) and 1-(2-Aminoethyl)piperazine (AEP), drastically increases the oxidative stability.

There seems to be a correlation between oxidative and biological degradability. Oxidative degradation tests can to a large extent, be used to predict biological degradability, but there is, fortunately, no exclusive relationship between the two properties, meaning that amines with high oxidative stability and ready biodegradability exist.

Oxidative and thermal stability do not correlate, so testing of both these properties seems necessary for solvent stability assessment.

Acknowledgments

Supporting information

Calculations: Uncertainty, Corrections of measured concentrations and Theoretical oxygen demand (ThOD)

Supplementary data for all included graphics

5. References

Blachly, C., Ravner, H., 1963. The effect of trace amounts of copper on the stability of monoethanolamine scrubber solutions. Naval Research Lab Washington DC.

Blachly, C.H., Ravner, H., 1966. Stabilization of Monoethanolamine Solutions in Carbon Dioxide Scrubbers. Journal of Chemical and Engineering Data 11, 401-403.

Brakstad, O.G., Booth, A., Eide-Haugmo, I., Skjaeran, J.A., Sorheim, K.R., Bonaunet, K., Vang, S.H., da Silva, E.F., 2012. Seawater biodegradation of alkanolamines used for CO2-capture from natural gas. International Journal of Greenhouse Gas Control 10, 271-277.

Brakstad, O.G., Sorensen, L., Zahlsen, K., Bonaunet, K., Hyldbakk, A., Booth, A.M., 2018. Biotransformation in water and soil of nitrosamines and nitramines potentially generated from amine-based CO2 capture technology. International Journal of Greenhouse Gas Control 70, 157-163.

Bui, M., Adjiman, C.S., Bardow, A., Anthony, E.J., Boston, A., Brown, S., Fennell, P.S., Fuss, S., Galindo, A., Hackett, L.A., Hallett, J.P., Herzog, H.J., Jackson, G., Kemper, J., Krevor, S., Maitland, G.C., Matuszewski, M., Metcalfe, I.S., Petit, C., Puxty, G., Reimer, J., Reiner, D.M., Rubin, E.S., Scott, S.A., Shah, N., Smit, B., Trusler, J.P.M., Webley, P., Wilcox, J., Mac Dowell, N., 2018. Carbon capture and storage (CCS): the way forward. Energy & Environmental Science 11, 1062-1176.

Cerniglia, C., Perry, J., 1975. Metabolism of n-propylamine, isopropylamine, and 1, 3-propane diamine by Mycobacterium convolutum. Journal of bacteriology 124, 285-289.

Chi, S., Rochelle, G.T., 2002. Oxidative Degradation of Monoethanolamine. Industrial & Engineering Chemistry Research 41, 4178-4186.

Ciftja, A.F., Hartono, A., Svendsen, H.F., 2014. Experimental study on carbamate formation in the AMP–CO2–H2O system at different temperatures. Chemical engineering science 107, 317-327.

da Silva, E.F., Lepaumier, H., Grimstvedt, A., Vevelstad, S.J., Einbu, A., Vernstad, K., Svendsen, H.F., Zahlsen, K., 2012. Understanding 2-ethanolamine degradation in postcombustion CO2 capture. Industrial & Engineering Chemistry Research 51, 13329-13338.

Davis, J.D., 2009. Thermal degradation of aqueous amines used for carbon dioxide capture.

Davis, J.W., Carpenter, C.L., 1997. Environmental assessment of the alkanolamines, Reviews of environmental contamination and toxicology. Springer, pp. 87-137.

DNP, 2020. Dictionary of Natural Products. CRC Press, Taylor & Francis Group, http://dnp.chemnetbase.com/faces/chemical/ChemicalSearch.xhtml.

Eide-Haugmo, I., 2011. Environmental impacts and aspects of absorbents used for CO_2 capture.

Eide-Haugmo, I., Brakstad, O.G., Hoff, K.A., da Silva, E.F., Svendsen, H.F., 2012. Marine biodegradability and ecotoxicity of solvents for CO2-capture of natural gas. International Journal of Greenhouse Gas Control 9, 184-192.

Fredriksen, S., Jens, K.-J., 2013. Oxidative degradation of aqueous amine solutions of MEA, AMP, MDEA, Pz: A review. Energy Procedia 37, 1770-1777.

Fytianos, G., Callot, R., Svendsen, H.F., Knuutila, H.K., 2015. Quantitative determination of amines used in post-combustion CO2 capture process by ion chromatography. International Journal of Greenhouse Gas Control 42, 372-378.

Gouedard, C., Rey, A., Cuzuel, V., Brunet, J., Delfort, B., Picq, D., Dugay, J., Vial, J., Pichon, V., Launay, F., 2014. Amine degradation in CO2 capture. 3. New degradation products of MEA in liquid phase: amides and nitrogenous heterocycles. International Journal of Greenhouse Gas Control 29, 61-69.

Henry, I.A., Kowarz, V., Østgaard, K., 2017. Aerobic and anoxic biodegradability of amines applied in CO2-capture. International Journal of Greenhouse Gas Control 58, 266-275.

Hutchinson, R.J., Smith, J.R.L., Twigg, M.V., 1984. Amine oxidation. Part 15. A product and stoicheiometric study of the oxidation of aminoalcohols by vanadium (V) ions in aqueous perchloric acid. Journal of the Chemical Society, Perkin Transactions 2, 1583-1587.

IEA, 2020. Energy Technology Perspectives 2020. IEA, Paris.

IPCC, 2014. Climate Change 2014: Synthesis Report. Contribution of Working Groups I, II and III to the Fifth Assessment Report of the Intergovernmental Panel on Climate Change, [Core Writing Team, R.K. Pachauri and L.A. Meyer (eds.)]. IPCC, Geneva, Switzerland.

ISO, 1999. ISO Guideline ISO/DIS 10253 Water quality - Marine algal growth inhibition test with *Skeletonema costatum* and *Phaeodactylum tricornutum*.

Knuutila, H., Asif, N., Vevelstad, S.J., Svendsen, H.F., 2014. Formation and Destruction of NDELA in 30 wt% MEA (Monoethanolamine) and 50 wt% DEA (Diethanolamine) Solutions. Oil & Gas Science and Technology–Revue d'IFP Energies nouvelles 69, 805-820.

Lepaumier, H., da Silva, E.F., Einbu, A., Grimstvedt, A., Knudsen, J.N., Zahlsen, K., Svendsen, H.F., 2011. Comparison of MEA degradation in pilot-scale with lab-scale experiments. Energy Procedia 4, 1652-1659.

Lepaumier, H., Picq, D., Carrette, P.-L., 2009a. Degradation study of new solvents for CO_2 capture in post-combustion, Energy Procedia, pp. 893-900.

Lepaumier, H., Picq, D., Carrette, P.L., 2009b. New amines for CO2 Capture. I. Mechanisms of amine degradation in the presence of CO2. Industrial and Engineering Chemistry Research 48, 9061-9067.

Lepaumier, H., Picq, D., Carrette, P.L., 2009c. New amines for CO2 Capture. II. Oxidative degradation mechanisms. Industrial and Engineering Chemistry Research 48, 9068-9075.

Leung, D.Y., Caramanna, G., Maroto-Valer, M.M., 2014. An overview of current status of carbon dioxide capture and storage technologies. Renewable and Sustainable Energy Reviews 39, 426-443.

Ma'mun, S., Jakobsen, J.P., Svendsen, H.F., Juliussen, O., 2006. Experimental and modeling study of the solubility of carbon dioxide in aqueous 30 mass% 2-((2-aminoethyl) amino) ethanol solution. Industrial & engineering chemistry research 45, 2505-2512.

Marcus, R.J., Zwolinski, B.J., Eyring, H., 1954. The electron tunnelling hypothesis for electron ex-change reactions. The Journal of Physical Chemistry 58, 432-437.

Martin, S., Lepaumier, H., Picq, D., Kittel, J., de Bruin, T., Faraj, A., Carrette, P.-L., 2012. New amines for CO2 capture. IV. Degradation, corrosion, and quantitative structure property relationship model. Industrial & Engineering Chemistry Research 51, 6283-6289.

OECD, 1992. Test No. 306: Biodegradability in Seawater.

Price, K.S., Waggy, G.T., Conway, R.A., 1974. Brine shrimp bioassay and seawater BOD of petrochemicals. Journal (Water Pollution Control Federation), 63-77.

Reynolds, A.J., Verheyen, T.V., Adeloju, S.B., Chaffee, A.L., Meuleman, E., 2015. Evaluation of methods for monitoring MEA degradation during pilot scale post-combustion capture of CO2. International Journal of Greenhouse Gas Control 39, 407-419.

Reynolds, A.J., Verheyen, T.V., Meuleman, E., 2016. Degradation of amine-based solvents, in: Feron, P.H.M. (Ed.), Absorption-Based Post-combustion Capture of Carbon Dioxide. Woodhead Publishing, pp. 399-423.

Richner, G., Puxty, G., Carnal, A., Conway, W., Maeder, M., Pearson, P., 2015. Thermokinetic properties and performance evaluation of benzylamine-based solvents for CO2 capture. Chemical Engineering Journal 264, 230-240.

Rieder, A., Dhingra, S., Khakharia, P., Zangrilli, L., Schallert, B., Irons, R., Unterberger, S., van Os, P., Goetheer, E., 2017. Understanding solvent degradation: A study from three different pilot plants within the OCTAVIUS project. Energy Procedia 114, 1195-1209.

Rochelle, G.T., 2009. Amine scrubbing for CO2 capture. Science 325, 1652-1654.

Rochelle, G.T., 2012. Thermal degradation of amines for CO2 capture. Current Opinion in Chemical Engineering 1, 183-190.

Rogelj, J., Shindell, D., Jiang, K., Fifita, S., Forster, P., Ginzburg, V., Handa, C., Kheshgi, H., Kobayashi, S., Kriegler, E., Mundaca, L., Séférian, R., Vilariño, M.V., 2018. Mitigation Pathways Compatible with 1.5°C in the Context of Sustainable Development. In: *Global Warming of 1.5°C. An IPCC Special Report on the impacts of global warming of 1.5°C above pre-industrial levels and related global greenhouse gas emission pathways, in the context of strengthening the global response to the threat of climate change, sustainable development, and efforts to eradicate poverty*. IPCC.

Rooney, P., Bacon, T., DuPart, M., 1996. Effect of heat stable salts on MDEA solution corrosivity. Hydrocarbon processing (International ed.) 75, 95-103.

Rooney, P., DuPart, M., Bacon, T., 1997. Effect of heat stable salts on MDEA solution corrosivity: Part 2. Hydrocarbon Processing 76.

Rosenblatt, D., Hull, L., De Luca, D., Davis, G., Weglein, R., Williams, H., 1967. Oxidations of amines. II. Substituent effects in chlorine dioxide oxidations. Journal of the American Chemical Society 89, 1158-1163.

Silverman, R.B., 1995. Radical ideas about monoamine oxidase. Accounts of chemical research 28, 335-342.

Smith, P.J., Mann, C.K., 1969. Electrochemical dealkylation of aliphatic amines. The Journal of Organic Chemistry 34, 1821-1826.

Strazisar, B.R., Anderson, R.R., White, C.M., 2003. Degradation pathways for monoethanolamine in a CO2 capture facility. Energy & fuels 17, 1034-1039.

Supap, T., Idem, R., Tontiwachwuthikul, P., 2011. Mechanism of formation of heat stable salts (HSSs) and their roles in further degradation of monoethanolamine during CO2 capture from flue gas streams. Energy Procedia 4, 591-598.

Vevelstad, S.J., Grimstvedt, A., Einbu, A., Knuutila, H., da Silva, E.F., Svendsen, H.F., 2013a. Oxidative degradation of amines using a closed batch system. International Journal of Greenhouse Gas Control 18, 1-14.

Vevelstad, S.J., Grimstvedt, A., Elnan, J., da Silva, E.F., Svendsen, H.F., 2013b. Oxidative degradation of 2-ethanolamine: The effect of oxygen concentration and

temperature on product formation. International Journal of Greenhouse Gas Control 18, 88-100.

Vevelstad, S.J., Grimstvedt, A., Knuutila, H., da Silva, E.F., Svendsen, H.F., 2014. Influence of experimental setup on amine degradation. International Journal of Greenhouse Gas Control 28, 156-167.

Vevelstad, S.J., Johansen, M.T., Knuutila, H., Svendsen, H.F., 2016. Extensive dataset for oxidative degradation of ethanolamine at 55–75° C and oxygen concentrations from 6 to 98%. International Journal of Greenhouse Gas Control 50, 158-178.

Voice, A.K., Closmann, F., Rochelle, G.T., 2013. Oxidative Degradation of Amines With High-Temperature Cycling. Energy Procedia 37, 2118-2132.

Voice, A.K., Rochelle, G.T., 2011. Oxidation of amines at absorber conditions for CO_2 capture from flue gas. Energy Procedia 4, 171-178.

Zhang, R., Yang, Q., Liang, Z., Puxty, G., Mulder, R.J., Cosgriff, J.E., Yu, H., Yang, X., Xue, Y., 2017. Toward efficient CO2 capture solvent design by analyzing the effect of chain lengths and amino types to the absorption capacity, bicarbonate/carbamate, and cyclic capacity. Energy & Fuels 31, 11099-11108.

Supporting information

Stability of structurally varied aqueous amines for CO$_2$ capture

Vanja Buvik [a], Solrun J. Vevelstad [b], Odd G. Brakstad [c] and Hanna K. Knuutila [a][7]

[a] Department of Chemical Engineering, Norwegian University of Science and Technology (NTNU), NO-7491 Trondheim, Norway

[b] SINTEF Industry, NO-7465 Trondheim, Norway

[c] SINTEF Ocean, NO-7465 Trondheim, Norway.

Calculations

Uncertainty

Calculation of standard deviation (SD) within an average ($\bar{x}$) of n samples is done according to

$$SD = \sqrt{\frac{\sum_{i=1}^{n}(x_i - \bar{x})^2}{n-1}},$$

where x_i represents the measured concentration of each sample.

Correction of measured concentrations

Correction from CO$_2$-loaded to CO$_2$-free solution using the amine concentration measured by amine titration ($C_{\text{CO}_2 \text{ loaded}}$) in mol kg^{-1} and mass concentration of CO$_2$ measured by TIC (C_{CO_2}) was performed according to equation

---

[7] Corresponding author: hanna.knuutila@ntnu.no

$$C_{CO_2\ free} = \frac{C_{CO_2\ loaded} \cdot (C_{CO_2} + 1000\ g)}{1000\ g}.$$

Correction for water and degradation compound loss throughout the experiment, assuming it to be linear with the equation $Loss\ (in\ \%) = d \cdot x$, depending on the day ($d$) and the slope increment (x) was calculated according to

$$C_{corrected} = C_{CO_2\ free} - d \cdot x \cdot C_{CO_2\ free}.$$

Theoretical oxygen demand (ThOD)

$$\text{ThOD}_{NH_3} = \frac{12 \cdot (2C + 0.5(H - Cl - 3N) + 3S + 2.5P + 0.5Na - O)}{MW} \qquad \text{Eq. 1}$$

$$\text{ThOD}_{NO_2} = \frac{12 \cdot (2C + 0.5(H - Cl) + 3S + 1.5N + 2.5P + 0.5Na - O)}{MW} \qquad \text{Eq. 2}$$

Calculations of the theoretical oxygen demand (ThOD) for the complete biodegradation of a substrate, forming NH_3 or NO_2 were performed according to Eq. 1 and 2, where the oxygen demand depends on number of carbon, hydrogen, chlorine, nitrogen, sulphur, phosphorus, sodium and oxygen atoms in the molecule, as well as its molecular mass (MW).

$$\% \text{ of ThOD} = \frac{m_{O_2}}{m_{ThOD}} \cdot 100\% \qquad \text{Eq. 3}$$

Biodegradability was then calculated according to Eq. 3, using the amount of oxygen consumed (m_{O_2}) divided by the theoretical oxygen demand (m_{ThOD}).

Supplementary data

A validation of the experimental conditions was performed, by subjecting MEA to the oxidative conditions with and without addition of iron sulfate. The presence of iron clearly gives a higher degradability of the amine solution and was maintained throughout the rest of the experiments. Secondly, a test was also made to validate the condenser temperature, where MMEA was run once with less cooling, as this amine is known to form volatile alkylamine degradation products and a lower boiling point than MEA. The results show close to the same amine loss, shown in Table S1, indicating that even a cooling temperature of 5 °C can maintain as much of the degradation compounds in the liquid phase as possible.

Table S1: Results of validation experiments with and without iron addition and condenser temperature varied. Amine loss measured by amine titration.

Amine	c_{FeSO4} [mM]	$T_{condenser}$ (°C)	Amine loss (%)
MEA	0.5	5	53 ± 6
	0.0		5 ± 1
MMEA	0.5	5	41 ± 2
		17	39 ± 2
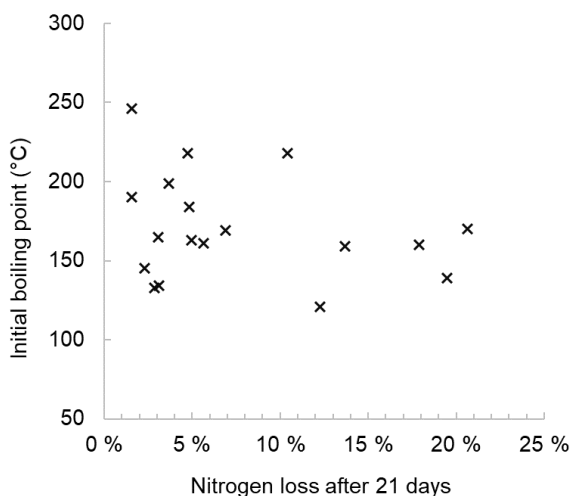
Figure S1: Amine boiling point plotted against the amount of nitrogen loss observed after 21 days under oxidatively degrading conditions.

213

Table S2: Concentrations of total nitrogen in start and end samples of oxidative degradation experiments. Average concentrations measured are given with standard deviation of parallels. Uncertainty within each parallel is maximum ±2% (uncertainty of analytical method).

Amine	Total Nitrogen [$mol_N kg^{-1}$]	
	start	day 21
MEA	5.03	3.99 ± 0.20
MEA (no CO_2)	-	-
MMEA	4.04 ± 0.02	3.49 ± 0.03
DMMEA	3.50	3.39 ± 0.01
DGA	3.03 ± 0.001	2.72 ± 0.01
AP	4.28	4.07 ± 0.04
DEEA	2.11	1.99 ± 0.01
DMPA	2.64	2.51 ± 0.005
TEA	2.13	2.10 ± 0.01
MDEA	2.26	2.23 ± 0.09
PZ	7.17	7.01 ± 0.05
EAE	3.08	2.87 ± 0.06
MAPA	6.19	4.98 ± 0.15
AMP	3.13	3.03 ± 0.10
MIPA	3.83	3.14 ± 0.13
AEP	8.03	7.64 ± 0.05
1-(2HE)PP	3.03	2.91 ± 0.06
DMAPA	7.63	7.41 ± 0.12
1DMA2P	2.99	2.11 ± 0.10
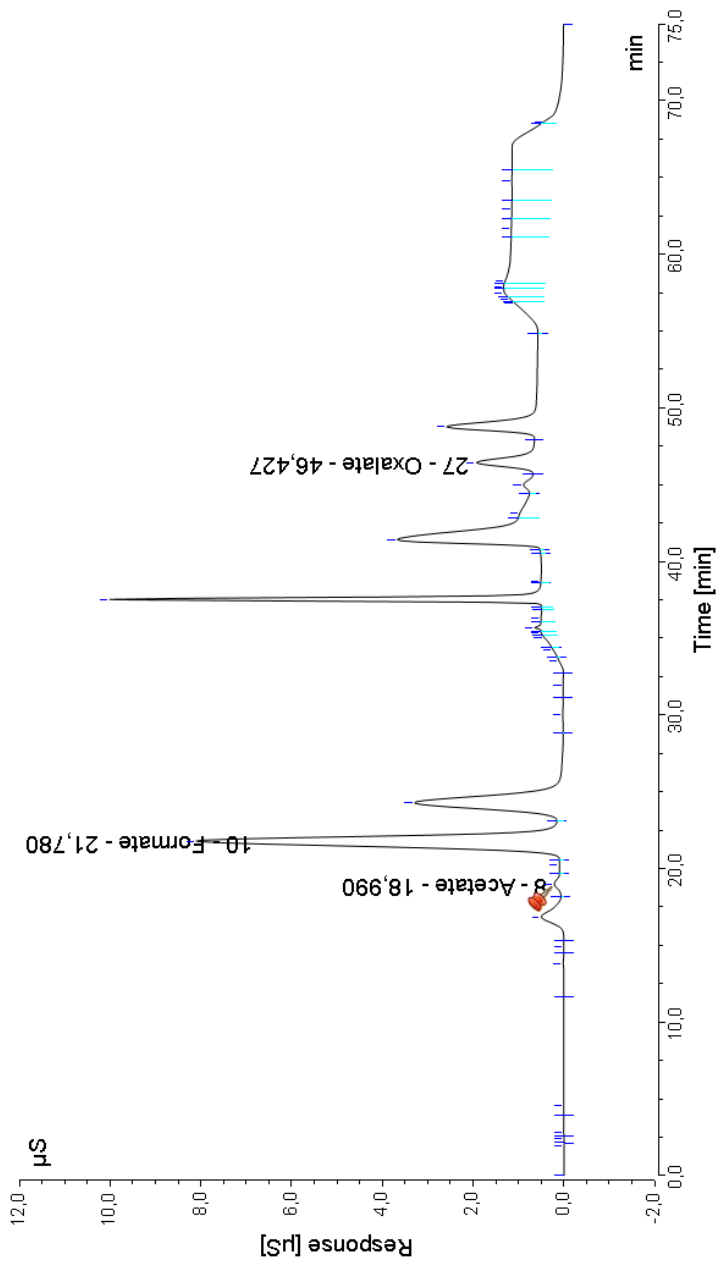
Figure S2: The anion chromatogram of an oxidatively degraded 30 wt% MEA (*aq.*) solution. The peaks that could be identified and quantified, using analytical standards are labelled. Further peaks originate from other anionic degradation compounds.

Table S3: Titration and TIC data from oxidative degradation experiments of 30wt% amines (*aq.*). F_{CO2} = 2% and $T_{condenser}$ = 5 °C unless otherwise specified. Where values are not given, analysis has not been performed, but values extrapolated from the data of samples taken before and after. R1-R6 represent six individual reactors in two separate setups. They are all constructed identically.

| | MEA 30wt% (*aq.*) | | | | |
| | Titration | CO$_2$-conc. | α | CO$_2$-free conc. | Water loss corr. |
Day	[mol$_{alkalinity}$/kg]	[g/kg]	[mol$_{CO2}$/mol$_{alkalinity}$]	[mol$_{alkalinity}$/kg]	[mol$_{alkalinity}$/kg]
0	4.339	77.37	0.41	4.675	4.675
R1 day 2	4.166			4.477	4.512
R2 day 2	4.187			4.506	4.542
R3 day 2	4.195			4.521	4.557
R1 day 3	3.946	74.51	0.43	4.240	4.291
R2 day 3	4.021	76.23	0.43	4.328	4.379
R3 day 3	4.118	77.64	0.43	4.437	4.490
R1 day 7	3.417	61.34	0.41	3.626	3.727
R2 day 7	3.586	66.30	0.42	3.824	3.930
R3 day 7	3.803	69.79	0.42	4.068	4.181
R1 day 10	2.862			3.038	3.159
R2 day 10	3.138			3.346	3.479
R3 day 10	3.362			3.596	3.739
R1 day 14	2.277	36.76	0.37	2.361	2.492
R2 day 14	2.592	43.64	0.38	2.705	2.855
R3 day 14	2.883	49.46	0.39	3.025	3.193
R1 day 17	2.019			2.093	2.234
R2 day 17	2.299			2.400	2.562
R3 day 17	2.546			2.672	2.852
R1 day 21	1.723	24.64	0.33	1.765	1.912
R2 day 21	2.012	30.49	0.34	2.073	2.246
R3 day 21	2.209	35.16	0.36	2.287	2.477

| | MEA 30wt% (*aq.*), without CO$_2$ | | | | |
| | Titration | CO$_2$-conc. | α | CO$_2$-free conc. | Water loss corr. |
Day	[mol$_{alkalinity}$/kg]	[g/kg]	[mol$_{CO2}$/mol$_{alkalinity}$]	[mol$_{alkalinity}$/kg]	[mol$_{alkalinity}$/kg]
0	4.913			4.913	4.913
R4 day 3	4.941			4.941	4.896
R5 day 3	4.956			4.956	4.909
R6 day 3	4.972			4.972	4.914
R4 day 7	4.965			4.965	4.861
R5 day 7	5.006			5.006	4.894
R6 day 7	4.954			4.954	4.819
R4 day 10	5.001			5.001	4.851
R5 day 10	5.036			5.036	4.875
R6 day 10	5.022			5.022	4.826
R4 day 14	4.981			4.981	4.772
R5 day 14	5.065			5.065	4.838
R6 day 14	5.079			5.079	4.802
R4 day 17	5.059			5.059	4.801
R5 day 17	5.063			5.063	4.788
R6 day 17	5.099			5.099	4.761
R4 day 21	5.072			5.072	4.752
R5 day 21	5.142			5.142	4.797
R6 day 21	5.163			5.163	4.740

MEA 30wt% (*aq.*), without FeSO₄				
	Titration	CO₂-conc.	α	CO₂-free conc.	Water loss corr.
Day	[mol$_{alkalinity}$/kg]	[g/kg]	[mol$_{CO2}$/mol$_{alkalinity}$]	[mol$_{alkalinity}$/kg]	[mol$_{alkalinity}$/kg]
0	4.538	83.16	0.42	4.916	4.916
R2 day 3	4.544	87.84	0.44	4.943	4.901
R3 day 3	4.503	90.35	0.46	4.910	4.867
R2 day 7	4.531	82.03	0.41	4.902	4.802
R3 day 7	4.516	81.61	0.41	4.884	4.784
R2 day 10	4.576			4.952	4.810
R3 day 10	4.562			4.939	4.796
R2 day 14	4.566	82.17	0.41	4.941	4.741
R3 day 14	4.573	82.56	0.41	4.951	4.751
R2 day 17	4.599			4.974	4.732
R3 day 17	4.587			4.969	4.727
R2 day 21	4.540	83.70	0.42	4.920	4.621
R3 day 21	4.582	83.29	0.41	4.964	4.664

MMEA 30wt% (*aq.*), condenser temperature 5 °C				
	Titration	CO₂-conc.	α	CO₂-free conc.	Water loss corr.
Day	[mol$_{alkalinity}$/kg]	[g/kg]	[mol$_{CO2}$/mol$_{alkalinity}$]	[mol$_{alkalinity}$/kg]	[mol$_{alkalinity}$/kg]
R1 day 0	3.716	70.93	0.43	3.980	3.980
R2 day 0	3.706	70.45	0.43	3.968	3.968
R3 day 0	3.705	69.61	0.43	3.963	3.963
R1 day 3	3.606	66.81	0.42	3.606	3.634
R2 day 3	3.658	67.61	0.42	3.658	3.683
R3 day 3	3.590	67.33	0.43	3.590	3.612
R1 day 7	3.236	58.68	0.41	3.236	3.295
R2 day 7	3.252	59.31	0.41	3.252	3.302
R3 day 7	3.198	57.72	0.41	3.198	3.243
R1 day 10	2.975	52.07	0.40	2.975	3.052
R2 day 10	2.979	53.97	0.41	2.979	3.044
R3 day 10	2.912	51.60	0.40	2.912	2.970
R1 day 14	2.672	46.52	0.40	2.672	2.769
R2 day 14	2.672	46.46	0.40	2.672	2.754
R3 day 14	2.574	45.42	0.40	2.574	2.646
R1 day 17	2.478	42.94	0.39	2.478	2.588
R2 day 17	2.468	42.96	0.40	2.468	2.560
R3 day 17	2.375	41.39	0.40	2.375	2.456
R1 day 21	2.256	39.65	0.40	2.256	2.379
R2 day 21	2.264	40.19	0.40	2.264	2.368
R3 day 21	2.159	38.88	0.41	2.159	2.250

MMEA 30wt% (*aq.*), condenser temperature 17 °C				
	Titration	CO₂-conc.	α	CO₂-free conc.	Water loss corr.
Day	[mol$_{alkalinity}$/kg]	[g/kg]	[mol$_{CO2}$/mol$_{alkalinity}$]	[mol$_{alkalinity}$/kg]	[mol$_{alkalinity}$/kg]
0	3.643	67.57	0.42	3.980	3.889
R1 day 3	3.355			3.558	3.605
R2 day 3	3.359			3.564	3.596
R3 day 3	3.303			3.500	3.535
R1 day 7	2.973	53.36	0.41	3.236	3.227
R2 day 7	3.000	54.22	0.41	3.252	3.230
R3 day 7	2.909	52.23	0.41	3.198	3.130
R1 day 10	2.721			2.850	2.974

Day	Titration [mol_alkalinity/kg]	CO₂-conc. [g/kg]	α [mol_CO2/mol_alkalinity]	CO₂-free conc. [mol_alkalinity/kg]	Water loss corr. [mol_alkalinity/kg]
R2 day 10	2.774			2.910	2.999
R3 day 10	2.641			2.763	2.853
R1 day 14	2.482	41.85	0.38	2.672	2.742
R2 day 14	2.529	43.50	0.39	2.672	2.752
R3 day 14	2.376	40.06	0.38	2.574	2.583
R1 day 17	2.322			2.411	2.589
R2 day 17	2.355			2.448	2.575
R3 day 17	2.219			2.300	2.427
R1 day 21	2.146	35.05	0.37	2.256	2.423
R2 day 21	2.170	35.76	0.37	2.264	2.392
R3 day 21	2.050	33.14	0.37	2.159	2.262

DMMEA 30wt% (*aq.*) 2% CO₂					
Day	Titration [mol_alkalinity/kg]	CO₂-conc. [g/kg]	α [mol_CO2/mol_alkalinity]	CO₂-free conc. [mol_alkalinity/kg]	Water loss corr. [mol_alkalinity/kg]
0	3.161	59.07	0.42	3.348	3.348
R1 day 3	3.208	22.49	0.16	3.280	3.328
R2 day 3	3.210	24.61	0.17	3.289	3.328
R3 day 3	3.199	23.03	0.16	3.273	3.319
R1 day 7	3.119	20.89	0.15	3.184	3.293
R2 day 7	3.123	21.52	0.16	3.190	3.279
R3 day 7	3.109	20.98	0.15	3.175	3.280
R1 day 10	3.072	20.96	0.16	3.137	3.290
R2 day 10	3.103	21.20	0.16	3.169	3.294
R3 day 10	3.058	20.96	0.16	3.123	3.271
R1 day 14	3.000	20.25	0.15	3.060	3.270
R2 day 14	3.024	21.11	0.16	3.088	3.260
R3 day 14	3.009	20.66	0.16	3.071	3.275
R1 day 17	2.943	20.43	0.16	3.003	3.252
R2 day 17	2.969	21.20	0.16	3.032	3.236
R3 day 17	2.931	20.50	0.16	2.991	3.232
R1 day 21	2.860	20.23	0.16	2.918	3.217
R2 day 21	2.913	20.90	0.16	2.974	3.222
R3 day 21	2.851	20.22	0.16	2.909	3.199

DMMEA 30wt% (*aq.*) 16.5% CO₂					
Day	Titration [mol_alkalinity/kg]	CO₂-conc. [g/kg]	α [mol_CO2/mol_alkalinity]	CO₂-free conc. [mol_alkalinity/kg]	Water loss corr. [mol_alkalinity/kg]
0	3.116	49.16	0.36	3.269	3.269
R4 day 3	3.078	100.66	0.74	3.388	3.340
R5 day 3	3.126	80.04	0.58	3.376	3.324
R4 day 7	3.115	100.94	0.74	3.430	3.317
R5 day 7	3.067	97.62	0.72	3.366	3.244
R4 day 10	3.143	102.66	0.74	3.465	3.303
R5 day 10	3.104	99.78	0.73	3.414	3.236
R4 day 14	3.153	102.80	0.74	3.478	3.249
R5 day 14	3.149	97.76	0.71	3.457	3.206
R4 day 17	3.185	100.96	0.72	3.507	3.226
R5 day 17	3.164	97.93	0.70	3.473	3.166
R4 day 21	3.231	101.64	0.71	3.559	3.208
R5 day 21	3.215	98.79	0.70	3.533	3.147

DGA 30wt% (*aq.*)					
	Titration	CO_2-conc.	α	CO_2-free conc.	Water loss corr.
Day	[$mol_{alkalinity}$/kg]	[g/kg]	[mol_{CO2}/$mol_{alkalinity}$]	[$mol_{alkalinity}$/kg]	[$mol_{alkalinity}$/kg]
0	2.698	52.91	0.45	2.841	2.840
R1 day 3	2.620	45.60	0.40	2.740	2.772
R2 day 3	2.656	46.70	0.40	2.780	2.807
R3 day 3	2.649	46.29	0.40	2.772	2.806
R1 day 7	2.485	42.73	0.39	2.591	2.649
R2 day 7	2.515	43.71	0.39	2.625	2.678
R3 day 7	2.529	43.43	0.39	2.639	2.705
R1 day 10	2.355			2.355	2.431
R2 day 10	2.427			2.528	2.601
R3 day 10	2.420			2.519	2.610
R1 day 14	2.186	37.64	0.39	2.269	2.370
R2 day 14	2.275	39.03	0.39	2.363	2.459
R3 day 14	2.296	38.78	0.38	2.385	2.505
R1 day 17	2.087			2.162	2.279
R2 day 17	2.177			2.257	2.368
R3 day 17	2.171			2.171	2.304
R1 day 21	2.003	33.67	0.38	2.070	2.209
R2 day 21	2.092	34.81	0.38	2.165	2.296
R3 day 21	2.098	34.87	0.38	2.171	2.335

AP 30wt% (*aq.*)					
	Titration	CO_2-conc.	α	CO_2-free conc.	Water loss corr.
Day	[$mol_{alkalinity}$/kg]	[g/kg]	[mol_{CO2}/$mol_{alkalinity}$]	[$mol_{alkalinity}$/kg]	[$mol_{alkalinity}$/kg]
0	3.755	71.63	0.43	4.024	4.024
R1 day 3	3.683	78.61	0.49	3.972	3.972
R2 day 3	3.700	78.07	0.48	3.988	3.988
R1 day 7	3.619	82.91	0.52	3.920	3.918
R2 day 7	3.600	76.08	0.48	3.874	3.872
R1 day 10	3.601	73.91	0.47	3.868	3.865
R2 day 10	3.577	74.42	0.47	3.843	3.840
R1 day 14	3.515	72.86	0.47	3.771	3.767
R2 day 14	3.550	73.60	0.47	3.811	3.807
R1 day 17	3.466	73.84	0.48	3.722	3.718
R2 day 17	3.501	73.75	0.48	3.759	3.755
R1 day 21	3.414	71.27	0.47	3.657	3.652
R2 day 21	3.452	71.98	0.47	3.700	3.695

DEEA 30wt% (*aq.*) 16.5% CO_2					
	Titration	CO_2-conc.	α	CO_2-free conc.	Water loss corr.
Day	[$mol_{alkalinity}$/kg]	[g/kg]	[mol_{CO2}/$mol_{alkalinity}$]	[$mol_{alkalinity}$/kg]	[$mol_{alkalinity}$/kg]
R1 day 0	1.826	58.53	0.73	1.933	1.933
R2 day 0	2.378	46.24	0.44	2.488	2.488
R1 day 3	1.856	57.92	0.71	1.964	1.951
R2 day 3	2.374			2.534	2.512
R1 day 7	1.891	58.39	0.70	2.001	1.971
R2 day 7	2.373	67.36	0.64	2.533	2.482
R1 day 10	1.874	58.73	0.71	1.984	1.940
R2 day 10	2.386			2.547	2.473
R1 day 14	1.894	58.54	0.70	2.005	1.943
R2 day 14	2.405	67.81	0.64	2.568	2.462

	Titration [mol_alkalinity/kg]	CO$_2$-conc. [g/kg]	α [mol_CO2/mol_alkalinity]	CO$_2$-free conc. [mol_alkalinity/kg]	Water loss corr. [mol_alkalinity/kg]
R1 day 17	1.916	58.77	0.70	2.029	1.953
R2 day 17	2.374			2.535	2.410
R1 day 21	1.914	58.87	0.70	2.026	1.933
R2 day 21	2.410	46.24	0.44	2.522	2.417

DEEA 30wt% (*aq.*) 3.5% CO$_2$					
	Titration	CO$_2$-conc.	α	CO$_2$-free conc.	Water loss corr.
Day	[mol_alkalinity/kg]	[g/kg]	[mol_CO2/mol_alkalinity]	[mol_alkalinity/kg]	[mol_alkalinity/kg]
0	1.914	45.12	0.54	2.000	2.000
R1 day 3	1.929	35.25	0.42	1.997	1.981
R2 day 3	1.917	35.19	0.42	1.984	1.971
R1 day 7	1.922	34.57	0.41	1.988	1.952
R2 day 7	1.929	34.97	0.41	1.996	1.967
R1 day 10	1.938	34.07	0.40	2.004	1.952
R2 day 10	1.935	34.54	0.41	2.002	1.960
R1 day 14	1.936	32.81	0.39	2.000	1.927
R2 day 14	1.939	33.38	0.39	2.004	1.945
R1 day 17	1.965	32.96	0.38	2.030	1.940
R2 day 17	1.942	33.17	0.39	2.006	1.935
R1 day 21	1.954	35.47	0.41	2.023	1.913
R2 day 21	1.943	35.41	0.41	2.012	1.923

DMPA 30wt% (*aq.*) 3.5% CO2					
	Titration	CO$_2$-conc.	α	CO$_2$-free conc.	Water loss corr.
Day	[mol_alkalinity/kg]	[g/kg]	[mol_CO2/mol_alkalinity]	[mol_alkalinity/kg]	[mol_alkalinity/kg]
0	2.648	80.09	0.69	2.860	2.860
R1 day 3	2.794			2.880	2.854
R3 day 3	2.812	28.89	0.23	2.893	2.873
R1 day 7	2.834			2.916	2.855
R3 day 7	2.787	28.89	0.24	2.867	2.807
R1 day 10	2.843			2.923	2.835
R3 day 10	2.791	28.06	0.23	2.869	2.783
R1 day 14	2.846			2.921	2.798
R3 day 14	2.811	26.56	0.21	2.885	2.764
R1 day 17	2.857			2.933	2.783
R3 day 17	2.824	26.58	0.21	2.899	2.752
R1 day 21	2.850			2.930	2.746
R3 day 21	2.794	28.29	0.23	2.873	2.692

DMPA 30wt% (*aq.*) 16.5% CO$_2$					
	Titration	CO$_2$-conc.	α	CO$_2$-free conc.	Water loss corr.
Day	[mol_alkalinity/kg]	[g/kg]	[mol_CO2/mol_alkalinity]	[mol_alkalinity/kg]	[mol_alkalinity/kg]
0	2.711	85.11	0.71	2.941	2.941
R3 day 3	2.699	62.83	0.53	2.869	2.847
R3 day 7	2.588	63.22	0.56	2.751	2.703
R3 day 10	2.718	63.47	0.53	2.890	2.818
R3 day 14	2.729	63.02	0.52	2.901	2.799
R3 day 17	2.753	62.20	0.51	2.925	2.800
R3 day 21	2.768	61.92	0.51	2.939	2.785

TEA 30wt% (*aq.*) 3.5% CO$_2$					
	Titration	CO$_2$-conc.	α	CO$_2$-free conc.	Water loss corr.
Day	[mol_alkalinity/kg]	[g/kg]	[mol_CO2/mol_alkalinity]	[mol_alkalinity/kg]	[mol_alkalinity/kg]
0	1.959	42.23	0.49	2.041	2.042
R2 day 3	2.032	3.70	0.04	2.039	2.022

	Titration				
R3 day 3	2.041			2.049	2.031
R2 day 7	2.037	5.88	0.07	2.049	2.008
R3 day 7	2.053	5.84	0.06	2.065	2.023
R2 day 10	2.044	3.75	0.04	2.052	1.992
R3 day 10	2.051			2.058	1.999
R2 day 14	2.066	3.59	0.04	2.073	1.989
R3 day 14	2.092	3.28	0.04	2.098	2.014
R2 day 17	2.056	3.69	0.04	2.063	1.962
R3 day 17	2.098			2.106	2.002
R2 day 21	2.092	3.42	0.04	2.099	1.971
R3 day 21	2.099	3.63	0.04	2.107	1.978

	TEA 30wt% (*aq.*) 16.5% CO_2				
	Titration	CO_2-conc.	α	CO_2-free conc.	Water loss corr.
Day	[mol$_{alkalinity}$/kg]	[g/kg]	[mol$_{CO2}$/mol$_{alkalinity}$]	[mol$_{alkalinity}$/kg]	[mol$_{alkalinity}$/kg]
0	1.938	32.06	0.38	2.000	2.000
R5 day 3	2.009	23.01	0.26	2.055	2.021
R6 day 3	2.015	24.91	0.28	2.065	2.031
R5 day 7	2.033	23.76	0.27	2.081	2.001
R6 day 7	2.044	24.90	0.28	2.094	2.015
R5 day 10	2.056	24.14	0.27	2.106	1.992
R6 day 10	2.063	24.89	0.27	2.114	2.000
R5 day 14	2.087	23.79	0.26	2.136	1.977
R6 day 14	2.073	24.88	0.27	2.124	1.965
R5 day 17	2.113	24.34	0.26	2.164	1.971
R6 day 17	2.089	25.69	0.28	2.143	1.949
R5 day 21	2.151	24.54	0.26	2.204	1.965
R6 day 21	2.114	25.53	0.27	2.167	1.928

	MDEA 30wt% (*aq.*) 16.5% CO_2				
	Titration	CO_2-conc.	α	CO_2-free conc.	Water loss corr.
Day	[mol$_{alkalinity}$/kg]	[g/kg]	[mol$_{CO2}$/mol$_{alkalinity}$]	[mol$_{alkalinity}$/kg]	[mol$_{alkalinity}$/kg]
R6 day 0	2.414	43.74	0.41	2.519	2.519
R4 day 0	2.414	37.00	0.35	2.503	2.503
R6 day 3	2.416	59.66	0.56	2.560	2.515
R4 day 3	2.401	61.64	0.58	2.549	2.524
R6 day 7	2.482	59.86	0.55	2.630	2.525
R4 day 7	2.427	60.55	0.57	2.574	2.516
R6 day 10	2.492	61.04	0.56	2.644	2.493
R4 day 10	2.439	60.70	0.57	2.587	2.504
R6 day 14	2.525	61.61	0.55	2.681	2.469
R4 day 14	2.460	61.59	0.57	2.612	2.496
R6 day 17	2.545	60.18	0.54	7.176	2.441
R4 day 17	2.477	62.18	0.57	7.027	2.491
R6 day 21	2.594	61.58	0.54	2.754	2.437
R4 day 21	2.501	62.12	0.56	2.657	2.483

	MDEA 30wt% (*aq.*) 2% CO_2				
	Titration	CO_2-conc.	α	CO_2-free conc.	Water loss corr.
Day	[mol$_{alkalinity}$/kg]	[g/kg]	[mol$_{CO2}$/mol$_{alkalinity}$]	[mol$_{alkalinity}$/kg]	[mol$_{alkalinity}$/kg]
0	2.374	42.94	0.41	2.476	2.476
R4 day 3	2.485	16.01	0.15	2.525	2.503
R5 day 3	2.481			2.519	2.494
R4 day 7	2.484	15.98	0.15	2.524	2.473

Day	Titration [mol_alkalinity/kg]	CO2-conc. [g/kg]	α [mol_CO2/mol_alkalinity]	CO2-free conc. [mol_alkalinity/kg]	Water loss corr. [mol_alkalinity/kg]
R5 day 7	2.455	15.10	0.14	2.492	2.435
R4 day 10	2.499	16.06	0.15	2.539	2.467
R5 day 10	2.497			2.535	2.453
R4 day 14	2.488	16.05	0.15	2.528	2.427
R5 day 14	2.502	15.19	0.14	2.540	2.426
R4 day 17	2.523			2.563	2.441
R5 day 17	2.518			2.555	2.416
R4 day 21	2.512	15.54	0.14	2.551	2.400
R5 day 21	2.540	14.49	0.13	2.577	2.406

PZ 30wt% (*aq.*)					
Day	Titration [mol_alkalinity/kg]	CO2-conc. [g/kg]	α [mol_CO2/mol_alkalinity]	CO2-free conc. [mol_alkalinity/kg]	Water loss corr. [mol_alkalinity/kg]
0	6.550	71.38	0.25	7.018	7.018
R1 day 3	6.482	87.01	0.31	7.046	7.017
R6 day 3	6.301	107.34	0.39	6.977	6.954
R1 day 7	6.459	91.08	0.32	7.047	6.979
R6 day 7	6.326	107.45	0.39	7.006	6.952
R1 day 10	6.454	92.16	0.32	7.049	6.950
R6 day 10	6.374	108.11	0.39	7.063	6.986
R1 day 14	6.518	92.66	0.32	7.122	6.985
R6 day 14	6.396	109.29	0.39	7.095	6.987
R1 day 17	6.584			7.176	7.009
R6 day 17	6.354			7.027	6.896
R1 day 21	6.563	87.09	0.30	7.135	6.928
R6 day 21	6.503	102.39	0.36	7.168	7.006

EAE 30wt% (*aq.*)					
Day	Titration [mol_alkalinity/kg]	CO2-conc. [g/kg]	α [mol_CO2/mol_alkalinity]	CO2-free conc. [mol_alkalinity/kg]	Water loss corr. [mol_alkalinity/kg]
0	3.227	62.34	0.44	3.428	3.428
R1 day 3	3.045	55.24	0.41	3.213	3.194
R2 day 3	3.026	55.95	0.42	3.195	3.176
R1 day 7	2.911	51.18	0.40	3.060	3.014
R2 day 7	2.869	50.60	0.40	3.014	2.968
R1 day 10	2.735	48.90	0.41	2.869	2.804
R2 day 10	2.720	48.02	0.40	2.851	2.785
R1 day 14	2.580	45.31	0.40	2.697	2.606
R2 day 14	2.516	44.59	0.40	2.628	2.537
R1 day 17	2.428			2.528	2.4172
R2 day 17	2.353			2.447	2.3366
R1 day 21	2.204	36.66	0.38	2.284	2.148
R2 day 21	2.127	35.44	0.38	2.202	2.065

MAPA 30wt% (*aq.*)					
Day	Titration [mol_alkalinity/kg]	CO2-conc. [g/kg]	α [mol_CO2/mol_alkalinity]	CO2-free conc. [mol_alkalinity/kg]	Water loss corr. [mol_alkalinity/kg]
0	6.392	60.79	0.22	6.781	6.781
R1 day 3	5.803	91.82	0.36	6.336	6.295
R2 day 3	5.943	84.72	0.32	6.447	6.394
R1 day 7	5.465	107.90	0.45	6.055	5.960
R2 day 7	5.518	108.40	0.45	6.116	5.992
R1 day 10	5.220	104.13	0.45	5.763	5.628
R2 day 10	5.405	108.49	0.46	5.991	5.815

Day	Titration [mol_alkalinity/kg]	CO₂-conc. [g/kg]	α [mol_CO2/mol_alkalinity]	CO₂-free conc. [mol_alkalinity/kg]	Water loss corr. [mol_alkalinity/kg]
R1 day 14	4.954	97.40	0.45	5.436	5.246
R2 day 14	5.225	104.45	0.45	5.771	5.524
R1 day 17	4.767	91.66	0.44	5.203	4.822
R2 day 17	5.092	100.00	0.45	5.601	5.098
R1 day 21	4.422	84.11	0.43	4.794	4.403
R2 day 21	4.901	96.11	0.45	5.372	4.825

AMP 30wt% (*aq.*)					
	Titration	CO₂-conc.	α	CO₂-free conc.	Water loss corr.
Day	[mol$_{alkalinity}$/kg]	[g/kg]	[mol$_{CO2}$/mol$_{alkalinity}$]	[mol$_{alkalinity}$/kg]	[mol$_{alkalinity}$/kg]
R3(1) day 0	3.142	61.60	0.45	3.335	3.335
R3(2) day 0	3.142	58.87	0.43	3.327	3.327
R3(1) day 3	3.250	32.85	0.23	3.356	3.328
R3(2) day 3	3.257	35.14	0.25	3.371	3.334
R3(1) day 7	3.300	31.63	0.22	3.405	3.339
R3(2) day 7	3.270	33.41	0.23	3.379	3.293
R3(1) day 10	3.298	31.64	0.22	3.402	3.309
R3(2) day 10	3.275	33.55	0.23	3.385	3.261
R3(1) day 14	3.323	32.27	0.22	3.430	3.299
R3(2) day 14	3.276	35.50	0.25	3.393	3.220
R3(1) day 17	3.347	31.91	0.22	3.454	3.295
R3(2) day 17	3.285	35.01	0.24	3.400	3.191
R3(1) day 21	3.363	32.01	0.22	3.471	3.275
R3(2) day 21	3.309	35.83	0.25	3.427	3.169

MIPA 30wt% (*aq.*)					
	Titration	CO₂-conc.	α	CO₂-free conc.	Water loss corr.
Day	[mol$_{alkalinity}$/kg]	[g/kg]	[mol$_{CO2}$/mol$_{alkalinity}$]	[mol$_{alkalinity}$/kg]	[mol$_{alkalinity}$/kg]
0	3.950	76.97	0.44	4.254	4.254
R1 day 3	3.743	70.07	0.43	4.005	3.977
R2 day 3	3.812	71.38	0.43	4.084	4.056
R1 day 7	3.437	62.15	0.41	3.650	3.585
R2 day 7	3.594	66.17	0.42	3.831	3.766
R1 day 10	3.236	57.26	0.40	3.421	3.327
R2 day 10	3.476	63.29	0.41	3.696	3.602
R1 day 14	2.923	50.82	0.40	3.072	2.941
R2 day 14	3.227	57.87	0.41	3.414	3.283
R1 day 17	2.715	48.07	0.40	2.846	2.687
R2 day 17	3.096	55.32	0.41	3.268	3.109
R1 day 21	2.456	42.34	0.39	2.560	2.364
R2 day 21	2.919	52.75	0.41	3.073	2.877

AEP 30wt% (*aq.*)					
	Titration	CO₂-conc.	α	CO₂-free conc.	Water loss corr.
Day	[mol$_{alkalinity}$/kg]	[g/kg]	[mol$_{CO2}$/mol$_{alkalinity}$]	[mol$_{alkalinity}$/kg]	[mol$_{alkalinity}$/kg]
0	4.485	48.06	0.24	4.701	4.701
R1 day 3	4.485	77.60	0.39	4.833	4.571
R2 day 3	4.485	75.57	0.38	4.824	4.635
R1 day 7	4.255	84.86	0.45	4.616	4.577
R2 day 7	4.269	84.99	0.45	4.632	4.613
R1 day 10	4.288	86.20	0.46	4.657	4.601
R2 day 10	4.283	85.38	0.45	4.649	4.621
R1 day 14	4.290	85.44	0.45	4.657	4.578
R2 day 14	4.304	86.29	0.46	4.676	4.636

Day	Titration [mol_alkalinity/kg]	CO_2-conc. [g/kg]	α [mol_CO2/mol_alkalinity]	CO_2-free conc. [mol_alkalinity/kg]	Water loss corr. [mol_alkalinity/kg]
R1 day 17	4.329	85.44	0.45	4.698	4.603
R2 day 17	4.307	86.18	0.45	4.678	4.630
R1 day 21	4.302	85.56	0.45	4.670	4.552
R2 day 21	4.360	86.57	0.45	4.737	4.678

1-(2HE)PP 30wt% (*aq.*)					
	Titration	CO_2-conc.	α	CO_2-free conc.	Water loss corr.
Day	[mol_alkalinity/kg]	[g/kg]	[mol_CO2/mol_alkalinity]	[mol_alkalinity/kg]	[mol_alkalinity/kg]
0	2.168	59.00	0.62	2.296	2.296
R4 day 3	2.135	83.42	0.89	2.313	2.286
R5 day 3	2.157	86.28	0.91	2.343	2.300
R4 day 7	2.164	85.55	0.90	2.349	2.285
R5 day 7	2.179	85.02	0.89	2.364	2.279
R4 day 10	2.160	85.02	0.89	2.344	2.253
R5 day 10	2.190	86.96	0.90	2.381	2.253
R4 day 14	2.197	86.24	0.89	2.387	2.256
R5 day 14	2.226	86.97	0.89	2.420	2.242
R4 day 17	2.211	86.95	0.89	2.403	2.244
R5 day 17	2.246	87.32	0.88	2.443	2.226
R4 day 21	2.229	87.61	0.89	2.425	2.226
R5 day 21	2.258	89.82	0.90	2.460	2.187

DMAPA 30wt% (*aq.*)					
	Titration	CO_2-conc.	α	CO_2-free conc.	Water loss corr.
Day	[mol_alkalinity/kg]	[g/kg]	[mol_CO2/mol_alkalinity]	[mol_alkalinity/kg]	[mol_alkalinity/kg]
0	5.589	54.29	0.22	5.893	5.893
R1 day 3	5.425	85.83	0.36	5.891	5.861
R2 day 3	5.418	83.56	0.35	5.871	5.836
R1 day 7	5.381	97.58	0.41	5.906	5.836
R2 day 7	5.416	98.36	0.41	5.949	5.866
R1 day 10	5.416	98.49	0.41	5.949	5.848
R2 day 10	5.438	99.76	0.42	5.980	5.860
R1 day 14	5.365	97.92	0.41	5.891	5.750
R2 day 14	5.467	100.90	0.42	6.019	5.850
R1 day 17	5.416	98.38	0.41	5.948	5.776
R2 day 17	5.501	100.18	0.41	6.052	5.846
R1 day 21	5.433	98.21	0.41	5.967	5.754
R2 day 21	5.523	100.22	0.41	6.077	5.821

1DMA2P 30wt% (*aq.*), 8% CO_2					
	Titration	CO_2-conc.	α	CO_2-free conc.	Water loss corr.
Day	[mol_alkalinity/kg]	[g/kg]	[mol_CO2/mol_alkalinity]	[mol_alkalinity/kg]	[mol_alkalinity/kg]
0	2.710	54.40	0.46	2.858	2.858
R4 day 3	2.595	58.47	0.51	2.746	2.709
R5 day 3	2.560			2.702	2.662
R4 day 7	2.481	57.00	0.52	2.620	2.540
R5 day 7	2.411	56.60	0.53	2.576	2.460
R4 day 10	2.376	56.06	0.54	2.511	2.396
R5 day 10	2.300			2.441	2.321
R4 day 14	2.281	68.74	0.68	2.384	2.284
R5 day 14	2.192	65.72	0.68	2.192	2.175
R4 day 17	2.225	56.91	0.58	2.225	2.172
R5 day 17	2.131	55.36	0.59	2.131	2.062
R4 day 21	2.141	51.99	0.55	2.141	2.040

R5 day 21	2.033	45.00	0.50	2.125	1.906

Table S4: Summary of results from different analytical methods, quantifying the amine loss and heat stable salt (HSS) accumulation after 21 days under oxidative conditions. Uncertainty given as standard error within parallel experiments. LC-MS analysis was only performed for one experiment each.

Amine	Amine titration	IC	LC-MS	HSS [mol kg^{-1}]
AEP	0 ± 1%		-	0.03 ± 0.01
AMP	3 ± 2%		-	0.00 ± 0.001
AP	9 ± 1%	8 ± 4%	-	0.06 ± 0.01
DEEA	4 ± 0.4%	5%	-	0.01 ± 0.002
DMAPA	2 ± 1%		-	0.01 ± 0.0001
DMMEA	4 ± 0.4%	9 ± 8%	-	0.02 ± 0.001
DGA	20 ± 2%	19 ± 8%	-	0.11 ± 0.02
DMPA	5 ± 1%	8 ± 3%	17%	0.01 ± 0.002
EAE	39 ± 2%	35 ± 5%	-	0.20 ± 0.02
1-(2HE)PP	4 ± 1%		-	0.00 ± 0.002
MAPA	32 ± 4%	41 ± 8%	41%	0.05 ± 0.01
MDEA	2 ± 1%		-	0.01 ± 0.003
MEA	53 ± 6%	52 ± 5%	46%	0.33 ± 0.002
MIPA	38 ± 9%		-	0.12 ± 0.02
MMEA	41 ± 2%	37 ± 2%	37%	0.13 ± 0.1
PZ	1 ± 1%		-	0.00 ± 0.001
TEA	4 ± 1%		-	0.01 ± 0.001

Table S5: Amine loss in oxidative and thermal degradability studies

Amine	Oxidative degradation		Davis 2009		Eide-Haugmo 2011	
	Amine loss	$(c_{lost})/(c_{lost,MEA})$	Amine loss	$(c_{lost})/(c_{lost,MEA})$	Amine loss	$(c_{lost})/(c_{lost,MMEA})$
MEA	53 %	1.00	37 %	1.00	56 %	0.58
MMEA	41 %	0.77	-	-	96 %	1.00
DMMEA	4 %	0.08	-	-	29 %	0.30
MAPA	32 %	0.60	-	-	50 %	0.52
DEEA	4 %	0.08	-	-	14 %	0.15
MDEA	2 %	0.04	37 %	1.00	37 %	0.39
DMAPA	2 %	0.04	-	-	60 %	0.63
DGA	20 %	0.38	7 %	0.19	6 %	0.07
AP	9 %	0.17	13 %	0.35	21 %	0.22
TEA	4 %	0.08	-	-	10 %	0.10
PZ	1 %	0.02	0 %	0.00	-	-
AMP	3 %	0.06	9 %	0.24	5 %	0.05
MIPA	38 %	0.72	-	-	19 %	0.20
AEP	0 %	0.00	37 %	1.00	-	-

Table S6: Measured concentrations of organic acids by anion IC. Concentrations in red are below the quantification limit and have therefore not been included.

Amine	Reactor	ID	m_{sample} [g]	m_{water} [g]	$C_{formate,dil}$ (ppm)	$C_{form,orig}$ (ppm)	$C_{acetate,dil}$ (ppm)	$C_{ac,orig}$ (ppm)	$C_{oxalate,dil}$ (ppm)	$C_{ox,orig}$ (ppm)
AEP	Mix	AEP1	0.05933	7.29656	1.68	209	-	-	-0.04	-4
AMP	Mix	AMP1	0.06242	7.13435	-0.19	-22	0.01	2	-0.16	-19
AP	R1	AP3	0.04544	5.93319	6.50	855	-	-	0.36	47
	R2	AP4	0.06732	6.11475	8.07	741	-	-	0.31	28
DEEA	Mix	DEEA1	0.06269	6.58165	-0.10	-11	-0.02	-2	-0.13	-14
DGA/ 2-2-AEE	R1	DGA1	0.02155	6.00323	12.94	3618	0.24	66	0.56	157
	R2	DGA2	0.02082	6.17566	9.88	2940	0.15	43	0.45	135
	R3	DGA3	0.02084	6.15724	8.28	2453	-	-	0.40	119
DMAPA	Mix	DMAPA1	0.06338	6.67958	-0.08	-9	0.00	0	-0.20	-21
1DMA2P	R4	1DMA2P1	0.05800	6.37481	1.92	212	0.33	37	0.33	37
	R5	1DMA2P2	0.05827	6.43518	1.82	203	0.33	37	0.28	31
DMMEA	Mix	DMMEA1	0.06208	6.46168	6.46	679	0.01	1	0.23	24
DMPA	R3	DMPA2	0.06657	6.17192	-	-	0.12	12	0.29	27
DMPA	Mix	DMPA3	0.06469	6.46978	2.56	267	0.23	24	0.12	13
EAE	R2	EAE1	0.02155	6.45277	9.75	2930	1.83	550	4.67	1403
	R3	EAE2	0.02061	6.73907	10.21	3348	1.88	617	4.90	1607
1-(2HE)PP	Mix	HEPP1	0.05901	6.44074	-0.02	-2	-0.06	-6	-0.18	-20
MAPA	R1	MAPA1	0.06058	6.20262	12.70	1313	1.49	154	0.33	34
	R2	MAPA2	0.06106	6.28508	8.08	840	-	-	0.13	13
MDEA	R4	MDEA1	0.06410	6.92249	1.10	120	-0.03	-4	-0.08	-9
MEA	Mix	MEA1	0.02108	6.35388	23.96	7245	0.65	196	3.58	1084
	Mix	MEA1	0.02108	6.35388	24.13	7298	0.68	206	3.37	1020
	R2	MEA2	0.02147	6.72174	20.15	6330	0.73	228	3.00	944
	R3	MEA3	0.02130	6.55473	17.60	5434	0.79	243	2.45	758
MIPA	Mix	MIPA1	0.02107	6.27327	7.09	2118	4.22	1262	0.60	179
MMEA	R1	MMEA1	0.02103	6.55799	10.44	3265	0.96	299	2.13	665
	R1	MMEA1-2	0.04151	6.47344	20.59	3232	1.96	308	3.92	616
	R2	MMEA2	0.02109	6.12129	11.57	3368	1.07	311	2.37	690
	R3	MMEA3	0.02085	6.28982	11.47	3473	0.95	289	3.27	990
PZ	Mix	PZ1	0.06654	6.60707	0.27	27	0.14	14	-0.20	-20
TEA	Mix	TEA1	0.06528	7.35366	0.07	8	0.06	7	-0.15	-17

Table S7: Dissolved oxygen (DO) concentration in biodegradability tests of amines after given number of days of incubation.

Test substance	Replicate	DO [mg L^{-1}]			
		Day 0	Day 7	Day 14	Day 28
1DMA2P	1	7.26	7.08	6.89	6.67
	2		6.97	6.77	6.59
DMMEA	1	7.27	7.26	4.18	3.67
	2		7.31	4.22	3.61
AEP	1	7.33	7.29	6.97	6.45
	2		7.35	7.00	6.44
1-(2HE)PP	1	7.40	7.29	7.07	6.61
	2		7.27	6.97	6.75
DMAPA	1	7.29	7.20	6.66	3.58
	2		7.27	6.92	3.58
Aniline	1	7.40	6.41	3.39	2.99
	2		6.45	3.29	2.88
Sea water	1	7.40	7.34	7.10	6.79
	2		7.34	7.05	6.81

Table S8: Biological oxygen demand (BOD) in biodegradability tests of amines after given number of days of incubation, calculated from amount of test substance added and DO concentration.

Test substance	Replicate	BOD [mg g^{-1}test substance]					
		Day 0	Day 7	Day 14	Day 28	Inhibition test	Abiotic test
1DMA2P	1	0.07	0.13	0.09	0.06	1.83	-0.03
	2		0.18	0.15	0.10	1.84	-0.05
DMMEA	1	0.06	0.04	1.34	1.45	3.03	-0.05
	2		0.01	1.32	1.48	3.16	-0.02
AEP	1	0.03	0.02	0.05	0.17	1.83	-0.04
	2		0.00	0.04	0.18	1.75	-0.05
1-(2HE)PP	1	0.00	0.02	0.00	0.09	1.85	-0.04
	2		0.03	0.05	0.02	1.70	-0.02
DMAPA	1	0.05	0.07	0.20	1.59	3.17	0.01
	2		0.03	0.08	1.59	3.17	-0.03
Aniline	1	0.00	0.44	1.73	1.79	-	-
	2		0.42	1.78	1.84	-	-

Chapter 7

Addition of potassium iodide reduces oxidative degradation of monoethanolamine (MEA)

This chapter contains the work conducted with stable salts as oxidative degradation inhibitors, in the form of an article published in the online journal Chemical Engineering Science: X. In this work we studied sodium chloride and potassium iodide's impact on a series of properties of aqueous MEA solutions, only to discover a very positive degradation inhibiting effect of potassium iodide under oxidative conditions.

Addition of potassium iodide reduces oxidative degradation of monoethanolamine (MEA)

Vanja Buvik, Ricardo R. Wanderley, Hanna K. Knuutila[*]

Department of Chemical Engineering, Norwegian University of Science and Technology (NTNU), NO-7491 Trondheim, Norway

Abstract

We introduce the addition of stable salts to aqueous MEA as a way of inhibiting oxidative degradation reactions. We performed oxidative degradation studies in aqueous MEA containing sodium chloride (NaCl) and potassium iodide (KI). These "salted amine solvents" have been shortened to SAS. The 2.0 %wt. and 1.0 %wt. KI SAS show remarkable oxidative degradation behaviour. Loss of alkalinity after 42 days of oxidative degradation experiments with the 1.0 %wt. KI SAS was of 4%, whereas that of aqueous MEA was of 40% after only 21 days. We evaluated how the addition of stable salts impacts CO_2 solubility, viscosity, and thermal degradation and corrosion behaviour and verify negligible deviations from aqueous MEA. Thus, addition of stable salts affects oxidative degradation phenomena without deranging CO_2 solubility or mass transfer rates. With the promising inhibition behaviour of KI on MEA degradation, this work presents the initial steps towards making it a commercially viable degradation inhibitor.

Keywords

CO_2 absorption, amine solvents, solvent stability, inhibitors, degradation inhibition

---

[*] Corresponding author. Tel.: +47 73594119
E-mail address: hanna.knuutila@ntnu.no

1 Introduction

The use of aqueous amine solvents for CO_2 absorption is the state-of-the-art technology for post-combustion CO_2 capture (Rochelle, 2016). Amine scrubbing is at the forefront of greenhouse gas control techniques for climate change mitigation. However, this is still a very capital-intensive process, and cutting costs is an essential step for large scale deployment(Bui et al., 2018). The expenses associated with amine degradation have been estimated as making up close to 10% of the total cost of CO_2 capture via amine scrubbing (Vega et al., 2014). Oxidative degradation is the most significant degradation pathway for amine loss experienced in industrial CO_2 capture applications (Lepaumier et al., 2011) (Vega et al., 2014). Finding a suitable inhibitor for oxidative degradation in aqueous amine solvents is crucial for reducing costs and increasing the feasibility of CO_2 capture technologies.

Degradation is as much an operational as an economic problem, bringing forth operational interruptions, incurring in solvent and plant replacement costs, and increasing emissions, which impacts the environmental footprint of the process. The benchmark solvent for amine-based flue gas scrubbing, monoethanolamine (MEA), is known for its tendency to undergo rapid and uncontrollable oxidative degradation. Experience from pilot campaigns with MEA proves that degradation is often the reason for ending a campaign (Dhingra et al., 2017).

Mechanistically, oxidative degradation is not as well understood as the thermal degradation pathways within the process, and different routes for the formation of a multitude of identifiable degradation compounds have been suggested (Lepaumier et al., 2009; Vevelstad et al., 2011; Vevelstad et al., 2016). It is commonly accepted that the initial step of the oxidative degradation mechanism is a radical reaction, where the amine reacts with dissolved oxygen originating from the flue gas. Such radical reactions are assumed to be catalysed by dissolved metals such as iron and copper, which have proven to increase degradation rates in laboratory scale studies (Blachly and Ravner, 1963; Goff, 2005; Sexton and Rochelle, 2009). In the initial reaction step, volatile ammonia, and organic acids such as formic, acetic, and oxalic acid are formed. These acids can react further with one another or with other amine molecules to create further degradation compounds, and are also known to give rise to corrosion of the construction material (Rooney and DuPart, 2000).

As a means of tackling the issues of degradation and corrosion in CO_2 capture plants, a plethora of degradation inhibitors have been suggested. There are typically three categories of oxidative degradation inhibitors for amine solutions:

Oxygen or peroxide scavengers.

Chelating agents.

Stable salts.

The first approach to finding degradation inhibitors was published in 1964, when Blachly and Ravner tested ethylenediaminetetraacetic acid (EDTA) as a chelating agent for inhibiting the reaction between amine and metals by forming chelate complexes with metal ions. They also successfully proposed bicine as an efficient peroxide scavenger, which proved to be an excellent degradation inhibitor in metal-free solutions (Blachly and Ravner, 1964). Their findings have since been employed for aiding CO_2 separation in nuclear submarines (Blachly and Ravner, 1965, 1966), and EDTA has remained an attractive inhibitor, being thoroughly tested by many researchers (Chi and Rochelle, 2002; Goff and Rochelle, 2006; Lee et al., 2012; Sexton and Rochelle, 2009; Supap et al., 2011). More recently, a number of other chelating agents and oxygen/peroxide scavengers have been assessed in Fytianos et al. (2016).

One big issue with these two categories of inhibitors is that these materials lose effect with time and require replenishing throughout the process. On the other hand, Goff and Rochelle (2006) tested a range of heat stable salts as degradation inhibitors including potassium chloride (KCl), potassium bromide (KBr) and potassium formate ($CHKO_2$) in concentrations between 10 and 1000 mM, observing a small decrease of ammonia formation rate with both KBr and $CHKO_2$. The great advantage of salt addition, compared to scavenging additives, is that these salts simply change the properties of the solvent without getting exhausted with time. As such, their need for replenishing is minimal. Another significant advantage of employing stable salts for reduction of amine degradability is their toxicity when compared to many suggested degradation inhibitors, such as reactive vanadium or copper salts. Halide containing stable salts were already pointed out as inhibitors for the oxidative degradation of organic acids by Lee and Rochelle (1987). Their work proved that iodide (I^-) worked as a powerful scavenger for sulfate (SO_4^{2-}), inhibiting its oxidation of the organic acid ($Cl^- < Br^- < I^-$). A recently published patent also identifies iodide as an effective oxidative degradation inhibitor in the context of organic acids (Sjostrom et al., 2020).

In this study, we have analysed the effects of adding two stable inorganic salts to aqueous monoethanolamine (MEA) solvents. These salts are sodium chloride (NaCl) and potassium iodide (KI). The 30 %wt. MEA (*aq.*) with added salts have been denominated "salted amine solvents", or simply SAS. Their effects have been evaluated in terms of changes in CO_2 solubility both at 40 and 120 °C, shifts in viscosity of loaded and unloaded solvents, and overall effects on oxidative degradation, thermal degradation, and corrosion phenomena in loaded MEA solutions. Our results show that oxidative degradation is inhibited with addition of both salts, and that the salts do not seem to be consumed through the course of our experiments (i.e., their activity in inhibiting amine loss is not lost with time). In the case of potassium iodide, this is achieved without a significant gain in viscosity. Additionally, in neither case is there a significative loss of CO_2 solubility nor an increase in thermal degradation or corrosion phenomena. These results are

encouraging for the use of potassium iodide as an oxidative degradation inhibitor in the context of aqueous amine scrubbing.

2 Materials and methods

2.1 Chemicals

Monoethanolamine (CAS: 141-43-5, purity $\geq$99.0%), ferrous sulfate heptahydrate ($FeSO_4 \cdot 7H_2O$, CAS: 7782-63-0, purity $\geq$ 99.0%) and potassium iodide (KI, CAS: 7681-11-0, purity $\geq$ 99.0%) were purchased from Merck Life Science/Sigma Aldrich Norway, and sodium chloride (NaCl, CAS: 7647-14-5) was purchased at a local grocery store and was of the brand JOZO. Oxygen (O_2, N5.0) and carbon dioxide (CO_2, N5.0) gases were purchased from AGA, and deionized water was obtained from a local water purification system at NTNU.

2.2 Oxidative degradation experiments

2.2.1 Setup 1 (three parallel reactors)

Oxidative degradation experiments were performed at absorber conditions in custom made open, water bath-heated, double-jacketed glass reactors (approximately 250 mL) as shown in Figure 7.1. The reactor temperature was maintained at 60 °C and the water bath-cooled Graham condensers at 5 °C. Each reactor was filled with 200 mL of the gravimetrically prepared solvent mixture, which was pre-loaded to 0.4 mol of CO_2 per mol MEA and contained 0.5 mM iron sulfate ($FeSO_4 \cdot 7H_2O$). A mixture of 98% oxygen (O_2) and 2% carbon dioxide (CO_2) gas was sparged through the solutions at a rate of 60 mL min^{-1} from Alicat mass flow controllers and through Pyrex® glass gas distribution tubes of porosity grade 1, under constant magnetic stirring for the total experimental time of three-six weeks. Empty gas wash bottles were used as safety solvent traps between the mass flow controllers and the gas distribution tubes in case of power outage. Sampling was performed on days 3, 7, 10, 14 and 17 (as well as 21, 28 and 35 for the six-week experiment), through a septum on top of each reactor. Each experiment was performed in two or three parallels, and the data presented in this work is given as the average values, with the standard deviation of the sample average as uncertainty. Experiments were primarily conducted in Setup 1, but validation was done with Setup 2, against published data for MEA stability.
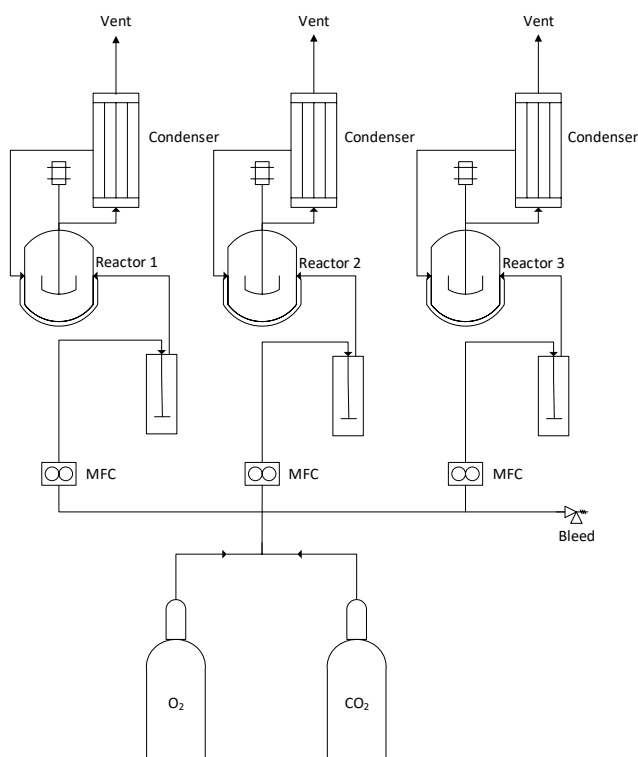
Figure 7.1. Schematic of oxidative degradation Setup 1.

2.2.2 Setup 2 (single reactor)

1 L 30 %wt. MEA (*aq.*) with 2.0 %wt. KI, preloaded with 0.4 mol_{CO2} mol_{MEA}^{-1} and $FeSO_4$ (1 mM), was added to an open batch setup described in Vevelstad et al. (2016). The setup belongs to SINTEF Industry and consists of a double-jacketed, water-bath heated glass reactor, kept at 55 °C, with a double water-cooled Graham condenser, continuous magnetic stirring and sparging with water-saturated gas (98% O_2; 0.350 L min^{-1} and 2% CO_2; 7.5 mL min^{-1}). A recycle gas stream (50 L h^{-1}) is bubbled through the solution for increased mass transfer from gas to liquid phase. This is precisely the same apparatus employed by Vevelstad et al. (2016). The experiment was performed for three weeks with regular sampling and the results were compared to that of 30 %wt MEA without addition of iron as given in Vevelstad et al. (2016).

2.3 Thermal degradation experiments

Thermal degradation experiments were performed in accordance with Eide-Haugmo et al. (2011) in stainless steel 316 cylinders with diameters of 0.5 inch and volumes of approximately 11 mL equipped with Swagelok® end caps. The cylinders were filled with 8 mL of the solution, which was pre-loaded to 0.4 mol_{CO2} mol_{MEA}^{-1} and kept at 135 °C for up to five weeks. Each sampling involved the removal of two metal

235

cylinders per experiment and the analyses of their contents, meaning that the sample taken after three weeks was kept uninterruptedly at 135 °C for three weeks, etc. The cylinders were weighed on a Mettler-Toledo ME204 analytical scale (taring range 0-220 g and readability 0.0001 g) prior to the filling with solution, as well as after the sample was removed, before and after the cylinders were washed with sulfuric acid (H_2SO_4, 0.1 M) to remove iron carbamate ($FeCO_3$) and other corrosion products from the stainless steel surface. The solutions were analysed for amine concentration by titration, and CO_2 loading was verified by TIC procedures and sent for ICP-MS analysis.

2.4 Vapor-liquid equilibrium experiments

A schematic drawing of the VLE apparatus employed in this work is shown in Figure 7.2. This apparatus and its standard operating procedure are the same as used in past studies by our group (Bernhardsen et al., 2019; Hartono et al., 2017). What follows is a quick recapitulation of what has been reported previously.
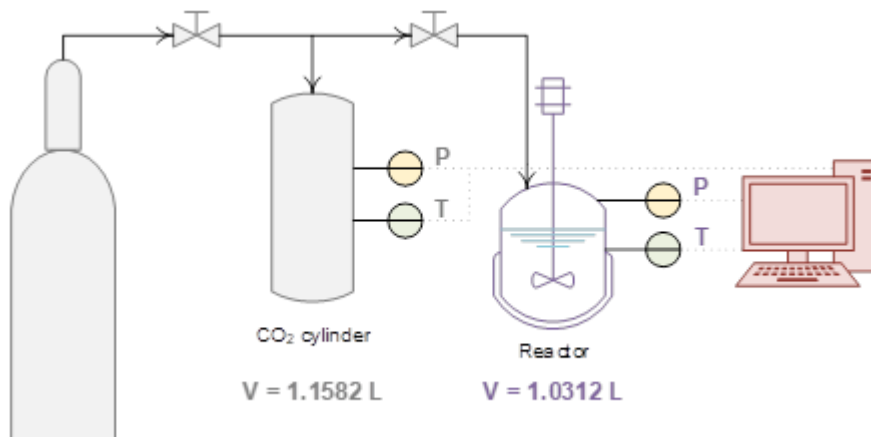
Figure 7.2. Schematic of the vapor-liquid equilibrium setup.

The setup consists essentially of a steel cylinder containing pressurized CO_2 and a stirred glass autoclave coupled to a Julabo temperature controller. Fresh solution containing water, amine and salt is prepared gravimetrically and fed to the reactor. This reactor is then vacuumed, so that the vapor phase in the autoclave should consist only of solvent molecules in equilibrium with the liquid phase. The temperature controller is set to its designed setpoint and the stirrer is turned on to approximately 500 rpm. After this setpoint is reached and enough time is given for temperature and pressure to reach equilibrium both inside the CO_2 cylinder and the reactor, the valve connecting these two equipments is opened. Gas flows from the cylinder to the autoclave. Once enough CO_2 is injected, the valve is closed. Once again, one must wait until temperature and pressure reach an equilibrium in both equipments. If required, the CO_2 cylinder must be refilled. A new injection is made when

temperature and pressure are stable again, and this cycle is repeated until the autoclave reaches its maximum safe pressure of 600 kPa.

The volume comprised between the two valves and the CO_2 cylinder shown in Figure 7.2 has been previously calibrated, and so has the volume comprised between the second valve and the autoclave. The volume of the liquid phase is considered constant throughout the experiment, being estimated by knowledge of the amount of solvent fed to the reactor plus its density, here assumed to be the same density of aqueous MEA 30 %wt. at 40 °C as obtained by Amundsen et al. (2009). With volumes, temperatures, and pressures for both the cylinder and the vapor phase of the autoclave before and after each injection, mass balance calculations can be performed to evaluate CO_2 loadings versus total pressure. In our work, the Peng-Robinson equation of state has been chosen for estimating the molar quantity of CO_2 at all times.

This methodology does not allow for the direct evaluation of CO_2 partial pressures, though these can be obtained by subtraction if one assumes that the solvent vapor pressure is kept constant throughout the experiment. After the procedure is finished, the solvent left in the reactor is titrated so that one can compare if the loading calculated by mass balance is consistent with the loading evaluated analytically. A match of ±3% between these final loading values is considered sufficient for validating our methodology. Additionally, our data is reported in the Appendix with confidence intervals obtained by following the procedure outlined by Wanderley et al. (2020).

2.5 Viscosity experiments

All viscosity experiments carried in this work were undertaken at 25 °C in an Anton Paar MCR rheometer with a double gap measuring cell (Evjen et al., 2019; Hartono et al., 2014; Skylogianni et al., 2019). This apparatus operates at atmospheric pressures. The double gap cell is filled with about 3.6 mL of solvent and semi-closed, so that there is little contact between the solution and the surrounding air and chemical stability can be assumed (i.e. there is negligible loss of CO_2 to the atmosphere even in loaded solutions). Once the liquid is enclosed, a rotor is set in motion. The shear rates in the standard operational procedure vary between 10 and 1000 s^{-1}. A computer connected to the equipment records shear stress versus shear rate values, producing the dynamic viscosity as the slope between these two variables. Hartono et al. (2014) have reported confidence intervals of ±2% for the dynamic viscosities obtained with this procedure, an interval that we assume to be valid for our data as well.

The loaded solvents evaluated in the Section 0 were obtained by preparing a fresh solution, loading part of it with CO_2 up to values above 0.5 mol_{CO2} mol_{MEA}^{-1} and then mixing loaded and fresh solvent in different proportions. After these partially loaded solutions are prepared, they are analytically titrated through the methods explained in Section 0. The values reported for the loadings are the values obtained analytically.

2.6 Analytical methods

The concentration of amine in the solutions was determined by titration with sulfuric acid (H_2SO_4, 0.1 M), a procedure with an uncertainty of $\leq 2\%$ according to Ma'mun et al. (2005). The concentration of CO_2 was determined by Total Inorganic Carbon (TIC) analysis, on a Shimadzu TOC-L_{CPH} analyzer, also with an uncertainty of $\leq 2\%$. For all the samples, the concentration of amine is back calculated to the solution without CO_2 and corrected for loss of water assuming a linear loss of water throughout the experiment, as the total mass of the solution is only known for the start and end solutions. The CO_2 loadings reported in this study are simply the ratios between CO_2 and amine concentrations obtained by these two methods.

Inductively coupled plasma mass spectrometry (ICP-MS) analyses were performed on a High Resolution Inductive coupled plasma ELEMENT 2 from Thermo Electronics. The samples were diluted in purified water (18.2 mΩ) from a Merck Millipore ICW-3000™ Water Purification System and digested with HNO_3 prior to analysis. The results were verified against certified reference material and the relative standard deviation (RSD) for three scans of a sample varies from sample to sample.

Anion exchange ion chromatography (IC) was used to quantify the iodide concentration in the 2.0 %wt. KI SAS oxidative degradation experiments. The instrument used was a Thermo Scientific™ Dionex™ ICS-5000 IC system, connected to an ICW-3000 Millipore water purification system and equipped with an ASRS300 suppressor (2mm), a carbonate removal device and conductivity detection. The column was a IonPac AS15 2×250mm with an AG15 guard column 2×50mm and column temperature 30 °C. An eluent generator provided a KOH gradient with the profile 13 mM for 10 minutes, then an increase to 45 mM between 10 and 15 minutes, kept at 45 mM from 15 to 49 minutes, then 13 mM for the remaining time. The total run time for each analysis is 60 minutes. Quantification of iodide concentrations were performed based on calibration in a concentration range of 0–116 ppm of iodide in the form of KI and dilution of the fresh and degraded samples to the corresponding concentration range. Peak areas were used for calculating iodide concentration.

3 Results and discussion

3.1 Oxidative degradation

The addition of both NaCl and KI reduce the oxidative degradability of aqueous 30 %wt. MEA (*aq*.) significantly, as shown in Figure 7.3. Of the two, KI is the strongest inhibitor of oxidative degradation. Whereas 30 %wt. MEA experiences a loss of 40 ± 4% alkalinity after three weeks under the conditions applied in this work (assumed to directly correlate to the concentration of MEA), the addition of NaCl to the solvent results in a loss of alkalinity of only 24 ± 5%, and the addition of KI reduces this loss

to as little as 4 ± 1%. This shows that the increase of salinity of the solvent has a positive effect in terms of degradability, making MEA less degradable under oxidative conditions. As no significant difference in stability was seen neither between the 2.0 %wt. and 7.5 %wt. NaCl SAS, nor between the 1.0 and 2.0 %wt. KI SAS, it can be inferred that, if the salt employed possesses certain properties, its concentration is of less importance. Moreover, a SAS with 15 %wt. NaCl was tested in the same setup. Although oxidative stability was in the same range as the two other NaCl SAS, the reproducibility of the parallels was low, and that data is not reported in this study. An important factor behind these effects might be that we are approaching a saturation limit of the NaCl in solution, especially if water is lost or degradation compounds are formed, thus influencing the solubility of the salt. A reduction in KI concentration to 0.2 %wt. gave much more oxidative degradation than the higher concentrations of KI as can be seen in Figure 7.4.
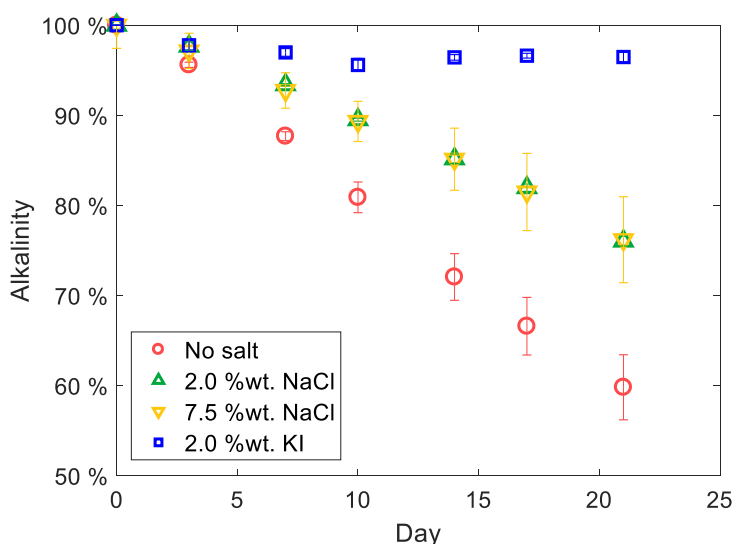

Figure 7.3. Amine conservation during the oxidative degradation experiments in Setup 1 with 30 wt%. MEA (*aq.*), with and without salt addition. Absolute amine concentrations back-calculated to CO_2-free solution, measured and corrected by titration and TIC analysis. Error bars represent standard error of the 2 or 3 parallel experiments.
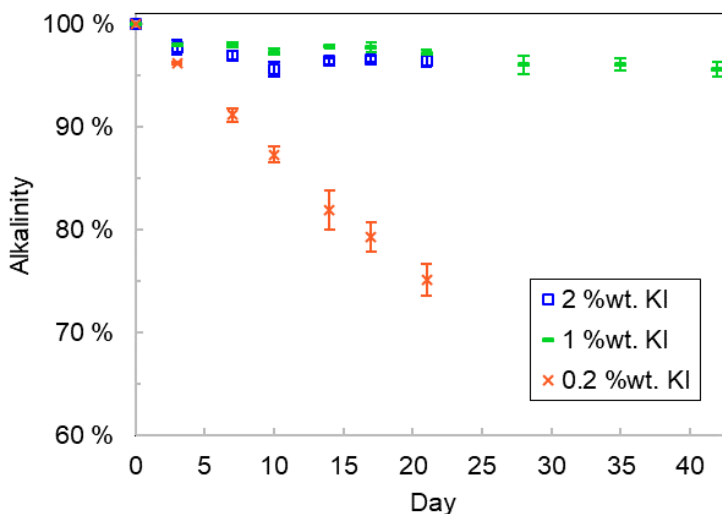
Figure 7.4. Oxidative degradation of 30 %wt. MEA (*aq.*) in Setup 1 with different concentrations of KI added. Absolute amine concentrations back-calculated to CO2-free solution, measured and corrected by titration and TIC analysis. Error bars represent standard error of the 2 or 3 parallel experiments.

As Figure 7.4 shows, the degradation inhibition is equally strong with 1.0 %wt. KI as it is with 2.0 %wt. Upon decreasing the concentration to 0.2 %wt. KI, there is a slight degradation inhibition observed, similar to that of the NaCl SAS shown in Figure 7.3. It should be noted that also for the 0.2 %wt. KI SAS there is no plateau in the degradation curve and the rate of degradation is steady throughout the experiment. To investigate whether the inhibition effect would wear off with the 1.0 %wt. KI case, if the KI is indeed consumed by the reaction, the 1.0 %wt. KI experiment was run twice as long as the other experiments. After six weeks, no significant amine loss was observed.

In the case of all the KI SAS, it was observed that the typical yellow/orange coloration characteristic of iron-containing solutions faded away in the course of the three weeks of experiment, while a red precipitate accumulated on the reactor walls. This effect was less visible in the 0.2 %wt. KI SAS than in 2.0 and 1.0 %wt., but still evident. We therefore hypothesize that KI reduces the solubility of iron oxide in 30 %wt. MEA (*aq.*), promoting precipitation. For this reason, 2.0 %wt. KI SAS was also studied in another oxidative degradation setup and compared to literature data for pure 30 %wt. MEA (*aq.*, without iron) from Vevelstad et al. (2016). The results and comparison are given in Figure 7.5. As the literature shows significant degradation of MEA (~25% loss after three weeks) even in the absence of iron, the fact that no significant amine loss was seen in the 2.0 %wt. KI SAS confirms that salting out of metal from the solution is not the only effect causing the solvent to be more stable under oxidative conditions.

Additionally, anion exchange chromatography showed no loss of iodide through the duration of the 21 days of oxidative degradation experiments in the 2 %wt KI case, which indicates that iodide is not being consumed while it inhibits the degradation reactions. The results of this analysis can be viewed in the Appendix.

Since both oxidative degradation setups used in these experiments use continuous agitation of the liquid, both by magnetic stirring (~ 200 rpm) and bubbling the gas into the solution, mass transfer from gas to liquid phase should not be the limiting factor for whether degradation takes place or not. Setup 2 has the advantage of recycling the gas phase and thereby enhancing the total gas flow into the liquid phase, making mass transfer of oxygen as high as possible throughout the experiment.
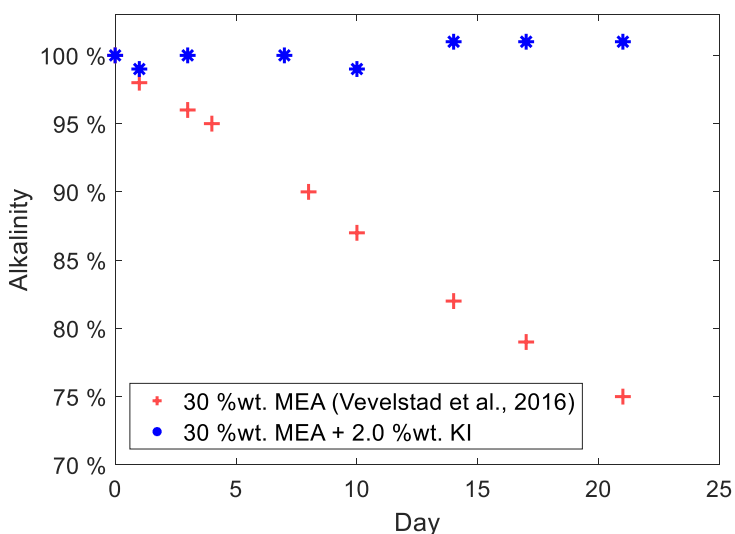
Figure 7.5: Validation of oxidative degradation of 2.0 %wt. KI SAS with iron against 30 %wt. MEA without iron from Vevelstad et al. (2016) in Setup 2.

We would like to address the hypothesis that the salts might shield the amine from being degraded by being themselves oxidized instead, thus being "sacrificed" for the amine. If the salts are being consumed during the oxidation process, this will decrease their value as inhibitors because of the subsequent need for replenishing. This hypothesis is particularly interesting in elucidating the good performance of potassium iodide, which is known for being readily oxidized (Altshuller et al., 1959).

Figure 7.6 shows the amount of amine degradation avoided by employing the SAS. There are three important things to notice in this image. The first one is that the degradation avoided with the use of potassium iodide does not reach a maximum, or a plateau, in the course of the 21 days of oxidation experiments. Such a plateau would have been expected in case of KI consumption, as eventually one would observe iodide depletion in the solvent. For comparison, a plateau does start to appear for the

NaCl SAS, though very incipiently. Incidentally, the second point of notice is that, if salt was indeed being consumed in this reaction, one would expect to see different curves for 2.0 %wt. and 7.5 %wt. NaCl – which clearly have very distinct amounts of "reactants". Finally, the SAS prepared in these experiments have very small molar amounts of NaCl and KI. Let us suppose that KI reacts with oxygen in a 1:1 molar basis, shielding MEA that would otherwise react with oxygen following an assumed 1:1 stoichiometry. By the end of day 21, having avoided the loss of almost 2 mol kg^{-1} MEA in the SAS containing 2.0 %wt. KI, one could expect to have instead lost 2 mol·kg^{-1} KI. However, this SAS contains merely 0.120 mol kg^{-1} of KI. If potassium iodide is indeed being consumed by oxygen, it is doing so in a basis far below 1:1 and indeed experiencing no reduction in inhibition capacity, as the lack of a plateau demonstrates. For these three reasons, we do not believe that salt consumption explains the differences in degradation behaviours alone, though it might certainly contribute with them to some extent. Contrary to the previous studies of halides as degradation inhibitors Lee and Rochelle (1987), we cannot see that it is a scavenging effect that is seen in these experiments, as the degradation rate is stable over time and iodide concentration is preserved. Conversely, our results agree with the observation by Sjostrom et al. (2020) that iodide is not consumed in this process.
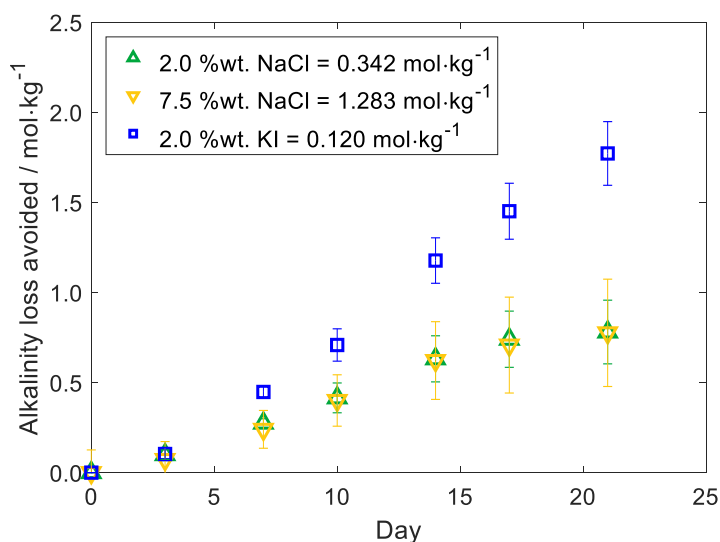
Figure 7.6. Avoidance of oxidative degradation brought by the addition of inorganic salts to aqueous 30 %wt. MEA (*aq*.). Error bars represent standard deviations of calculated values with sets of parallel experiments.

The mechanism through which potassium iodide inhibits oxidative organic acid degradation is not very well understood. Both inhibitors Lee and Rochelle (1987) and Sjostrom et al. (2020) suggest a direct mechanism through which, for example in the context of limestone scrubbing, iodide is oxidized to iodine by reacting with SO_4^{2-}

and then reduced back to iodide after reacting with excess sulphite (SO_3^{2-}) (Lee and Rochelle, 1987). Conversely, iodide could also react with some of the metal ions in solution, preventing their activity in catalysing oxidative degradation reactions (Sjostrom et al., 2020), which could also explain its application in inhibiting corrosion phenomena (Khadom et al., 2018). At any rate, the equilibrium between oxidation and reduction reactions in the solvent would enable iodide to be constantly regenerated in solution without being consumed. There might also exist other effects through which stable salts such as potassium iodide inhibit oxidative degradation. It might be, as Goff and Rochelle (2006) suggest, that these salts are effective simply through salting-out of O_2. A reduction of dissolved oxygen concentrations will surely decrease oxidative degradation rates, explaining the observed phenomena. It could also be that the increase in ionic strength of the solvent upon salt addition affects its molecular structure (Marcus, 2009b, 2012), promoting the creation of rigid solvation shells that are disadvantageous for many radical reaction mechanisms (Marcus, 1964; Marcus et al., 1954). These two phenomena could explain inhibition even when using stable salts that are not known for being easily oxidized.

Whether the degradation inhibition effect seen in the NaCl SAS experiments is sufficient to justify its implementation as a degradation inhibitor on a commercial scale can be discussed. This relatively small effect can possibly be explained by salting out of oxygen, achieving a lower oxygen solubility, although using the Schumpe parameters (Weisenberger and Schumpe, 1996) predicted in Buvik et al. (2020) to calculate the solubility of oxygen in loaded MEA, the relative contributions of NaCl and KI to the salting out of gases is very small compared to that of $MEAH^+$ and $MEACOO^-$. The fact that iron oxide-like precipitates were not observed in the NaCl SAS also suggests that there is a different inhibition effect taking place here than in KI SAS.

On the process level fears that iodide will be lost upon conventional thermal reclaiming of the spent solvent should be mitigated by the facts that (1) implementation of potassium iodide as a degradation inhibitor could perhaps reduce the need for thermal reclamation to one fourth of the frequency of its current requirement and (2) methodologies for recovery of iodide are known to literature (Sjostrom et al., 2020). At any rate, a feasibility study shall be carried out in the future to evaluate how easy it is to implement these iodide recovery techniques. Since cases of increased foaming upon inhibitor addition in MEA have been observed (Thitakamol and Veawab, 2008), this should therefore be investigated in future tests of KI as a degradation inhibitor.

It will be, of course, crucial to test KI as a degradation inhibitor under more realistic conditions before it should be implemented in the CO_2 capture process. Previous studies of degradation inhibitors have shown that certain inhibitors are only efficient at absorber conditions and lose their properties when tested in a cyclic system (Nielsen, 2018; Voice and Rochelle, 2014). This will therefore be an important next

step towards the potential commercialization of the KI inhibitor. However, before testing KI inhibitor on cyclic CO_2 capture systems, one should assess SAS's impact on the vapor-liquid equilibrium (VLE), the viscosity, thermal degradation, and corrosion tendency to ensure that the SAS does not render the solvents unfeasible for CO_2 capture process applications. Results from these tests will be discussed before concluding remarks.

3.2 Thermal degradation

The thermal stability of aqueous MEA with and without added NaCl or KI have no significant difference, as can be seen in Figure 7.7. After 5 weeks in stainless steel cylinders at 135 °C, all the four tested solutions had amine/alkalinity losses between 22–25%, regardless of the type of salt and salt concentration.
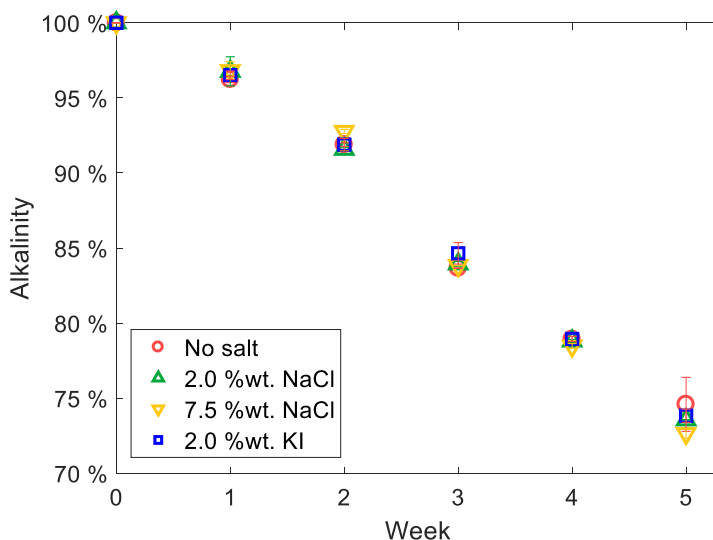
Figure 7.7. Amine loss over time in the five-week thermal degradation experiments with 30wt% MEA (aq.), respectively with and without salt addition, at 135 °C. The concentrations given are corrected to CO_2-free solution and error bars represent the standard error of the two parallel samples.

ICP-MS analysis of the end samples in the thermal degradation study shows comparable concentrations of iron (Fe), nickel (Ni), chromium (Cr) and molybdenum (Mo) in all the SAS solutions, as in aqueous 30 %wt. MEA without salt addition (Figure 7.8). Only the 7.5 %wt. NaCl SAS shows a significantly higher iron concentration than the other solutions. This indicates that the 2.0 %wt. SAS solutions do not influence the corrosivity of MEA. As a comparison, a cylinder that contained just deionized water was also subjected to thermal degradation conditions for five weeks, and close to no dissolved metals could be detected by ICP-MS.
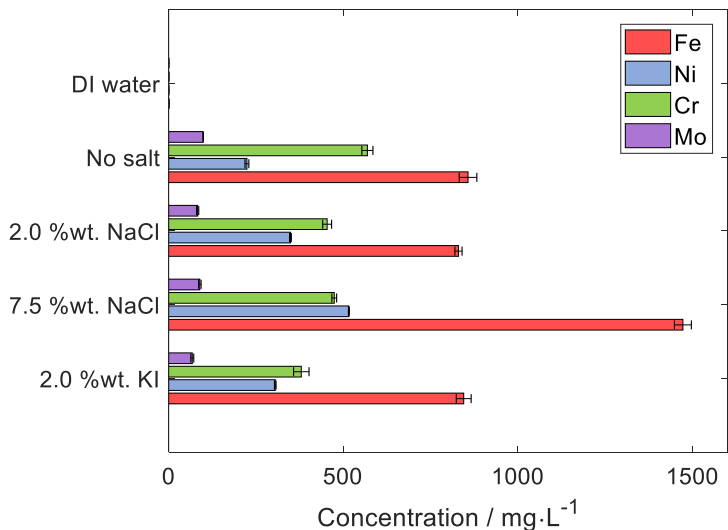
Figure 7.8. Average metal concentration in the two parallel samples analysed after 5 weeks of thermal degradation by ICP-MS. Error bars represent the average relative standard deviation of the analyses.

The cylinders were weighed both after rinsing with water and after 24 hours soaking in 0.1 M H_2SO_4, so that the cylinder mass loss could be used to assess corrosivity in addition to ICP-MS data. The absolute mass losses during the experimental period are very low (< 0.05% at most). This is due to the relative total mass of the cylinders of about 170 g. A mass loss due to corrosion in < 5 weeks is therefore relatively small, but still a statistically significant difference could be observed between the different salt solutions. Figure 7.9 shows that the lowest cylinder mass losses are seen in those that contained 30 %wt. MEA with 2.0 %wt. KI, while the highest losses are in those containing 7.5 %wt. NaCl, despite the statistical significance of these measurements being low. According to this test, all solutions seem to induce the same degree of cylinder destruction as salt-free MEA, something that confirms the ICP-MS results. Since this method is sensitive to corrosion-unrelated causes of cylinder loss, such as chipping, it is not a perfect indication of corrosion and shows a relatively high uncertainty.

245
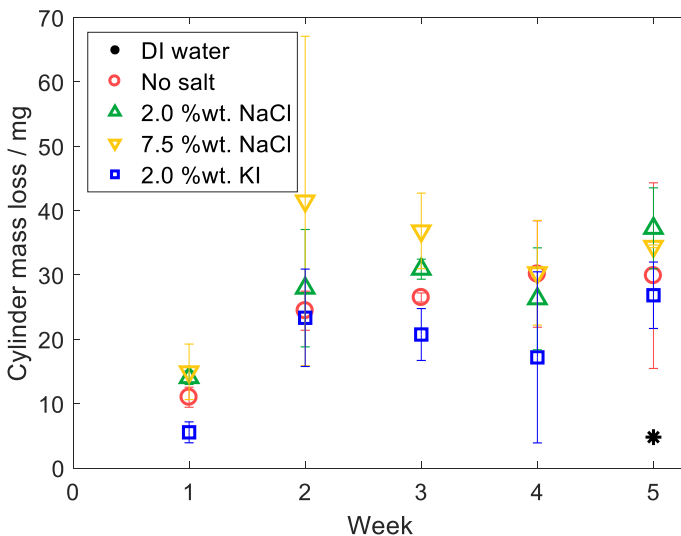
Figure 7.9. Loss of mass of stainless-steel cylinders during the thermal degradation experiments with 30wt% MEA (aq.), as well as a set of end-sample cylinders containing only deionized water. Error bars represent the standard error of the two cylinders used for each time of sampling for each solution. The total cylinder mass without solution is 170 g.

3.3 Vapor-liquid equilibrium

Figure 7.10 shows a comparison between the vapor-liquid equilibria (VLE) of unsalted 30 %wt. MEA (*aq.*) with that of SAS both at 40 °C and at 120 °C. The data referring to the unsalted solvent comes from Wanderley et al. (2020). Though the curves shown in Figure 7.10 are for CO_2 partial pressure (p_{CO2}) versus loadings (*α*), we must reinforce that the methodology described in Section 0 is able to produce only total pressure versus loading, meaning that the CO_2 partial pressures have to be estimated from the original data set. As a result, some data points referring to lower CO_2 partial pressures have to be eliminated since their values end up being smaller than the inherent propagated uncertainties of ± 0.34 kPa. Complete disclosure of the total pressures and loadings measured throughout our experiments, together with their uncertainties, can be found in the Appendix to this study.

246
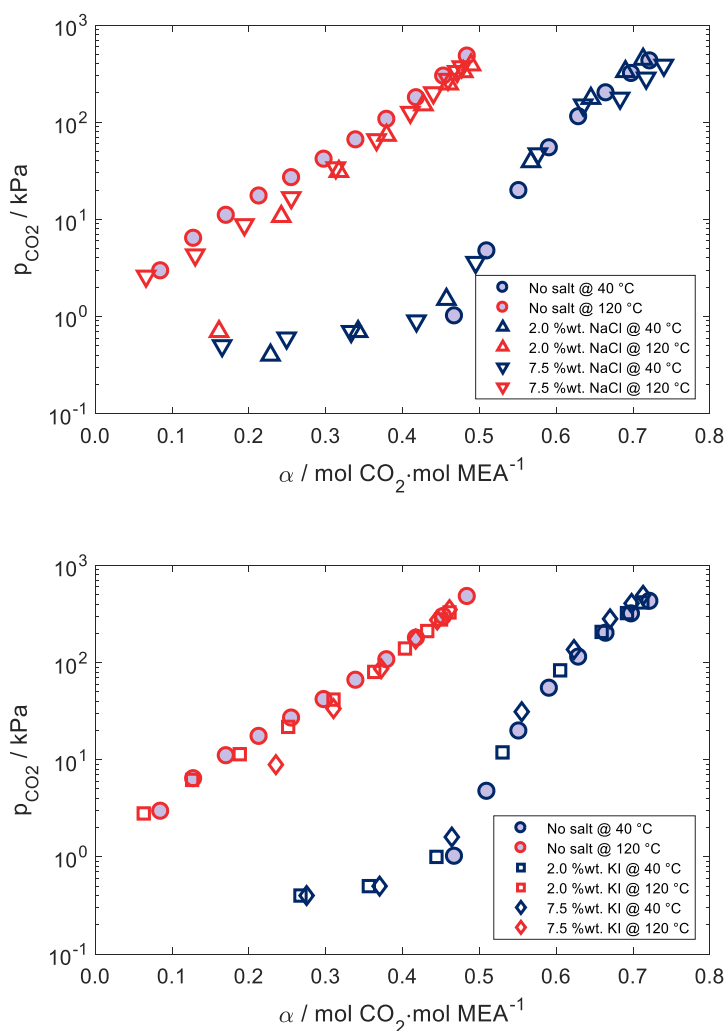
Figure 7.10. Estimated CO_2 partial pressure versus CO_2 loading for salted 30 %wt. MEA (*aq.*) compared to the VLE for the unsalted amine obtained from Wanderley et al. (2020).

Once we account for the uncertainties, which are particularly meaningful for the lower CO_2 partial pressure data points, what results from Figure 7.10 is nearly an overlap between the VLE curves for the unsalted 30 %wt. MEA (*aq.*) and the SAS. It is even unclear whether the SAS experience a loss of CO_2 solubility or not. Looking at the blue scattered data points, both for solutions with NaCl and KI, it seems that a small shift in equilibrium towards less CO_2 conversion might be observed with the SAS at 40 °C. As such, both the blue △ and ▽ data points and the blue □ and ◇ data points are slightly to the left of the curves for unsalted MEA in top and bottom images alike. There are three outlying points for the SAS with 7.5 %wt. NaCl at 40 °C (uppermost blue ▽ markers at the top image). In this experiment, we observed

precipitation of white solids at high CO_2 pressures, likely of sodium bicarbonate ($NaHCO_3$). This demonstrates a clear risk of employing too concentrated SAS for CO_2 absorption. At 120 °C, on the other hand, there are indications of a slight *increase* in CO_2 solubility for the SAS, with both the red △ and ▽ data points and the red □ and ◇ data points falling a bit to the right of the curves for unsalted MEA.

These contradictory small shifts in equilibrium at 40 °C and at 120 °C could imply a very small reduction in cyclic capacity for the SAS. However, it is difficult to interpret Figure 7.10 as anything but an overlap of VLEs curves. It appears to us that, other than the caveat of precipitation issues at high NaCl concentrations, one can conclude an insignificant shift in absorption capacity when employing the SAS.

3.4 Viscosity

Figure 7.11 shows how the viscosities of SAS increase with loading at 25 °C when compared to that of unsalted 30 %wt. MEA as measured by Amundsen et al. (2009). Once again, the full data set together with its uncertainties is found in the Appendix to this study.
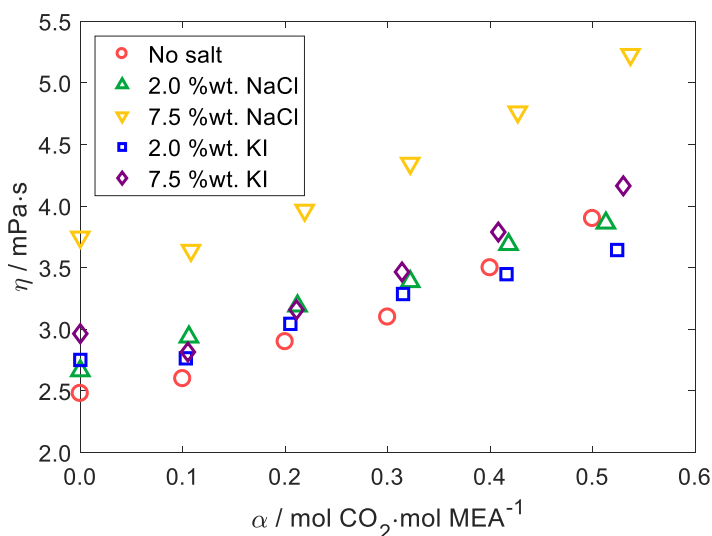
Figure 7.11. Viscosity versus CO_2 loading for salted 30 %wt. MEA compared to that for the unsalted amine obtained from Amundsen et al. (Amundsen et al., 2009) at 25 °C.

As expected, the addition of inorganic salts promotes an increase in solvent viscosity. This seems to happen both with NaCl, which is structure-making at 25 °C, and with KI, which is structure-breaking (Marcus, 2009a). However, NaCl does indeed increase the viscosity of aqueous MEA more than KI. This is particularly evident in the SAS with 7.5 %wt. salt, wherein the 7.5 %wt. NaCl SAS (yellow ▽ markers) clearly has the highest viscosity at all loadings while that of the 7.5 %wt. KI SAS

(purple ◇ markers) almost overlaps with both the 2.0 %wt. SAS. This might be a consequence of the SAS with KI having lower ionic strength than the SAS with NaCl on account of KI having higher molecular mass than NaCl. KI has a molecular mass of 166.00 g mol^{-1} compared to 58.44 g mol^{-1} of NaCl, meaning that the ionic strength of the unloaded NaCl SAS is almost three times as big as that of the unloaded KI SAS. As shown by Esteves et al. (2001), higher viscosities might be attributed to higher ionic strengths.

The viscosity of the SAS with 2.0 %wt. salt is very similar to that of aqueous MEA, and there appears to be even a crossing-over for both 2.0 %wt. NaCl and KI SAS at around $\alpha \approx 0.4$ and 0.5 mol$_{CO2}$ mol$_{MEA}$$^{-1}$ respectively (see where the yellow △ markers and blue □ markers overlap with the red stars in Figure 7.11). This is a very interesting behaviour. In fact, except for the 7.5 %wt. NaCl SAS, the viscosities of the SAS apparently increase less steeply with loading than that of aqueous 30 %wt. MEA (*aq.*). To our knowledge, there is no explanation for this observed behaviour in the Debye-Hückel theory (Esteves et al., 2001), which suggests that such phenomena might be attributed to unexpected solute-solute interaction between the inorganic salt electrolytes and the products of the MEA–CO$_2$ reaction.

In other words, the impact of mixing both inorganic salts to aqueous 30 %wt. MEA (*aq.*) on solvent viscosity is not nearly as noticeable as one would expect. This is good, as it signalizes that transport phenomena in SAS will probably not be significantly depressed due to the addition of salts.

4 Conclusion

The increase in oxidative stability upon addition of just 1.0 %wt. potassium iodide is remarkable. With the KI SAS system we have achieved an oxidative stability comparable to tertiary and sterically hindered amines under the given conditions. Both the tested salts give an increased stability and, based on the salt concentration tested, the type of salt seems to matter much more than its concentration. Regarding thermal stability, no significant difference is observed between the SAS and fresh, salt-free MEA, and in terms of corrosivity the ICP-MS results indicate that the 2.0 %wt. SAS solutions are comparable to salt-free MEA. However, the higher concentration of dissolved iron in the 7.5 %wt. NaCl SAS hints towards a higher corrosion potential when using this formulation.

The addition of stable salts has little effect on the vapor-liquid equilibrium between CO$_2$ and the solvent (except for the 7.5 %wt. NaCl SAS case, where precipitation was observed at 40 °C). It also has an almost negligible impact on the viscosity of loaded and unloaded solvents at 25 °C, with the potential of becoming completely negligible at higher temperatures. In other words, the reduction of CO$_2$ physical solubility, the shift in chemical equilibria and the increase in viscosity should not be a cause of concern regarding the SAS.

The nature of the phenomena behind this reduction in degradation potential with potassium iodide is yet to be properly understood. Future studies are required to assess if there is indeed no salt depletion during the oxidation of the solvent. The KI SAS is a promising degradation inhibitor for absorption-based CO_2 capture based on the current results. However, to further validate its applicability, testing in cyclic systems and pilots is needed.

Acknowledgements

5 References

Altshuller, A.P., Schwab, C.M., Bare, M., 1959. Reactivity of Oxidizing Agents with Potassium Iodide Reagent. Analytical Chemistry 31, 1987-1990.

Amundsen, T.G., Øi, L.E., Eimer, D.A., 2009. Density and Viscosity of Monoethanolamine + Water + Carbon Dioxide from (25 to 80) °C. Journal of Chemical & Engineering Data 54, 3096-3100.

Bernhardsen, I.M., Trollebø, A.A., Perinu, C., Knuutila, H.K., 2019. Vapour-liquid equilibrium study of tertiary amines, single and in blend with 3-(methylamino) propylamine, for post-combustion CO2 capture. The Journal of Chemical Thermodynamics 138, 211-228.

Blachly, C., Ravner, H., 1963. The effect of trace amounts of copper on the stability of monoethanolamine scrubber solutions. Naval Research Lab Washington DC.

Blachly, C.H., Ravner, H., 1964. The stabilization of monoethanolamine solutions for submarine carbon dioxide scrubbers. Naval Research Lab Washington DC, Washington DC.

Blachly, C.H., Ravner, H., 1965. Studies of submarine carbon dioxide scrubber operation: effect of an additive package for the stabilization of monoethanolamine solutions. Naval Research Lab Washington DC.

Blachly, C.H., Ravner, H., 1966. Stabilization of Monoethanolamine Solutions in Carbon Dioxide Scrubbers. Journal of Chemical and Engineering Data 11, 401-403.

Bui, M., Adjiman, C.S., Bardow, A., Anthony, E.J., Boston, A., Brown, S., Fennell, P.S., Fuss, S., Galindo, A., Hackett, L.A., Hallett, J.P., Herzog, H.J., Jackson, G., Kemper, J., Krevor, S., Maitland, G.C., Matuszewski, M., Metcalfe, I.S., Petit, C., Puxty, G., Reimer, J., Reiner, D.M., Rubin, E.S., Scott, S.A., Shah, N., Smit, B., Trusler, J.P.M., Webley, P., Wilcox, J., Mac Dowell, N., 2018. Carbon capture and storage (CCS): the way forward. Energy & Environmental Science 11, 1062-1176.

Buvik, V., Bernhardsen, I.M., Figueiredo, R.V., Vevelstad, S.J., Goetheer, E., van Os, P., Knuutila, H.K., 2020. Measurement and prediction of oxygen solubility in post-combustion CO2 capture solvents. International Journal of Greenhouse Gas Control, 103205.

Chi, S., Rochelle, G.T., 2002. Oxidative Degradation of Monoethanolamine. Industrial & Engineering Chemistry Research 41, 4178-4186.

Dhingra, S., Khakharia, P., Rieder, A., Cousins, A., Reynolds, A., Knudsen, J., Andersen, J., Irons, R., Mertens, J., Abu Zahra, M., Van Os, P., Goetheer, E., 2017. Understanding and Modelling the Effect of Dissolved Metals on Solvent Degradation in Post Combustion CO2 Capture Based on Pilot Plant Experience. Energies 10.

Eide-Haugmo, I., Lepaumier, H., da Silva, E.F., Einbu, A., Vernstad, K., Svendsen, H.F., 2011. A study of thermal degradation of different amines and their resulting degradation products, 1st Post Combustion Capture Conference, pp. 17-19.

Esteves, M.J.C., Cardoso, M.J.E.d.M., Barcia, O.E., 2001. A Debye−Hückel Model for Calculating the Viscosity of Binary Strong Electrolyte Solutions. Industrial & Engineering Chemistry Research 40, 5021-5028.

Evjen, S., Wanderley, R., Fiksdahl, A., Knuutila, H.K., 2019. Viscosity, Density, and Volatility of Binary Mixtures of Imidazole, 2-Methylimidazole, 2,4,5-Trimethylimidazole, and 1,2,4,5-Tetramethylimidazole with Water. Journal of Chemical & Engineering Data 64, 507-516.

Fytianos, G., Vevelstad, S.J., Knuutila, H.K., 2016. Degradation and corrosion inhibitors for MEA-based CO2 capture plants. International Journal of Greenhouse Gas Control 50, 240-247.

Goff, G.S., 2005. Oxidative Degradation of Aqueous Monoethanolamine in CO2 Capture Processes: Iron and Copper Catalysis, Inhibition, and O2 Mass Transfer.

Goff, G.S., Rochelle, G.T., 2006. Oxidation inhibitors for copper and iron catalyzed degradation of monoethanolamine in CO2 capture processes. Industrial & engineering chemistry research 45, 2513-2521.

Hartono, A., Mba, E.O., Svendsen, H.F., 2014. Physical properties of partially CO2 loaded aqueous monoethanolamine (MEA). Journal of Chemical & Engineering Data 59, 1808-1816.

Hartono, A., Rennemo, R., Awais, M., Vevelstad, S.J., Brakstad, O.G., Kim, I., Knuutila, H.K., 2017. Characterization of 2-piperidineethanol and 1-(2-hydroxyethyl) pyrrolidine as strong bicarbonate forming solvents for CO2 capture. International Journal of Greenhouse Gas Control 63, 260-271.

Khadom, A.A., Abd, A.N., Ahmed, N.A., 2018. Potassium Iodide as a Corrosion Inhibitor of Mild Steel in Hydrochloric Acid: Kinetics and Mathematical Studies. Journal of Bio- and Tribo-Corrosion 4.

Lee, I.Y., Kwak, N.S., Lee, J.H., Jang, K.R., Shim, J.-G., 2012. Degradation and corrosivity of MEA with oxidation inhibitors in a carbon dioxide capture process. Journal of chemical engineering of Japan, 1201190322-1201190322.

Lee, Y.J., Rochelle, G.T., 1987. Oxidative Degradation of Organic Acid Conjugated with Sulfite Oxidation in Flue Gas Desulfurization: Products, Kinetics, and Mechanism. Environmental Science and Technology 21, 266-272.

Lepaumier, H., da Silva, E.F., Einbu, A., Grimstvedt, A., Knudsen, J.N., Zahlsen, K., Svendsen, H.F., 2011. Comparison of MEA degradation in pilot-scale with lab-scale experiments. Energy Procedia 4, 1652-1659.

Lepaumier, H., Picq, D., Carrette, P.L., 2009. New amines for CO2 Capture. I. Mechanisms of amine degradation in the presence of CO2. Industrial and Engineering Chemistry Research 48, 9061-9067.

Ma'mun, S., Nilsen, R., Svendsen, H.F., Juliussen, O., 2005. Solubility of carbon dioxide in 30 mass% monoethanolamine and 50 mass% methyldiethanolamine solutions. Journal of Chemical & Engineering Data 50, 630-634.

Marcus, R.A., 1964. Chemical and electrochemical electron-transfer theory. Annual review of physical chemistry 15, 155-196.

Marcus, R.J., Zwolinski, B.J., Eyring, H., 1954. The electron tunnelling hypothesis for electron ex-change reactions. The Journal of Physical Chemistry 58, 432-437.

Marcus, Y., 2009a. Effect of ions on the structure of water: Structure making and breaking, pp. 1346-1370.

Marcus, Y., 2009b. On water structure in concentrated salt solutions. Journal of Solution Chemistry 38, 513-516.

Marcus, Y., 2012. Ions in Water and Biophysical Implications. Springer.

Nielsen, P.T., 2018. Oxidation of Piperazine in Post-Combustion Carbon Capture Austin, TX.

Rochelle, G.T., 2016. Conventional amine scrubbing for CO2 capture. Elsevier Inc., pp. 35-67.

Rooney, P.C., DuPart, M.S., 2000. Corrosion in alkanolamine plants: causes and minimization. CORROSION 2000. NACE International.

Sexton, A.J., Rochelle, G.T., 2009. Catalysts and inhibitors for oxidative degradation of monoethanolamine. International Journal of Greenhouse Gas Control 3, 704-711.

Sjostrom, S., Baldrey, K.E., Senior, C., 2020. Control of Wet Scrubber Oxidation Inhibitor and Byproduct Recovery.

Skylogianni, E., Wanderley, R.R., Austad, S.S., Knuutila, H.K., 2019. Density and Viscosity of the Nonaqueous and Aqueous Mixtures of Methyldiethanolamine and Monoethylene Glycol at Temperatures from 283.15 to 353.15 K. Journal of Chemical & Engineering Data 64, 5415-5431.

Supap, T., Idem, R., Tontiwachwuthikul, P., Saiwan, C., 2011. Investigation of degradation inhibitors on CO_2 capture process. Energy Procedia 4, 583-590.

Thitakamol, B., Veawab, A., 2008. Foaming behavior in CO2 absorption process using aqueous solutions of single and blended alkanolamines. Industrial & engineering chemistry research 47, 216-225.

Vega, F., Sanna, A., Navarrete, B., Maroto-Valer, M.M., Cortés, V.J., 2014. Degradation of amine-based solvents in CO2 capture process by chemical absorption. Greenhouse Gases: Science and Technology 4, 707-733.

Vevelstad, S.J., Eide-Haugmo, I., Da Silva, E.F., Svendsen, H.F., 2011. Degradation of MEA; A theoretical study. Energy Procedia 4, 1608-1615.

Vevelstad, S.J., Johansen, M.T., Knuutila, H., Svendsen, H.F., 2016. Extensive dataset for oxidative degradation of ethanolamine at 55–75° C and oxygen concentrations from 6 to 98%. International Journal of Greenhouse Gas Control 50, 158-178.

Voice, A.K., Rochelle, G.T., 2014. Inhibitors of monoethanolamine oxidation in CO2 capture processes. Industrial and Engineering Chemistry Research 53, 16222-16228.

Wanderley, R.R., Pinto, D.D.D., Knuutila, H.K., 2020. Investigating opportunities for water-lean solvents in CO2 capture: VLE and heat of absorption in water-lean solvents containing MEA. Separation and Purification Technology 231, 115883-115883.

Weisenberger, S., Schumpe, A., 1996. Estimation of gas solubilities in salt solutions at temperatures from 273 K to 363 K. AIChE Journal 42, 298-300.

Appendix

Addition of potassium iodide reduces oxidative degradation of monoethanolamine (MEA)

Vanja Buvik, Ricardo R. Wanderley, Hanna K. Knuutila [*]

Department of Chemical Engineering, Norwegian University of Science and Technology (NTNU), NO-7491 Trondheim, Norway

Table A-1 and Table A-2 contain data regarding the VLE of the SAS with NaCl and KI respectively. In those tables, the CO_2 partial pressure (p_{CO2}) is calculated by subtracting the total pressure measured above the unloaded solvent ($\alpha = 0$ mol $CO_2 \cdot$mol MEA^{-1}) from each new total pressure measurement. The inherent uncertainties of all loadings are calculated based on the methodology described by Wanderley et al. (2020). For these calculations, the uncertainties of pressure measurements are $\pm$ 0.24 kPa, those of temperature measurements are $\pm$ 0.01 K and those of mass measurements are $\pm$ 0.01 g. The volumes of the CO_2 cylinders have been calibrated within an accuracy of $\pm$ 0.1%, while those of the reactors have $\pm$ 0.5% accuracy.

Table A-1. Vapor-liquid equilibrium data for SAS containing sodium chloride.

Aqueous 30 %wt. MEA + 2.0 %wt. NaCl at 40 °C		
α / $mol_{CO2} \cdot mol_{MEA}^{-1}$	p / kPa	p_{CO_2} / kPa
0	6.3 ± 0.2	—
0.1146 ± 0.0002	6.4 ± 0.2	—
0.2280 ± 0.0002	6.7 ± 0.2	0.4 ± 0.3
0.3424 ± 0.0003	7.0 ± 0.2	0.7 ± 0.3
0.4573 ± 0.0003	7.8 ± 0.2	1.5 ± 0.3
0.5674 ± 0.0004	45.5 ± 0.2	39.2 ± 0.3
0.6448 ± 0.0004	182.1 ± 0.2	175.8 ± 0.3
0.6896 ± 0.0005	338.2 ± 0.2	331.9 ± 0.3
0.7127 ± 0.0006	450.5 ± 0.2	444.2 ± 0.3

[*] Corresponding author. Tel.: +47 73594119
E-mail address: hanna.knuutila@ntnu.no

Aqueous 30 %wt. MEA + 2.0 %wt. NaCl at 120 °C		
α / $mol_{CO2} \cdot mol_{MEA}^{-1}$	p / kPa	pCO_2 / kPa
0	174.0 ± 0.2	—
0.0829 ± 0.0002	171.4 ± 0.2	—
0.1612 ± 0.0002	174.7 ± 0.2	0.7 ± 0.3
0.2415 ± 0.0003	184.7 ± 0.2	10.7 ± 0.3
0.3165 ± 0.0003	205.1 ± 0.2	31.1 ± 0.3
0.3785 ± 0.0004	247.3 ± 0.2	73.3 ± 0.3
0.4274 ± 0.0004	324.8 ± 0.2	150.8 ± 0.3
0.4601 ± 0.0005	421.3 ± 0.2	247.3 ± 0.3
0.4788 ± 0.0006	505.1 ± 0.2	331.1 ± 0.3
0.4888 ± 0.0006	562.6 ± 0.2	388.6 ± 0.3
Aqueous 30 %wt. MEA + 7.5 %wt. NaCl at 40 °C		
α / $mol_{CO2} \cdot mol_{MEA}^{-1}$	p / kPa	pCO_2 / kPa
0	6.5 ± 0.2	—
0.0824 ± 0.0001	6.8 ± 0.2	—
0.1650 ± 0.0002	7.0 ± 0.2	0.5 ± 0.3
0.2488 ± 0.0002	7.1 ± 0.2	0.6 ± 0.3
0.3332 ± 0.0002	7.2 ± 0.2	0.7 ± 0.3
0.4182 ± 0.0003	7.4 ± 0.2	0.9 ± 0.3
0.4953 ± 0.0003	10.1 ± 0.2	3.6 ± 0.3
0.5763 ± 0.0003	53.7 ± 0.2	47.2 ± 0.3
0.6346 ± 0.0004	156.8 ± 0.2	150.3 ± 0.3
0.6825 ± 0.0004	183.1 ± 0.2	176.6 ± 0.3
0.7172 ± 0.0004	290.7 ± 0.2	284.2 ± 0.3
0.7401 ± 0.0005	392.2 ± 0.2	385.7 ± 0.3
Aqueous 30 %wt. MEA + 7.5 %wt. NaCl at 120 °C		
α / $mol_{CO2} \cdot mol_{MEA}^{-1}$	p / kPa	pCO_2 / kPa
0	159.5 ± 0.2	—
0.0659 ± 0.0001	162.1 ± 0.2	2.6 ± 0.3
0.1305 ± 0.0002	163.8 ± 0.2	4.3 ± 0.3
0.1935 ± 0.0002	168.3 ± 0.2	8.8 ± 0.3
0.2548 ± 0.0003	176.2 ± 0.2	16.7 ± 0.3
0.3132 ± 0.0003	193.4 ± 0.2	33.9 ± 0.3
0.3655 ± 0.0003	225.5 ± 0.2	66.0 ± 0.3
0.4101 ± 0.0004	285.6 ± 0.2	126.1 ± 0.3
0.4398 ± 0.0004	360.2 ± 0.2	200.7 ± 0.3
0.4593 ± 0.0005	435.3 ± 0.2	275.8 ± 0.3
0.4707 ± 0.0005	491.6 ± 0.2	332.1 ± 0.3
0.4774 ± 0.0006	530.9 ± 0.2	371.4 ± 0.3

Table A-2. Vapor-liquid equilibrium data for SAS containing potassium iodide.

Aqueous 30 %wt. MEA + 2.0 %wt. KI at 40 °C		
α / $mol_{CO2} \cdot mol_{MEA}^{-1}$	p / kPa	pCO_2 / kPa
0	7.1 ± 0.2	—
0.0903 ± 0.0001	7.2 ± 0.2	—
0.1780 ± 0.0002	7.4 ± 0.2	—
0.2671 ± 0.0002	7.5 ± 0.2	0.4 ± 0.3
0.3560 ± 0.0003	7.6 ± 0.2	0.5 ± 0.3
0.4438 ± 0.0003	8.1 ± 0.2	1.0 ± 0.3

α / $mol_{CO2}\cdot mol_{MEA}^{-1}$	p / kPa	pCO_2 / kPa
0.5305 ± 0.0003	19.0 ± 0.2	11.9 ± 0.3
0.6055 ± 0.0003	90.3 ± 0.2	83.2 ± 0.3
0.6594 ± 0.0004	214.0 ± 0.2	206.9 ± 0.3
0.6915 ± 0.0004	330.3 ± 0.2	323.2 ± 0.3
0.7116 ± 0.0005	423.3 ± 0.2	416.2 ± 0.3

Aqueous 30 %wt. MEA + 2.0 %wt. KI at 120 °C

α / $mol_{CO2}\cdot mol_{MEA}^{-1}$	p / kPa	pCO_2 / kPa
0	174.9 ± 0.2	—
0.0628 ± 0.0001	177.7 ± 0.2	2.8 ± 0.3
0.1259 ± 0.0002	181.1 ± 0.2	6.2 ± 0.3
0.1879 ± 0.0003	186.3 ± 0.2	11.4 ± 0.3
0.2508 ± 0.0003	196.7 ± 0.2	21.8 ± 0.3
0.3101 ± 0.0003	216.5 ± 0.2	41.6 ± 0.3
0.3625 ± 0.0004	255.1 ± 0.2	80.2 ± 0.3
0.4034 ± 0.0004	314.5 ± 0.2	139.6 ± 0.3
0.4318 ± 0.0005	386.1 ± 0.2	211.2 ± 0.3
0.4499 ± 0.0005	452.7 ± 0.2	277.8 ± 0.3
0.4608 ± 0.0006	503.5 ± 0.2	328.6 ± 0.3

Aqueous 30 %wt. MEA + 7.5 %wt. KI at 40 °C

α / $mol_{CO2}\cdot mol_{MEA}^{-1}$	p / kPa	pCO_2 / kPa
0	6.2 ± 0.2	—
0.0915 ± 0.0001	6.4 ± 0.2	—
0.1821 ± 0.0002	6.6 ± 0.2	—
0.2752 ± 0.0002	6.7 ± 0.2	0.4 ± 0.3
0.3695 ± 0.0003	6.4 ± 0.2	0.5 ± 0.3
0.4637 ± 0.0003	7.8 ± 0.2	1.6 ± 0.3
0.5549 ± 0.0003	37.4 ± 0.2	31.2 ± 0.3
0.6229 ± 0.0004	142.5 ± 0.2	136.3 ± 0.3
0.6700 ± 0.0004	288.1 ± 0.2	281.9 ± 0.3
0.6975 ± 0.0005	412.7 ± 0.2	406.5 ± 0.3
0.7133 ± 0.0005	498.7 ± 0.2	492.5 ± 0.3

Aqueous 30 %wt. MEA + 7.5 %wt. KI at 120 °C

α / $mol_{CO2}\cdot mol_{MEA}^{-1}$	p / kPa	pCO_2 / kPa
0	173.5 ± 0.2	—
0.0805 ± 0.0002	169.1 ± 0.2	—
0.1594 ± 0.0002	173.3 ± 0.2	—
0.2345 ± 0.0003	182.4 ± 0.2	8.9 ± 0.3
0.3097 ± 0.0003	207.1 ± 0.2	33.6 ± 0.3
0.3722 ± 0.0004	259.9 ± 0.2	86.4 ± 0.3
0.4173 ± 0.0004	347.8 ± 0.2	174.3 ± 0.3
0.4454 ± 0.0005	447.8 ± 0.2	274.3 ± 0.3
0.4606 ± 0.0006	524.6 ± 0.2	351.1 ± 0.3

Table A-3. Viscosities of loaded salted solvents with aqueous 30 %wt. MEA measured at 25 °C. The confidence interval of each viscosity is assumed to be of ±2% following Hartono et al. (Hartono et al., 2014).

30 %wt. MEA +			30 %wt. MEA +			30 %wt. MEA +			30 %wt. MEA +		
α	/	η / mPa s	α	/	η / mPa s	α	/	η / mPa s	α	/	η / mPa s
0.000		2.664	0.000		3.749	0.000		2.752	0.000		2.965
0.106		2.938	0.108		3.641	0.103		2.765	0.105		2.816
0.212		3.190	0.219		3.967	0.205		3.045	0.211		3.159
0.322		3.388	0.322		4.348	0.315		3.287	0.314		3.466
0.418		3.689	0.427		4.765	0.416		3.448	0.408		3.790
0.513		3.863	0.537		5.231	0.524		3.644	0.530		4.165

The calculation of standard deviation (SD) within an average ($\bar{x}$) of n samples is done according to Eq. (A1), where x_i represents the measured concentration of each sample.

$$SD = \sqrt{\frac{\sum_{i=1}^{n}(x_i - \bar{x})^2}{n-1}} \tag{A1}$$

The correction from CO_2-loaded to CO_2-free solution using the amine concentration measured by amine titration ($C_{CO_2\,loaded}$) in mol·kg^{-1} and mass concentration of CO_2 measured by TIC (C_{CO_2}) was performed according to Eq. (A2).

$$C_{CO_2\,free} = \frac{C_{CO_2\,loaded} \cdot (C_{CO_2} + 1000\ \text{g})}{1000\ \text{g}} \tag{A2}$$

The correction for water and degradation losses was made assuming a linear loss of H_2O throughout the experiment. This is shown in Eq. (A3), where d is time in days and x is a coefficient regressed by taking the total amount of mass lost at the end of the experiment and dividing it by the duration of the procedure.

$$C_{corrected} = C_{CO_2\,free} \cdot (1 - d \cdot x) \tag{A3}$$

Table A–4. Oxidative degradation data from Setup 1. The calculations for CO$_2$ loading are made assuming that the alkalinity measured by titration stands for MEA concentration in the solvent.

Aqueous 30 %wt. MEA

Day	Alkalinity (w/ CO$_2$) [mol kg^{-1}]	CO$_2$ concentration [g kg^{-1}]	Loading [mol$_{CO2}$ mol$_{MEA}^{-1}$]	Alkalinity (w/o CO$_2$) [mol kg^{-1}]	Alkalinity (corrected) [mol kg^{-1}]
0	4.479	80.12	0.41	4.838	4.838
3a	4.322	80.24	0.42	4.669	4.634
3b	4.321	81.71	0.43	4.674	4.633
3c	4.285	79.49	0.42	4.625	4.609
7a	3.997	73.89	0.42	4.293	4.218
7b	4.034	74.06	0.42	4.332	4.244
7c	4.008	73.02	0.41	4.301	4.265
10a	3.673	66.73	0.41	3.918	3.820
10b	3.828	69.51	0.41	4.094	3.975
10c	3.741	67.47	0.41	3.994	3.946
14a	3.287	53.86	0.37	3.464	3.343
14b	3.519	59.27	0.38	3.727	3.576
14c	3.405	57.04	0.38	3.599	3.539
17a	3.032	48.37	0.36	3.179	3.044
17b	3.317	54.81	0.38	3.499	3.327
17c	3.194	52.83	0.38	3.363	3.294
21a	2.725	42.77	0.36	2.842	2.692
21b	3.042	48.92	0.37	3.191	2.997
21c	2.933	46.50	0.36	3.069	2.992

Aqueous 30 %wt. MEA + 2.0 %wt. NaCl

Day	Alkalinity (w/ CO$_2$)	CO$_2$ concentration	Loading	Alkalinity (w/o CO$_2$)	Alkalinity (corrected)

Day	Alkalinity (w/ CO2) [mol kg^{-1}]	CO2 concentration [g kg^{-1}]	Loading [mol$_{CO2}$ mol$_{MEA}$$^{-1}$]	Alkalinity (w/o CO2) [mol kg^{-1}]	Alkalinity (corrected) [mol kg^{-1}]
0	4.497	80.37	0.41	4.858	4.858
3a	4.407	86.96	0.45	4.790	4.761
3b	4.398	84.04	0.44	4.768	4.729
7a	4.250	83.65	0.45	4.605	4.541
7b	4.247	87.71	0.47	4.620	4.533
10a	4.112	80.33	0.44	4.443	4.354
10b	4.122	82.84	0.46	4.464	4.343
14a	3.924	80.03	0.46	4.238	4.119
14b	3.985	83.81	0.48	4.319	4.156
17a	3.842	76.71	0.45	4.136	3.996
17b	3.858	78.02	0.46	4.159	3.968
21a	3.615	72.38	0.46	3.876	3.713
21b	3.635	71.64	0.45	3.895	3.675

Aqueous 30 %wt. MEA + 7.5 %wt. KI

Day	Alkalinity (w/ CO2) [mol kg^{-1}]	CO$_2$ concentration [g kg^{-1}]	Loading [mol$_{CO2}$ mol$_{MEA}$$^{-1}$]	Alkalinity (w/o CO$_2$) [mol kg^{-1}]	Alkalinity (corrected) [mol kg^{-1}]
0a	4.528	97.93	0.49	4.971	4.971
0b	4.467	84.59	0.43	4.845	4.845
3a	4.381	102.45	0.53	4.830	4.798
3b	4.404	87.98	0.45	4.791	4.738
7a	4.182	96.87	0.53	4.588	4.517
7b	4.320	90.30	0.48	4.710	4.588
10a	4.047	94.22	0.53	4.428	4.331
10b	4.249	84.45	0.45	4.608	4.437

Day	Alkalinity (w/ CO$_2$) [mol kg^{-1}]	CO$_2$ concentration [g kg^{-1}]	Loading [mol$_{CO2}$ mol$_{MEA}$$^{-1}$]	Alkalinity (w/o CO$_2$) [mol kg^{-1}]	Alkalinity (corrected) [mol kg^{-1}]
14a	3.862	87.58	0.52	4.200	4.071
14b	4.159	86.50	0.47	4.519	4.285
17a	3.699	84.03	0.52	4.010	3.860
17b	4.073	84.31	0.47	4.416	4.139
21a	3.481	78.62	0.51	3.755	3.581
21b	3.912	80.12	0.47	4.226	3.898

Aqueous 30 %wt. MEA + 2.0 %wt. KI

Day	Alkalinity (w/ CO$_2$) [mol kg^{-1}]	CO$_2$ concentration [g kg^{-1}]	Loading [mol$_{CO2}$ mol$_{MEA}$$^{-1}$]	Alkalinity (w/o CO$_2$) [mol kg^{-1}]	Alkalinity (corrected) [mol kg^{-1}]
0	4.9002	85.78	0.43	4.900	4.900
3a	4.8480	90.23	0.46	4.848	4.823
3b	4.8291	—	—	4.829	4.793
3c	4.7844	—	—	4.784	4.756
7a	4.8338	89.51	0.46	4.834	4.776
7b	4.8222	89.62	0.46	4.822	4.738
7c	4.8091	89.17	0.46	4.809	4.742
10a	4.7853	88.73	0.46	4.785	4.704
10b	4.7616	—	—	4.762	4.643
10c	4.8015	—	—	4.801	4.705
14a	4.8450	89.30	0.46	4.845	4.730
14b	4.8787	89.96	0.46	4.879	4.708
14c	4.8733	90.35	0.46	4.873	4.737
17a	4.8758	90.14	0.46	4.876	4.735
17b	4.9307	—	—	4.931	4.721
17c	4.9145	—	—	4.915	4.747
21a	4.8988	90.80	0.46	4.899	4.724

Day	Alkalinity (w/ CO$_2$) [mol kg^{-1}]	CO$_2$ concentration [g kg^{-1}]	Loading [mol$_{CO2}$ mol$_{MEA}$$^{-1}$]	Alkalinity (w/o CO$_2$) [mol kg^{-1}]	Alkalinity (corrected) [mol kg^{-1}]
21b	4.9621	91.76	0.46	4.962	4.702
21c	4.9639	91.17	0.46	4.964	4.755

Aqueous 30 %wt. MEA + 1.0 %wt. KI

Day	Alkalinity (w/ CO$_2$) [mol kg^{-1}]	CO$_2$ concentration [g kg^{-1}]	Loading [mol$_{CO2}$ mol$_{MEA}$$^{-1}$]	Alkalinity (w/o CO$_2$) [mol kg^{-1}]	Alkalinity (corrected) [mol kg^{-1}]
0	4.5015	89.35	0.45	4.904	4.904
3a	4.4428	89.14	0.46	4.839	4.804
3b	4.4602	85.84	0.44	4.843	4.801
3c	4.4665	85.78	0.44	4.850	4.812
7a	4.8338	87.95	0.41	4.898	4.816
7b	4.8222	87.55	0.41	4.893	4.794
7c	4.8091	92.31	0.44	4.898	4.809
10a	4.7853	—	—	4.872	4.755
10b	4.7616	—	—	4.923	4.780
10c	4.8015	—	—	4.909	4.782
14a	4.5141	—	—	4.952	4.786
14b	4.5651	—	—	5.009	4.805
14c	4.5408	—	—	4.983	4.801
17a	4.5683	99.14	0.49	5.021	4.816
17b	4.5952	98.43	0.49	5.047	4.799
17c	4.5421	97.99	0.49	4.987	4.767
21a	4.5800	99.56	0.49	5.036	4.782
21b	4.6142	99.88	0.49	5.075	4.766
21c	4.5756	98.77	0.49	5.028	4.753
28a	4.6816	90.45	0.44	5.105	4.762
28b	4.6797	91.40	0.44	5.107	4.693

	Alkalinity (w/ CO$_2$) [mol kg^{-1}]	CO$_2$ concentration [g kg^{-1}]	Loading [mol$_{CO2}$ mol$_{MEA}^{-1}$]	Alkalinity (w/o CO$_2$) [mol kg^{-1}]	Alkalinity (corrected) [mol kg^{-1}]
28c	4.6259	90.15	0.44	5.043	4.676
35a	4.7194	92.01	0.44	5.154	4.721
35b	4.8223	93.42	0.44	5.273	4.738
35c	4.7197	91.18	0.44	5.150	4.681
42a	4.7979	91.74	0.43	5.238	4.710
42b	4.8923	94.80	0.44	5.356	4.704
42c	4.7786	91.73	0.44	5.217	4.647

Aqueous 30 %wt. MEA + 0.2 %wt. KI

Day	Alkalinity (w/ CO$_2$) [mol kg^{-1}]	CO$_2$ concentration [g kg^{-1}]	Loading [mol$_{CO2}$ mol$_{MEA}^{-1}$]	Alkalinity (w/o CO$_2$) [mol kg^{-1}]	Alkalinity (corrected) [mol kg^{-1}]
0	4.4848	76.95	0.39	4.830	4.830
3a	4.3374	81.28	0.43	4.690	4.656
3b	4.3365	80.90	0.42	4.687	4.646
3c	4.3193	82.05	0.43	4.674	4.640
7a	4.1758	81.16	0.44	4.515	4.439
7b	4.1412	77.89	0.43	4.464	4.373
7c	4.1428	80.31	0.44	4.475	4.400
10a	4.0521	-	-	4.368	4.263
10b	4.0051	-	-	4.313	4.188
10c	3.9973	-	-	4.309	4.206
14a	3.8893	73.60	0.43	4.176	4.035
14b	3.7364	75.27	0.46	4.018	3.855
14c	3.8248	75.16	0.45	4.112	3.974
17a	3.7722	-	-	4.046	3.881
17b	3.6793	72.83	0.45	3.947	3.753
17c	3.7472	72.94	0.44	4.020	3.856

	Alkalinity (w/ CO$_2$)	CO$_2$ concentration	Loading	Alkalinity (w/o CO$_2$)	Alkalinity (corrected)
21a	3.6349	71.13	0.44	3.893	3.697
21b	3.5319	69.36	0.45	3.777	3.547
21c	3.5869	70.43	0.45	3.839	3.646

Validation: oxidative degradation of 2.0 %wt. KI SAS

Table A-5. Data for the validation oxidative degradation experiment with 2.0 %wt. KI SAS in oxidative degradation Setup 2.

Aqueous 30 %wt. MEA + 2.0 %wt. KI

Day	Alkalinity (w/ CO$_2$) [mol kg^{-1}]	CO$_2$ concentration [g kg-1]	Loading [mol$_{CO2}$ mol$_{MEA}^{-1}$]	Alkalinity (w/o CO$_2$) [mol kg^{-1}]	Alkalinity (corrected) [mol kg^{-1}]
0	4.4606	79.66	0.41	4.816	4.816
1	4.4010	87.71	0.45	4.787	4.785
3	4.4224	87.12	0.45	4.808	4.802
7	4.4224	87.01	0.45	4.807	4.794
10	4.4105	86.13	0.44	4.790	4.771
14	4.4434	99.55	0.51	4.886	4.858
17	4.4742	94.23	0.48	4.896	4.862
21	4.4984	92.23	0.47	4.913	4.872

Table A-6. Thermal degradation data. The calculations for CO_2 loading are made assuming that the alkalinity measured by titration stands for MEA concentration in the solvent.

Aqueous 30 %wt. MEA

Week	Alkalinity (w/ CO_2)	CO_2 concentration	Loading	Alkalinity (w/o CO_2)
	[mol kg^{-1}]	[g kg^{-1}]	[mol$_{CO2}$ mol$_{MEA}^{-1}$]	[mol kg^{-1}]
0	4.5111	81.787	0.41	4.880
1A	4.3627	78.076	0.41	4.703
1B	4.3496	78.119	0.41	4.689
2A	4.1729	73.515	0.40	4.480
2B	4.1894	71.256	0.39	4.488
3A	3.8268	66.883	0.40	4.083
3B	3.8272	66.461	0.39	4.082
4A	3.6324	62.215	0.39	3.858
4B	3.6227	61.315	0.38	3.845
5A	3.5131	53.815	0.35	3.702
5B	3.3908	55.324	0.37	3.578

Aqueous 30 %wt. MEA + 2.0 %wt. NaCl

Week	Alkalinity (w/ CO_2)	CO_2 concentration	Loading	Alkalinity (w/o CO_2)
	[mol kg^{-1}]	[g kg^{-1}]	[mol$_{CO2}$ mol$_{MEA}^{-1}$]	[mol kg^{-1}]
0	4.5025	82.238	0.42	4.873
1A	4.4104	76.857	0.40	4.749
1B	4.3439	77.907	0.41	4.682
2A	4.1624	72.905	0.40	4.466
2B	4.1530	73.663	0.40	4.459
3A	3.8303	66.507	0.39	4.085
3B	3.8414	66.210	0.39	4.096
4A	3.6159	61.147	0.38	3.837
4B	3.6209	61.550	0.39	3.844
5A	3.3935	56.054	0.38	3.584
5B	3.3940	56.248	0.38	3.585

Aqueous 30 %wt. MEA + 7.5 %wt. NaCl

Week	Alkalinity (w/ CO_2)	CO_2 concentration	Loading	Alkalinity (w/o CO_2)
	[mol kg^{-1}]	[g kg^{-1}]	[mol$_{CO2}$ mol$_{MEA}^{-1}$]	[mol kg^{-1}]
0	4.5237	79.036	0.40	4.881
1A	4.4091	76.507	0.39	4.746
1B	4.3690	76.995	0.40	4.705

2A	4.2150	73.035	0.39	4.523
2B	4.2250	73.008	0.39	4.533
3B	3.8362	66.773	0.40	4.092
4A	3.5996	62.564	0.39	3.825
4B	3.6129	61.673	0.39	3.836
5A	3.3467	56.261	0.38	3.535
5B	3.3676	56.217	0.38	3.557

Aqueous 30 %wt. MEA + 2.0 %wt. KI

Week	Alkalinity (w/ CO_2) [mol kg^{-1}]	CO_2 concentration [g kg^{-1}]	Loading [mol$_{CO2}$ mol$_{MEA}^{-1}$]	Alkalinity (w/o CO_2) [mol kg^{-1}]
0	4.4594	83.147	0.42	4.830
1A	4.3370	76.967	0.40	4.671
1B	4.3286	74.691	0.39	4.652
2A	4.1328	70.562	0.39	4.424
2B	4.1519	72.286	0.40	4.452
3A	3.8643	64.435	0.38	4.113
3B	3.8158	65.165	0.39	4.064
4A	3.6014	60.385	0.38	3.819
4B	3.5952	58.960	0.37	3.807
5A	3.3662	54.800	0.37	3.551
5B	3.3980	53.931	0.36	3.581

Table A-7. Results of the ICP-MS analysis of samples subjected to 5 weeks at 135 °C. RSD is that of the three parallel injections of each sample.

Sample	m_{sample} [g]	m_{water} [g]	$C_{Fe,ICP}$ [µg L^{-1}]	$C_{Fe,original}$ [mg L^{-1}]	Fe (RSD%)	$C_{Cr,ICP}$ [µg L^{-1}]	$C_{Cr,original}$ [mg L^{-1}]	Cr (RSD%)
MEA A	0.4977	14.5156	29015.4	875.3	3.0	7558.7	228.0	0.6
MEA B	0.4950	14.2848	28119.5	839.6	0.68	7374.5	220.2	1.3
2.0% NaCl A	0.5002	14.6645	27619.2	837.3	1.9	11563.7	350.6	4.3
2.0% NaCl B	0.5052	14.3824	27919.5	822.8	2.6	11773.8	347.0	1.0
7.5% NaCl A	0.5224	14.9120	50431.6	1490.0	0.36	17442.1	515.3	0.8
7.5% NaCl B	0.5282	14.7574	50302.0	1455.7	0.43	17866.7	517.0	1.3
2.0% KI A	0.5024	14.5337	28738.5	860.1	2.0	10253.4	306.9	0.6
2.0% KI B	0.4996	14.4445	27748.5	830.0	0.58	10154.7	303.7	1.5
Water A	0.4525	14.4200	10.4	0.34	4.3	0.67	0.022	20.2
Water B	0.4520	13.1932	12.4	0.37	3.6	0.81	0.024	9.7

Sample	m_{sample} [g]	m_{water} [g]	$C_{Ni,ICP}$ [µg L^{-1}]	$C_{Ni,original}$ [mg L^{-1}]	Ni (RSD%)	$C_{Mo,ICP}$ [µg L^{-1}]	$C_{Mo,original}$ [mg L^{-1}]	Mo (RSD%)
MEA A	0.4977	14.5156	19240.8	580.4	0.73	3290.2	99.3	3.1
MEA B	0.4950	14.2848	18684.5	557.9	0.42	3303.3	98.6	4.3
2.0% NaCl A	0.5002	14.6645	15269.7	462.9	2.3	2811.8	85.2	4.9
2.0% NaCl B	0.5052	14.3824	15098.5	444.9	1.2	2743.5	80.8	2.4
7.5% NaCl A	0.5224	14.9120	15886.7	469.4	1.8	2937.9	86.8	3.1
7.5% NaCl B	0.5282	14.7574	16554.4	479.1	0.34	3173.5	91.8	3.5
2.0% KI A	0.5024	14.5337	13214.3	395.5	2.1	2358.7	70.6	2.4
2.0% KI B	0.4996	14.4445	12174.0	364.2	1.2	2161.4	64.7	1.8
Water A	0.4525	14.4200	1.4	0.046	16.1	0.94	0.031	7.2
Water B	0.4520	13.1932	7.6	0.23	0.13	0.38	0.011	26.4

Table A-8. Cylinder masses before thermal degradation experiments and after finishing plus 24 hours of acid washing with 0.1 M H_2SO_4.

Initial cylinder weight / g

Week	1	2	3	4	5
MEA A	170.0131	170.0600	170.4835	170.2170	170.3419
MEA B	169.7770	170.3677	170.5990	170.7898	170.1838
2.0% NaCl A	169.9413	169.6453	170.4424	170.5775	169.8514
2.0% NaCl B	170.1657	170.7374	170.2237	170.1015	170.7888
7.5% NaCl A	169.7331	170.1711	170.2732	169.8243	170.3480
7.5% NaCl B	169.8257	170.3808	170.0477	170.2144	170.3045
2.0% KI A	170.5621	170.2748	170.0193	170.2499	170.0645
2.0% KI B	169.8234	169.9881	170.5398	170.5295	170.3911
Water A	—	—	—	—	169.9854
Water B	—	—	—	—	170.0475

Cylinder weight after acid wash / g

Week	1	2	3	4	5
MEA A	170.0032	170.0377	170.4565	170.1927	170.3018
MEA B	169.7649	170.3411	170.5730	170.7538	170.1641
2.0% NaCl A	169.9265	169.6109	170.4104	170.5456	169.8186
2.0% NaCl B	170.1524	170.7159	170.1939	170.0808	170.7471
7.5% NaCl A	169.7151	170.1477	170.2322	169.7882	170.3137
7.5% NaCl B	169.8138	170.3212	170.0150	170.1898	170.2699
2.0% KI A	170.5554	170.2461	169.9957	170.2233	170.0413
2.0% KI B	169.8190	169.9701	170.5219	170.5217	170.3606
Water A	—	—	—	—	169.9809
Water B	—	—	—	—	170.0424

Table A-9. Anion exchange ion chromatography analysis of iodide concentrations after oxidative degradation in aqueous 30 %wt. MEA + 2.0 %wt. KI.

Sample	m_{sample} [g]	m_{water} [g]	Area [µS min]	C_{KI} (w/ CO_2) (ppm)	C_{KI} (w/o CO_2) (ppm)	(%wt.)	C_{KI} (corrected) (ppm)	(%wt.)
Blank	—	—	0	—	—	—	—	—
I⁻ std. 0 ppm	—	—	0	—	—	—	—	—
I⁻ std. 5.84 ppm	—	—	2.21	—	—	—	—	—
I⁻ std. 11.5 ppm	—	—	4.02	—	—	—	—	—
I⁻ std. 28.4 ppm	—	—	8.97	—	—	—	—	—
I⁻ std. 57.7 ppm	—	—	16.56	—	—	—	—	—
I⁻ std. 90.4 ppm	—	—	24.86	—	—	—	—	—
I⁻ std. 116 ppm	—	—	33.01	—	—	—	—	—
2.0% KI start	0.0132	1.749	28.7067	101.7	14742	1.5	14742	1.5
2.0% KI A day 21	0.0133	1.7794	30.6354	108.7	15967	1.6	15441	1.5
2.0% KI B day 21	0.0134	1.7314	32.9905	117.2	16656	1.7	15883	1.6
2.0% KI C day 21	0.0135	1.8016	30.905	109.6	16085	1.6	15466	1.5

Chapter 8

Experimental assessment of the environmental impact of ethanolamine

This chapter contains expermineal work in collaboration with the department of biology at NTNU in the form of a short paper submitted to and peer reviewed by the Trondheim CCS conference in 2021 (TCCS-11). The goal of this work was to come one step closer to assessing the environmental impact of amines in a more holistic manner. We wanted to be able to identify the pathways the amine and degradation compounds took thourhgout the simulated amine spill situations, but did not find good extraction or analytical methods for recovering the substances from the plants or soil. We did however manage to get an interesting assessement of the impact the amine had on the plant/soil system, which hopefully represents the beginning of future studies of the environmental faith of amines.

Experimental assessment of the environmental impact of ethanolamine

Vanja Buvik[1], Richard Strimbeck[2], Hanna K. Knuutila[1]*

[1] Department of Chemical Engineering, NTNU, NO-7491 Trondheim, Norway

[2] Department of Biology, NTNU, NO-7491, Trondheim, Norway

Abstract

The environmental impact of ethanolamine, a common amine for carbon dioxide capture, was experimentally investigated in laboratory scale microcosms. By exposing the plant-soil systems to varying amounts of ethanolamine, we assessed the effects a potential leakage or spill to the surroundings of an industrial site including vegetation. The results of this study show that small amounts of ethanolamine have no significant impact of the health of the plants in the scope of three weeks after treatment. Plant health was affected negatively by larger amounts of ethanolamine, but the plants treated with larger ethanolamine concentrations also seemed to be healthier, lusher, and greener after three weeks of observation. Unfortunately, this positive observation, indicating an actual fertilizing effect by ethanolamine on the plants could not be verified. In the TCCS-11 presentation we will show the results of this experimental study, their statistical interpretation, as well the implications the results have.

Keywords:

Biodegradation, Amine stability, CO_2 capture, Ecotoxicity, Plant health

8.1   Introduction

One of the most efficient ways of performing capture of carbon dioxide (CO_2) from industrial sources is using amine solvents. This is one of the most mature technologies available for large scale CO_2 capture, as it has been developed and tested over nearly a century. (Kohl and Nielsen, 1997; Leung et al., 2014; Rochelle, 2009) Amines bind chemically to the CO_2 molecules in a reaction that can be reversed upon heating up the solvent. Chemical stability of the amine is a necessity in the capture process, where it needs to withstand temperature cycling as well as oxidative conditions. (Reynolds et al., 2016) If the amine reaches the environment through emissions or spills from the capture facility, however, stability may no longer be a desirable property. Anything that reaches the environment should have the ability to get

---

* Corresponding author. Tel.: +47 73594119
E-mail address: hanna.knuutila@ntnu.no

incorporated into the environment as non-toxic components that can be consumed by organisms making changes to them or the environment.

Biodegradation is the process of breaking down larger into smaller molecules, performed by microorganisms. Because of the plethora of different microorganisms capable of performing biodegradation, biodegradability can follow manifold pathways. Amines used in CO_2 capture consist of hydrogen (H), carbon (C), oxygen (O) and nitrogen (N) and will ideally be broken down to CO_2, water (H_2O) and ammonia (NH_3), or other small molecules that can be available for plants to use as nutrients.

Assessment of biodegradability of chemicals which are used or considered for use in industrial applications is of immense importance, for mapping potential environmental risks of a spill or leakage of the chemical. A range of biodegradability test guidelines have been developed by the Organisation for Economic Co-operation and Development (OECD), for testing new chemicals, and these are commonly used for assessing new chemicals for industrial use. (OECD, 2002)

Table 8.1: Summary of the results of previous biodegradation studies of MEA.

Type	Conditions	Results	Reference
Soil	aerobic and anaerobic	MEA degraded aerobically and anaerobically	(Ndegwa et al., 2004)
Soil	aerobic and anaerobic	MEA degraded aerobically and anaerobically	(Wong et al., 2004)
Sea water	Aerobic with varying temperatures	Overall high degradability of MEA	(Brakstad et al., 2012)
Sea water	aerobic	MEA readily biodegradable	(Eide-Haugmo et al., 2012)
Fresh water	aerobic	MEA is readily biodegradable	(Henry et al., 2017)
Bioreactors	aerobic	MEA successfully degraded	(Kim et al., 2010)
Bioreactors	aerobic and anaerobic	MEA completely degradable upon PO43- addition	(Mrklas et al., 2004)

8.1.1 Biodegradation of ethanolamine (MEA)

Ethanolamine is naturally occurring (DNP, 2020), a feature that seems to make the amines more likely to be biodegradable than synthetic ones (Eide-Haugmo, 2011). It has for decades been the benchmark solvent for CO_2 capture and many biodegradation studies have already been performed both aerobically and anaerobically in soils (Ndegwa et al., 2004; Wong et al., 2004), in sea water (Brakstad et al., 2012; Eide-Haugmo et al., 2012), fresh water(Henry et al., 2017) and in lab-scale bioreactors under aerobic and anaerobic conditions (Kim et al., 2010; Mrklas et al., 2004). Some of these studies have also been performed according to the previously mentioned OECD guidelines. A quick summary of the findings of these studies is given in Table 8.1, and it can be observed that all have proven MEA to indeed be biodegradable. Additionally, Eide-Haugmo et al. (Eide-Haugmo et al., 2012) found that the ecotoxicity of MEA is also acceptably low in the marine species *Skeletonema costatum*.

In this work we try to take the conclusions from all these earlier studies one step further, to assess whether there are any immediate effects of an amine leakages to surrounding plants and soils. The experimental setup is, to our knowledge, novel in the field and provides a further perspective of the biocompatibility and environmental effects of amines and specifically ethanolamine.

8.2 Materials and methods

8.2.1 Materials

Ethanolamine (CAS: 141-43-5, purity $\geq$99.0%) was purchased from Merck Life Science/Sigma Aldrich Norway. Flowering soil ($^1/_3$ cow manure and $^2/_3$ turf, long-term composted over three years) and a mixture of grass seeds for outdoor use, were purchased from a local garden equipment store.

8.2.2 Experimental design

6 sets of 6 pots of 8x8x8 cm were filled with approximately 400 mL, which was thoroughly watered before soil and grass seeds were sowed on its surface in the density recommended on the seed package. The grass was watered twice a week, from a dish under the pots for the entire duration of the experiment. After 46 days, when the grass had grown at least 5-8 cm (see Figure 8.1) and a root system had the time to develop in the soil, one single randomized treatment was conducted per pot.

Figure 8.1: Example of grass length before the single treatment with MEA was conducted.

Each set of 6 pots were given one 10 mL addition of water or MEA with Table 8.2. The liquid was carefully distributed over the soil surface with a disposable syringe, without applying it directly on the plants. The order of treatment was randomized within each set.

275

Table 8.2: Treatments overview. Each treatment consisted of 10 mL of the given solution.

Treatment	% MEA
T1	0 (control)
T2	1.0
T3	2.5
T4	5.0
T5	7.5
T6	10

In summary this means that for each of the 6 treatments there were 6 individual samples, randomly located in different sample sets.

Table 8.3: Explanation of the scoring sheet used for assessing the plant health in the experiment.

Score	Percentage of brown leaves
0	0
1	1-10
2	11-30
3	31-60
4	61-90
5	91-100

8.2.3   Assessment of plant health

Regular visual scoring of plant health was performed according to Table 8.3 on day 4, 7, 11, 13, 18 and 21. Every scoring was performed by the same observer, without knowledge of which treatment each given system had been given.

Figure 8.2: Browning observed in one set of 6 different, randomized plant pots 11 days after treatment with MEA.

8.2.4 Statistical tests

A Kruskal-Wallis test was performed to determine the statistical significance in the difference of plant health observed in these experiments. This is a non-parametric statistical test, suitable for the comparison of individual samples and it does not assume a normal distribution of residuals. Variance is quantified as adjusted p-values and an adjusted $p \leq 0.05$ represents a significant difference between two treatments at a given time. The Bonferroni method was used for p-value adjustment.

A Friedman test, which is a non-parametric test for non-replicated data with complete block design, was performed to determine the statistical significance of the change in plant health over time. Kendall's W, as shown in Eq. 1, where $X2$ is the Friedman test statistic value, N the sample size and K the number of measurements. Cohen's interpretation of effect size was used to determine the size of the effect observed within each treatment.

$$W = \frac{X2}{N}(K-1)$$
Eq. 1
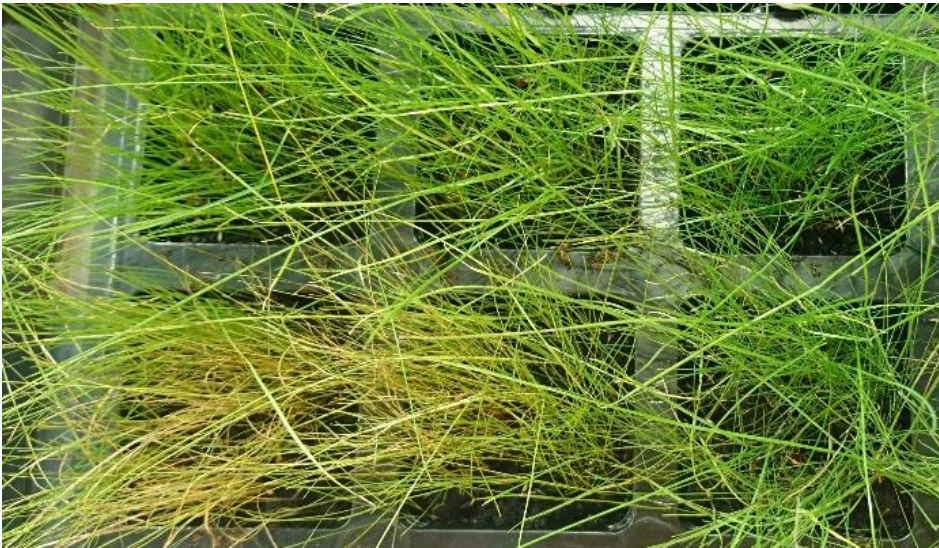
Bonferroni p-value adjustment was used for the identification of statistical difference between the treatments.

8.3 Results

8.3.1 Plant health

Browning was typically observed from day three to some degree, and then increasing. An example of the grass health as it was observed some days after treatment can be seen in Figure 8.2, The results of the plant health testing throughout three weeks after treatment with different amounts of MEA is depicted the means of each treatment in Figure 8.3 and medians in Figure 8.4. There is a clear trend seen from T4 to T6, whereas the health of the plants receiving treatments T1 (control) to T3 are more similar and no effect can be immediately distinguished. The statistical relevance of both these and the remaining results were determination by a Kruskal-Wallis test as well as a Friedman test.
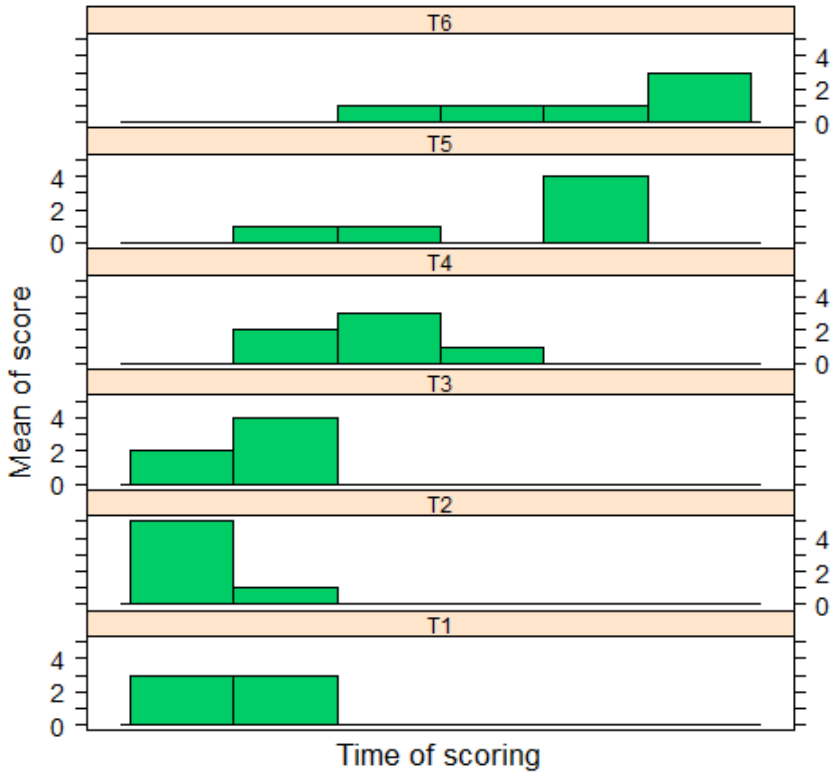
Figure 8.3: Means of plant health score for all treatments at different times of scoring.
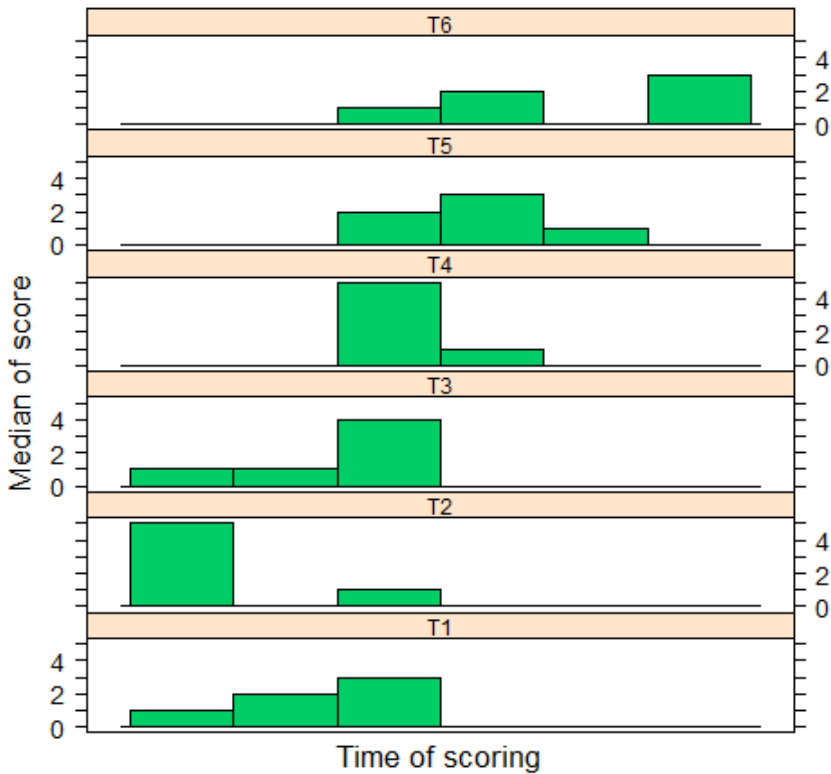
Figure 8.4: Medians of plant health score for all treatments at different times of scoring.

As seen in Figure 8.5, the Kruskal Wallis test shows that a higher degree of browning was seen on day 21 with T5 and T6 compared to T1-T3. On day 4, no significant differences were observed between any treatments, but at day 7, T6 showed more browning than T3 ($p < 0.01$). The difference between these two treatments remained significant throughout the whole experiment. After 11 days T6 had more browning than T1-T3 ($p < 0.3$ in all cases) and this is when T5 also started being browner than T2 ($p = 0.02$).

	T1	T2	T3	T4	T5
T2	1				
T3	1	1			
T4	0.9	0.4	0.9		
T5	0.03	0.01	0.03	1	
T6	0.04	0.01	0.04	1	1

Figure 8.5: Adjusted p-values for the average plant scores on day 21. Treatments which have $p \leq 0.05$ are statistically different from one another and can be described as giving different response in the plant health.

At no time of scoring was there a significant difference in browning between T1-T4, meaning that the addition of 1.0-5.0% MEA into the plant-soil systems makes no difference from not adding any MEA, the plant health is deemed the same.

The overall change in plant health over time was quantified by the Friedman test to be *large*. Within treatments, the effect was *small* in T1 and T2, *moderate* in T3 and T4 and *large* in T5 and T6 using Kendall's W and the Cohen interpretation of effect size. The effects of the treatments were studied using multiple pairwise comparisons and the Bonferroni adjusted p-values are given in Figure 8.6. According to these results treatments T3 to T6 have differences in plant health over time compared to T1 (control) to T3.

	T1	T2	T3	T4	T5
T2	0.7				
T3	1	1			
T4	$4 \cdot 10^{-3}$	$9 \cdot 10^{-6}$	$1 \cdot 10^{-4}$		
T5	$4 \cdot 10^{-6}$	$7 \cdot 10^{-8}$	$2 \cdot 10^{-7}$	0.04	
T6	$2 \cdot 10^{-8}$	$7 \cdot 10^{-10}$	$1 \cdot 10^{-9}$	$7 \cdot 10^{-5}$	1

Figure 8.6: Adjusted p-values for the mean of the plant scores through the entire experiment time of 21 days. Statistical significance given at $p \leq 0.05$.

Interestingly, a few weeks after the experiment was concluded, the pots containing plants treated with T5 and T6 seemed lusher and healthier than the plants where less MEA had been added. Since the observer from the duration of the experiment was not available, this data could not be logged. Attempts were made to extract remaining MEA and potential degradation compounds from the soil using a KOH extraction

method followed by centrifuging and filtering. No MEA could be observed in the soil extracts in the subsequent cation IC analysis. This phenomenon could either be due to an insufficiently low detection limit, having the strong signal of K^+ in the chromatogram, or it could be simply because the MEA was already biodegraded. Further research is needed to conclude on this matter.

8.4 Discussion and conclusions

Just like previous biodegradability ecotoxicity testing, these experiments show that MEA is not harmful for a plant-soil system, at least in small doses. For the three weeks after treatment with MEA there was no observable difference between plant-soil systems given up to 0.5 mL of MEA per 400 mL soil. This must mean that the buffer capacity of the soil is good enough to account for the potential pH increase when adding MEA, as well as that there's no observable toxic effect on the plants. The higher concentrations of MEA had a significant impact on the plants, making them browner in the experimental observation time of three weeks. In these cases, it can be hypothesized that the MEA has a negative impact in the soil, either by killing off some of the microbes or damaging the root systems of the plants. This is likely to be caused by the high pH of the MEA causing a chemical burn. The less likely explanation is that MEA has a toxic effect causing the plants to go brown. This is less likely because of previous testing, but also because of the subsequent healing of the plants after the end of the experiment.

The fact that the plants which had received a higher concentration of MEA actually seemed healthier after the experiment had ended, than those with less or no MEA added, indicates that the MEA that initially may have made the plants health decline, now was biodegraded into components that acted as nutrients for the plants. Nitrogen is a valuable nutrient in the plant kingdom, that the plants need to absorb from soil and water, as they are not able to convert nitrogen from air. Hence, the addition of nitrogen in the form of MEA may initially be harmful, but then have been biologically (biodegraded) converted to bioavailable small molecules by the soil microbes. Since, unfortunately, this observation took place after the experiment was ended and could not be logged by the same observer as throughout the scorings given in this paper, this effect could not be quantified and would be interesting to study in future work. This would most definitely be an interesting starting point for any further studies of the environmental impact of amines.

Acknowledgements

References

Brakstad, O.G., Booth, A., Eide-Haugmo, I., Skjaeran, J.A., Sorheim, K.R., Bonaunet, K., Vang, S.H., da Silva, E.F., 2012. Seawater biodegradation of alkanolamines used for CO2-capture from natural gas. International Journal of Greenhouse Gas Control 10, 271-277.

DNP, 2020. Dictionary of Natural Products. CRC Press, Taylor & Francis Group, http://dnp.chemnetbase.com/faces/chemical/ChemicalSearch.xhtml.

Eide-Haugmo, I., 2011. Environmental impacts and aspects of absorbents used for CO_2 capture.

Eide-Haugmo, I., Brakstad, O.G., Hoff, K.A., da Silva, E.F., Svendsen, H.F., 2012. Marine biodegradability and ecotoxicity of solvents for CO2-capture of natural gas. International Journal of Greenhouse Gas Control 9, 184-192.

Henry, I.A., Kowarz, V., Østgaard, K., 2017. Aerobic and anoxic biodegradability of amines applied in CO2-capture. International Journal of Greenhouse Gas Control 58, 266-275.

Kim, D.-J., Lim, Y., Cho, D., Rhee, I.H., 2010. Biodegradation of monoethanolamine in aerobic and anoxic conditions. Korean Journal of Chemical Engineering 27, 1521-1526.

Kohl, A.L., Nielsen, R.B., 1997. Chapter 2 - Alkanolamines for Hydrogen Sulfide and Carbon Dioxide Removal, in: Kohl, A.L., Nielsen, R.B. (Eds.), Gas Purification (Fifth Edition). Gulf Professional Publishing, Houston, pp. 40-186.

Leung, D.Y., Caramanna, G., Maroto-Valer, M.M., 2014. An overview of current status of carbon dioxide capture and storage technologies. Renewable and Sustainable Energy Reviews 39, 426-443.

Mrklas, O., Chu, A., Lunn, S., Bentley, L.R., 2004. Biodegradation of monoethanolamine, ethylene glycol and triethylene glycol in laboratory bioreactors. Water, air, and soil pollution 159, 249-263.

Ndegwa, A.W., Wong, R.C., Chu, A., Bentley, L.R., Lunn, S.R., 2004. Degradation of monoethanolamine in soil. Journal of Environmental Engineering and Science 3, 137-145.

OECD, 2002. Detailed Review Paper on Biodegradability Testing.

Reynolds, A.J., Verheyen, T.V., Meuleman, E., 2016. Degradation of amine-based solvents, in: Feron, P.H.M. (Ed.), Absorption-Based Post-combustion Capture of Carbon Dioxide. Woodhead Publishing, pp. 399-423.

Rochelle, G.T., 2009. Amine scrubbing for CO2 capture. Science 325, 1652-1654.

Wong, R.C., Bentley, L., Ndegwa, A., Chu, A., Gharibi, M., Lunn, S.R., 2004. Biodegradation of monoethanolamine in soil monitored by electrical conductivity measurement: an observational approach. Canadian geotechnical journal 41, 1026-1037.

Chapter 9

Conclusions and recommendations for future work

In this chapter, some overarching conclusions from the work included in this thesis will be listed with some suggestions to what future work should follow based on them.

9.1 Conclusions

Altogether, this work contributes to the knowledge base on how we can manage degradation of amine solvents by providing new information on oxygen solubility, stabilising effects of amine structures and potential for a novel inhibitor. Management strategies related to oxygen removal can in the future use the knowledge gathered in chapter 5 to assess the effectiveness of their technology, as well as predicting the amount of oxygen initially present. For future solvent development of new solvents for CO_2 capture, the findings of chapter 6 will be useful, by having made correlations between structure and amine stability, enhancing an already existing knowledge base by providing new data and data on amines not yet assessed under oxidising conditions. Potassium iodide was proven to be a good oxidation inhibitor for aqueous ethanolamine at simulated absorber conditions.

Based on all the data we could access on degradation in pilot plant studies presented in chapter 3, there is no single compound that seems to represent degradation, or the health of the ethanolamine (MEA) solvent well enough to recommend monitoring of any one compound. It does, however look like solvent pre-treatment is very efficient in extending the solvent lifetime, and that, if any parameters are more recommended to keep an eye on than others, it must be the total HSS concentration of the solution in combination with ammonia in the cleaned flue gas, or in the water wash. When it comes to other, and proprietary solvents, there is simply not sufficient data available to draw any conclusions. Degradation behaviour is highly solvent specific and should be treated as such. There is a lack of general reporting routines, documentation of analytical procedures used, and guidelines for solvent monitoring at all. This is of course not something that would be easily implemented with many industrial competitors wanting the advantage of keeping data to themselves, but it could potentially accelerate solvent and process development by a lot.

When it comes to the quantification of dissolved O_2 in amine solvents there are still some unknowns that need to be figured out. Firstly, because there are limited methods for quantification available to aid the validation process and secondly, because the chemical reactions taking place within the liquid phase makes the conditions deviate from the classic case of physical solubility. The work presented in chapter 5 contributes with a thorough testing of commercially available dissolved oxygen sensors, made for water testing, for measurement of dissolved oxygen also in solvents for CO_2 capture. The work concludes that there is no significant difference in oxygen solubility between different amine solvents. It also concludes that it is difficult to measure dissolved O_2 in CO_2 loaded MEA in water, which is assumed to be because of the rapid oxygen consumption taking place because of degradation reactions even at relatively low temperatures. This difficulty is not present for the more stable amine MDEA in water. A first approach to making a model for predicting O_2 solubility was made for MEA, using speciation data for the ionic compounds found in the CO_2

loaded amine, and a model originally developed by Schumpe et al. (1978). This model can be extended for further amines.

The results shown in chapter 6 show that most modifications of the amine structure compared to MEA are more stable. The results also suggest that the carbamate of the amines should be considered to play a larger role in the degradation mechanisms than earlier assumed. Most of the early works looking at MEA degradation product formation, the ones that suggested the mechanisms widely used to explain degradation still, were in CO_2 free systems. The fact that we do not see significant oxidative degradation of 30wt% MEA (*aq.*) without CO_2 but do with CO_2 present suggest that it at least partakes catalytically in the degradation reactions. Our study also shows, in agreement with several other studies (Muchan et al., 2021; Vevelstad et al., 2013; Vevelstad et al., 2014), that even a chain extension stabilises the amine, perhaps because of the decreased chance of radical formation and stabilisation of the C-N bond (Muchan et al., 2021).

In chapter 7 a new inhibitor to prevent oxidative degradation in aqueous amines is presented. Potassium iodide (KI) proved to successfully inhibit oxidative degradation in laboratory scale oxidation experiments, without having a negative impact on thermal stability, density, viscosity, or the kinetics of CO_2 absorption and desorption. The inhibitor also does not appear to get spent throughout the inhibition and may therefore not need replenishment in the process.

The work presented in chapter 8 is a first approach to studying the environmental fate of amines with a more holistic approach than independent studies of biodegradability or ecotoxicity. We saw that a spill of MEA may, at least initially, harm a plant/soil system, making the plants health decline. This effect is possibly caused by the elevated pH in the soil and on the plants' roots, when exceeding the soils immediate buffering capacity. There were, however, indications that following an initial decline, an improved plant health could be seen. This small study rises further questions about the biological effects which amines can have if they reach the environment, both negative and potentially positive.

9.2   Suggestions for future work

Despite of seemingly representing the oxidation processes of the temperature swing CO_2 absorption process, by producing the same degradation products, the oxidative degradation experiments we are performing in our laboratories have their limitations. Firstly, as noted also in earlier studies, the most abundant oxidative degradation products in the laboratory are not the most abundant in pilot scale. Secondly, we observed that when the KI oxidative degradation inhibitor, which worked perfectly for inhibiting laboratory scale oxidative degradation did not seem to fully inhibit degradation in during temperature swing absorption and desorption experiments. These results just came in after testing in SINTEF Industry's cyclic solvent

degradation (SDR) rig (Einbu et al., 2013) and are therefore not included in this thesis. In this experiment, some classical oxidative degradation compounds were indeed suppressed, but the amine loss was not reduced compared to inhibitor-free ethanolamine. It seems that the inhibition of certain oxidative degradation pathways may have enhanced other degradation mechanisms and thereby actually increased the amine loss. The inhibitor did, however, seem to inhibit the formation of compounds that give rise to the solvent discolouration that is normally observed in MEA. Despite of the purely thermal degradation experiments performed in our labs showing similar stability of the MEA with KI as without, the effect seen at temperature swing conditions did not. In the future, degradation experiments should therefore aim to include the large-scale effects, by performing absorption and desorption, as well as the increase and decrease of temperature, to actually be able to predict the amine's behaviour in larger scale.

Further work on oxygen measurement in amine solutions is required to assure whether quantification of dissolved oxygen and oxygen solubility is possible. This would require either more work on dissolved oxygen sensors made for water testing, or with some luck, a further quantification method that can be used to validate the sensors. The Schumpe model presented in this work can also be extended for other amines, to predict their oxygen solubility. To facilitate this, speciation studies of the CO_2-loaded amines, as well as the measured solubility of an inert gas like N_2O in it, would be necessary.

Another inherent property of the amine solvents, which is not fully understood, is the solubility of metals into them. We see how increasing degradation usually correlates with increasing metal concentrations in the solution, but the mechanism behind this has not yet been explained. It would be interesting to see what metal-degradation product complexes are formed in the degraded solutions. It would also be very useful to develop a direct method for measurement of dissolved iron, and other metals in the solutions, for monitoring the state of the solvent and the CO_2 capture plant, preferably one that would distinguish between metal ions or complexes, and other metal particles.

The environmental faith of amines is an important factor to include in future evaluations of solvents. An interesting effect we observed in the study presented in Chapter 8 was what happened after the actual experiment was over. The plants that had been treated with MEA seemed to experience a "bounce back" effect after initially having suffered from the higher concentrations of amine added to their pots. After the end of the experiment, the plant that had received the largest dose of MEA, looked the least healthy after three weeks, but a few weeks after that again, they looked healthier than ever. This effect would be very interesting to follow up on and continue the study. Nitrogen is a valuable resource in nature and bioavailable nitrogen can be of limited availability, maybe the nitrogen contained in MEA, fresh or degraded could be considered used as or transformed into fertiliser? Of course, this

would require a lot more research, but it could potentially solve the issues of disposing of the used amine solvents. On the same topic, it would also be immensely interesting to find ways of extracting and analysing the amines in the soil/plant-systems over time. Does the MEA (or other amines) remain in the soil and remain intact for long, or does it degrade, or transform rapidly? What does it degrade into, and what contributes to the degradation? Will any soil microbiome be as efficient at providing bioavailable nitrogen for the plants? A study comparable to that of Rankin et al. (2014), where the biodegradability of fluorotelomer-based polymers was monitored in soil-plant microcosms under aerobic conditions. They used advanced analytical methods like direct MALDI-TOF and indirect LC-MS/MS of the soil samples. Because of the relatively small size of the amines and their derivatives, these analytical methods may not be ideal in our case, especially not the MALDI-TOF, but the principle would be interesting to use on amines if possible.

9.3 References

Einbu, A., DaSilva, E., Haugen, G., Grimstvedt, A., Lauritsen, K.G., Zahlsen, K., Vassbotn, T., 2013. A new test rig for studies of degradation of CO2 absorption solvents at process conditions; comparison of test rig results and pilot plant data for degradation of MEA. Energy Procedia 37, 717-726.

Muchan, P., Supap, T., Narku-Tetteh, J., Idem, R., 2021. Assessment of the Relationship between Degradation and Emission Activities of Carbon Capture Amines Based on their Chemical Structures, 15th Greenhouse Gas Control Technologies Conference.

Rankin, K., Lee, H., Tseng, P.J., Mabury, S.A., 2014. Investigating the biodegradability of a fluorotelomer-based acrylate polymer in a soil–plant microcosm by indirect and direct analysis. Environmental science & technology 48, 12783-12790.

Schumpe, A., Adler, I., Deckwer, W.D., 1978. Solubility of oxygen in electrolyte solutions. Biotechnology Bioengineering 20, 145-150.

Vevelstad, S.J., Grimstvedt, A., Einbu, A., Knuutila, H., da Silva, E.F., Svendsen, H.F., 2013. Oxidative degradation of amines using a closed batch system. International Journal of Greenhouse Gas Control 18, 1-14.

Vevelstad, S.J., Grimstvedt, A., Knuutila, H., da Silva, E.F., Svendsen, H.F., 2014. Influence of experimental setup on amine degradation. International Journal of Greenhouse Gas Control 28, 156-167.

NTNU
Norwegian University of
Science and Technology